Copy No. 41

RESEARCH REPORT

ON

OPTIMAL CONTROL FOR SATELLITE ATTITUDE MANEUVERS

(Contract No. NAS 5-10191 and NAS 5-10349)

APR 1968

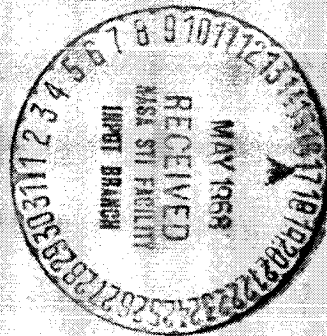### VOLUME 1: MATHEMATICAL ANALYSIS

RESEARCH REPORT

on

OPTIMAL CONTROL FOR SATELLITE ATTITUDE MANEUVERS

Prepared by

G. Stephen Jones
Thomas Englar
Wallace Parr
E. V. Schuman
Arrigo Cellina

of

The Mathematical Sciences Group
7100 Baltimore Avenue
College Park, Maryland

Z = Euler Angles

FLIGHT VEHICLE

$$\alpha = \begin{bmatrix} \phi \\ \theta \\ \psi \end{bmatrix}$$

$$\omega = \begin{bmatrix} \omega_1 \\ \omega_2 \\ \omega_3 \end{bmatrix}$$

$$u = \begin{bmatrix} u_1 \\ u_2 \\ u_3 \end{bmatrix}$$

$$T = \begin{bmatrix} T_1 \\ \vdots \\ T_{16} \end{bmatrix}$$

GRAVITY AND SOLAR TORQUE
Appendices B & C

SENSORS
(NOISE AND NONLINEARITY)
Appendix F

SATELLITE DYNAMICS
Part I

Xmit, A/D
Part IV

PRE-FILTER
(BAD POINT DISCARD)
Part IV

Z

Z

Z

ESTIMATION AND CONTROL

FILTER
Appendix F

$$\begin{bmatrix} \hat{\alpha} \\ \hat{\omega} \end{bmatrix}$$

FILTER CHANGES
$\begin{bmatrix} \hat{\alpha}_o \\ \hat{\omega}_o \end{bmatrix}$ k, δ, τ Appendix F

CONTROL COMPUTER
Part II

CHANGE OF
λ, T/I, b
Part II
Appendix E

THRUSTER TORQUES
Part IV

RECEIVER, VERIFICATION, ACTUATION
Part IV

THRUSTER SELECTOR
Part IV

CHANGE OF THRUSTER SELECTION
Part IV

LAG τ

COMMAND DECISIONS

OVERALL BLOCK DIAGRAM

This report has been written in partial fulfillment of Contract NAS5-10349 carried out by the Mathematical Sciences Group with the support of the Systems Analysis and Electric Propulsion Section of the Goddard Space Flight Center. This report constitutes a final report for the subject contract and is intended to serve as a reference document for controls engineers faced with the task of design and construction of optimal attitude control for space vehicles.

Under Contract NAS5-10191 a synthesis for suboptimal attitude maneuvering control for synchronous earth-pointing satellites was performed using six degree of freedom nonlinear dynamics for rigid body satellites being perturbed by gravity gradient and solar pressure torques and misalignment of attitude control thrusters. Under the Contract NAS5-10349 this analysis was extended to include the real effects of sensors such as noise and derived rate data. Thruster real effects are also incorporated related to on-time delays, minimum pulse restrictions, and rise time and decay behavior. Analysis has also been performed to allow elastic deformation of members supporting a solar panel on the satellite. Computer programs have been constructed for control synthesis and simulation purposes in the digital member of a digital-analogue hybrid computer. In addition, analoguous computer software has been constructed for fully digital simulation study.

Extensive simulation studies have been carried out using the MSG control synthesis program and much information has been obtained which can be of direct application in the proper design

of satellite controls hardware. Of particular interest in this direction are the trade-off studies between minimum time and minimum fuel consumption in making standard maneuvers. A deeper investigation has revealed some extremely interesting results concerning the influence of the real effects of sensors and thrusters on these trade-offs. These studies are fully documented herein.

Although the results of this study are quite general and not restricted in any essential way to a specific satellite, they are highly relevant for possible utilization with the ATS-F and -G satellites. In particular, solar and gravity gradient torques are computed with the physical characteristics of these satellites in mind. Of significant practical importance is the determination that the control synthesis simultaneously possesses highly versatile capabilities and sufficient simplicity for feasible onboard implementation. Ground station operation is anticipated to be necessary only for incorporating secondary adaptive modifications to system parameters and for transmitting slewing commands.

Control strategies discussed herein are particularly well suited for applications where a precise time sequence of attitude maneuvers is required and conservation of fuel is a major consideration. Such characteristics are of central importance to missions involving the mapping of the surface of the earth or the surveillance of surface or near surface activities such as weather, plane flights, missile launchings, explosions, etc. It is also feasible to consider tracking missions of one space vehicle by another using the synthesis developed.

In addition to the interesting qualitative and quantitative results of simulation studies documented, this report contains a complete detailed development of the theoretical foundation behind these studies. The many theoretical aspects of the dynamics involved have been carefully recorded for easy reference. Discussion of the relevant control theory is included as well as the complete synthesis of the relevant optimal feedback control policy constructed around a very flexible performance index weighting time, fuel, and energy in the system.

Acknowledgements

TABLE OF CONTENTS

LIST OF SYMBOLS

s-system   =   A satellite or orbital coordinate system with $\vec{s}_2$ pointing at the center of the earth and $\vec{s}_3$ pointing northward and parallel to the axis of rotation of the earth.

S-system   =   A satellite related coordinate system parallel to the s-system but with origin at the center of the earth.

b-system   =   The body coordinate system with $\vec{b}_2$ pointing at an initial latitude and longitude.

B-system   =   The body coordinate system with $\vec{B}_2$ pointing at a target (or terminal) latitude and longitude.

r-system   =   A reference coordinate system with $\vec{r}_2$ pointing at an initial latitude and longitude.

R-system   =   A reference coordinate system with $\vec{R}_2$ pointing at a target (or terminal) latitude and longitude.

p-system   =   A principal moment of inertia system with axis along the body principal moments of inertia and $\vec{p}_2$ parallel to the axis of symmetry of the body, positive toward the earth.

e-system   =   An inertial earth system.

C-system   =   An earth-sun coordinate system with $\vec{C}_2$ pointing from the sun to the earth.

$A^{\leftarrow}_{pq}$ = The matrix satisfying $(\vec{v})_p = A^{\leftarrow}_{pq}(\vec{v})_q$. That is, the transformation which takes a vector with components in the q-coordinate system into a vector with components in the p-coordinate system.

$C(\theta, \Psi, \phi)$ = A special case of the matrix $A^{\leftarrow}_{pq}$ where both the p-system and q-system are orthonormal systems and where the elements of the matrix are written in terms of the Euler angles θ, Ψ, ϕ.

$(\theta_{pq}, \Psi_{pq}, \phi_{pq})$ = The Euler angles which satisfy the equation $A^{\leftarrow}_{pq} = C(\theta_{pq}, \Psi_{pq}, \phi_{pq})$. That is, the angles which rotate the q-system <u>into</u> the p-system. (Defined to be the (pitch, yaw, roll) angles, respectively.)

$B(L, \ell, \gamma)$ = A special case of the matrix $A^{\leftarrow}_{pq}$ where the matrix elements can be written in terms of latitude (L), longitude difference (ℓ) and rotation angle (γ).

L, L_I, L_T = Latitude, initial latitude, target (or terminal) latitude of a point on the surface of the earth.

ℓ, ℓ_I, ℓ_T = Difference in longitude, initial difference in longitude, target (or terminal) difference in longitude between a point on the surface of the earth and the longitude of the point directly below the satellite. The difference is positive for points east of the satellite longitude.

γ_I = Rotation angle of the b-system about the r_2 axis.

γ_T = Rotation angle of the B-system about the R_2 axis.

$\vec{\omega}$ = The angular velocity of the body with respect to the s-system.

ω_i = The components of the angular velocity in the p-system.

$D(\Psi_{bs}, \phi_{bs})$ = The matrix transforming the time derivatives of the Euler angles into $(\vec{\omega})_b$ -- the angular velocity of the body in terms of the b-system. (Also a matrix of the form $A^{\leftarrow}_{pq}$ where p is the b-system and q is the non-orthogonal system $(\vec{s}_3, \vec{s}_2', \vec{b}_1)$.

α_i = Normalizing constants for the r and R system unit vectors.

$\widehat{uv}$ = The angle between the vectors $\vec{u}$ and $\vec{v}$.

r_e = Radius of the earth.

r_s = Radius of the satellite orbit.

k = r_s/r_e .

M^{-1} = Inverse of a matrix M.

M^T = Transpose of a matrix M.

M^L = Linearization of a matrix M, i.e., angles θ small enough so that $\sin \theta \cong \theta$, $\cos \theta \cong 1$, $\theta^n = 0$ for $n = 2,3,\ldots$.

$h(t)$ = Angular momentum of body.

n = Total torque of body about center of mass.

     = $n_C + n_D$, where n_C is control torque and n_D is disturbance torque.

I_i = Moment of inertia about i^{th} principal axis, $i = 1,2,3$.

COORDINATE SYSTEM AND TRANSFORMATION SUMMARY

The matrices used for coordinate transformations are presented here for references:

$$C(\theta, \psi, \phi) = \begin{pmatrix} C\psi C\theta & C\psi S\theta & S\psi \\ -S\phi S\psi C\theta - C\phi S\theta & -S\phi S\psi S\theta + C\phi C\theta & S\phi C\psi \\ -C\phi S\psi C\theta + S\phi S\theta & -C\phi S\psi S\theta - S\phi C\theta & C\phi C\psi \end{pmatrix}$$

$$B(L, \ell, \gamma) = \begin{bmatrix} \dfrac{\cos\gamma}{\alpha_1}(k - \cos L \cos\ell) & \dfrac{-\cos}{\alpha_1}\cos L \sin\ell & \dfrac{\alpha_1}{\alpha_2}\sin\gamma \\[1em] \dfrac{-\sin\gamma}{\alpha_1\alpha_2}\sin L \cos L \sin\ell & \dfrac{-\sin\gamma}{\alpha_1\alpha_2}\sin L(k - \cos L \cos\ell) & \\[2em] \dfrac{\cos L \sin\ell}{\alpha_2} & \dfrac{(k - \cos L \cos\ell)}{\alpha_2} & \dfrac{\sin L}{\alpha_2} \\[2em] \dfrac{-\sin\gamma}{\alpha_1}(k - \cos L \cos\ell) & \dfrac{\sin\gamma}{\alpha_1}\cos L \sin\ell & \dfrac{\alpha_1}{\alpha_2}\cos\gamma \\[1em] \dfrac{-\cos\gamma}{\alpha_1\alpha_2}\sin L \cos L \sin\ell & \dfrac{-\cos\gamma}{\alpha_1\alpha_2}\sin L(k - \cos L \cos\ell) & \end{bmatrix}$$

The normalizing constants α_i are defined on page 43.

$$D(\psi, \phi) = \begin{pmatrix} 1 & 0 & \sin\psi \\ 0 & -\cos\phi & \sin\phi \cos\psi \\ 0 & \sin\phi & \cos\phi \cos\psi \end{pmatrix}$$

$$D^L(\psi, \phi) = \begin{pmatrix} 1 & 0 & \psi \\ 0 & -1 & \phi \\ 0 & \phi & 1 \end{pmatrix}$$

$$D^{-1}(\psi, \phi) = \begin{pmatrix} 1 & -\tan\psi\,\sin\phi & -\tan\psi\,\cos\phi \\ 0 & -\cos\phi & \sin\phi \\ 0 & \sec\psi\,\sin\phi & \sec\psi\,\cos\phi \end{pmatrix}$$

$$[D^{-1}(\psi, \phi)]^L = \begin{pmatrix} 1 & 0 & -\psi \\ 0 & -1 & \phi \\ 0 & \phi & 1 \end{pmatrix}$$

(1) $b_i \to s_i$

$$(\vec{u})_s = A_{sb}^{\leftarrow}(\vec{u})_b = C(\theta_{sb}, \psi_{sb}, \phi_{sb})\,(\vec{u})_b$$

$$= C^T(\theta_{bs}, \psi_{bs}, \phi_{bs})\,(\vec{u})_b = B^T(L_I, \ell_I, \gamma_I)\,(\vec{u})_b$$

(2) $s_i \to R_i$

$$(\vec{u})_R = A_{Rs}(\vec{u})_s = C(\theta_{Rs}, 0, \phi_{Rs})\,(\vec{u})_s$$

$$= B(L_T, \ell_T, 0)\,(\vec{u})_s$$

12

(3) $b_i \rightarrow R_i$

$$(\vec{u})_R = A_{Rb}^{\leftarrow}(\vec{u})_b = C(\theta_{Rb}, \psi_{Rb}, \phi_{Rb})\ (\vec{u})_b$$

$$= C^T(\theta_{bR}, \psi_{bR}, \phi_{bR})\ (\vec{u})_b = A_{Rs}^{\leftarrow}\ A_{sb}^{\leftarrow}\ (\vec{u})_b$$

$$= C(\theta_{Rs},\ 0,\ \phi_{Rs})C^T(\theta_{bs}, \psi_{bs}, \phi_{bs})\ (\vec{u})_b$$

(4) $e_i \rightarrow s_i$

$$(\vec{u})_s = A_{se}^{\leftarrow}(\vec{u})_e = C(\theta(t)_{se},0,0)(\vec{u})_e$$

where $\theta(t)_{se} = \Omega(t - t_o) + \theta(t_o)$, Ω is the rate of rotation of the earth, t_o an arbitrary time.

(5) $b_i \rightarrow p_i$

$$(\vec{u})_p = A_{pb}(\vec{u})_b = C(\theta_{pb}, \psi_{pb}, \phi_{pb})\ (\vec{u})_b$$

$$= C^T(\theta_{bp}, \psi_{bp}, \phi_{bp})\ (\vec{u})_b$$

(6) $(\vec{s}_3,\ \vec{s}_2',\ b_1) \rightarrow b_i$

$$(\vec{\omega}) = A_{(s_3,\ s_2',\ b_1^{\leftarrow}),b}(\vec{\omega})_{(s_3,\ s_2',\ b_1)}$$

$$= D(\psi_{bs}, \phi_{bs})\begin{pmatrix} \dot{\phi}_{bs} \\ \dot{\psi}_{bs} \\ \dot{\theta}_{bs} \end{pmatrix} \simeq D^L(\psi_{bs}, \phi_{bs})\begin{pmatrix} \dot{\phi}_{bs} \\ \dot{\psi}_{bs} \\ \dot{\phi}_{bs} \end{pmatrix}$$

(7) $(\overset{>}{R}_3, \overset{>}{R}'_2, b_1) \rightarrow b_i$

$$(\overset{>}{\omega})_b = D(\psi_{bR}, \phi_{bR}) \begin{pmatrix} \dot{\phi}_{bR} \\ \dot{\psi}_{bR} \\ \dot{\theta}_{bR} \end{pmatrix} \simeq D^L(\psi_{bR}, \phi_{bR}) \begin{pmatrix} \dot{\phi}_{bR} \\ \dot{\psi}_{bR} \\ \dot{\theta}_{bR} \end{pmatrix}$$

(8) $b_i \rightarrow (s_3, s'_2, b_1)$

$$\begin{pmatrix} \dot{\phi}_{bs} \\ \dot{\psi}_{bs} \\ \dot{\theta}_{bs} \end{pmatrix} = D^{-1}(\psi_{bs}, \phi_{bs}) (\overset{>}{\omega})_b \simeq [D^{-1}(\psi_{bs}, \phi_{bs})]^L (\overset{>}{\omega})_b$$

(9) $b_i \rightarrow (R_3, R'_2, b_1)$

$$\begin{pmatrix} \dot{\phi}_{bR} \\ \dot{\psi}_{bR} \\ \dot{\theta}_{bR} \end{pmatrix} = D^{-1}(\psi_{bR}, \phi_{bR}) (\overset{>}{\omega})_b \simeq [D^{-1}(\psi_{bR}, \phi_{bR})]^L (\overset{>}{\omega})_b$$

Spacecraft Dynamics Model

The development of techniques for the construction of economical high-accuracy attitude control mechanisms is a problem of pressing importance to the objectives of NASA and the industry built around and dependent upon earth satellites. In this document and the study it describes the authors respectfully report that significant progress both practical and theoretical has been made in answer to this need.

This report is divided into seven main parts and five appendices which may be read independently depending on the needs and interest of the reader. *Part I* together with *Appendices A, B,* and *C* develop fully the kinematics and dynamics of a single body satellite moving in a synchronous orbit around the earth's equator. All transformations between the various coordinate systems encountered are fully described as well as the transformations between latitude and longitude coordinated ground tracks and Euler angles tied to the body of the satellite or to an attitude target position. A mathematical model is developed describing the dynamics for attitude maneuvers of earth oriented satellites incorporating the following considerations:

1) Six degree of freedom nonlinear dynamics.

2) Disturbance torques resulting from solar pressure acting on a parabolic dish.

3) Disturbance torques resulting from gravity gradient considerations.

4) Misalignment of attitude control thrusters relative to the satellite principal axes.

5) Incomplete feedback resulting from data acquisition restrictions.

6) Effects of elastic deformation of satellite members supporting solar panels.

In *Part II* and *Appendix E* a brief discussion of relevant optimal control theory is presented and a detailed synthesis of optimal control strategy is developed for the dynamics described in *Part I*. Control policies described herein and developed during the prerequisite study are adaptive in the sense that weighting parameters are incorporated in the performance criterion to allow trade-off between speed of response and fuel consumption. It is also possible by adjusting parameters to strengthen the stability of the system at the expense of optimality in speed of response and fuel consumption and conversely. The control synthesis is particularly well suited for applications where a precise time sequence of attitude maneuvers is required and conservation of fuel is a major consideration.

In *Part III* a comprehensive and detailed account of results acquired through simulation studies is presented. A series of experiments is described which test and illustrate the performance

of the control strategy under systematic variations of the large number of parameters built into the system. In particular, trajectories are illustrated for different initial and target angular positions. The stability of the feedback control has been illustrated by subjecting the simulated vehicle to a large unaccounted for disturbance during a slewing maneuver. A variety of optimizations based on compromise weightings between speed of response, energy in the system, and fuel economy were tested and curves indicating the trade-off characteristics of these performance parameters are presented. The effects of incomplete feedback resulting from sample data and the cross-coupling effects of large initial rates are also illustrated. Curves were computed representing the effects of gravity gradient and solar pressure torques and large random torques on the control of the vehicle.

In Part IV the analysis and simulation results associated with the introduction of noise, derived rate data, and other imperfections in sensor hardware are outlined. The application of a linear filter for deriving rate data from noisy angular data is set forth in Appendix F. The effects of real thruster characteristics on the control of the vehicle are discussed and illustrated in Part IV. A number of the parametric studies illustrated in Part III are repeated in Part IV with the incorporation of real sensors and thrusters. The program has the capability of handling torques which are not aligned with the vehicle principal axes. The method of simulation and also how these disturbance torques are compensated for are described in Appendix J.

In *Part V* elastic dynamics generally are discussed and a limited result of simulation study is presented. It is anticipated that more complete and detailed investigations of elastic effects will be carried out in future work. In Appendix D a lumped parameter analysis of a single rigidly attached elastic member is presented.

Part VI consists of *Appendices A* through *E* which in general contain much of the detailed mathematical analysis backing up the illustrations and conclusions set forth in *Parts I* through *V*.

A detailed discussion and the logical flow of the digital and digital-analogue simulation computer programs are set forth in *Part VII*. Included also are complete program listings, instructions for the operation of these programs, and specifications of some of the tests performed in establishing the functional correctness of subroutine components of the system. *Part VII* is presented under separate cover.

It should be pointed out that the constraint of feasible implementation has been imposed on the control synthesis described herein. This constraint has necessitated some minor deviation from strict theoretical optimality with respect to the performance criterion. In the strict theoretical sense, therefore, the control synthesis should be described as "near" optimal.

A number of important techniques were developed in this study for quantitatively assessing and predicting the performance of attitude control systems. Of particular importance is the ability of the synthesis to predict the fuel requirements of a satellite in carrying out specified maneuvering missions. Conversely given a satellite design with a specified fuel storage capacity, the synthesis can be used to determine what maneuvering missions are at least theoretically feasible.

In addition to its fuel predicting capability, the synthesis developed herein is capable of time synchronization of satellite maneuvers with the movement of other vehicles while simultaneously maintaining fuel optimality subject to the requirement of speed of response. In time synchronization of sequential operations the control policy is adaptive or self-calibrating. That is, feedback adapts the control policy to arrive at specified targets at specified times. This capability is particularly useful in situations where accurate apriori estimates of environmental disturbances are not possible to obtain.

Many of the capabilities of the control synthesis discussed in this report are new in the engineering art of 3-axis control of attitude maneuvers. It is strongly felt that the techniques developed point the way by which the design of attitude control hardware can be substantially improved. The results presented have been subjected to extensive experimentation in which the characteristics are standard hardware have been included. The conclusions strongly support the feasibility of the control strategy developed (or a slightly modified one) for implementation in a wide range of space vehicles.

Basic Problem Formulation

With respect to some specified orthonormal reference axis system let ϕ, ψ, θ denote the Euler angles of deviation of the principal axes of inertia of a single body satellite. Our reference axis is chosen such that the satellite will have the desired attitude when the deviation angles ϕ, ψ, and θ are zero. Let ξ be the vector whose components are ϕ, ψ, and θ. That is,

$$\xi = \begin{bmatrix} \phi \\ \psi \\ \theta \end{bmatrix} \cdot \tag{1}$$

Let $A(\xi)$ denote the matrix

$$\begin{bmatrix} 1 & 0 & \sin\psi \\ 0 & -\cos\phi & \sin\phi\cos\psi \\ 0 & \sin\phi & \cos\phi\cos\psi \end{bmatrix}, \tag{2}$$

and let

$$\omega = \begin{bmatrix} \omega_1 \\ \omega_2 \\ \omega_3 \end{bmatrix} \tag{3}$$

denote the angular velocity vector with components taken about the principal axes of inertia. We have the relationship

$$\omega = A(\xi)\dot{\xi}, \tag{4}$$

where $\dot{\xi}$ is the time derivative of the vector function ξ. The vector equation for angular velocity is

$$I\dot{\omega} + \omega \times I\omega = Bu + f(\xi,\omega,t) \tag{5}$$

where

$$I = \text{diag}\ [I_1,\ I_2,\ I_3]$$

is the moment of inertia matrix for the principal axis system, u is

the control torque vector, and B is a matrix representing the mis-

alignment of control torques with respect to the principal axis system.

$f(\xi,\omega,t)$ represents environmental disturbance torques affecting the rotating

of a satellite. In particular, f incorporates torques generated by solar

flux and variations in the gravitational field. f might also include dis-

turbances on attitude motion resulting from other processes going on in the

satellite.* The time dependency of f expresses itself primarily in the

solar torques, which are influenced by the position of the sun. The change

in these torques is small in the period encompassed by a slewing maneuver,

however, so we assume that f is time independent, this is even

more strongly indicated by the fact that these torques are very small compared

with the control torque. This leaves us with

$$f(\xi,\omega,t_o) = \begin{bmatrix} f_1(\xi,\omega,t_o) \\ f_2(\xi,\omega,t_o) \\ f_3(\xi,\omega,t_o) \end{bmatrix} = \begin{bmatrix} T_1 \\ T_2 \\ T_3 \end{bmatrix}$$

as the contribution of solar pressure and gravity gradient forces.

The control vector function

$$u = \begin{bmatrix} u_1 \\ u_2 \\ u_3 \end{bmatrix} \tag{6}$$

is subject to constraints $|u_1| \leq k_1$, $|u_2| \leq k_2$, and $|u_3| \leq k_3$,

---

*We shall not consider elastic effects here, but refer the interested reader to Part I.

where k_1, k_2, and k_3 are specified positive constants. For an arbitrary vector

$$V = \begin{bmatrix} v_1 \\ v_2 \\ v_3 \end{bmatrix}$$

let

$$\| v \| = \left(\sum_{i=1}^{3} v_i^2 \right)^{1/2}$$

As a practical design requirement the parameters k_i, $i = 1, 2, 3,$ are specified such that

$$k_i > \|(B - I)u\| + \|f(\xi,\omega)\| , \quad i=1, 2, 3 \qquad (7)$$

for all considered values of ξ, ω, and u. This requirement simply indicates that our means for exerting control torque dominates the disturbance torques it must counteract and that disturbance resulting from misalignment is not sufficient to disrupt this situation.

The basic objective in this study was to synthesize and carry out simulation experients with a control function u such that:

(a) Transfers of attitude position for a satellite take

place within physically imposed constraints and with

22

sufficient speed to be useful in a specified mission.

(b) The energy put into the system in making transfer is constrained so as not to endanger the stability of the system.

(c) The expenditure of fuel or power required in carrying out transfer is held to the minimum consistent with imposed constraints and other specified objectives such as speed of response.

These objectives are quantitatively measured by means of an appropriate performance criterion which can be adaptively changed through parametric variations. In accordance with the imposed performance criterion a feedback control function $V(\xi,\omega)$ is constructed such that when $V(\xi,\omega)$ is substituted in equation (4), the system

$$I_1\dot{\omega}_1 = (I_2 - I_3)\omega_2\omega_3 + b_{11}v_1 + b_{12}v_2 + b_{13}v_3 + T_1$$

$$I_2\dot{\omega}_2 = (I_3 - I_1)\omega_1\omega_3 + b_{21}v_1 + b_{22}v_2 + b_{23}v_3 + T_2$$

$$I_3\dot{\omega}_3 = (I_1 - I_2)\omega_1\omega_2 + b_{31}v_1 + b_{32}v_2 + b_{33}v_3 + T_3 \tag{8}$$

$$\dot{\phi} = \omega_1 - \tan\psi\sin\phi\omega_2 - \tan\psi\cos\phi\omega_3$$

$$\dot{\psi} = -\cos\phi\omega_2 + \sin\phi\omega_3$$

$$\dot{\theta} = \sec\psi\sin\phi\omega_2 + \sec\psi\cos\phi\omega_3$$

performs optimally with respect to above objectives and imposed constraints.

At an arbitrary but specified time t_0 we consider the system at an arbitrary state ξ_0, ω_0 and our general objective is to drive the system to the state $0,0$ at some time t_1 later. With the performance criterion used in control synthesis it is possible to impose a variety of control strategies. In particular, one strategy could be to effect the movement from ξ_0, ω_0 to $0,0$ with velocity components constrained in magnitude to be less than some specified constant and with the time of arrival on target specified to be no later than a specified time $t^* > t_0$ if possible. If it is not possible to arrive on target at or before time t^*, then the system would be required to arrive on target as quickly as possible. Within specified velocity and time constraints the system would be required to use a minimum of fuel. An alternative strategy would be to rigidly constrain velocity and fuel and minimize the time required to carry out the motion.

The control laws used throughout the report are selected on the basis of the following performance index

$$P = \int_{t_o}^{t_1} \left(\lambda_1 + \lambda_{12} \left(\frac{I_1 \omega_1}{k_1} \right)^2 + \lambda_{22} \left(\frac{I_2 \omega_2}{k_2} \right)^2 + \lambda_{32} \left(\frac{I_3 \omega_3}{k_3} \right)^2 \right.$$
$$\left. + \lambda_{13} \left(\frac{|u_1|}{k_1} \right) + \lambda_{23} \left(\frac{|u_2|}{k_2} \right) + \lambda_{33} \left(\frac{|u_3|}{k_3} \right) \right) dt \ .$$

For fixed t_o and free t_1, the objective of the control is to minimize P. The mathematics of this development is covered in Part II; here we only mention the type of control which is obtained.

The control settings called for by optimization are constrained

to $\qquad u_i = \{k_i, \ 0, \ -b_i, \ -k_i\} \ .$

(For definition of b_i in functional terms see page 74.) That is, control will not ever assume other values in the interval $[-k_i, \ k_i] \ .$

Ideally, a trajectory is controlled by a sequence of controls with only three changes of control setting.

For practical reasons this mode has been simplified so that controls called for are "bang-off-bang," that is

$$u_i = \{ k_i, \ 0, \ -k_i \}$$

and a trajectory ideally contains only two changes of setting.

The large number of parameters in the performance index gives this control computer a tremendous range of flexibility in applications. Some of these are described in the next section.

Control Capabilities

Under the constraints imposed, a variety of optimization schemes are feasible with the general synthesis developed. The fundamental formulation involves the specification of a time of arrival on a designated earth target (given in latitude and longitude) from an arbitrary initial angular position and rotational rate. Arrival on target is interpreted as assuming a desired attitude position with rotational rates exactly counteracting the effect of the earth's rotation. The control synthesis is such as to require the satellite to slew and arrive on target at the specified time and to carry out this maneuver with a minimum expenditure of fuel. The specified time of arrival will, in general, be a function of initial position, initial rates, target position, and constraint parameters. In particular, specified time of arrival can be set as the minimum time required for the maneuver subject to constraints imposed on thrust levels of control jets.

The control policy generally can be described as "bang-off-bang" which simply means that control thrusters are either on full or off at any given time during a maneuver. Strict mathematical optimality would, in general, also require a phase in which the control exactly counteracts the disturbance torques. However, it was determined that only a small loss of theoretical optimality would result from dropping this phase and substantial simplification would be achieved. Dropping the counteracting phase, therefore, may be correctly considered as a move in the direction of practical optimality.

It is, of course, impossible to graphically represent optimal trajectories in a six dimensional state space. However, a good indication of solution behavior may be obtained by superimposing three 2-dimensional projected trajectories on the same coordinate frame. In particular, if we plot ϕ, ψ, and θ against ω_1, ω_2, and ω_3 respectively, then typical superimposed projected trajectories are represented by Figure 1. The components u_1, u_2, and u_3 of the control vector u essentially control the (ϕ, ω_1)-projection, the (ψ, ω_2)-projection, and the (θ, ω_3)-projection respectively. The target state is placed at the origin of our state space and consequently at the origin of each projected subspace. Initial rates in the illustration are taken to be zero with respect to the target state and ϕ_0, ψ_0, and θ_0 represent initial angular positions. Optimal strategy is set so as to require arrival on target in minimum time.

For purposes of comparison in Figure 1, maximum control thrust in each projected plane is normalized to 1 with respect to a specified thrust to inertia ratio. With respect to this normalization the (ϕ, ω_1)-projected trajectory begins furtherest from target position. Note that for the (ϕ, ω_1)-trajectory full control thrust is first applied in the positive direction and then immediately applied in the negative direction. In common terminology the control with respect to this axis is "bang-bang." During the near horizontal portions of the (ψ, ω_2)-trajectory and the (θ, ω_3)-trajectory note that the control thrusters are off. That is, between applications of extreme positive and extreme negative control the vehicle with respect to motion in these projected planes is allowed to drift. In common terminology the control with respect to the (ψ, ω_2)-trajectory and the (θ, ω_3)-trajectory is "bang-off-bang."
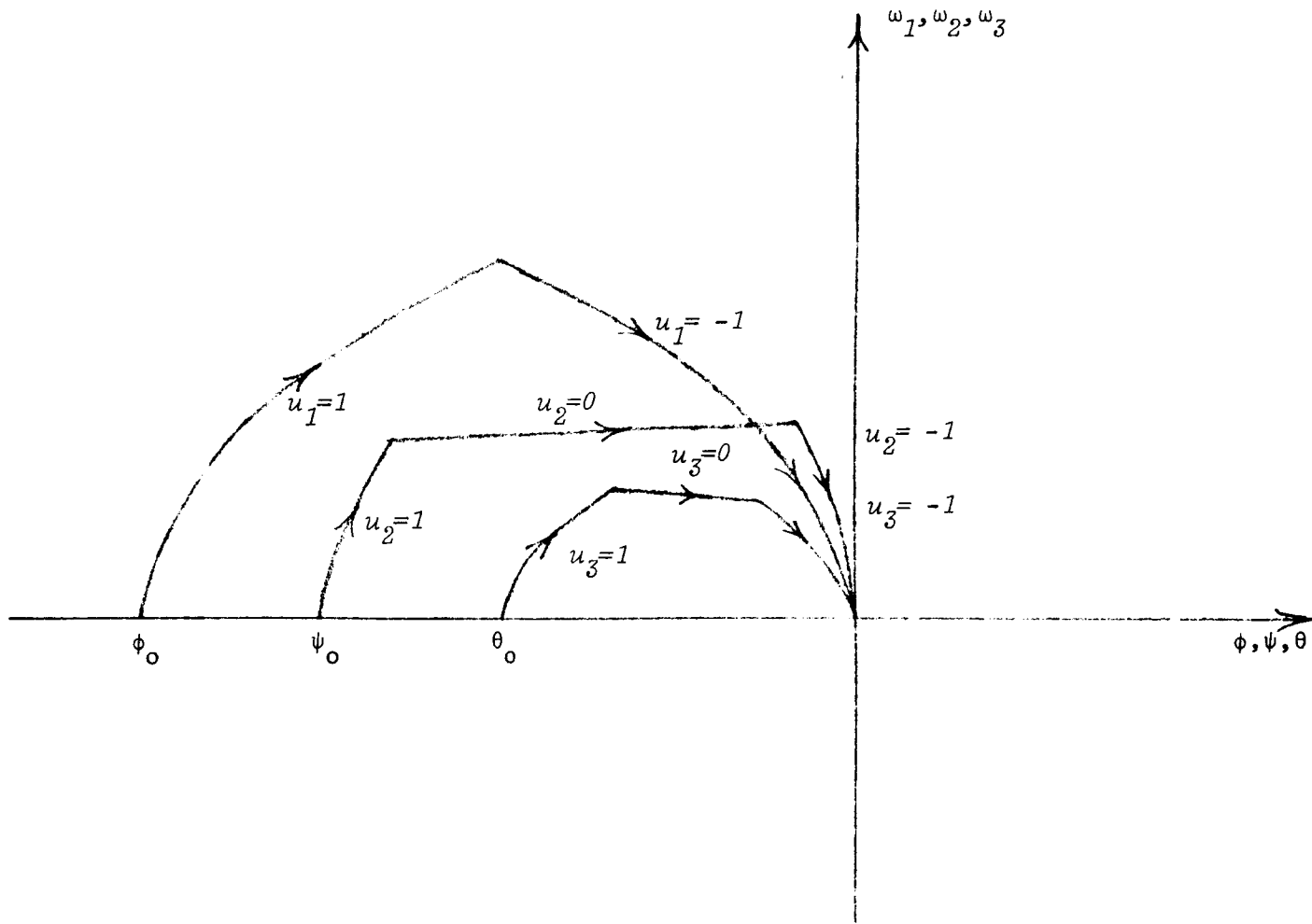
Figure 1

Figure 2 illustrates optimal projected trajectories when the
specified time of arrival on target is greater than minimum possible
time. Note that for the non-time optimal case a drift phase appears
in all three projected trajectories. Such drift phases in any parti-
cular formulation may be the result of the fuel consumption constraint
or the rate-limiting constraint which may be imposed to improve stability
and keep unacceptable elastic perturbations from developing. In both
Figure 1 and Figure 2 the slopes of projected trajectories during
drift phases are functions of the perturbations acting on the system.
If perturbations and inertial cross-coupling were not incorporated,
then the trajectories would be exactly horizontal during drift phases.
During phases of active control, the trajectory slopes are functions
of perturbations, cross-coupling, and the ratio of control thrusts
to inertial resistance.

A distinctive feature of the control strategy developed
herein is that regardless of the weighting factors assigned to the
various parameters involved in determining optimality, all projected
trajectories arrive on target simultaneously. If such time of arrival
synchronization is not present, then it can be shown that the
strategy can be improved and therefore is not optimal. The logic
involved in effecting this simultaneous time of arrival for the
projected trajectories is referred to as "time synchronization"
and it is the fundamental link between optimality for the three
projected trajectories separately and optimality for the total
system.
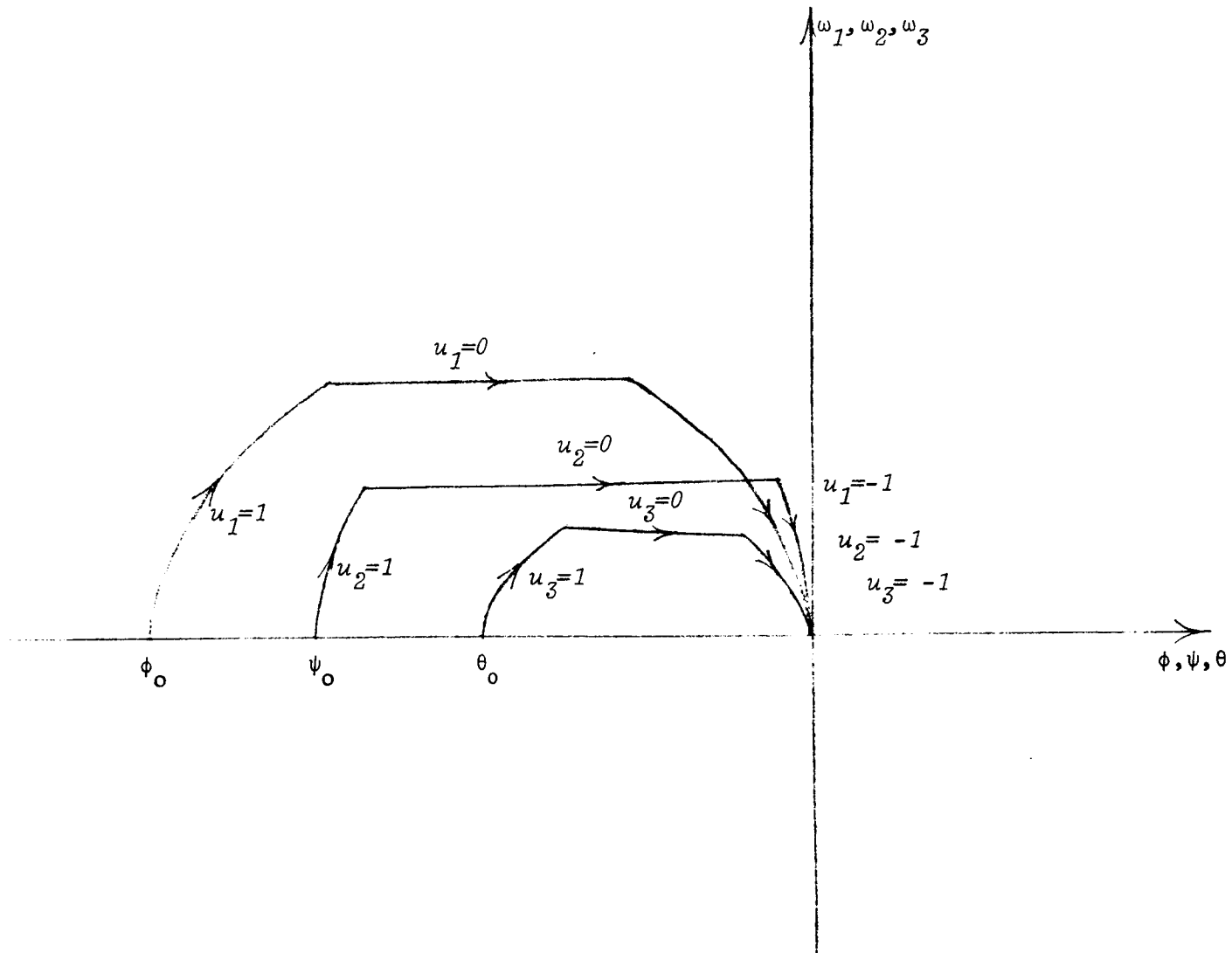
Figure 2

Other modes of optimization may be formulated where one may determine the "best" utilization of a specified fuel allocation with respect to carrying out a mission involving a series of attitude maneuvers. Since both time and fuel requirements are readily predictable through this synthesis, a highly significant logical design tool has been created. It is possible to apply mathematical (linear or nonlinear) programming techniques to carry out a large variety of projects of importance to NASA and other space oriented agencies. One immediate and obvious application could be the optimal programming of experiments carried out through the use of earth satellites and involving extensive attitude maneuvers. Optimal timed surveillance of a number of earth sites by a satellite or network of satellites is also feasible. Among the most exciting outcomes of this study are the implications of feasibility for tracking space vehicles with earth-oriented satellites. In particular, for Apollo and other manned flights such tracking would provide a capability for continuous uninterrupted surveillance and communication. In addition, improved accuracy in orbital data could result from the reduction of atmospheric interference. The synthesis developed could also be used to detect the need for, and to communicate adaptive corrections for improving performance during rendezvous and other more complicated mission maneuvers.

PART I

SATELLITE ATTITUDE KINEMATICS AND DYNAMICS

1. *Coordinate Systems.*

Given a synchronous, equatorial satellite, we wish to set up coordinate systems at the c. g. (center of gravity) of the satellite and at the center of the earth in order to describe the orientation of the satellite.

(a) The $\vec{s}_i$ system. The origin of the $\vec{s}_i$ system is at the c. g. of the satellite. Let $\vec{s}_2$ be a unit vector pointing to the center of the earth. Take $\vec{s}_3$ as a unit vector parallel to the axis of rotation of the earth and pointing northward. For a satellite in the plane of the equator, $\vec{s}_2$ and $\vec{s}_3$ are orthogonal. Choose $\vec{s}_1$ so that the system ($\vec{s}_1$, $\vec{s}_2$, $\vec{s}_3$) is a right-handed orthonormal system. (See Figure 1.1.) The $\vec{s}_i$ system is set up as a reference for the other coordinate systems.

(b) The $\vec{r}_i$ system. The origin of the $\vec{r}_i$ system is at the c. g. of the satellite. Let $\vec{r}_2$ be a unit vector pointing at a prescribed latitude and longitude on the surface of the earth. Choose $\vec{r}_3$ to be a unit vector orthogonal to $\vec{r}_2$ and lying in the plane containing $\vec{r}_2$ and $\vec{s}_3$. Choose the positive direction of $\vec{r}_3$ so as to make the smaller of the two possible angles with $\vec{s}_3$ (that is, $\vec{r}_3$ makes the smallest angle with $\vec{s}_3$ of any vector which is orthogonal to $\vec{r}_2$.). (See Figure 1.2.) Let $\vec{r}_1$ be chosen to give a right-handed orthonormal system. The $\vec{r}_i$ system is set up to determine the desired attitude of the satellite, that is, what direction ($\vec{r}_2$) the antenna should point for a prescribed latitude and longitude and within what cone (of $\vec{r}_3$) the sensors should point to locate certain stars.

(c) The $\vec{b}_i$ system. The $\vec{b}_i$ system is the same as the $\vec{r}_i$ system except for a rotation by a fixed angle ($-\gamma$) about the $\vec{r}_2$ axis.
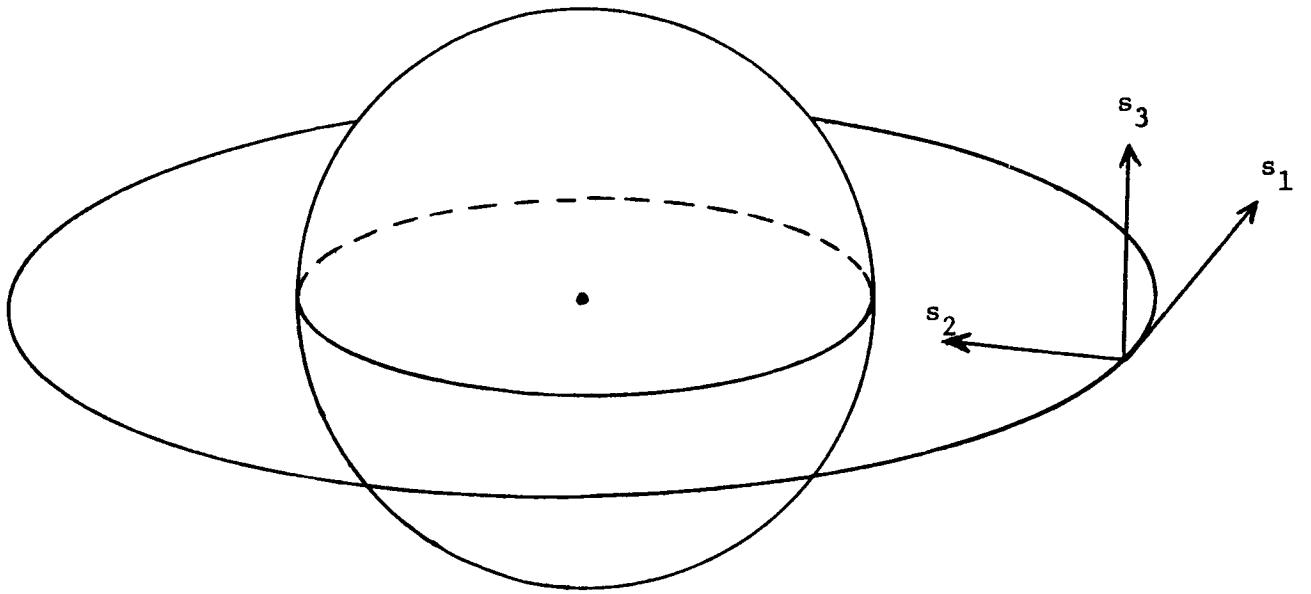
Figure 1.1
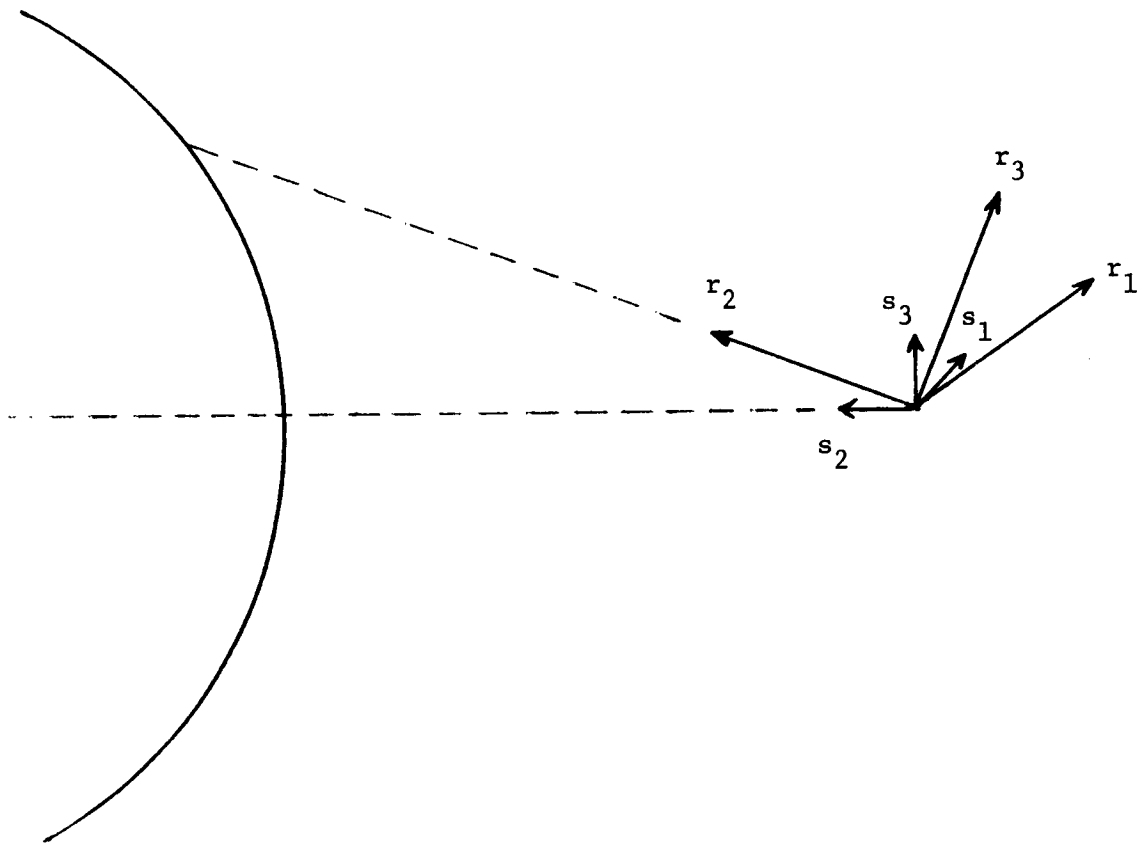
Figure 1.2

The $\vec{b}_i$ system is a body fixed system and is set up to describe the orientation of the satellite.

(d) The $\vec{p}_i$ system. The origin of the $\vec{p}_i$ system is at the c. g. of the satellite. The unit vectors $\vec{p}_i$ point along the principal axes for the moment of inertia. The $\vec{p}_i$ system is set up for use in the equations of motion of the satellite about its c. g.

(e) The $\vec{S}_i$ system. The $\vec{S}_i$ system is the same as the $\vec{s}_i$ system except for the origin of $\vec{S}_i$. That is, $(\vec{S}_1, \vec{S}_2, \vec{S}_3)$ are, respectively, parallel to $(\vec{s}_1, \vec{s}_2, \vec{s}_3)$, but the origin of the $\vec{S}_i$ system is at the center of the earth while the origin of the $\vec{s}_i$ system is at the c. g. of the satellite. The $\vec{S}_i$ system is set up to relate the $\vec{r}_2$ vector to latitude and longitude on the surface of the earth.

2. _Transformation From One Coordinate System To Another._

We are interested in obtaining an expression for the transformation or rotation $A_{bs}^{\leftarrow}$ from the $\vec{s}_i$ system to the $\vec{b}_i$ system. Such a rotation can be represented in matrix form in two different ways. First, the elements a_{ij} of $A_{bs}^{\leftarrow}$ can be written in terms of the scalar products $(\vec{b}_i \cdot \vec{s}_j)$ of unit vectors in the two systems. Secondly, $A_{bs}^{\leftarrow}$ can be written in terms of a set of Euler angles. Equating corresponding terms in the forms for $A_{bs}^{\leftarrow}$ will then enable us to solve for the Euler angles.

We will investigate in this section the scalar product form for $A_{bs}^{\leftarrow}$. In the next section, we will examine the Euler angles.

Let $\vec{\omega}$ be a fixed vector and resolve $\vec{\omega}$ into components in the $\vec{s}_i$ system:

$$\vec{\omega} = v_1\vec{s}_1 + v_2\vec{s}_2 + v_3\vec{s}_3 \quad . \tag{1.2.1}$$

Similarly, resolve $\vec{\omega}$ into components in the $\vec{b}_i$ system:

$$\vec{\omega} = u_1\vec{b}_1 + u_2\vec{b}_2 + u_3\vec{b}_3 \quad . \tag{1.2.2}$$

To obtain the relation between the two sets of components, we define the

matrix $A_{bs}^{\leftarrow}$ to satisfy:

$$\begin{pmatrix} u_1 \\ u_2 \\ u_3 \end{pmatrix}_b = A_{bs}^{\leftarrow} \begin{pmatrix} v_1 \\ v_2 \\ v_3 \end{pmatrix}_s \quad . \tag{1.2.3}$$

That is, $A_{bs}^{\leftarrow}$ is the matrix which transforms components in the $\vec{s}_i$ system

to components in the $\vec{b}_i$ system.

In element notation (1.2.3) can be written:

$$u_1 = a_{11}v_1 + a_{12}v_2 + a_{13}v_3 \tag{1.2.4}$$

$$u_2 = a_{21}v_1 + a_{22}v_2 + a_{23}v_3$$

$$u_3 = a_{31}v_1 + a_{32}v_2 + a_{33}v_3 \quad .$$

Equating (1.2.1) and (1.2.2):

$$u_1\vec{b}_1 + u_2\vec{b}_2 + u_3\vec{b}_3 = v_1\vec{s}_1 + v_2\vec{s}_2 + v_3\vec{s}_3 \quad . \tag{1.2.5}$$

Taking the scalar product of (1.2.5) with $\vec{b}_1$, we have:

$$u_1 = (\vec{b}_1 \cdot \vec{s}_1)v_1 + (\vec{b}_1 \cdot \vec{s}_2)v_2 + (\vec{b}_1 \cdot \vec{s}_3)v_3 \tag{1.2.6}$$

(for $\vec{b}_i$ an orthonormal system). Since the v_i are arbitrary, comparing

(1.2.4) and (1.2.6) gives:

$$a_{11} = (\vec{b}_1 \cdot \vec{s}_1), \ a_{12} = (\vec{b}_1 \cdot \vec{s}_2), \ a_{13} = (\vec{b}_1 \cdot \vec{s}_3) \quad . \tag{1.2.7}$$

In general, we have:

$$a_{ij} = (\vec{b}_i \cdot \vec{s}_j) \quad .$$

(1.2.8)

In a similar way, the inverse mapping $A_{sb}^{\leftarrow}$ from the $\vec{b}_i$ system

to the $\vec{s}_i$ system given by

$$\begin{pmatrix} v_1 \\ v_2 \\ v_3 \end{pmatrix}_s = A_{sb}^{\leftarrow} \begin{pmatrix} u_1 \\ u_2 \\ u_3 \end{pmatrix}_b$$

(1.2.9)

has elements $b_{ij} = (\vec{s}_i \cdot \vec{b}_j)$. Thus one transformation is the transpose

of the other. That is:

$$A_{sb}^{\leftarrow} = A_{bs}^{\rightarrow T} \quad \text{or} \quad A_{bs}^{\rightarrow -1} = A_{bs}^{\rightarrow T}$$

(1.2.10)

where $A_{bs}^{\rightarrow T}$ denotes the transpose and $A_{bs}^{\rightarrow -1}$ denotes the inverse of $A_{bs}^{\rightarrow}$. That

is, each matrix involved is an orthogonal matrix.

For $\vec{s}_i$ an orthornormal system, (1.2.4) may also be written as:

$$\vec{b}_1 = a_{11}\vec{s}_1 + a_{12}\vec{s}_2 + a_{13}\vec{s}_3$$

$$\vec{b}_2 = a_{21}\vec{s}_1 + a_{22}\vec{s}_2 + a_{23}\vec{s}_3$$

(1.2.11)

$$\vec{b}_3 = a_{31}\vec{s}_1 + a_{32}\vec{s}_2 + a_{33}\vec{s}_3 \quad .$$

To verify (1.2.11), take the scalar products with $\vec{s}_1$, $\vec{s}_2$, and $\vec{s}_3$, respectively,

and compare with (1.2.8). Therefore, one may obtain the elements a_{ij} from

(1.2.11) by expressing the $\vec{b}_i$ vectors in terms of the $\vec{s}_i$ system.

The transformation $A_{bs}^{\leftarrow}$ from $\vec{s}_i$ components to $\vec{b}_i$ components may

be considered as the product of two transformations; the first, from $\vec{s}_i$

37

$\vec{r}_i$; the second, from $\vec{r}_i$ to $\vec{b}_i$. In matrix notation this is:

$$A_{bs}^{\leftarrow} = A_{br}^{\leftarrow} A_{rs}^{\leftarrow} \quad . \tag{1.2.12}$$

The transformation $A_{br}^{\leftarrow}$ is simply a rotation through an angle $(-\gamma)$ with $\vec{r}_2$ fixed. Consequently, $A_{br}^{\leftarrow}$ may be written:

$$A_{br}^{\leftarrow} = \begin{pmatrix} \cos\gamma & 0 & \sin\gamma \\ 0 & 1 & 0 \\ -\sin\gamma & 0 & \cos\gamma \end{pmatrix} . \tag{1.2.13}$$

To find $A_{rs}^{\leftarrow}$, we will use the technique of (1.2.11) and write:

$$\vec{r}_1 = b_{11}\vec{s}_1 + b_{12}\vec{s}_2 + b_{13}\vec{s}_3$$

$$\vec{r}_2 = b_{21}\vec{s}_1 + b_{22}\vec{s}_2 + b_{23}\vec{s}_3 \tag{1.2.14}$$

$$\vec{r}_3 = b_{31}\vec{s}_1 + b_{32}\vec{s}_2 + b_{33}\vec{s}_3$$

where the b_{ij} in (1.2.14) are the elements of the matrix $A_{rs}^{\leftarrow}$.

First, we solve for the $\vec{r}_2$ vector (which points at a given initial latitude and longitude on the surface of the earth). Let $\vec{u}_S$ be a vector with components in the S_i system and terminating at the given latitude and longitude. We then have

$$\vec{u}_S = \begin{pmatrix} r_e \cos L \cos(\ell+270°) \\ r_e \cos L \sin(\ell+270°) \\ r_e \sin L \end{pmatrix}_S = \begin{pmatrix} r_e \cos L \sin \ell \\ -r_e \cos L \cos \ell \\ r_e \sin L \end{pmatrix}_S . \tag{1.2.15}$$

(See Figures 2.1 and 2.2.) In equation (1.2.15) r_e is the radius of the (spherical) earth, L is the given latitude (north positive), and ℓ is

38

Figure 2.1

S_3

u_s

L

S_2

$\ell + 270°$

$r_e \cos L$
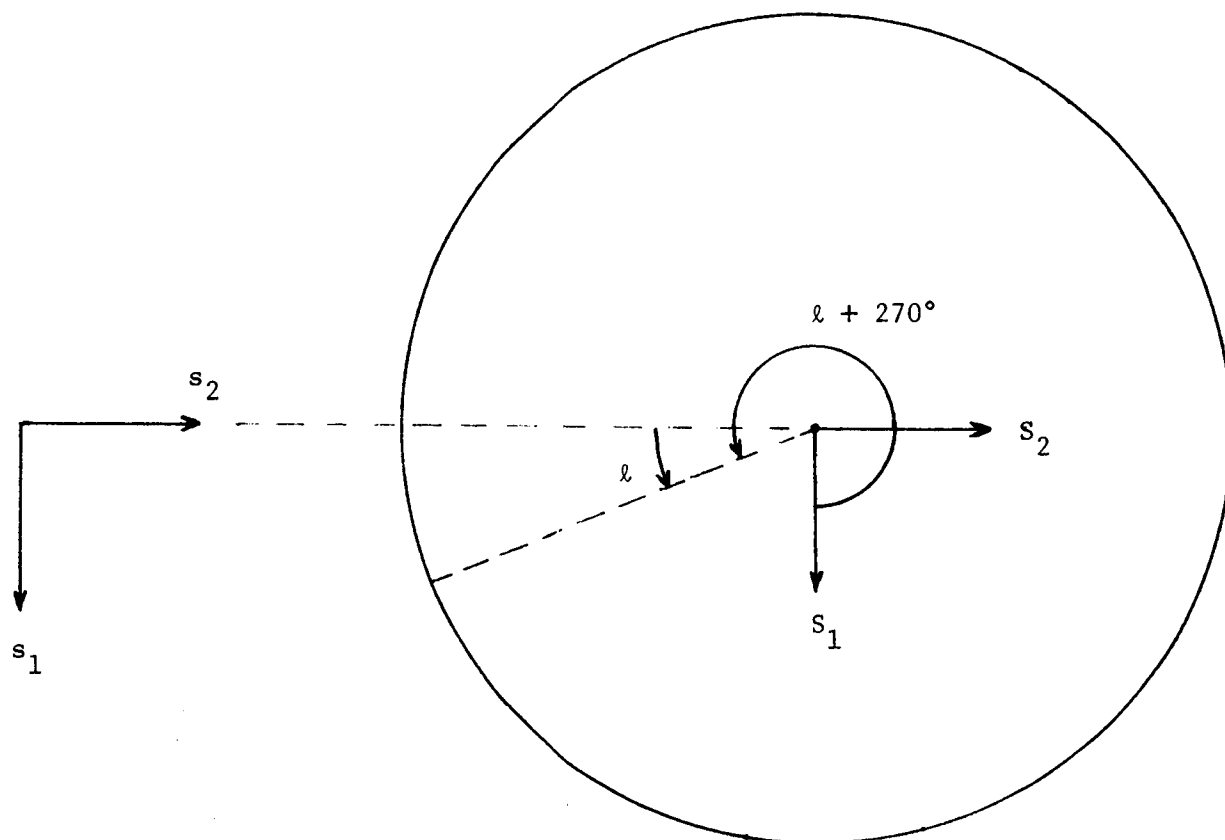
S_1
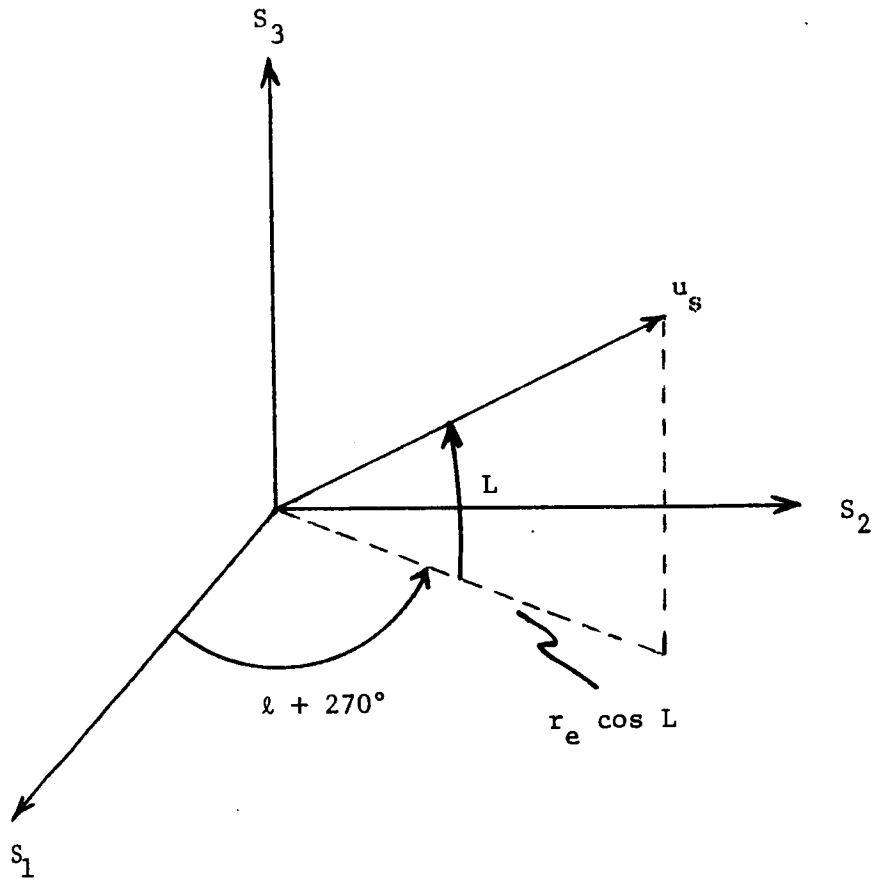
Figure 2.2

the given longitude minus the satellite longitude (longitude determined by a straight line from the satellite to the center of the earth). If the given longitude is east of the satellite, then ℓ is taken as positive.

To express $\vec{u}_S$ in the s_i system we need to perform a translation through a distance r_s (the distance of the satellite from the center of the earth).

Thus, we have:

$$\vec{u}_s = \vec{u}_S + r_s \vec{s}_2 \qquad (1.2.16)$$

or

$$\vec{u}_s = \begin{pmatrix} r_e \cos L \sin \ell \\ r_s - r_e \cos L \cos \ell \\ r_e \sin L \end{pmatrix}_s . \qquad (1.2.17)$$

We may now normalize $\vec{u}_s$ and set it equal to $\vec{r}_2$.

$$
\begin{aligned}
\vec{r}_2 = &\ \vec{s}_1 \ (\cos L \sin \ell)/\alpha_2 \\
&+ \vec{s}_2 \ (k - \cos L \cos \ell)/\alpha_2 \\
&+ \vec{s}_3 \ (\sin L)/\alpha_2
\end{aligned} \qquad (1.2.18)
$$

where $k \equiv r_s/r_e$ and the normalizing constant α_2 is:

$$
\begin{aligned}
\alpha_2 &\equiv \sqrt{(\cos L \sin \ell)^2 + (k - \cos L \cos \ell)^2 + (\sin L)^2} \\
&= \sqrt{1 + k^2 - 2 k \cos L \cos \ell}
\end{aligned} \qquad (1.2.19)
$$

We next solve for $\vec{r}_3$. From Figure 2.3, we have:

$$\alpha_3 \vec{r}_3 = \vec{s}_3 - (\vec{s}_3 \cdot \vec{r}_2) \vec{r}_2 \qquad (1.2.20)$$

where α_3 is the normalizing constant:

$$\alpha_3 = \sqrt{1 - (\vec{s}_3 \cdot \vec{r}_2)^2} \qquad . \qquad\qquad (1.2.21)$$
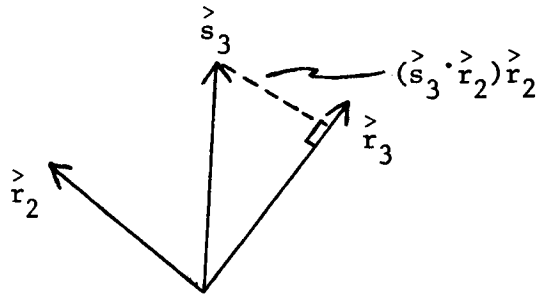
Figure 2.3

From (1.2.18):

$$(\vec{s}_3 \cdot \vec{r}_2) = \frac{\sin L}{\alpha_2} \qquad\qquad (1.2.22)$$

Consequently, from (1.2.21) and (1.2.22):

$$\alpha_3 = \sqrt{1 - \left(\frac{\sin L}{\alpha_2}\right)^2} = \frac{\sqrt{(\alpha_2)^2 - \sin^2 L}}{\alpha_2} \qquad\qquad (1.2.23)$$

and from (1.2.20), (1.2.22) and (1.2.18):

$$\alpha_3 \vec{r}_3 = \vec{s}_1 \left(\frac{-\sin L}{\alpha_2}\right) \left(\frac{\cos L \sin \ell}{\alpha_2}\right)$$
$$+ \vec{s}_2 \left(\frac{-\sin L}{\alpha_2}\right) \left(\frac{k - \cos L \cos \ell}{\alpha_2}\right) \qquad (1.2.24)$$
$$+ \vec{s}_3 \left(1 - \frac{\sin^2 L}{\alpha_2^2}\right) \qquad .$$

We may solve for $\vec{r}_1$ by noting that $\vec{r}_1$ is normal to $\vec{r}_2$ and $\vec{r}_3$ and, therefore, to $\vec{r}_2$ and $\vec{s}_3$. Thus

$$\alpha_1 \vec{r}_1 = (\alpha_2 \vec{r}_2) \times \vec{s}_3 \qquad\qquad (1.2.25)$$

or

$$\alpha_1 \vec{r}_1 = \vec{s}_1 \ (k - \cos L \cos \ell) \qquad (1.2.26)$$

$$- \vec{s}_2 \ (\cos L \sin \ell) \quad .$$

We also have:

$$\alpha_1 = \sqrt{(k - \cos L \cos \ell)^2 + (\cos L \sin \ell)^2} = \alpha_2 \alpha_3 \qquad (1.2.27)$$

or

$$\alpha_3 = \alpha_1 / \alpha_2 \quad . \qquad (1.2.28)$$

The matrix $A^{\leftarrow}_{rs} = (b_{ij})$ may now be written out using (1.2.14), (1.2.18), (1.2.24) and (1.2.26):

$$A^{\leftarrow}_{rs} = \begin{pmatrix} \dfrac{(k - \cos L \cos \ell)}{\alpha_1} & -\dfrac{\cos L \sin \ell}{\alpha_1} & 0 \\[3ex] \dfrac{\cos L \sin \ell}{\alpha_2} & \dfrac{(k - \cos L \cos \ell)}{\alpha_2} & \dfrac{\sin L}{\alpha_2} \\[3ex] \dfrac{-\sin L \cos L \sin \ell}{\alpha_1 \alpha_2} & \dfrac{(-\sin L)(k - \cos L \cos \ell)}{\alpha_1 \alpha_2} & \dfrac{\alpha_1}{\alpha_2} \end{pmatrix} \quad (1.2.29)$$

where α_3 has been eliminated from the third row.

Summarizing the α_i factors, we have:

$$\alpha_1 = \sqrt{(k - \cos L \cos \ell)^2 + (\cos L \sin \ell)^2} \qquad (1.2.30)$$

$$= \sqrt{\cos^2 L + k^2 - 2k \cos L \cos \ell}$$

$$\alpha_2 = \sqrt{(k - \cos L \cos \ell)^2 + (\cos L \sin \ell)^2 + (\sin L)^2} \qquad (1.2.31)$$

$$= \sqrt{(\alpha_1)^2 + \sin L)^2}$$

$$= \sqrt{1 + k^2 - 2k \cos L \cos \ell}$$

$$\alpha_3 = \alpha_1 / \alpha_2$$

The matrix $A_{bs} = (a_{ij})$ may also be written out using (1.2.12), (1.2.13) and (1.2.29).

$$a_{11} = \frac{\cos \gamma}{\alpha_1} (k - \cos L \cos \ell) - \frac{\sin \gamma}{\alpha_1 \alpha_2} \sin L \cos L \sin \ell \qquad (1.2.33a)$$

$$a_{12} = \frac{-\cos \gamma}{\alpha_1} \cos L \sin \ell - \frac{\sin \gamma}{\alpha_1 \alpha_2} \sin L (k - \cos L \cos \ell) \qquad (1.2.33b)$$

$$a_{13} = +(\sin \gamma) \frac{\alpha_1}{\alpha_2} \qquad (1.2.33c)$$

$$a_{21} = \frac{\cos L \sin \ell}{\alpha_2} \qquad (1.2.33d)$$

$$a_{22} = \frac{(k - \cos L \cos \ell)}{\alpha_2} \qquad (1.2.33e)$$

$$a_{23} = \frac{\sin L}{\alpha_2} \qquad (1.2.33f)$$

$$a_{31} = \frac{-\sin \gamma}{\alpha_1} (k - \cos L \cos \ell) - \frac{\cos \gamma}{\alpha_1 \alpha_2} \sin L \cos L \sin \ell \qquad (1.2.33g)$$

$$a_{32} = \frac{+\sin \gamma}{\alpha_1} \cos L \sin \ell - \frac{\cos \gamma}{\alpha_1 \alpha_2} \sin L (k - \cos L \cos \ell) \qquad (1.2.33h)$$

$$a_{33} = (\cos \gamma) \frac{\alpha_1}{\alpha_2} \qquad . \qquad (1.2.33i)$$

For uniformity of notation, we introduce the following matrix. The matrix whose elements are given by (1.2.33) depends upon three variables, the latitude L, the longitude ℓ and the angle of rotation γ. Let

$$B(L, \ell, \gamma) \equiv (a_{ij}) \qquad (1.2.34)$$

where the a_{ij} elements are given by (1.2.33). In this notation:

$$A_{bs} = B(L, \ell, \gamma) \qquad (1.2.35)$$

and

$$A_{rs} = B(L, \ell, 0) \qquad . \qquad (1.2.36)$$

3. *The Euler Angles.*

There are many different ways one could set up Euler angles
to define the orientation of a rigid body. We will describe in this
section a (ψ, θ, ϕ) system which corresponds to yaw, pitch and roll,
respectively, as if the satellite were an airplane flying along the
equator.

Suppose we wish to rotate the r_i system into the b_i system.
(See Figure 3.1.) First, we rotate about $\vec{r}_3$ through an angle θ. This
rotation has the matrix:

$$D = \begin{pmatrix} \cos\theta & \sin\theta & 0 \\ -\sin\theta & \cos\theta & 0 \\ 0 & 0 & 1 \end{pmatrix} . \qquad (1.3.1)$$

Secondly, we rotate about $\vec{r}_2'$ through an angle $(-\psi)$. This rotation has
the matrix

$$E = \begin{pmatrix} \cos\psi & 0 & \sin\psi \\ 0 & 1 & 0 \\ -\sin\psi & 0 & \cos\psi \end{pmatrix} . \qquad (1.3.2)$$
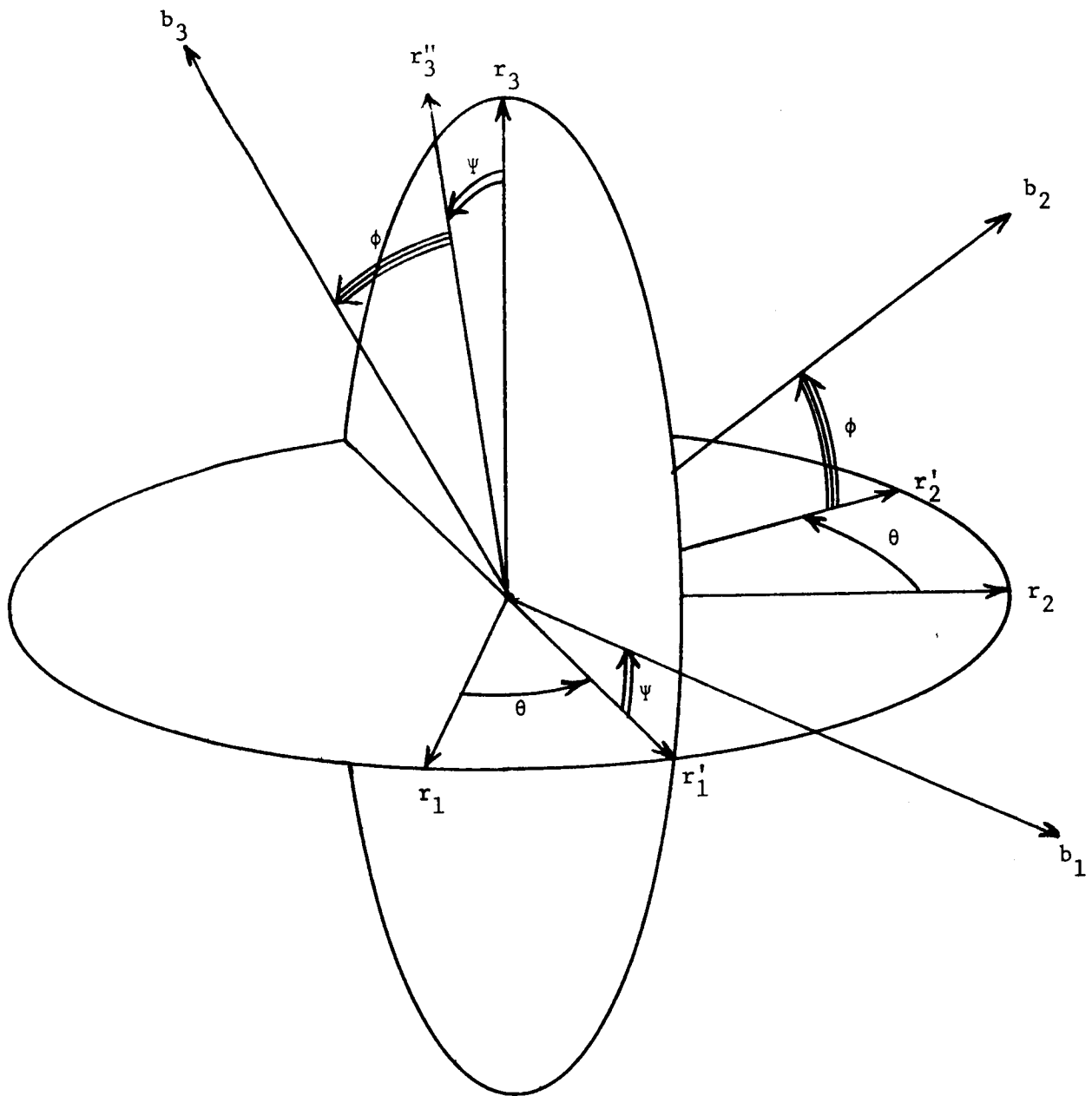
The Euler angles (θ, Ψ, ϕ) = (pitch, yaw, roll)

    a) θ rotated about $\vec{r}_3$.

    b) $(-\Psi)$ rotated about $\vec{r}_2'$.

    c) ϕ rotated about $\vec{b}_1$.

Figure 3.1

Finally, we rotate about $\vec{b}_1$ through an angle ϕ. This rotation has the matrix:

$$F = \begin{pmatrix} 1 & 0 & 0 \\ 0 & \cos\phi & \sin\phi \\ 0 & -\sin\phi & \cos\phi \end{pmatrix} \tag{1.3.3}$$

The elements C of the complete rotation may be obtained from the product of the successive rotations:

$$C = FED \quad . \tag{1.3.4}$$

We thus obtain:

$$C(\theta, \Psi, \theta) \equiv \begin{pmatrix} C\Psi C\theta & C\Psi S\theta & S\Psi \\ -S\phi S\Psi C\theta - C\phi S\theta & -S\phi S\Psi S\theta + C\phi C\theta & S\phi C\Psi \\ -C\phi S\Psi C\theta + S\phi S\theta & -C\phi S\Psi S\theta - S\phi C\theta & C\phi C\Psi \end{pmatrix} \tag{1.3.5}$$

where $C\Psi$ denotes $\cos\Psi$, $S\theta$ denotes $\sin\theta$, etc.

The rotation matrix C as defined in equation (1.3.5) can be used represent the rotation of any orthonormal coordinate system into any other orthonormal coordinate system if the appropriate angles (θ, Ψ, ϕ) are used. Thus $A^{\leftarrow}_{pq} = C(\theta_{pq}, \Psi_{pq}, \phi_{pq})$ indicates the rotation from the q_i system _into_ the p_i system. The angles indicated in Figure 3.1 are θ_{br}, Ψ_{br}, ϕ_{br}, and we have $A^{\leftarrow}_{br} = C(\theta_{br}, \Psi_{br}, \phi_{br})$. To indicate the rotation from the s_i system to the b_i system, we introduce the notation θ_{bs}, Ψ_{bs}, and ϕ_{bs} for those angles. Thus, the transformation $A^{\leftarrow}_{bs}$ of the previous section can be represented as:

$$A^{\leftarrow}_{bs} = C(\theta_{bs}, \Psi_{bs}, \phi_{bs}) \quad . \tag{1.3.6}$$

There are other representations for $A^{\leftarrow}_{bs}$. For example we can calculate the angles θ_{sb}, Ψ_{sb} and ϕ_{sb} for the rotation of the b_i system

into the s_i system. The last transformation is the inverse of the first, that is:

$$C(\theta_{bs}, \Psi_{bs}, \phi_{bs}) = C^{-1}(\theta_{sb}, \Psi_{sb}, \phi_{sb}) \qquad (1.3.7)$$

(although the two sets of angles are not simply related). However, each A and C matrix is an orthogonal matrix, and its inverse is equal to its transpose (compare equation (1.2.10)). Thus:

$$C^{-1}(\theta_{sb}, \Psi_{sb}, \phi_{sb}) = C^{T}(\theta_{sb}, \Psi_{sb}, \phi_{sb}) \qquad (1.3.8)$$

and from (1.3.3), (1.3.4) and (1.3.5):

$$A_{bs}^{\leftarrow} = C^{T}(\theta_{sb}, \Psi_{sb}, \phi_{sb}) \qquad (1.3.9)$$

is a second representation for $A_{bs}^{\leftarrow}$. Other representations are possible for writing $A_{bs}^{\leftarrow}$ as a product (compare equation (1.2.12)) and writing each factor in various forms.

We now wish to introduce two sets of latitude and longitude, the initial latitude and longitude denoted by (L_I, ℓ_I) and the terminal or target latitude and longitude denoted by (L_T, ℓ_T). For each set of latitude and longitude there will be an r_i and a b_i coordinate system. We will use the notation R_i and B_i for the r_i and b_i systems corresponding to the target latitude and longitude. The notation of r_i and b_i we now will associate with the initial latitude and longitude. Our primary interest is in finding the transformation $A_{Rb}^{\leftarrow}$ which takes the b_i system corresponding to the initial latitude into the R_i system corresponding to the target latitude.

The transformation $A_{Rb}^{\leftarrow}$ satisfies several different relations:

$$(\vec{u})_R = A_{Rb}^{\leftarrow}(\vec{u})_b \qquad (1.3.10)$$

$$A_{Rb}^{\leftarrow} = A_{Rs}^{\leftarrow} A_{sb}^{\leftarrow} \qquad (1.3.11)$$

$$A_{Rb}^{\leftarrow} = C(\theta_{Rb},\ \Psi_{Rb},\ \phi_{Rb}) \qquad (1.3.12)$$

$$A_{Rb}^{\leftarrow} = C^{T}(\theta_{bR},\ \Psi_{bR},\ \phi_{bR}) \qquad . \qquad (1.3.13)$$

Equation (1.3.10) is the defining equation for $A_{Rb}^{\leftarrow}$. Equation (1.3.11) follows

from considering $A_{Rb}^{\leftarrow}$ as the succession of the rotation $A_{sb}^{\leftarrow}$ and the rotation

$A_{Rs}^{\leftarrow}$. Equation (1.3.12) follows from the definition of the matrix C and

the Euler angles θ_{Rb}, Ψ_{Rb}, ϕ_{Rb}. Equation (1.3.13) follows from the Euler

angles θ_{bR}, Ψ_{bR}, ϕ_{bR} in rotating from R_i system to the b_i system (compare

equation (1.3.9)).

Similarly, the transformation $A_{sb}^{\leftarrow}$ used in (1.3.11) satisfies:

$$(\vec{u})_{s} = A_{sb}^{\leftarrow} (\vec{u})_{b} \qquad (1.3.14)$$

$$A_{sb}^{\leftarrow} = B^{T}(L_{I},\ \ell_{I},\ \gamma_{I}) \qquad (1.3.15)$$

$$A_{sb}^{\leftarrow} = C(\theta_{sb},\ \Psi_{sb},\ \phi_{sb}) \qquad (1.3.16)$$

$$A_{sb}^{\leftarrow} = C^{T}(\theta_{bs},\ \Psi_{bs},\ \phi_{bs}) \qquad , \qquad (1.3.17)$$

and $A_{Rs}^{\leftarrow}$ satisfies:

$$(\vec{u})_{R} = A_{Rs}^{\leftarrow} (\vec{u})_{s} \qquad (1.3.18)$$

$$A_{Rs}^{\leftarrow} = B(L_{T},\ \ell_{T},\ 0) \qquad (1.3.19)$$

$$A_{Rs}^{\leftarrow} = C(\theta_{Rs},\ 0,\ \phi_{Rs}) \qquad (1.3.20)$$

$$A_{Rs}^{\leftarrow} = C^{T}(\theta_{sR},\ \Psi_{sR},\ \phi_{sR}) \qquad . \qquad (1.3.21)$$

The angle $\Psi_{Rs} = 0$ follows from noting that equation (1.3.19) is the

same as (1.2.29) (with the use of L_T and ℓ_T), and comparing (1.2.29) with

equation (1.3.5) (with the Rs subscripts).

We wish to use equation (1.3.11) to solve for the Euler angles θ_{bR}, Ψ_{bR}, ϕ_{bR}. Substituting (1.3.13), (1.3.17) and (1.3.20) into (1.3.11), we have:

$$C^T(\theta_{bR},\ \Psi_{bR},\ \phi_{bR}) = C(\theta_{Rs},\ 0,\ \phi_{Rs})C^T(\theta_{bs},\ \Psi_{bs},\ \phi_{bs}), \qquad (1.3.22)$$

or taking the transpose of both sides:

$$C(\theta_{bR},\ \Psi_{bR},\ \phi_{bR}) = C(\theta_{bs},\ \Psi_{bs},\ \phi_{bs})C^T(\theta_{Rs},\ 0,\ \psi_{Rs}) \quad . \qquad (1.3.23)$$

One may express the matrix equation (3.23) in element form in the following way. The Euler angles θ_{bs}, Ψ_{bs}, ϕ_{bs} may be obtained from equating matrix elements in equations (1.3.17) and (1.3.15) using the definition of the matrix B ((1.2.33) and (1.2.34)) and the matrix C (equation (1.3.5)). We thus obtain for Ψ_{bs}, θ_{bs} and ϕ_{bs}, (where I denotes initial conditions)

$$\sin \Psi_{bs} = (\sin \gamma_I)\ \frac{\alpha_1^I}{\alpha_2^I} = a_{13} \qquad (1.3.24a)$$

$$\sin \phi_{bs} \cos \Psi_{bs} = \frac{\sin L_I}{\alpha_2^I} = a_{23} \qquad (1.3.24b)$$

$$\sin \theta_{bs} \cos \Psi_{bs} = \frac{-\cos \gamma_I}{\alpha_1^I} \cos L_I \sin \ell_I - \frac{\sin \gamma_I}{\alpha_1^I \alpha_2^I} \sin L_I(k - \cos L_I \cos \ell_I)$$

$$(1.3.24c)$$

Alternatively, we have:

$$\tan \phi_{bs} = \frac{\sin L_I}{\cos \gamma_I}\ \frac{1}{\alpha_1^I} = \frac{a_{23}}{a_{33}} \qquad (1.3.25a)$$

$$\tan \theta_{bs} = \frac{\cos \gamma_I \cos L_I \sin \ell_I - \sin \gamma_I \sin L_I(k - \cos L_I \cos \ell_I)}{\cos \gamma_I (k - \cos L_I \cos \ell_I) - \sin \gamma_I \sin L_I(\cos L_I \sin \ell_I)}$$

$$= a_{12}/a_{11}\ , \qquad (1.3.25b)$$

or:

$$\cos \phi_{bs} \cos \Psi_{bs} = \cos \gamma_I \frac{\alpha_1^I}{\alpha_2^I} = a_{33} \tag{1.3.26a}$$

$$\cos \theta_{bs} \cos \Psi_{bs} = \frac{\cos \gamma_I}{\alpha_1^I} (k - \cos L_I \cos \ell_I) - \frac{\sin \gamma_I}{\alpha_1^I \alpha_2^I} \sin L_I \cos L_I \sin \ell_I$$

$$= a_{11} \quad . \tag{1.3.26b}$$

The Euler angles θ_{Rs}, ϕ_{Rs} and Ψ_{Rs} are determined similarly from equation (1.3.19) and (1.3.20):

$$\Psi_{Rs} = 0 \quad . \tag{1.3.27a}$$

$$\sin \phi_{Rs} = \frac{\sin L_T}{\alpha_2^T} \tag{1.3.27b}$$

$$\sin \theta_{Rs} = \frac{-\cos L_T \sin \ell_T}{\alpha_1^T} \quad . \tag{1.3.27c}$$

These equations are actually of the same form as (1.3.24) with T (T denoting target conditions) replacing I and γ set to zero. Alternatively, we have:

$$\tan \phi_{Rs} = \frac{\sin L_T}{\alpha_1^T} \tag{1.3.28a}$$

$$\tan \theta_{Rs} = \frac{-\cos L_T \sin \ell_T}{(k - \cos L_T \cos \ell_T)} , \tag{1.3.28b}$$

or:

$$\cos \phi_{Rs} = \frac{\alpha_1^T}{\alpha_2^T} \tag{1.3.29a}$$

$$\cos \theta_{Rs} = \frac{(k - \cos L_T \cos \ell_T)}{\alpha_1^T} \tag{1.3.29b}$$

Finally, direct matrix multiplication of the right hand side of (1.3.23) and equating matrix elements gives us:

$$\sin \Psi_{bR} = \sin \phi_{Rs} \cos \Psi_{bs} \sin (\theta_{Rs} - \theta_{bs}) \tag{1.3.30a}$$

$$+ \cos \phi_{Rs} \sin \Psi_{bs}$$

$$\sin \theta_{bR} \cos \Psi_{bR} = \sin \phi_{Rs} \sin \Psi_{bs} + \cos \phi_{Rs} \cos \Psi_{bs} \sin(\theta_{bs} - \theta_{Rs})$$
$$\tag{1.3.30b}$$

$$\sin \phi_{bR} \cos \Psi_{bR} = - \sin \phi_{Rs} \cos \phi_{bs} \cos(\theta_{Rs} - \theta_{bs})$$

$$- \sin \phi_{Rs} \sin \phi_{bs} \sin \Psi_{bs} \sin(\theta_{Rs} - \theta_{bs})$$

$$+ \cos \phi_{Rs} \sin \phi_{bs} \cos \Psi_{bs} \tag{1.3.30c}$$

The angles θ_{bR}, Ψ_{bR}, ϕ_{bR} may be written directly in terms of (L_I, ℓ_I) and (L_T, ℓ_T) by substituting into equation (1.3.30) using equations (1.3.24) through (1.3.29). The same result may also be obtained by substituting equations (1.3.15) and (1.3.19) and (1.3.11) and equating matrix elements.

Another problem which may arise in these equations is the ground track problem, a type of inverse problem. For given Euler angles ϕ_{bR}, Ψ_{bR}, θ_{bR}, what direction is the satellite pointing? That is, for a fixed set (L_T, ℓ_T) how do the values of L_I, ℓ_I and γ_I vary as ϕ_{bR}, Ψ_{bR} and θ_{bR} vary? Rewriting the right hand side of (1.3.23) using (1.3.15) and (1.3.17) we have:

$$C(\theta_{bR}, \Psi_{bR}, \phi_{bR}) = B(L_I, \ell_I, \gamma_I) C^T(\theta_{Rs}, 0, \phi_{Rs}) \tag{1.3.31}$$

or:

$$B(L_I, \ell_I, \gamma_I) = C(\theta_{bR}, \Psi_{bR}, \phi_{bR}) C(\theta_{Rs}, 0, \phi_{Rs}) \tag{1.3.32}$$

(using the fact that $C^T = C^{-1}$ for the orthogonal matrix C). The right hand side of (1.3.32) is known since the θ_{bR}, Ψ_{bR}, ϕ_{bR} are now prescribed and θ_{Rs} and ϕ_{Rs} are determined by (L_T, ℓ_T) (equations (1.3.27), (1.3.28) and (1.3.29)). See Appendix A for the expression of the matrix equation (1.3.32) in element form.

One notes a difference in the use of equations (1.3.24) through (1.3.30) in the computer simulation runs and actual satellite operation. In actual operation, sensors in the satellite will be used to determine ϕ_{bs}, Ψ_{bs} and θ_{bs}. In simulation runs, the angles ϕ_{bs}, Ψ_{bs} and θ_{bs} are determined by equations (1.3.24) (or by an analog computer).

4. *Angular Velocities*

The angular velocities determined by the satellite sensors are the values $\dot{\phi}_{bs}$, $\dot{\psi}_{bs}$ and $\dot{\theta}_{bs}$, the rates of change with respect to time in the Euler angles between the b_i and s_i systems. However, the angular velocities used in the equations of motion (next section) are expressed about the b_i (or p_i) coordinate axes. It is thus necessary to obtain the transformation between these two representations of the angular velocity.

Let $\vec{\omega}$ be the angular velocity of the body (or b_i system) with respect to the s_i system. The angular velocities $\dot{\phi}_{bs}$, $(-\dot{\psi}_{bs})$ and $\dot{\theta}_{bs}$ may be considered as the components of $\vec{\omega}$ expressed in the non-orthogonal coordinate system $(\vec{s}_3, \vec{s}_2', \vec{b}_1)$ (see Figure 3.1 with r_i replaced by s_i). That is, we may write

$$\vec{\omega} = \dot{\theta}_{bs} \, \vec{s}_3 + (-\dot{\psi}_{bs}) \vec{s}_2' + \dot{\phi}_{bs} \, \vec{b}_1 \tag{1.4.1}$$

We wish to express the vector $\vec{\omega}$ in (1.4.1) in terms of the b_i system.

The terms on the right hand side of (1.4.1) may be transformed individually. Expressing the first term in the b_i system, we have

$$(\dot{\theta}_{bs} \, \vec{s}_3)_b = A^{\leftarrow}_{bs} (\dot{\theta}_{bs} \, \vec{s}_3)_s \tag{1.4.2}$$

or

$$(\dot{\theta}_{bs} \, \vec{s}_3)_b = C(\theta_{bs}, \psi_{bs}, \phi_{bs}) \cdot \begin{pmatrix} 0 \\ 0 \\ \dot{\theta}_{bs} \end{pmatrix}_s , \tag{1.4.3}$$

The expression used in (1.4.3) for $A^{\leftarrow}_{bs}$ was previously obtained in section 3 (equation (1.3.6)) and corresponds to a rotation through the three angles θ_{bs}, ψ_{bs}, ϕ_{bs}. Note that (1.4.3) could be altered (and still give the correct results) to:

$$(\dot{\theta}_{bs} \; \vec{s}_3)_b = C_3(\theta_{bs}, \; \Psi_{bs}, \; \phi_{bs}) \begin{pmatrix} 0 \\ 0 \\ \dot{\theta}_{bs} \end{pmatrix}_s \quad , \tag{1.4.4}$$

where C_3 is a matrix identical to C in the third column and arbitrary in the first and second columns. Equation (1.4.4) is possible because of the zeros occuring in the vector representation of $\dot{\theta}_{bs} \; \vec{s}_3$ in the s_i system.

The second term on the right hand side of (1.4.1) may be written:

$$(-\dot{\Psi}_{bs} \; \vec{s}_2')_b = A_{bs}^{\leftarrow}(-\dot{\Psi}_{bs} \; \vec{s}_2')_{s'} \tag{1.4.5}$$

or

$$(\dot{\Psi}_{bs} \; \vec{s}_2')_b = C(0, \; \Psi_{bs}, \; \phi_{bs}) \begin{pmatrix} 0 \\ -\dot{\Psi}_{bs} \\ 0 \end{pmatrix}_{s'} \quad . \tag{1.4.6}$$

The expression used in (1.4.6) for $A_{bs}^{\leftarrow}$, may be obtained by noting that the s_i' system goes into the b_i system by means of a rotation through the two angles Ψ_{bs}, ϕ_{bs} ($\theta_{bs} = 0$ for this case). In analogy with (1.4.4), we may rewrite (1.4.6) as:

$$(\dot{\Psi}_{bs} \; s_2')_b = C_2(0, \; \Psi_{bs}, \; \phi_{bs}) \begin{pmatrix} 0 \\ -\dot{\Psi}_{bs} \\ 0 \end{pmatrix}_{s'} \quad , \tag{1.4.7}$$

where C_2 is a matrix identical with C in the second column and arbitrary otherwise.

The third term on the right hand side of (1.4.1) is already expressed in the b_i system. However, for purposes of comparison, we may write:

$$(\dot{\phi}_{bs} \; \vec{b}_1)_b = C(0, \; 0, \; 0) \begin{pmatrix} \dot{\phi}_{bs} \\ 0 \\ 0 \end{pmatrix}_b \tag{1.4.8}$$

or

$$(\phi_{bs} \, \vec{b}_1)_b = C_1(0, 0, 0) \begin{pmatrix} \dot\phi_{bs} \\ 0 \\ 0 \end{pmatrix}_b \quad , \tag{1.4.9}$$

where C_1 is a matrix identical to C in the first column but arbitrary otherwise.

Using (1.4.4), (1.4.6) and (1.4.7) to rewrite (1.4.1) we have:

$$(\vec\omega)_b = C_3(\theta_{bs}, \Psi_{bs}, \phi_{bs}) \begin{pmatrix} 0 \\ 0 \\ \dot\theta_{bs} \end{pmatrix}_s \tag{1.4.10}$$

$$+ C_2(0, \Psi_{bs}, \phi_{bs}) \begin{pmatrix} 0 \\ -\dot\Psi_{bs} \\ 0 \end{pmatrix}_{s'} \quad .$$

$$+ C_1(0, 0, 0) \begin{pmatrix} \dot\phi_{bs} \\ 0 \\ 0 \end{pmatrix}_b \quad .$$

Making the three matrices in (1.4.10) equal, we may rewrite (1.4.10) as:

$$(\vec\omega)_b = D(\Psi_{bs}, \phi_{bs}) \begin{pmatrix} \dot\phi_{bs} \\ \dot\Psi_{bs} \\ \dot\theta_{bs} \end{pmatrix} \tag{1.4.11}$$

where D is a matrix which agrees with $C(\theta_{bs}, \Psi_{bs}, \phi_{bs})$ in the third column (θ_{bs} does not actually appear in the third column), agrees with $-C(0, \Psi_{bs}, \phi_{bs})$ in the second column, and agrees with $C(0, 0, 0)$ in the first column. Since θ_{bs} does not explicitly appear, D is a function of only two angles Ψ_{bs} and ϕ_{bs}.

The matrix $D(\Psi, \phi)$ may be written in full as:

$$D(\Psi, \phi) = \begin{bmatrix} 1 & 0 & \sin\Psi \\ 0 & -\cos\phi & \sin\phi\cos\Psi \\ 0 & +\sin\phi & \cos\phi\cos\Psi \end{bmatrix} \tag{1.4.12}$$

One may also obtain the equation:

$$(\vec{\omega})_b = D(\Psi_{bR}, \phi_{bR}) \begin{pmatrix} \dot{\phi}_{bR} \\ \dot{\Psi}_{bR} \\ \dot{\theta}_{bR} \end{pmatrix} \qquad (1.4.13)$$

in a similar manner.

The inverse of (1.4.11) or (1.4.13) may be obtained if $D(\Psi,\phi)$ is not singular. The determinant of $D(\Psi,\phi)$ is equal to $-\cos\Psi$. Thus, we may rewrite (1.4.13) as:

$$\begin{pmatrix} \dot{\phi}_{bR} \\ \dot{\Psi}_{bR} \\ \dot{\theta}_{bR} \end{pmatrix} = D^{-1}(\Psi_{bR}, \phi_{bR})\,(\vec{\omega})_b \qquad (1.4.14)$$

if $\cos\Psi_{bR} \neq 0$. We have explicitly that:

$$D^{-1}(\Psi,\phi) = \begin{pmatrix} 1 & -\tan\Psi\sin\phi & -\tan\Psi\cos\phi \\ 0 & -\cos\phi & \sin\phi \\ 0 & \sec\Psi\sin\phi & \sec\Psi\cos\phi \end{pmatrix} \qquad (1.4.15)$$

If we linearize the D and D^{-1} matrices (for Ψ small and ϕ small), we obtain:

$$D^L(\Psi,\phi) = \begin{pmatrix} 1 & 0 & \Psi \\ 0 & -1 & \phi \\ 0 & \phi & 1 \end{pmatrix} \qquad (1.4.16)$$

and

$$[D^{-1}(\Psi,\phi)]^L = \begin{pmatrix} 1 & 0 & -\Psi \\ 0 & -1 & \phi \\ 0 & \phi & 1 \end{pmatrix} . \qquad (1.4.17)$$

5. *Equations of Motion*

By Newton's second law as applied to angular momentum, we have:

$$\left(\frac{d\vec{h}}{dt}\right)_{inert} = \vec{n}(t) \tag{1.5.1}$$

where $\vec{h} = \vec{h}(t)$ is the angular momentum of the body, $\vec{n}(t)$ is the total applied torque about the center of mass and $\left(\frac{d}{dt}\right)_{inert}$ denotes the time derivative of a function taken in an inertial coordinate system.

We wish to express (1.5.1) relative to a rotating coordinate system, in particular, one fixed relative to the body. Let $\vec{G}(t)$ be any arbitrary vector depending on time. The change $\vec{dG}$ for a small change in time dt will differ when viewed in the inertial system as compared to the change viewed in the body system. The difference is due to the rotation of the body axes, and we can write:

$$(d\vec{G})body = (d\vec{G})inert + (d\vec{G})rotat \tag{1.5.2}$$

where $(d\vec{G})$ rotat arises solely from the rotation.

The change due solely to rotation may be written as:

$$(d\vec{G})rotat = \vec{G} \times d\vec{\lambda} \tag{1.5.3}$$

(see Figure 5.1). Then (1.5.2) becomes:

$$(d\vec{G})_{body} = (d\vec{G})_{inert} + \vec{G} \times d\vec{\lambda}. \tag{1.5.4}$$

Dividing by the differential time element dt, we have:

$$\left(\frac{d\vec{G}}{dt}\right)_{body} = \left(\frac{d\vec{G}}{dt}\right)_{inert} + \vec{G} \times \vec{\omega} , \tag{1.5.5}$$

where $\vec{W} = \frac{d}{dt}\vec{\lambda}$ is the angular velocity of the body. Equation (1.5.5) may also be written as:

$$\left(\frac{d\vec{G}}{dt}\right)_{inert} = \left(\frac{d\vec{G}}{dt}\right)_{body} + \vec{\omega} \times \vec{G} . \tag{1.5.6}$$
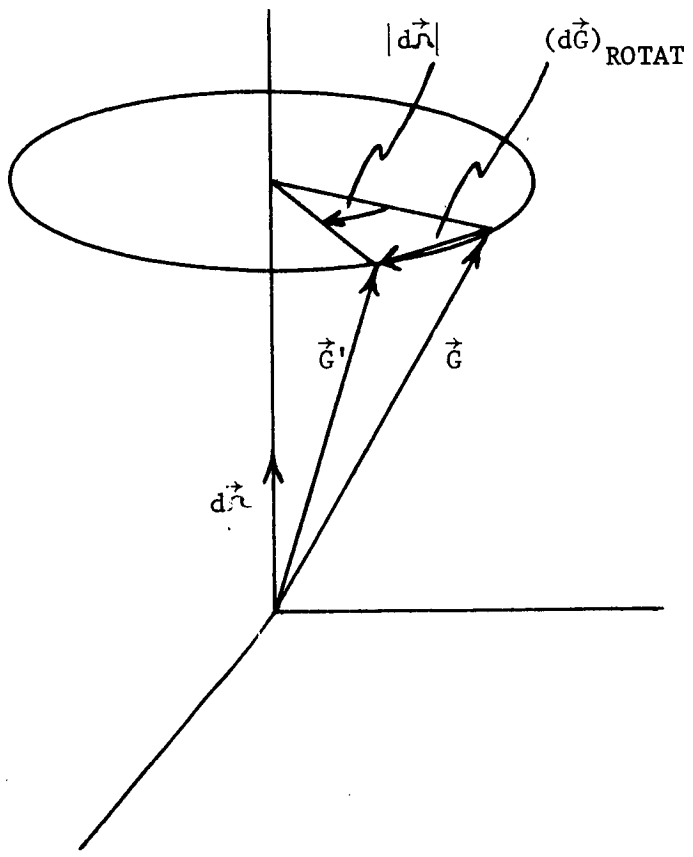
Figure 5.1

Applying (1.5.6) to (1.5.1), we have:

$$(\frac{d\vec{h}}{dt})_{body} + \vec{\omega} \times \vec{h} = \vec{n}(t), \tag{1.5.7}$$

an equation applying to any coordinate system fixed in the body. Now the angular momentum may be written as:

$$\vec{h}(t) = S \, \vec{\omega}(t) \quad , \tag{1.5.8}$$

where S is the moment of inertia tensor (as represented by a symmetric matrix). For S expressed relative to any coordinate system fixed in the body, we have that S is a constant matrix. Then (1.5.8) substituted into (1.5.7) yields:

$$(S)_{body} \, (\frac{d\vec{\omega}}{dt})_{body} + \vec{\omega} \times (S)_{body} \vec{\omega} = \vec{n}(t) \tag{1.5.9}$$

Equation (1.5.9) can be written in component form most simply in a certain body axes system. Since S is symmetric, a coordinate system can be chosen in which S is a diagonal matrix. Such a coordinate system is called the principal moment of inertia system and the diagonal elements (I_1, I_2, I_3) of the matrix S are called the principal moments of inertia. We have previously denoted the principal moment of inertia system as the P_i system.

Expressing (1.5.9) in component form in the p_i system yields:

$$I_1 \dot{\omega}_1 + (I_3 - I_2)\omega_2\omega_3 = n_1$$
$$I_2 \dot{\omega}_2 + (I_1 - I_3)\omega_1\omega_3 = n_2 \tag{1.5.10}$$
$$I_3 \dot{\omega}_3 + (I_2 - I_1)\omega_1\omega_2 = n_2$$

where $\dot{\omega}_1$ denotes the time derivative in the body system. These equations are the so-called Euler equations of motion for a rigid body with one point fixed.

The torque in equation (1.5.9) or (1.5.10) may be considered as the sum of a control torque and a disturbance torque:

$$\vec{n} = \vec{n}_c + \vec{n}_D \tag{1.5.11}$$

Equation (1.5.10) may then be rewritten:

$$I_1\dot{\omega}_1 = (I_2 - I_3)\omega_2\omega_3 + T_1 + b_{11}u_1 + b_{12}u_2 + b_{13}u_3$$

$$I_1\dot{\omega}_2 = (I_3 - I_1)\omega_1\omega_3 + T_2 + b_{21}u_1 + b_{22}u_2 + b_{23}u_3 \tag{1.5.12}$$

$$I_1\dot{\omega}_3 = (I_1 - I_2)\omega_1\omega_2 + T_3 + b_{31}u_1 + b_{32}u_2 + b_{33}u_3.$$

For completeness we add the angular rate equations used in the simulation (linearized from the full equation)

$$\dot{\phi} = \omega_1 - \psi\omega_3$$

$$\dot{\psi} = -\omega_2 + \phi\omega_3 \tag{1.5.13}$$

$$\dot{\theta} = \phi\omega_2 + \omega_3$$

If $\vec{n}_c$ is given in another coordinate system, say the b_i system, we may always transform to the p_i system as discussed in Section 3, e.g.

$$(\vec{n}_c)_p = A^+_{pb}(n_c)_b . \tag{1.5.14}$$

The disturbance torques $\vec{n}_D$ are discussed more fully in a later section and in the appendices.

6. *Simulation Program and Coordinate System Use*

Part VII of this report has been issued under separate cover. Part VII is a complete program description of both the analog and digital parts of the simulator. This includes input instructions for the digital program, setup instructions for the analog array, and detailed flow charts for each. In the present section we want to describe the simulation briefly and then, by using the flow chart appearing in Figure 6.1, relate the major junctions of information flow to the various coordinate systems, Euler angles, equations of motion, etc., that appear in the body of the report. Further detail on the analytical aspects is provided elsewhere in this report, further material, on the analog program (provided by Computing and Software, Inc.), and on the digital programs is contained in Part VII.

Two distinct simulation modes were available, runs could be made either on hybrid equipment or on a completely digital simulator. The analog computer used was an EAI Hydac 2000, the digital computer an SDS-9300.

In hybrid operation, the analog computer solved the differential equation describing the satellite dynamics and provided output via standard analog strip charts and x-y plotters (primarily used for phase plane plotting of the three satellite axes). The digital machine provided the analog with the control torques and the "natural" disturbance torques arising from solar and gravitational effects.

When using completely digital simulation, output could be specified at any multiple of the integration interval.

The remainder of this section appears in the form of Notes relating to the flow chart in Figure 6.1.

Digital
Data
Read   Note 1

Digital
Initialization
and Printout   Note 2

Analog
Initialization   Note 3

Calculate
Disturbance
Torques   Note 4

Calculate
Control
Torques   Note 5

Digital
Dynamics   Note 6

Analog
Dynamics   Note 6

Sensor
Simulation   Note 7

Disturbance
& Control
Torques D/A

Angles
& Rates
A/D

Calculate
Ground Track   Note 8

Output
Print   Note 9

Terminal
Conditions
Satisfied?   Note 10

no

yes

Stop

Dotted lines indicate flow during hybrid
Simulation. Digital Computer is SDS 9300
Analog Computer is EAI Hydac 2000

Figure 6.1:

Note 1: Data read from cards. Among these are ℓ_s (longitude of satellite subpoint), L_T and ℓ_T (latitude and longitude of target), L_I, ℓ_I, and γ_I (latitude and longitude of initial pointing, and the arbitrary initial rotation angle about the 2 (yaw) - axis), Euler angles bp relating body to principal axes, and the 12 thruster misalignment angles. Coordinates used: all. Subroutines used: Main.

Note 2: ℓ_s fixes the s_i coordinate system, L_T and ℓ_T determine the Euler angles θ_{Rs} (see equation 1.3.27). L_I, ℓ_I, and γ_I then determine the Euler angles θ_{bs} (see equation 1.3.24). The Euler angles θ_{Rs} and θ_{bs} determine the Euler angles θ_{bR} (see equation 1.3.30). The Euler angles θ_{bp} determine the matrix $A_{bp}^{\leftarrow} = C(\theta_{bp}, \psi_{bp}, \phi_{bp})$ (see equation 1.3.5). All initial rates are set to zero. Coordinates used: s_i, Rs, bs, bR, bp. Subroutines used: INIT and STUP.

Note 3: If hybrid simulation is used, initial conditions $(\theta_{bR}, \psi_{br}, \phi_{br})$ and thruster misalignment coefficients are setup on the analog computer.

Note 4: Disturbance torques due to solar radiation and gravity gradient are calculated here (see Appendices B and C, respectively). Since these torques are very small, an option to use constant torques is provided. All torques are expressed in the p_i system (using the matrix in section 2). The sum of these two torques is the disturbance torque sent to the analog in hybrid simulation.

Another disturbance torque arises from misalignment of the jets with respect to the principal axes. The overall disturbance torque (b) used in the computation of the control is the sum of torques $\{T_i\}$ (composed of solar, gravitational, and thrust misalignment) and the cross-coupling torques $\omega \times I\omega$. Coordinates used: p_i. Subroutines used: TOR.

64

<u>Note 5</u>: The control torques $\{u_i\}_1^3$ are calculated using the current (normalized values of θ_{bR}, ψ_{bR}, ϕ_{bR}, $\{\omega_i\}_1^3$, and $\{b_i\}_1^3$. (See Part II and Appendix E.)

The equations used in control computation are

$$\dot{y} = v + b$$

where: 1) y is the normalized vector ω, i.e.,

$$y = K^{-1}I\omega$$

$K = \text{diag}(b_{ii}k_i)$, $I = \text{diag}(I_i)$, I_i being the moment of inertia on the ith principal axis, k_i being the control bound in the ith axis, and b_{ii} being the projection of that control torque on the ith axis ($b_{ii} \neq 1$ if misalignment is present); 2) B is the normalized control vector whose components therefore, are either 0 or ± 1; 3) b is the normalized disturbance torques that is $K^{-1}I$ times the sum of cross coupling torques $I\omega \times \omega$, solar and gravitational torques T and the disturbance torques caused by misalignment of the control torques, e.g.

$$b_2 = \frac{1}{b_{22}k_2}((I_3 - I_1)\omega_1\omega_3 + T_2 + b_{21}u_1 + b_{23}u_3).$$

In addition the normalized form of equation 1.5.13 is used, i.e.

$$\dot{\alpha}_1 = \frac{I_1}{k_1}(\omega_1 - \psi_{bR}\omega_3)$$

$$\dot{\alpha}_2 = \frac{I_2}{k_2}(-\omega_2 + \phi_{bR}\omega_3)$$

$$\dot{\alpha}_3 = \frac{I_3}{k_3}(\omega_3 + \phi_{bR}\omega_2) \quad .$$

Coordinates used: p_i and bR. Subroutines used: REG .

<u>Note 6</u>: An option is provided here to calculate the satellite dynamics either digitally or by analog computer. The control torques u_i from Note 5 are used and the dynamic equations are integrated either on the analog or the digital computer. The analog device has the option of using a decaying control torque rather than a constant one (see Part III and Part VI). The digital program has the option of approximating the elastic effects of a boom (see Part V and Appendix D). Coordinates used: bR

and p_i. Subroutines used: MAIN, DER, RK – or analog.

Note 7: To simulate the sensor, only the values from Note 6 of the

angles θ_{bR}, $\cdots$ (no rates) are used. Using the linear approximation,

these are set equal to the sensor outputs, a Gaussian noise is added,

and the noisy angles are filtered to yield smooth values of θ_{bR}, ψ_{bR}, ϕ_{bR}

and $\dot\theta_{bR}$, $\dot\psi_{bR}$, $\dot\phi_{bR}$. After converting $(\dot\theta_{bR}, \dot\psi_{bR}, \dot\phi_{bR})$ to $(\vec\omega)p$, these

are the current angles and rates used next in Note 5 (see Part IV). Co-

ordinates used: bR and p_i. Subroutines used: MAIN.

Note 8: Using the angles θ_{bR}, $\cdots$ obtained from the full dynamics,

the ground track is computed (i.e., current latitude–longitude of

pointing). (See Appendix A.) Coordinates used: bR, rs, bs. Subroutines

used: GT.

Note 9: In hybrid simulation, no digital output appears during the run.

In digital simulation, printed output can be given at integral multiples

of the integration interval. Among other things, the state of the system

and its dervative, the ground track coordinates, and values of the torques

are printed. A complete format is given in Part VII. Cordinates used:

Subroutines used: OUT .

Note 10: The target is reached when the Euler angles θ_{bR} and rates $\dot\theta_{bR}$

have reached a prescribed neighborhood of the origin. In digital simulation,

a terminal print is given. Coordinates used: bR. Subroutines used: MAIN.

PART II

OPTIMAL ATTITUDE CONTROL SYNTHESIS

2.1 *The Model*

Let θ, ψ, ψ denote the euler angles of the principal axis system with respect to a reference coordinate system determined by a selected target point. Our primary objective is to drive these angles to zero. A control is to be synthesized which carries out this objective and simultaneously behaves optimally with respect to performance criteria and constraints to be described.

For our discussion in this part we introduce the vector notation

$$\xi = \begin{bmatrix} \theta \\ \psi \\ \phi \end{bmatrix}, \qquad (2.1.1)$$

$$A(\xi) = \begin{bmatrix} 1 & 0 & \sin \psi \\ 0 & -\cos \phi & \sin \phi \cos \psi \\ 0 & \sin \phi & \cos \phi \cos \psi \end{bmatrix}, \qquad (2.1.2)$$

$$\omega = \begin{bmatrix} \omega_1 \\ \omega_2 \\ \omega_3 \end{bmatrix}, \qquad (2.1.3$$

where ω is angular velocity about the center of gravity of the satellite.

The basic dynamics as developed in *Part I* for rigid body satellite attitude motion are represented by the equations

$$I\dot{\omega} + \omega \times I\omega = Bu + f(\xi, \omega), \tag{2.1.4}$$

and

$$A(\xi)\dot{\xi} = \omega \quad . \tag{2.1.5}$$

In equation (2.1.4)

$$I = \begin{bmatrix} I_1 & 0 & 0 \\ 0 & I_2 & 0 \\ 0 & 0 & I_3 \end{bmatrix} \tag{2.1.6}$$

is the moment of inertia matrix which is diagonal since I measures principal axes of inertia deviations relative to our reference system. u in equation (2.1.4) is a three parameter control torque vector, and B is a matrix representing the misalignment of control torques with respect to the principal axes system. B in general is assumed close to the identity matrix which we represent by E.

$$f(\xi,\omega) = \begin{bmatrix} f_1(\xi,\omega) \\ f_2(\xi,\omega) \\ f_3(\xi,\omega) \end{bmatrix} \tag{2.1.7}$$

represents environmental disturbance torques effecting the rotation of a satellite. In particular, f incorporates torques generated by solar flux

and variations in the gravitational field. F also includes other disturbances on attitude motion resulting from other processes going on in the satellite. The precise breakdown of this vector function is the subject of later sections and *Appendices B, C,* and *D* in particular. For purposes of our present discussion of control, we need only specify that it satisfies certain constraints which are specified shortly.

The control vector

$$u = \begin{bmatrix} u_1 \\ u_2 \\ u_3 \end{bmatrix} \qquad (2.1.8)$$

is subject to constraints $|u_1| \le k_1$, $|u_2| \le k_2$, and $|u_3| \le k_3$, where k_1, k_3, and k_3 are specified positive constants . For an arbitrary vector

$$v = \begin{bmatrix} v_1 \\ v_2 \\ v_3 \end{bmatrix} \quad ,$$

let

$$||v|| = \left(\sum_{i=1}^{3} v_i^2 \right)^{1/2} \qquad (2.1.9)$$

As a practical design requirement the parameters k_i, $i = 1, 2, 3$, are specified such that

$$k_i > ||(B - E)u|| + ||f(\xi,\omega)||, \quad i = 1, 2, 3 \qquad (2.1.10)$$

70

for all considered values of ξ, ω, and u. This requirement simply indicates that our means for exerting control torque dominates the disturbance torques it must counteract and that disturbance resulting from misalignment is not sufficient to disrupt this situation.

The basic objective in this development is to synthesize and present the results of simulation experiments with a control function u such that:

  (a) Transfers of attitude position for a satellite take place within physically imposed constraints and with sufficient speed to be useful in a specified mission.

  (b) The energy put into the system in making transfer is constrained so as not to endanger the stability of the system.

  (c) The expenditure of fuel or power required in carrying out transfer is held to the minimum consistent with imposed constraints and other specified objectives such as speed of response.

These objectives are quantitatively measured by means of an appropriate performance criterion which can be adaptively changed through parametric variations. In accordance with the imposed performance criterion a feedback control function $g(\xi,\omega)$ is constructed such that when $g(\xi,\omega)$ is substituted in equation (2.1.4), the system

$$I\dot{\omega} + \omega \times I\omega = Bg(\xi,\omega) + f(\xi,\omega) \tag{2.1.11}$$

performs optimally or nearly so with respect to above objectives and imposed constraints.

At an arbitrary but specified time t_o we consider the system at an arbitrary state ξ_o, ω_o and our general objective is to drive the system to the state 0,0 at sometime t_1 later. With the performance criterion used in control synthesis it is possible to impose a variety of control strategies. In particular, one strategy could be to effect the movement from ξ_o, ω_o to 0,0 with velocity components constrained in magnitude to be less than some specified constant and with the time of arrival on target specified to be no later than a specified time $t^* > t_o$ if possible. If it is not possible to arrive on target at or before time t^*, then the system would be required to arrive on target as quickly as possible. Within specified velocity and time constraints the system is required to use a minimum of fuel. An alternative strategy would be to rigidly constrain velocity and fuel and minimize the time required to carry out the motion.

2.2 *System Normalization and Simplification for Purposes of Control Synthesis*

For purposes of control synthesis it is convenient to normalize our system through the change of variables

$$y = \hat{K}^{-1}I\omega, \quad v = \hat{K}^{-1}u \quad \text{and} \quad A^*(\xi) = \hat{K}^{-1}IA(\xi), \qquad (2.2.1)$$

and

$$\hat{K} = \text{diag}\{b_{11}\,k_1,\ b_{22}\,k_2,\ b_{33}\,k_3\}\ . \qquad (2.2.2)$$

Our dynamical system in terms of these normalized variables takes the form

$$\dot{y} = v + b \qquad (2.2.3)$$

and

$$A^*(\xi)\dot{\xi} = y \qquad (2.2.4)$$

together with the composite perturbations

$$b = b(\xi,\ y,\ v) = \hat{K}^{-1}((B-\hat{B})\hat{K}v + f(\xi,\ I^{-1}\hat{K}y) - I^{-1}\hat{K}y \times \hat{K}y) \qquad (2.2.5)$$

where

$$\hat{B} = \text{diag}\{b_{11},\ b_{22},\ b_{33}\}$$

and

$$|v_i| \le 1 \quad \text{for} \quad i = 1,\ 2,\ 3\ . \qquad (2.2.6)$$

Subject to the performance criterion which we shall introduce shortly, we would ideally like to synthesize optimal control with these completely general dynamics. Unfortunately, however, for a variety of reasons this is not feasible. To begin with, the complexity of the function b makes the analysis involved in such a synthesis completely untractible. Furthermore, even if such precise synthesis were carried out, it would be far too

complicated for application to real systems. What we shall synthesize is a highly stable control for these general dynamics which is "near" optimal. This will be accomplished by synthesizing optimal control for a system which, from the point of view of control, closely approximates our general system.

Let b be an arbitrary constant vector whose components in magnitude are bounded less than 1. Consider the system of equations

$$\dot{y} = v + b \qquad\qquad (2.2.7)$$

and

$$A^*(\xi)\dot{\xi} = y \qquad\qquad (2.2.8)$$

together with the constraints $|v_i| \leq 1$, $i = 1, 2, 3$. Let us suppose for each point (ξ, y, b) that $v = p(\xi, y; b)$ is an optimal synthesis for this system. A "near" optimal synthesis for our general dynamics is given by the formula

$$v = p(\xi, y; b(\xi, y, 0)) \qquad\qquad (2.2.9)$$

under the reasonable assumption that b is relatively small and makes large value changes slowly. If misalignment of thrusters with the principal axes of inertia is relatively large, then improved performance is likely if v is given by the formula

$$v = p(\xi, y; b(\xi, y, p(\xi, y; b(\xi, y, 0)))). \qquad\qquad (2.2.10).$$

2.3 *The Performance Criterion*

Let y^2 and $|v|$ denote the vectors

$$\begin{bmatrix} y_1^2 \\ y_2^2 \\ y_3^2 \end{bmatrix} \quad \text{and} \quad \begin{bmatrix} |v_1| \\ |v_2| \\ |v_3| \end{bmatrix} \qquad (2.3.1)$$

respectively. For our performance criterion we shall require that controlled attitude slews be such that as to minimize the functional

$$J = \int_{t_o}^{t_1} (\lambda + \Gamma_2 \cdot y^2 + \Gamma_3 \cdot |v|) dt \qquad (2.3.2)$$

where t_o and t_1 are the initial time and time of arrival on target respectively. λ is a positive scalar parameter and Γ_1 and Γ_2 are vector parameters with positive components.

Minimizing J in the process of driving our satellite to the target attitude $\xi = 0$, $y = 0$ represents optimal performance with a weighted compromise between speed of acquisition, fuel consumption, and stability characteristics. Choosing different λ, Γ_2, and Γ_3 will result in a different weighting of these important performance factors. In particular, if we choose $\lambda \neq 0$, $\Gamma_2 = 0$, $\Gamma_3 = 0$, our control would be time optimal. However, time optimality for our system is not uniquely defined and we would not in general use this particular choice of parameters. We would use nonzero vectors for Γ_2 and Γ_3 which would use minimum fuel consistent to arriving on target in minimum time. If minimum time is not required, then Γ_2 and Γ_3 would be chosen so as to constrain further fuel consumption and angular rates.

Including the term $\Gamma_3 \cdot |v|$ in J has the effect of holding a lid on the amount of control force applied. This in turn acts as a constraint on the amount of fuel required. The term $\Gamma_2 \cdot y^2$ in J has the effect of constraining angular rates and thereby improving stability of performance. Having all components of Γ_2 positive dictates that optimal control for $||y||$ sufficiently large is automatically a despinning mode (See Section 3 of Appendix E).

We have qualitatively explained the effects of our parameterized performance criterion on system performance. Let us now illustrate how the parameterization can be used to yield specific types of system performance.

First let us define Γ_1 to be a vector such that

$$\Gamma_1 = \begin{bmatrix} \lambda_{11} \\ \lambda_{21} \\ \lambda_{31} \end{bmatrix} \tag{2.3.3}$$

where $\lambda_{11} + \lambda_{21} + \lambda_{31} = \lambda$, and let Γ_2 and Γ_3 in component form be

$$\Gamma_2 = \begin{bmatrix} \lambda_{12} \\ \lambda_{22} \\ \lambda_{32} \end{bmatrix} \quad \text{and} \quad \Gamma_3 = \begin{bmatrix} \lambda_{13} \\ \lambda_{23} \\ \lambda_{33} \end{bmatrix} . \tag{2.3.4}$$

Let

$$
\dot{z} =
\begin{bmatrix}
J_1 \\
J_2 \\
J_3
\end{bmatrix}
=
\int_{t_o}^{t_1}
\begin{bmatrix}
\lambda_{11} + \lambda_{12} y_1^2 + \lambda_{13}|v_1| \\
\lambda_{21} + \lambda_{22} y_2^2 + \lambda_{23}|v_2| \\
\lambda_{31} + \lambda_{32} y_3^2 + \lambda_{33}|v_3|
\end{bmatrix}
dt \qquad (2.3.5)
$$

be called the *performance vector* and let

$$
\Lambda =
\begin{bmatrix}
\lambda_{11} & \lambda_{12} & \lambda_{13} \\
\lambda_{21} & \lambda_{22} & \lambda_{23} \\
\lambda_{31} & \lambda_{32} & \lambda_{33}
\end{bmatrix}
\qquad (2.3.6)
$$

be called the *parameter matrix*. In conjunction we introduce the concept

of a *speed of response function* $t^*(\xi, y)$ which we assume has been defined

apriori based on hardware and mission considerations. $t^*(\xi, y)$ is a positive

real valued function which establishes that if the state of our system at

t_o is (ξ_o, y_o), then we strive for the state $(0,0)$ at time $t_o + t^*(\xi_o, y_o)$.

$t^*(\xi, y)$ may be defined simply as the minimum time required for arrival on

target from the position (ξ, ω). Let us also assume Γ_2 and Γ_3

have positive components which have been specified apriori on the basis

of hardware and mission considerations. They may, however, be subjected

to adaptive modification during a mission if this becomes desirable.

Assume $t^*(\xi, y)$ has been specified, we define

$$
|J_{t^*}| = \sum_{i=1}^{3} \int_{t_o}^{t^*(\xi_o, y_o)} (\lambda_{i1} + \lambda_{i2} y_i^2 + \lambda_{i3}(t^*(\xi_o, y_o))|v_i|) dt. \qquad (2.3.7)
$$

Optimal control defined relative to t^* and J is interpreted in terms

of minimizing $|J_{t^*}|$ in slewing from any point (ξ, y) in our operational

state to the target position $(C,0)$. The procedure followed herein accomplishes this to a high degree of approximation.

2.4 *System Splitting through a Nonlinear Change of Variables*

We have at this point reduced the dynamics to be considered to the system (2.2.7) and (2.2.8). Our performance criterion is incorporated through J as defined by (2.3.2). We shall now introduce a nonlinear change of variables as the first step in the development of a procedure whereby the control function as specified by (2.2.9) or (2.2.10) can be closely approximated.

Let us consider the functional equation

$$x(t) = - \int_{t}^{t_1} A^*(z(\tau))\dot{z}(\tau)d\tau \quad . \qquad (2.4.1)$$

where x and z are differentiable vector functions defined on the interval $[t_o, t_1]$ which vanish at t_1. It can be proved that for each function $x(t)$ there exists one and only one function $z(t)$ satisfying (2.4.1). *Hence there exists a one-to-one correspondence between the functions $x(t)$ and $z(t)$ related through equation (2.4.1).* Proof of this fact is given in *Appendix E.*

Now consider the system

$$\dot{y} = v + b \qquad (2.4.2)$$

$$\dot{x} = y \qquad (2.4.3)$$

together with J and the constraints on v as previously specified. Let ξ, y, $v = p(\xi, y:b)$ be functions defined on an interval $[t_o, t_1]$ which satisfy the system of equations (2.2.7) and (2.2.8) and are such that $\xi(t_1) = 0$ and $y(t_1) = 0$. Let x and ξ be related by the equation

$$x(t) = - \int_{t}^{t_1} A^*(\xi(\tau))\dot{\xi}(\tau)d\tau \quad . \qquad (2.4.4)$$

79

Proposition I: ξ, y, v = p(ξ,y:b) *is an optimal synthesis for the system of equations* (2.2.7) *and* (2.2.8) *relative to* J *if and only if*

x, y, v = q(x,y:b) *is an optimal synthesis for the system of equations* (2.4.2) *and* (2.4.3) *relative to* J *and*

$$p(\xi,y) = q(-\int_t^{t_1} A^*(\xi(\tau))\dot{\xi}(\tau)\tau,y) \quad . \tag{2.4.5}$$

Proof of this proposition is given in Section 4 of *Appendix E.*

Through the use of Proposition I we have a procedure for synthesizing optimal control for the system of equations (2.2.7) and (2.2.8) by considering optimal synthesis for the system (2.4.2) and (2.4.3) together with J. We observe that the latter system can be split into three, two-dimensional systems which are coupled only through J and b. The "carry over" synthesis is exact if given initial data $\xi(t_o) = \xi_o$, $y(t_o) = y_o$, the initial state vector

$$x(t_o) = x_o = -\int_{t_o}^{t_1} A^*(\xi(\tau))\dot{\xi}(\tau)d\tau \quad . \tag{2.4.6}$$

is exactly known. x_o is, of course, only known through the formula (2.4.4) but it can be computed through iteration to any degree of precision. A simple and adequately accurate estimate for x_o in most cases is given by the formula

$$x_o = \frac{1}{2}(A^*(0) + A^*(\xi_o))\xi_o \quad . \tag{2.4.7}$$

Since all terms on the right hand side of (2.4.7) are computable explicitly without integration, this estimate is highly desirable from the point of view of implementation.

2.5 *Control Synthesis for Split Dynamics*

In view of Proposition I it is now clearly reasonable to synthesize control with respect to the dynamics

$$
\left\{
\begin{aligned}
&\dot{y} = v + b \quad, \\[1mm]
&\dot{x} = y \quad, \\[1mm]
&J = \sum_{i=1}^{3} \int_{t_o}^{t_1} (\lambda_{i1} + \lambda_{i2} y_2^2 + \lambda_{i3}|v_i|)\, dt \quad, \\[1mm]
&|v_i| \leq 1 \quad, \qquad i=1,2,3.
\end{aligned}
\right.
\tag{2.5.1}
$$

This system is splittable for purposes of control synthesis into the following scalar systems:

$$
\left\{
\begin{aligned}
&\dot{y}_1 = v_1 + b_1 \quad, \\[1mm]
&\dot{x}_1 = y_1 \quad, \\[1mm]
&|v_1| \leq 1 \quad, \\[1mm]
&J = \int_{t_o}^{t_1} (\lambda_{11} + \lambda_{12} y_1^2 + \lambda_{13}|v_1|)\, dt \quad.
\end{aligned}
\right.
\tag{2.5.2}
$$

$$
\left\{
\begin{aligned}
&\dot{y}_2 = v_2 + b_2 \quad, \\[1mm]
&\dot{x}_2 = y_2 \quad, \\[1mm]
&|v_2| \leq 1 \quad, \\[1mm]
&J = \int_{t_o}^{t_1} (\lambda_{21} + \lambda_{22} y_2^2 + \lambda_{23}|v_2|)\, dt \quad.
\end{aligned}
\right.
\tag{2.5.3}
$$

$$\left\{ \begin{array}{l} \dot{y}_3 = v_3 + b_3 \;, \\[2em] \dot{x}_3 = y_3 \;, \\[2em] |v_3| \le 1 \;, \\[2em] J = \displaystyle\int_{t_o}^{t_1} (\lambda_{31} + \lambda_{32} y_3^2 + \lambda_{33}|v_3|)dt \;. \end{array} \right. \qquad (2.5.4)$$

Note that systems (2.5.2), (2.5.3), and (2.5.4) are coupled only through J and the vector parameter

$$\mathbf{b} = \begin{bmatrix} b_1 \\ b_2 \\ b_3 \end{bmatrix} \;. \qquad (2.5.5)$$

Note also that arrival time on target is the same for all three systems. This requirement is referred to as *time synchronization*. The simultaneous optimation of these systems does in fact constitute optimal synthesis for the total system represented by (2.4.1).

Operationally, unless a specific speed of response function is introduced, time of arrival on target is dictated by the initial specification of Λ which we denote by Λ_o. In terms of this parametric specification, times of arrival τ_1, τ_2, and τ_3 for the scalar systems (2.5.2), (2.5.3), and (2.5.4) respectively are computed. Time of arrival is then specified as $\tau = \max \{\tau_1, \tau_2, \tau_3\}$. Λ is then properly modified to a new matrix Λ_1 which will cause all three systems to arrive on target simultaneously at the specific time $t_o + \tau$. Note

that Λ_o is maintained in the computer at all times and Λ_1 is recomputed

at each sample interval. This is necessary, of course, to preserve the

closed loop character of the synthesis.

The details of the calculations of τ_1, τ_2, τ_3, and Λ_1 are

presented in Section 2 of Appendix E. Assuming, therefore, that parameters

matrix Λ_1 is properly specified, our synthesis is completed by considering

simultaneously the syntheses of three scalar component systems of the form

$$\left\{ \begin{array}{l} \dot{y} = v + b \\[2ex] \dot{x} = y \\[2ex] J = \displaystyle\int_{t_o}^{t_1} (\lambda_1 + \lambda_2 y^2 + \lambda_3 |v|)dt \quad . \\[2ex] |v| \leq 1 \end{array} \right. \tag{2.5.6}$$

Optimal v for such systems can be easily shown to take

on only the values 1, 0, $-b$, and -1. It is representable in closed

form as a function of x,y, and b as illustrated in Figures 2.1, 2.2,

and 2.3. In these illustrations b is assumed negative and less than 1.

For positive b the control is reflexed with respect to the y-axis. Note

that changing b has the effect of moving switching curves, but otherwise

does not change the qualitative behavior of the system. Assuming perfect

data from any point x,y a maximum of only three value changes in the

control is required for reaching the target.

For the practical implementation of this system, one can drop

the value of $-b$ for v without seriously effecting optimality. This

is accomplished by softening the control appropriately near the lines

$$y = \sqrt{\frac{\lambda_1 - \lambda_3 b}{\lambda_2}} \qquad \text{and} \qquad y = -\sqrt{\frac{\lambda_1 - \lambda_3 b}{\lambda_2}} \qquad .$$

Figure 2.1

Figure 2.2

85

2.18

$$b = -\frac{\lambda_1}{\lambda_3}$$

$-1 < b < -\dfrac{\lambda_1}{\lambda_3}$

u=-1

u=-b

u=0

u=+1

$\sqrt{\dfrac{-2\lambda_3 b}{\lambda_2}}$

$\sqrt{\dfrac{\lambda_1-\lambda_3 b}{\lambda_2}} +$

$\sqrt{\dfrac{\lambda_1-\lambda_3 b}{\lambda_2}}$

$-\sqrt{\dfrac{\lambda_1-\lambda_3 b}{\lambda_2}} + \sqrt{\dfrac{-2\lambda_3 b}{\lambda_2}}$

c_2

$-\sqrt{\dfrac{\lambda_1+\lambda_3 b}{\lambda_2}}$

u=+1

u=-1

u=0

u=-b

86
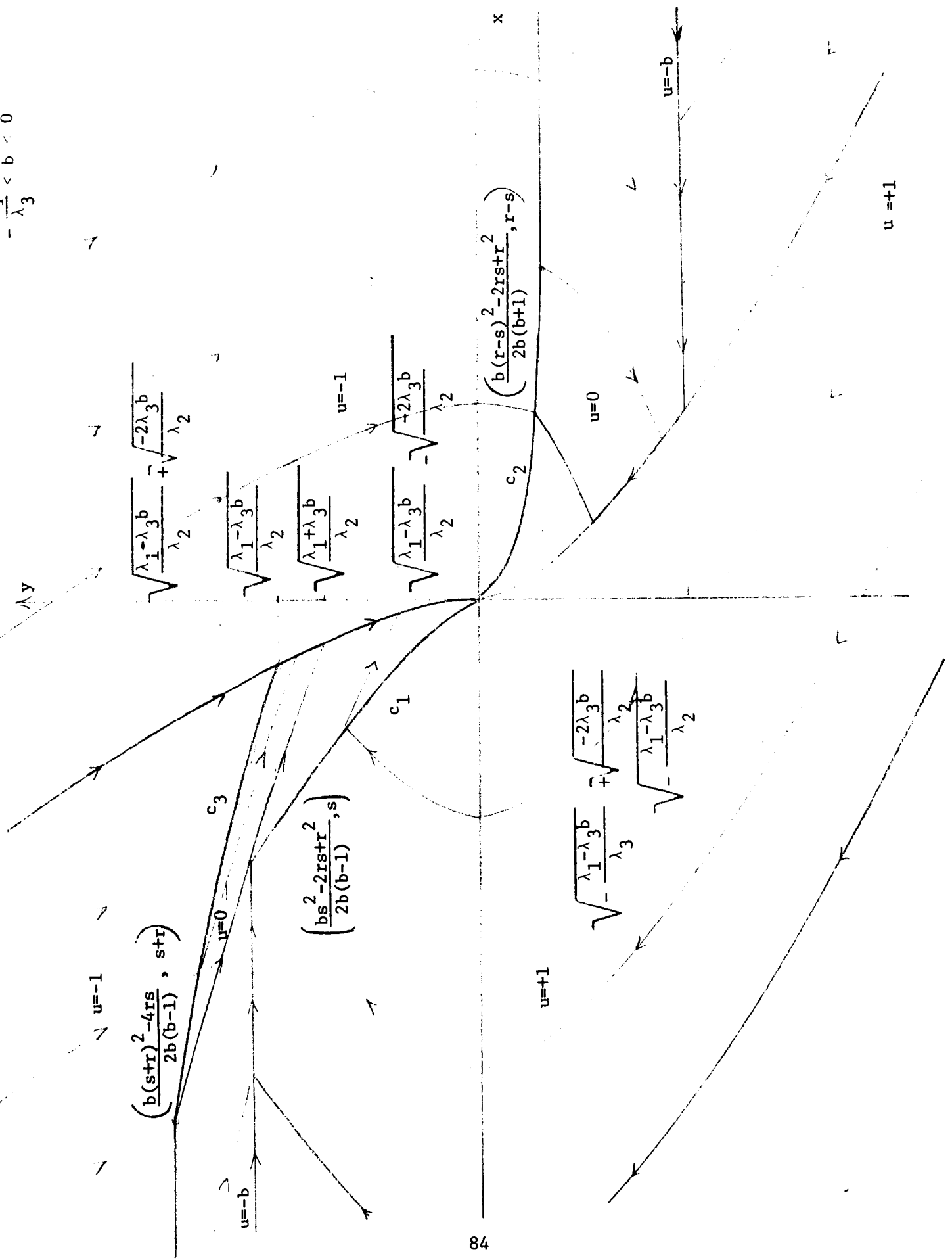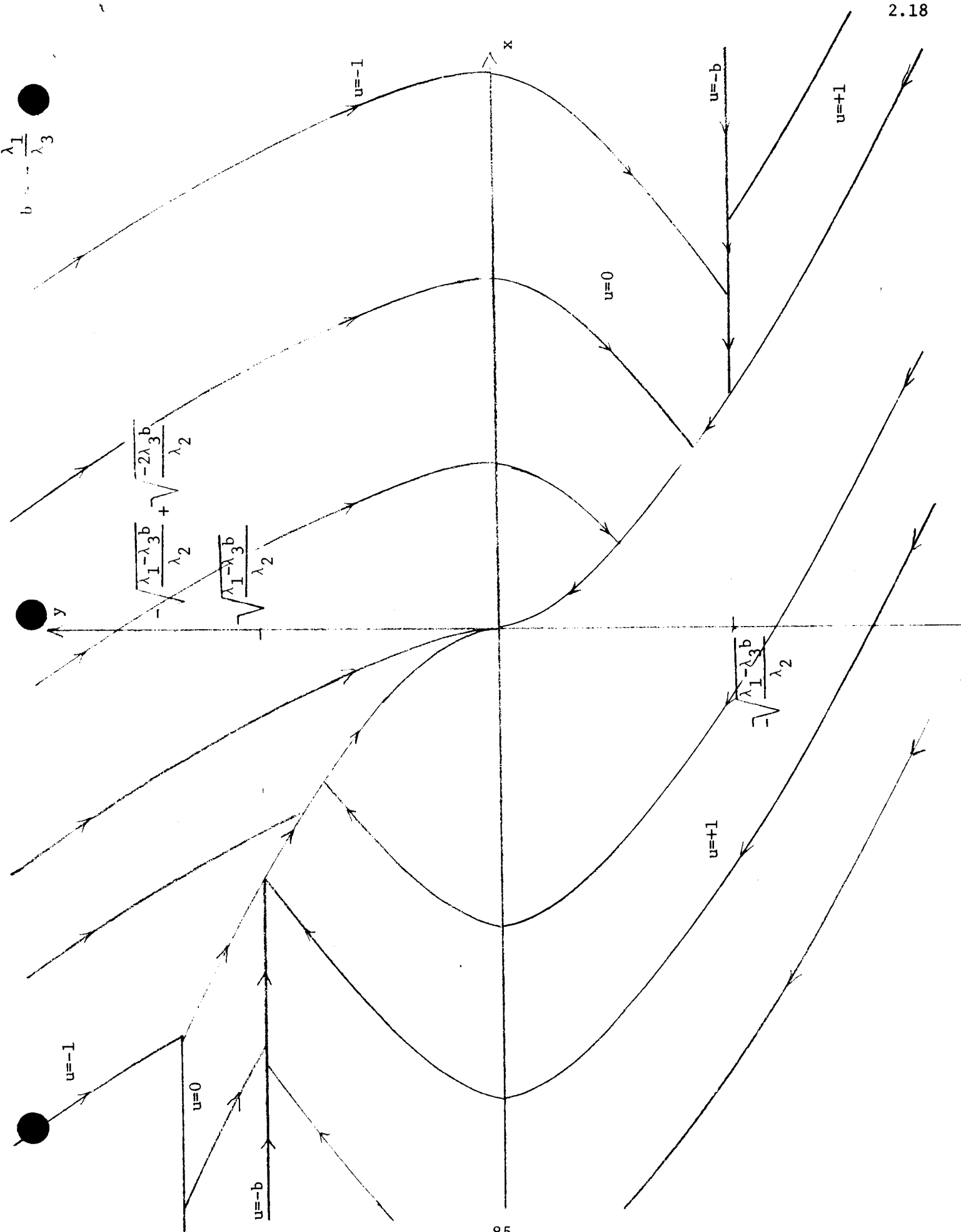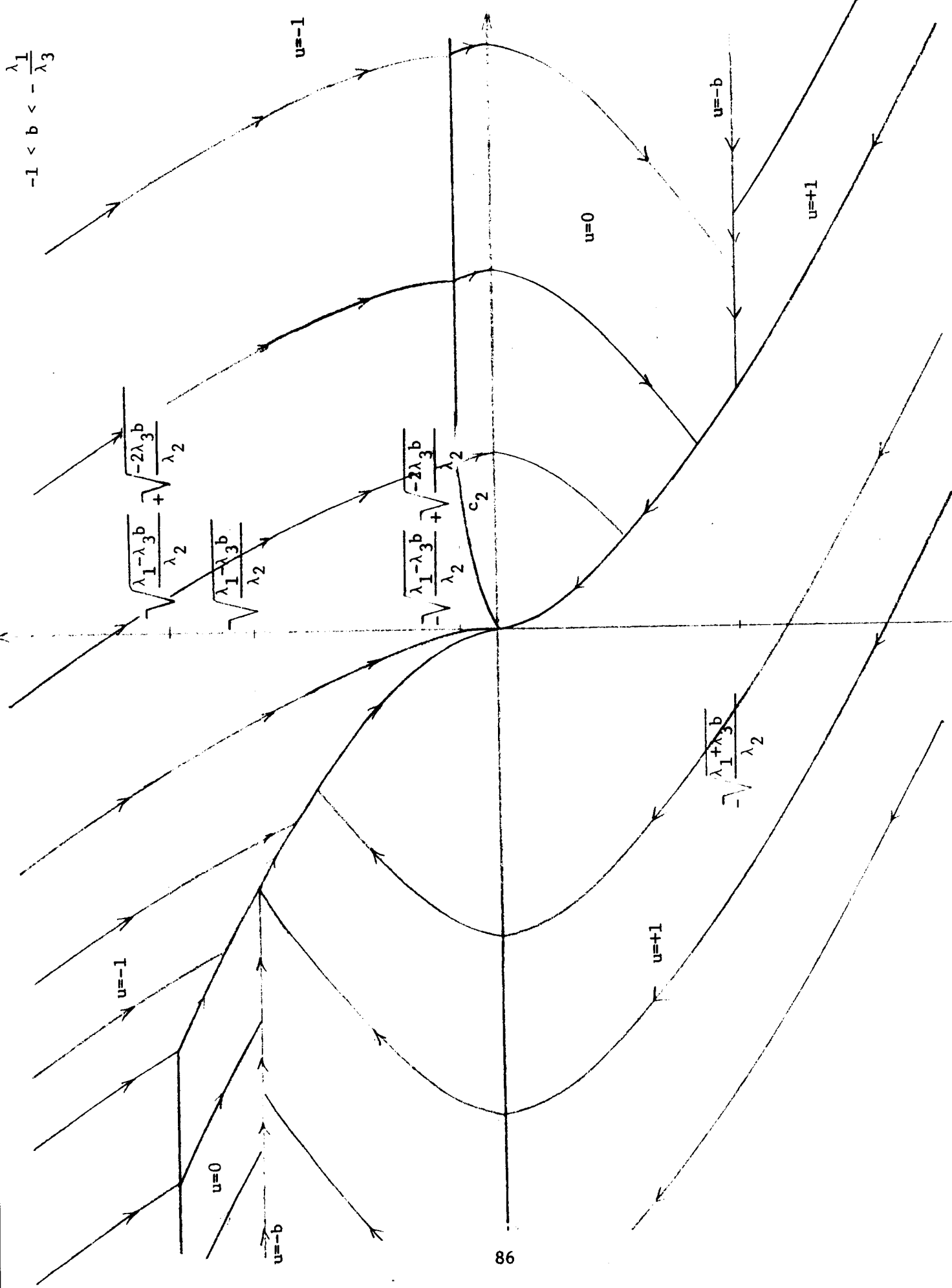
Figure 2.3

Optimal control as utilized and described herein and represented in Figures 2.1, 2.2, and 2.3 was derived through the use of the Pontryagin Maximal Principle. The details of the analysis necessary to establish the optimality of our results are presented in Section 1 of Appendix E.

PART III

SIMULATION STUDIES FOR ATTITUDE MANEUVERS USING OPTIMAL

CONTROL STRATEGY AND IDEAL SATELLITE DYNAMICS

*Simulation Studies for Attitude Maneuvers Using Optimal Control Strategy
and Ideal Satellite Dynamics*

Many simulation studies were performed in the process of check-
out. These began with single-axis problems and progressed to more complica-
ted cases. In this process we gained intuition about the control which
enabled us to draw up an experiment plan designed to demonstrate the proper-
ties of the system in a relatively demanding maneuver. Specifically, slews
from Mohave to Quito were chosen for illustration since they require a
reasonable rotation about both the pitch and roll axes and because both
Mohave and Quito are logical targets for such a satellite. Mohave is 35.3°
North Latitude, 116.9° West Longitude; Quito is .2° South Latitude, 78° West
Longitude. The resultant initial conditions in terms of the coordinate system
used in the program are a roll angle of .0993 radians, a yaw angle of 6.5×10^{-5}
radians and a pitch angle of .1065 radians. Since the holding mode takes over
when an angle is less than .0017 radians, the yaw angle is seen to be already in
this region and no thrust is required for this axis during this maneuver. The
angles above are computed for a satellite orbiting in the earth's equatorial
plane, at synchronous altitude and having a subpoint at longitude 100° West.

In this chapter we will analyze results obtained using the "ideal"
satellite. This is in distinction from the "real" satellite described in
section 4 and the "elastic" satellite described in section 5. In this con-
text, the ideal satellite has two distinguishing characteristics. Both angle
and rate information are available for use in control computation. The thrust
rise time and tailoff time are both zero and the thrust level is constant.

The satellite physical constants for all simulation appear in
the following table.

SPACECRAFT REFERENCE DESIGN CONSTANTS

AXIS	DESIGNATION	RATED THRUST (lbs.)	MOMENT ARM (ft.)	TORQUE (ft.-lbs.)	MOMENT OF INERTIA (slugs-ft^2)
pitch	θ	0.026	4.6	0.12	2000
roll	ϕ	0.017	4.6	0.08	3580
yaw	ψ	0.011	3.6	0.04	1970

NOTE: Above thrust and torque values for the yaw axis assume a couple.
Moment of inertia values are for the principal axes.
Maximum thruster misalignment angles are 1 degree in each axis.

The results described here came from two types of simulation. In one, all computations were done on an SDS 9300 digital computer. In the other, control values and solar and gravitational torques were computed digitally on the 9300 for use in the dynamics run on an EAI Hydac 2000. Angle and rate then came from the analog computer back to the digital.

The runs herein described were made on the hybrid computer unless specifically labeled otherwise.[*]

Figure 3.1 is a phase plane plot showing both the pitch and roll axes during this slew for a time optimal run ($\gamma = 1, 0, 0$). It should be noted that both angles go directly into the holding region with practically no overshoot or undershoot. (We refer to the holding region as one in which the angle is less than .002 radians and the rate is less than .5 x 10^{-4} radians per second.) For the roll axis, which requires the maximum time, the thrust is on for the first half of the slew and is reversed for the final half. For the pitch axis thrust is cut off when the rate reaches .00104 rad/sec and is reversed when the angle reaches -.008 radians. If the single axis control policy were adhered to with respect to the pitch axis, it would arrive on target considerably earlier than the roll axis with a resultant waste of fuel. Time

[*] Complete description of the hybrid setup appears in Part VII, Sect 5 - 9.

synchronization causes the cut-off, which causes both axes to reach the origin at approximately the same time, the roll axis being the later, but using no more fuel than is absolutely necessary.

Figure 3.2 is a phase plane plot for the Mohave to Quito slew showing the roll axis behavior for three different cost functions; Figure 3.3 shows the pitch axis for these same runs.

From these graphs it appears that the effect of fuel weighting is the same as that for rate weighting. This is certainly true for a fixed initial condition. That is for a given slew, any control law obtained by some $(1, \lambda_2, 0)$ weighting could also be obtained by using a $(1, 0, \lambda_3)$ weighting. However, if the initial conditions were changed, for instance by making both initial angles smaller, the trajectories given by the two weightings would not be the same. This may be verified by comparing the (curved) switching line imposed by fuel weighting with the (flat) line given by energy weighting. These may intersect at one point but will not coincide.

Figure 3.4 shows the ground track, i.e., the trace of the earth's latitude and longitude to which the yaw axis points as the satellite performs a Mohave-Quito maneuver. Two runs are displayed here, one being the time optimal, the other being fuel limited, both with the satellite subpoint at 100° West Longitude. These were hybrid runs, the plots being done simultaneously on the analog x - y plotter, the great circle added by hand.

Figure 3.5 is the same time optimal run as appears on Figure 3.4. However, it was drawn from digital computer output, enabling us to perform a little more analysis of the curve and the time sequence. The initial (0-17 seconds) trace should be approximately a straight line with slope equal to the ratio of the torque/moment ratios in the two axes.

$$\frac{\Delta\theta}{\Delta\phi} = \frac{-116.9 + 114.14}{35.3 - 34.25} = -\frac{2.76}{1.05} = 2.61; \quad \frac{(T/I)_\theta}{(T/I)_\phi} = \frac{\frac{.12}{2000}}{\frac{.08}{3580}} = 1.5 \cdot 1.79 = 2.68$$

The trace in the region (17-106 sec) is approximately an S-curve with inflection point occurring at the roll control sign change (67 seconds).

Notice that 33.75 - 16 = 17.75 degrees of latitude are covered in the 50 second interval (17 - 16) while only 16 - 2.5 = 13.5 are covered in the dynamically symmetric interval (67 - 106). This occurs, of course, because a one degree change in roll at a latitude of 35° covers about $\frac{1}{\cos 35°}$ as much as at latitude zero.

We can also speculate about the relation of the track to a great circle. Little can be said except that the track will virtually never follow the G(reat) C(ircle) but will probably always approximate it. We have seen above that the track will start tangent to the G. C. only if the torque/moment ratios are properly set. Further, we notice that the track does not cross the G. C. at 67 seconds. We gather that in order to follow the G. C. the target and initial conditions must be symmetric with respect to the satellite subpoint, and both axes must actuate controls together.

The time resolution on the digital printout is one second and the time periods seem to be within this accuracy. That is, there are 17 seconds negative and 16 seconds positive on-time in pitch. There are 67 seconds negative and 64 seconds positive on-time in roll. Roll control cut off by reaching the dead band, prior to passing through Quito, which could account for the three second discrepancy.

Now consider the terminal behavior. From 67 to 106 seconds the curve flattens as latitude (roll) rate slows. Then at 106 the pitch rate begins to slow more quickly even than roll. Hence the curve turns down. At 122 seconds longitude (pitch) error is zero and the trace moves vertically to the final latitude. This is, of course, a result of the failure to have perfect synchronization.

This failure to have perfect simulation is primarily caused by the purposely introduced bias in the synchronization calculation. That is, we expect the axes with shorter times to come in several seconds before the longest-time axis. This is done to avoid the choice of longest-time axis switching back and forth.

Figure 3.6 is a graph resulting from a series of runs in which λ_1 and λ_3 were fixed at 1 and 0 respectively, but λ_2, the fuel weighting factor, was varied from 0 to 8. The graph shows clearly the fuel-time trade-off for the Mohave-Quito slew. For example, the minimum time possible for this maneuver is about 131 seconds. However, allowing an additional 20 seconds would effect a saving of approximately one-third the fuel, a factor of no small import.

Figure 3.7 exhibits phase plane plots of the roll axis in executing a slew from 70° South Latitude, 100° West Longitude to 70° North Latitude, 100° West Longitude, the satellite being at 100° West Longitude. The figure shows clearly the efficiency of the control in executing this maneuver, this being a near maximum slew for the satellite. In all three cases the holding region was entered directly with neither undershoot nor overshoot.

Figure 3.8 shows the resultant shift in the time-fuel curve if the control torque is increased or decreased by 11%. If we examine the curve with the increased torque we see that for the time optimal case, $(\lambda_2 = 0)$, both time and fuel are less than time and fuel for the standard torque. Indeed, the entire curve is below and to the left of the standard curve, indicating a saving in time and fuel for all cost functions.

This is to be expected since the increased thrust was obtained by an increase in I_{sp} and not by an increase in mass flow rate. If increased thrust came from increased flow rate then clearly time would be less but at time-optimal for instance more fuel would be used. This is true since minimum time is proportional to $\sqrt{thrust}^{-1}$ in the single axis case.

Among the single axis runs which we have made on the hybrid computer, one involving large, known disturbance torques was particularly interesting and could be very relevant to the application if, for instance, a single thruster should become locked open.

Figure 3.9 exhibits a pitch slew of this type, with a disturbance torque one-half of the control torque. This figure was hand drawn from an analog x-y plot and also shows the trajectory with no disturbance torques. In pitch the dynamics are

$$\ddot{\theta} = 6 \cdot 10^{-5} + b$$

and we here let $b = 3 \cdot 10^{-5}$.

Then the second quadrant switching curve is

$$\dot{\theta}^2 = -6 \cdot 10^{-5}\theta$$

and the fourth quadrant switching curve is

$$\dot{\theta}^2 = -18 \cdot 10^{-5}\theta \quad .$$

One may think of this problem with equal validity as being characteristic of unequal bounds on the control torque rather than as a problem with disturbance torques. In such a case we observe that control in the interval $[-a, b]$ will always imply a longer minimum time and a smaller switching rate than the minimum time with control in the interval $[-\frac{a+b}{2}, \frac{a+b}{2}]$.

Of course there is an obvious distinction between unequal control bounds and disturbance torques in that with unequal control bounds the origin is an equilibrium whereas disturbance torques will require compensation to keep the system near the origin.

Figure 10 shows another single axis experiment, this time with degraded thrust. Here the actual torque available is only 75% of that which the control computer expects. This necessarily leads to overshoot. However, the system is most sensitive to unknown thrust changes in time-optimal control and any change toward reducing the rates will reduce over-shoot. This is evident from the graph.

We can comment again on the non-equivalence of λ_2 and λ_3 weighting. It is apparent that for some weighting, say $\lambda = (1, 4, 0)$, the first and second switching points could be made the same as for $\lambda = (1, 0, 0.001)$. In the known-torque case the trajectories would both go to the origin then and be identical. However, because of the overshoot we can observe a difference.

When the $(1, 2, 0)$ trajectory overshoots and goes into the fourth quadrant with an angle of about 0.5° it hits the C_1 curve (see page 84) at a much lower point than it did when the angle was 16°. This causes the observed "flat". Notice that no such behavior occurs in the $(1, 0, 0.001)$ trajectory.
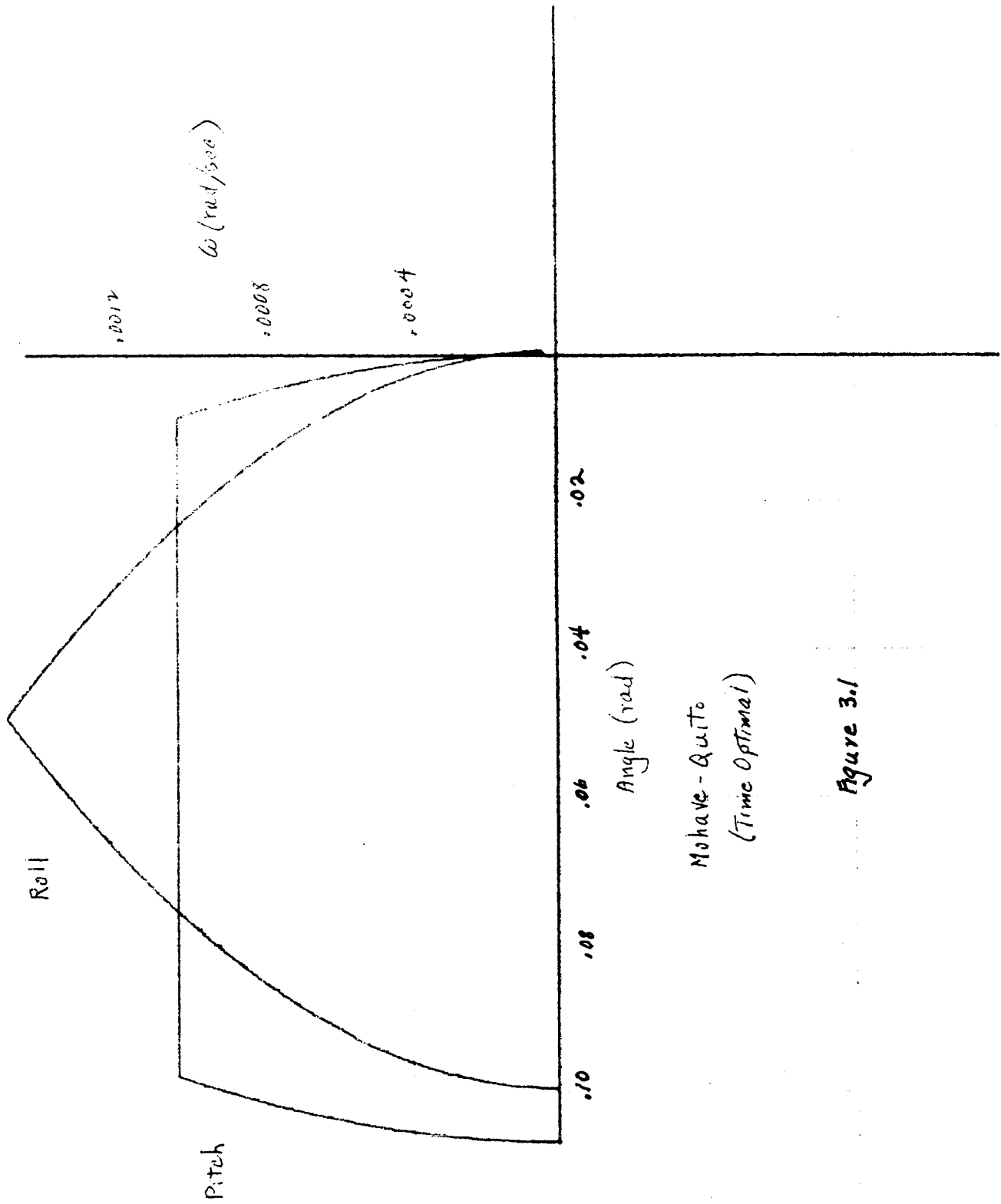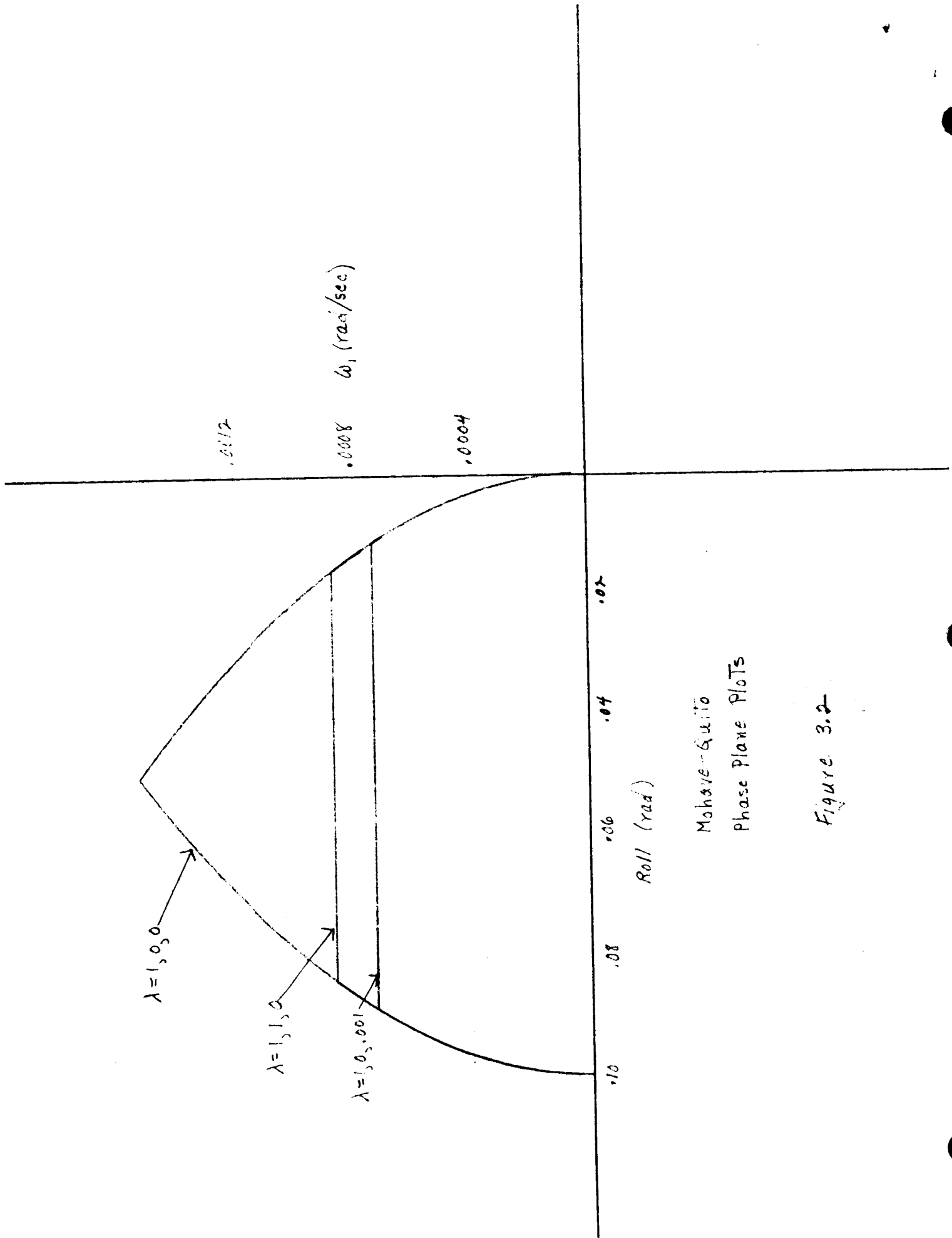
Mohave - Quito
(Time Optimal)

Figure 3.1

Mohave-Quito
Phase Plane Plots

Figure 3.2

ω₁ (rad/sec)

.0012

.0008

.0004

Roll (rad)

.02   .04   .06   .08   .10

λ = 1,0,0

λ = 1,0,0

λ = 1,0,.001

Pitch (rad)

Mohave - Quito

Phase Plane Plots
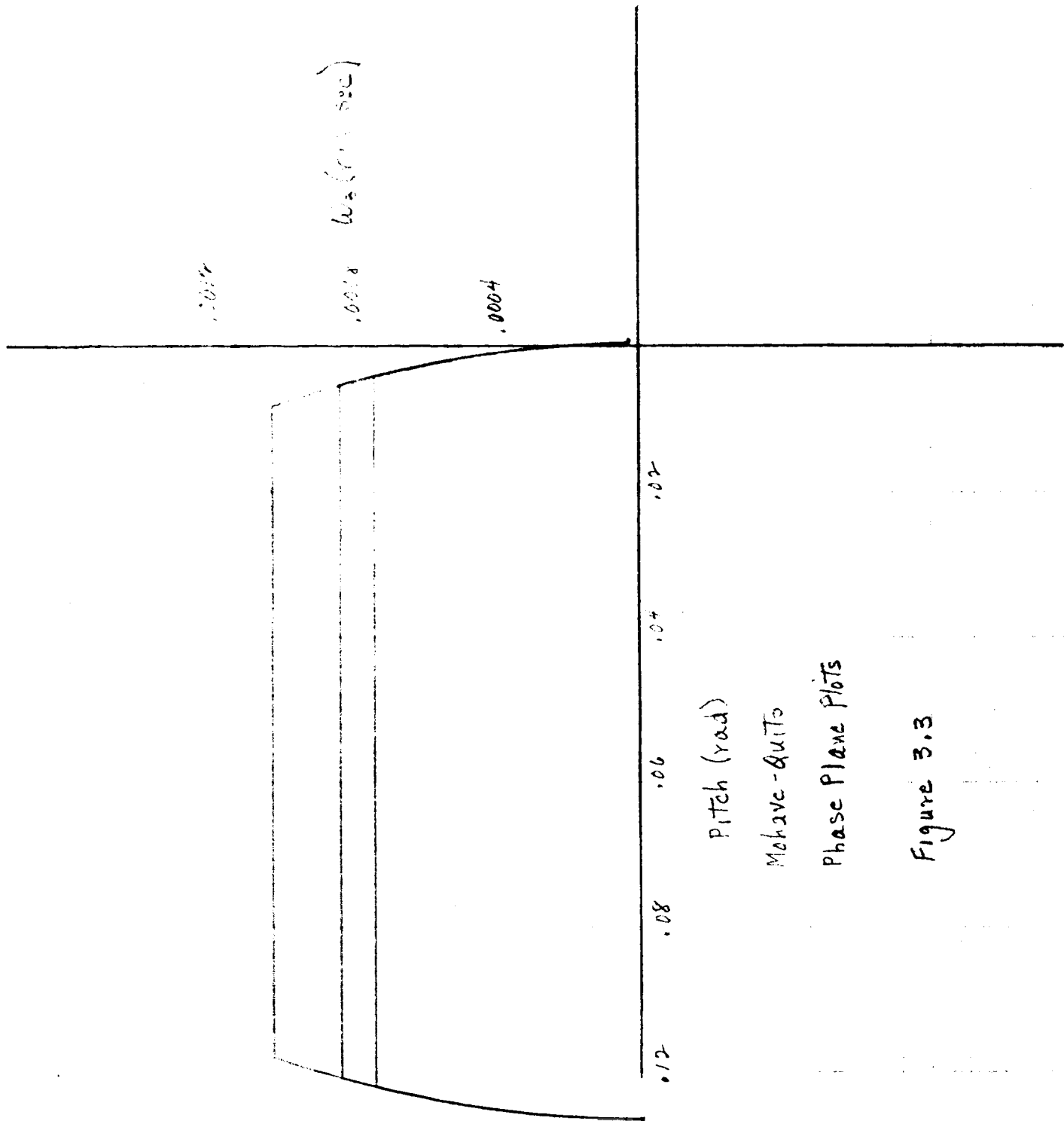
Figure 3.3

FIG. 3.4 Ground Track for Mohave-Quito Slew.

Mohave→

Rosman→.

North
latitude

Time Optimal
λ = 1, 0, 0

Non Time Optimal
λ = 1, 2, 0

Quito

West Longitude

FIG. 3.5 Ground Track for Mohave-Quito Slew.

99

Figure 8.6.

Full Disc Slews.

ω (radians/sec)

.024

.016

.008

λ=1,0,0

λ=1,2,0

λ=1,0,.001

AXIS ⊥ − β (radians)

−.08

−.16

−.24

−.32
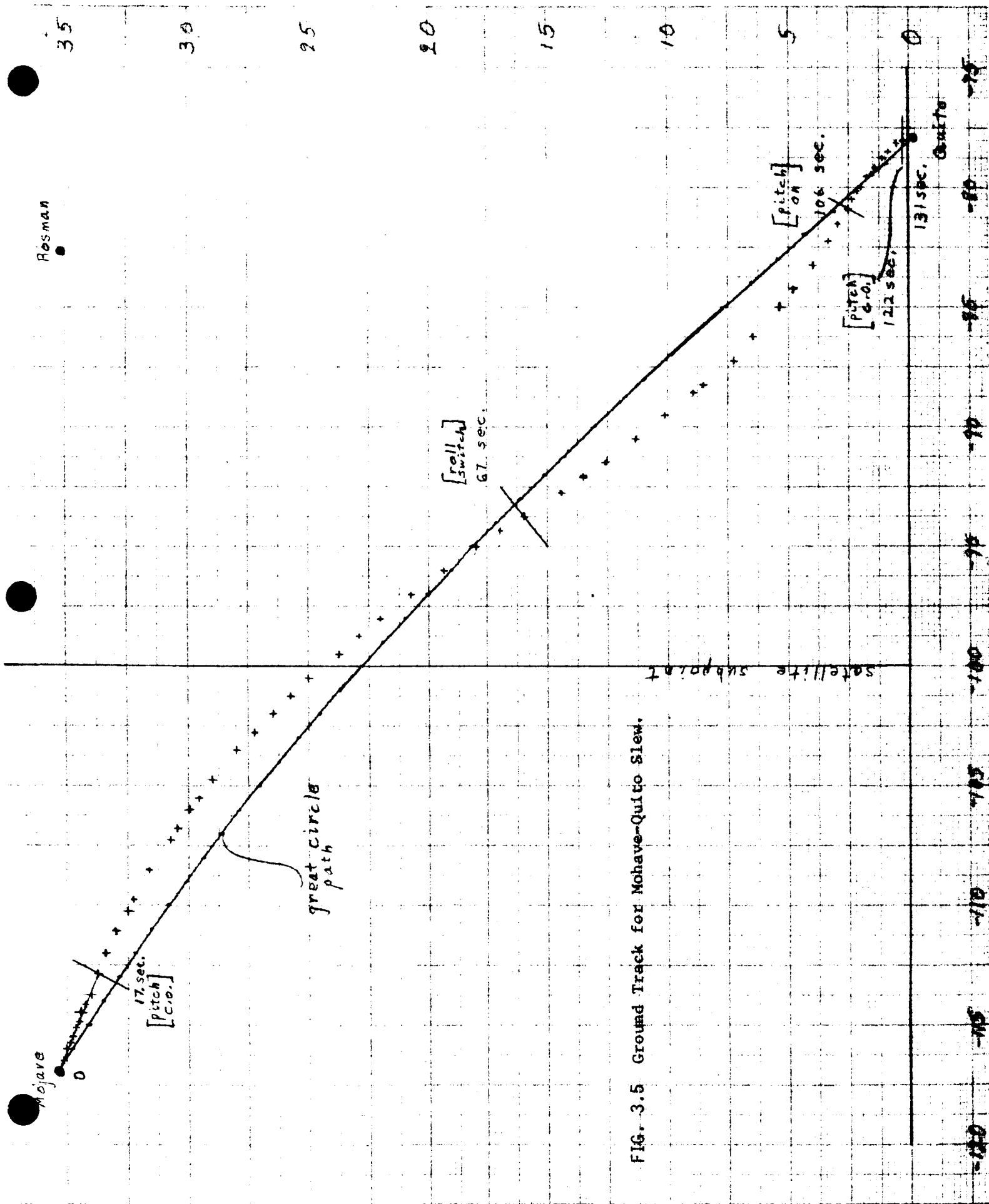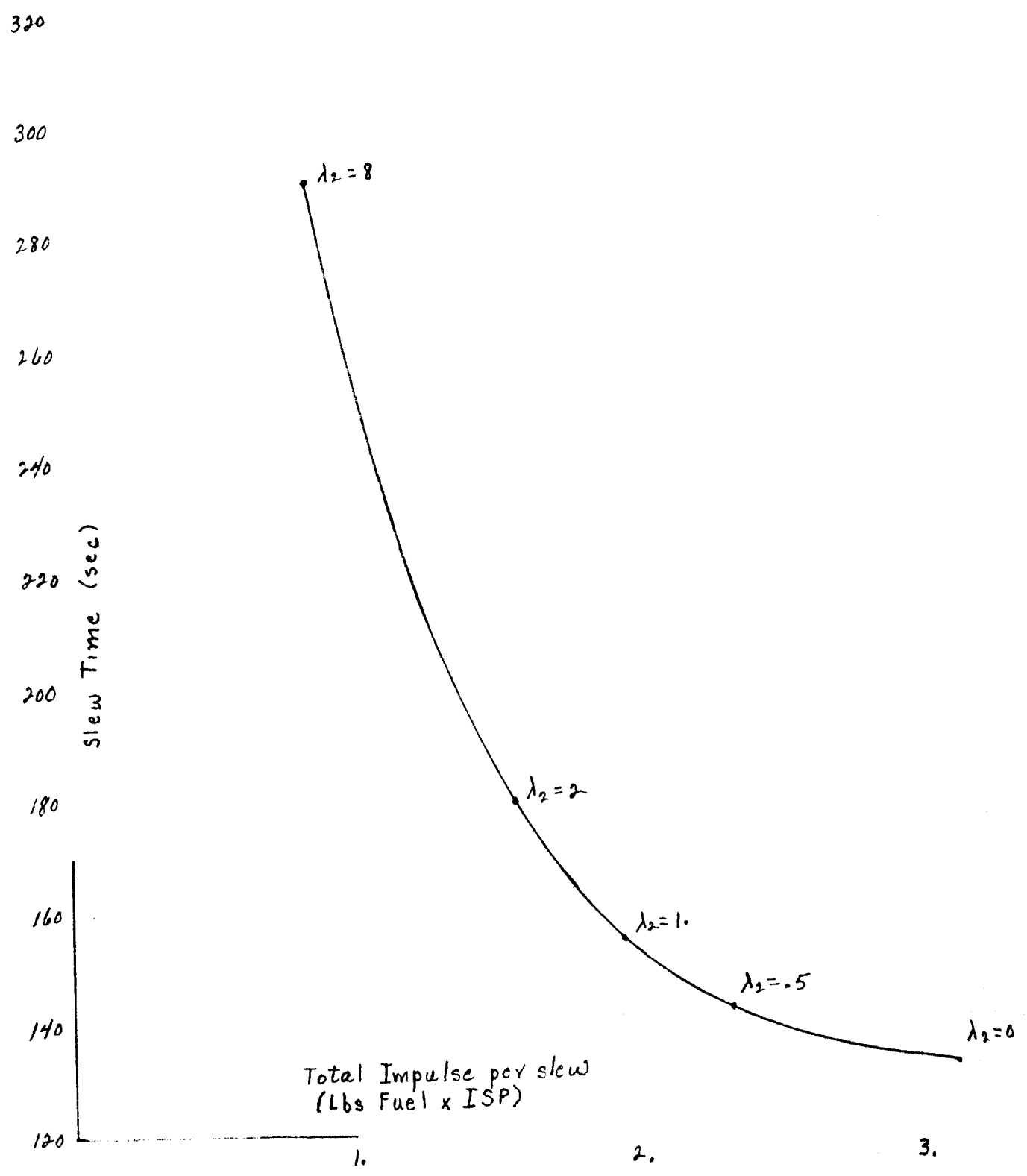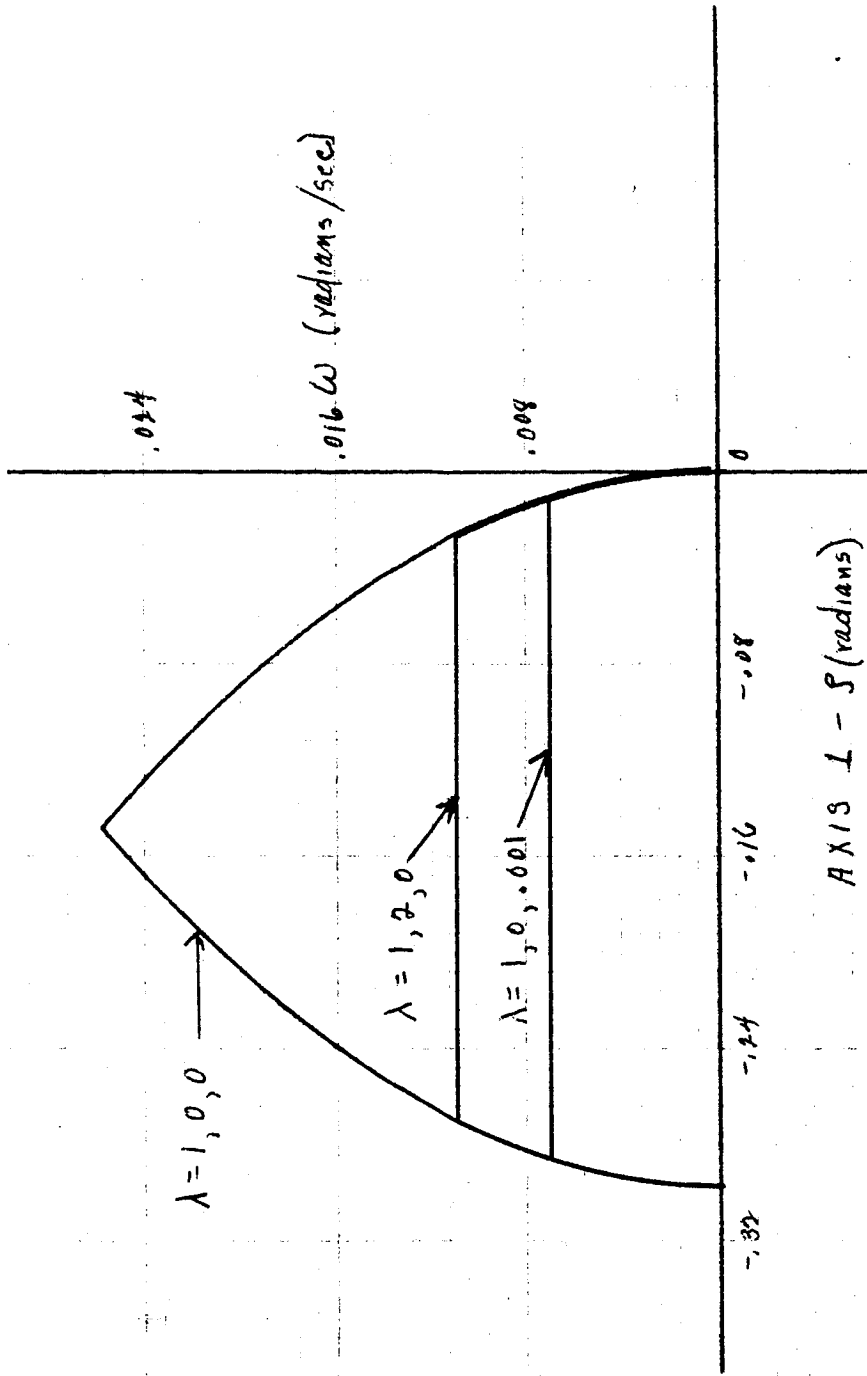
70° S. LAT., 100° W. LONG.
to
70° N. LAT., 100° W. LONG.

Figure 3-7

FIGURE 3.8

TIME – FUEL CURVES FOR IDEAL THRUSTER
(MOJAVE – QUITO)

102

FIG. 3.9 Phase plane plot – Disturbance torque equal one-half control torque.

FIGURE 3.10

PHASE PLANE 140 DEGREE GROUND TRACK MANEUVER
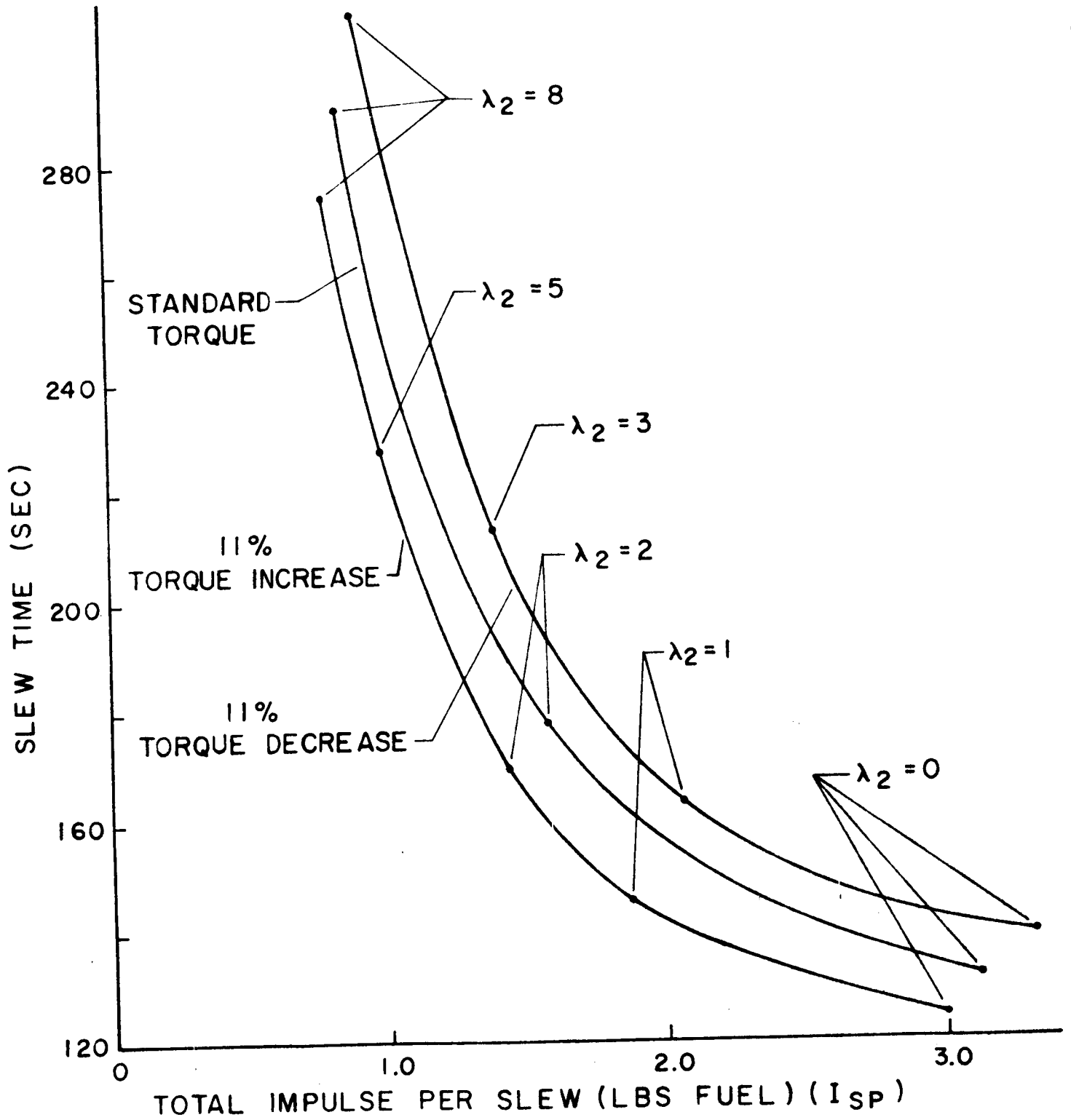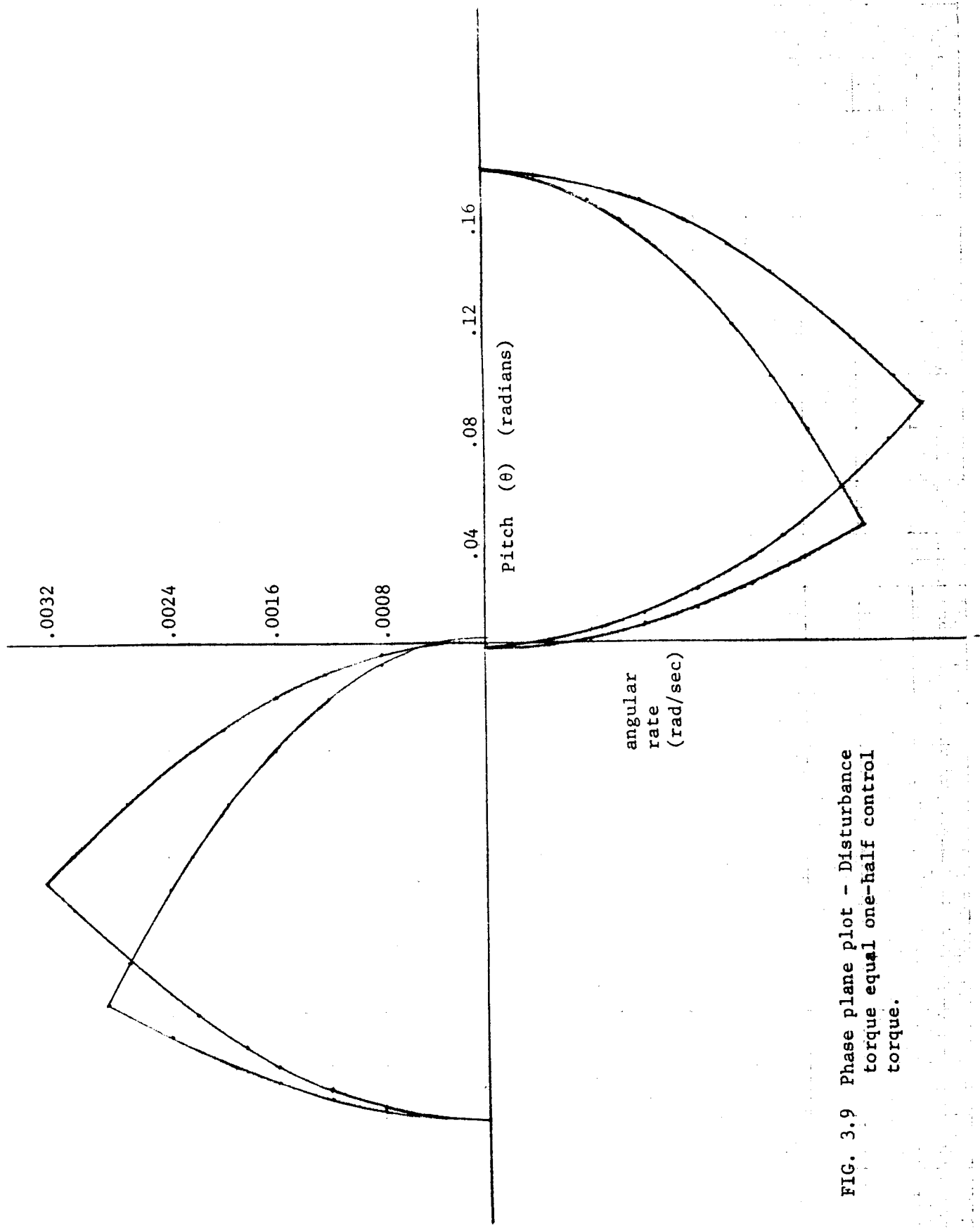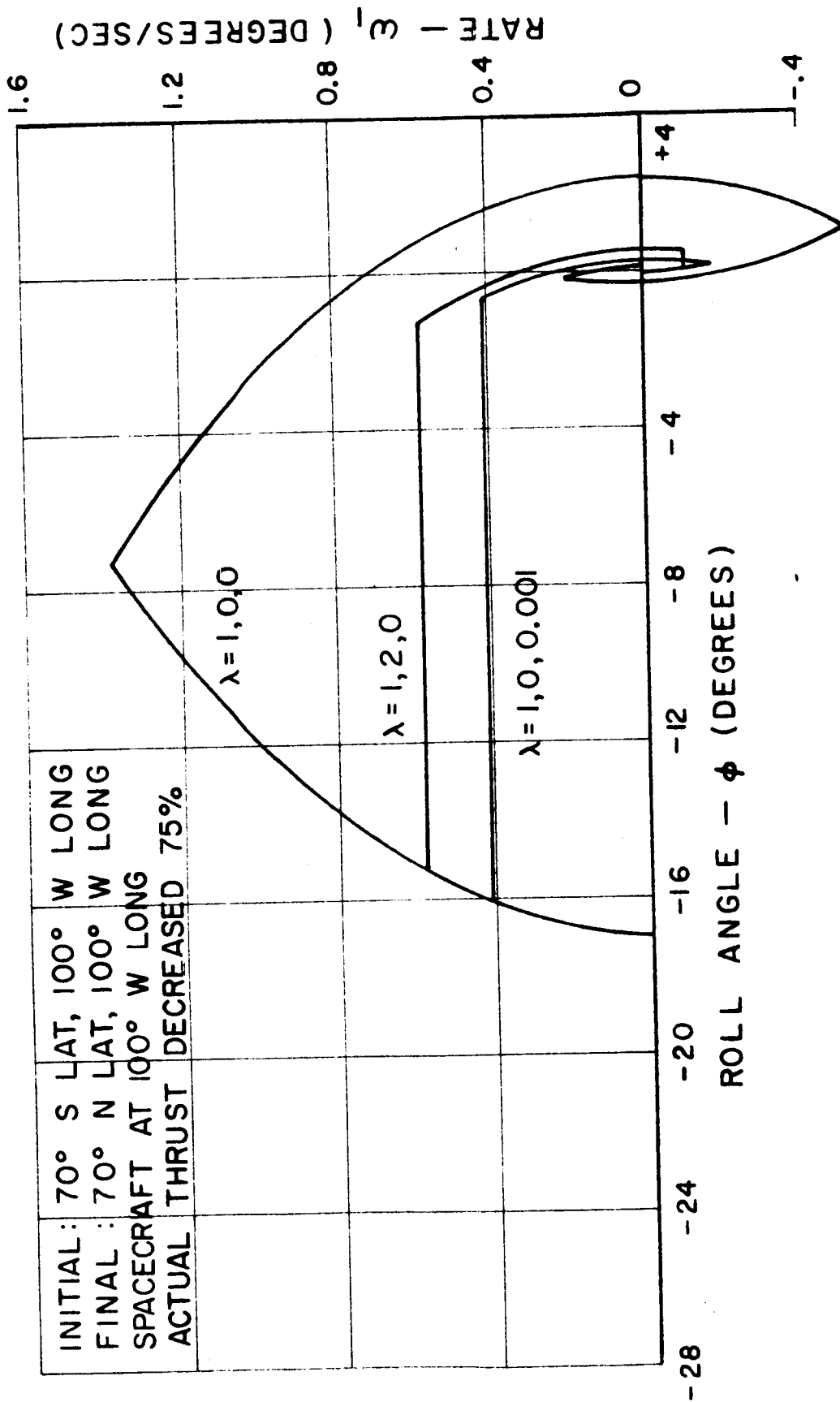
PART IV

THE EFFECTS OF REALISTIC CHARACTERISTICS OF SENSORS

AND THRUSTERS ON SYSTEM PERFORMANCE

I. *Introduction*

Previous chapters have discussed in some detail the synthesis
of the control law and its application under certain ideal situations
where the satellite is rigid, its state is known perfectly, and ideal
thrusters are available. In Chapter V a short investigation will be
made into the effects of vehicle flexibility.

In this chapter, however, we wish to consider the effects of
certain characteristics of the real thrusters, and, in addition, test
the filter used to process sensor information when only noisy angles are
available. The simulation set-up is the same as that described in Part III
except that all runs with real thruster simulation have been made on the
hybrid computer.

The overall block diagram shown as frontispiece to this report
presents the major functional parts of the simulation complex. This
could be considered as a ground-based simulation model, a spacecraft
onboard control model, or a spacecraft-to-ground linkage and control
model. The pre-filter refers to processing of sensor outputs to verify
the presence of useable data or to reject signals which can be shown to
lie outside of prescribed measurement bounds. Thruster selection is in-
cluded to allow for more than one control jet on a given axis (redundancy),
and the selection input command would be by telemetry link or digital
input to the onboard control system. The sensor-to-filter link can be
considered as spacecraft to ground telemetry, or straight forward analog
to digital conversion within a simulation system.

Real thruster effects considered in this section deal with mathematical modeling of thrust magnitude versus time resulting from rise-time transients, thrust level decay during extended pulse operation, and tail-off behavior. First order exponential response is assumed for approximation of real behavior. The control impulse (H_1) added to the spacecraft during thrust turn-on is given by:

$$H_1 = \int_0^{t_1} A(1 - e^{-\lambda_1 t})dt$$

where A is defined as the initial steady state thrust magnitude, t_1 is duration of turn-on command, and λ_1 is the reciprocal rise time constant. During extended thrust-on periods, the actual steady state level can decrease as the result of regulation system behavior. This can occur in the form of variations in mass flow rate or variations in specific impulse due to thermal transients. The control impulse (H_2) added to the spacecraft during this interval can be represented by:

$$H_2 = \int_{t_1}^{t_2} A[1 - K(1 - e^{-\lambda_2(t-t_1)})]dt$$

where K is the steady state bias constant in control torque, t_2 is time of thrust-off command (assuming no valve lag), and λ_2 is the reciprocal thrust decay constant.

The thrust tail-off behavior results from stored energy in the propulsion device that does not reduce instantly to zero upon off command. The control impulse (H_3) added to the spacecraft during this interval is given by:

$$H_3 = \int_{t_2}^{\infty} \left\{ A[1 - K(1 - e^{-\lambda_2(t_2-t_1)})]e^{-\lambda_3(t-t_2)} \right\} dt$$

106A

where λ_3 is the reciprocal tail-off time constant. The total impulse added to the spacecraft (H_t) during a full jet firing cycle from on-to-off is the sum of H_1 plus H_2 plus H_3. Typical values of real effect constants used in the study program are:

$$\lambda_1 = 10 \text{ seconds}^{-1}$$
$$\lambda_2 = 0.0115 \text{ seconds}^{-1}$$
$$\lambda_3 = 3.333 \text{ seconds}^{-1}$$
$$K = 0.3913$$

The relative importance of each control impulse term, H_1, is dependent upon time constants involved and the total jet-on time required to perform a given slewing maneuver. The above constants are representative values supplied by the government for a thermal storage resistojet using a sonic metering orifice and operating in the millipound thrust regime. Large angle slewing operations, such as from Mohave to Quito tracking stations, would require on-times in the range of 120 seconds or more based upon actual simulation data. For such cases rise and tail-off impulse variations are but a small percentage of the total impulse needed to perform the given maneuver. Early simulation tests revealed that only the thrust decay effects were of importance in such slewing operations. However, for very small angle slewing modes (e.g. 0.2 degrees) the total control impulse becomes small and rise-tail-off effects are now important.

The above thruster simulation model assumes that positive and negative torques are generated within the same control device. In the subject case, the device would be a multijet version of a heated-gas thruster. In this approach, control impulse H_2 would continue to

decrease upon switchover from a positive roll jet to the negative roll jet. If, however, separate control jets are employed on each thrust direction, a separate simulation model is required for H_2 to properly represent expected thrust level variations.

The control computer assumes that the force available to it is a constant, whereas the real thruster has a decay characteristic. In order to predict the correct switching points for thruster operation, it is necessary to incorporate either a fine-tuning of control torque input or adjust control policy to account for thrust-time behavior. If not compensated, this would invariably lead to overshoot relative to the target. This leads to no instability or failure to terminate at zero, but does introduce a rather wasteful circling of the origin before equilibrium is reached. Certain rather simple procedures are described for alleviating this problem.

Naturally when the sensors provide only angle data, this confusion is even greater since rate derivation is based partly on knowledge of the thrust level.

The complete derivation of the filter appears in Appendix F and only an outline will be given here. The sensor (polaris tracker and vertical indicator) information is linearly approximated by the Euler angles $(\phi, \theta, \Psi)_{br}$, so to avoid any possibility of hybrid timing problems caused by long computation times, the Euler angles themselves (corrupted by additive gaussian noise) were used as sensor outputs. These in turn went through a constant gain Kalman filter to produce the rate and angle estimates upon which control was based.

Since commands to initiate a slew will come from the ground, we assumed that the filter would start each slew with correct angle and rate estimates, especially since the initialization of these quantities could itself be the command to slew.

Our conclusions, in brief, were

1) With the present filter, the lack of rate information does not seem to inflict any added costs.

2) Real thrusters involve added costs but these penalities decrease automatically as the trajectory is removed from time-optimality.

II. *Experiments*

The basic slew here is Mojave-Quito, time-optimal.

1) <u>Noiseless with filter</u>. This run was made using the filter but with no noise on the signal. That is, only angle data was available, but it was correct.

The runs are indistinguishable from the runs in which the state is fully known.

2) <u>Filter with noise of standard deviation, $\sigma = .00063$</u>. This is the realistic sensor case as described in Appendix F. Again the run is indistinguishable from the ideal case. To illustrate this, the phase plane plots of ϕ and θ appear in Figure 4.1 and 4.2, the time traces of ϕ, u_1, and u_3 in Figure 4.3. Notice that there are no additional actuations and the satellite goes directly to zero.

3) <u>Noiseless with filter and real thruster</u>.

This gave us some interesting results. The phase plane plots of ϕ and θ appear in Figure 4.4 and 4.5, the time traces of ϕ, u_1, and u_3 appear in Figure 4.6. Examine Figure 4.5 first.

This axis (pitch) is under control of the time synchronization since it is "closer" to the origin in terms of the quantity $\dfrac{\theta(0)I_3}{T_3}$.

Therefore the time during which thrust decay takes place is only about 18 seconds (see the two u_3 bursts in Figure 4.6). This leads us to

expect only a small overshoot in θ since the control force is close to what the control computer expects. In fact, comparing Figure 4.2 and Figure 4.5, we find that a small undershoot in Experiment 2 is nicely eliminated. This is the type behavior expected in non time-optimal runs and gives us one method of compensating for thrust decay.

Figure 4.4 shows the problems, and there are at least two. First there is a bad overshoot caused by the fact that the switching curve is incorrect for the available thrust. Second there is an early change of sign caused by the filter's lagging estimate of the state. As a small additional time passes, the filter obtains a better estimate, reverses sign to go up to the switching curve and then comes down on such a short axis that the reduced thrust is unimportant.

Actually this run is a gratifying check on the filter operation. The previous two runs have been so close to the ideal that there could easily be a suspicion that the filter was not using external data at all. Here we see that such is not the case. At the time when the ideal model would be at the origin, the filter was aware of the error and did not shut off control. Because the thrust is lower than expected, there is a tendency to estimate the rate too far in the direction of thrust. This is illustrated in the early switch (second switch). Then as time passes the third and fourth switches are made bringing the satellite home.

A discussion of thrust decay compensations in the control computer will be deferred until after the last experiment is described.

4) **Filter, real thruster, σ = 0.00063**

The discussion of experiment 3 was heavily weighted toward explanation of the trajectory by means of the filter behavior. This is because the behavior under reduced thrust is predictable, consisting of decreasing overshoots until the deadzone is reached. Any departure from this pattern is necessarily a result of the filter behavior. In the present experiment we can see more evidence of this.

Looking at Figures 4.8 and 4.9, we see that θ goes to the origin in the usual way, as we would expect, thus entering the fine pointing mode.

Looking at Figure 4.7 we see almost the same behavior of ϕ as in experiment 3 . There is the premature second switch caused by over-estimating the rate. But now the combination of the noisy observations and the underestimation of rate during negative control causes the filter to think the satellite is home before it actually is. This at present would cause the entry to holding mode prematurely. Nevertheless because the angle is small, such a change of mode would no doubt be successful. The trajectory was allowed to continue, however, and very shortly an entry to the actual deadzone occurred.

If estimation problems were occurring for large angles, this lag in the estimator could be corrected by increasing the gain. At low signal levels, however, the filter must depend upon its knowledge of the dynamics and when that is faulty as here, the thrust being low, the filter will show errors.

5) **Thrust decay compensation by thrust understatement.**

The thrust decay problem can be alleviated by understatement of the thrust. This can be done precisely, very much in the same logical

way as the time synchronization is done. However, the switching curve is not too sensitive to this as the Figures 4.10 - 4.12 show and we can do it much more roughly.

The thrust in each axis as known to the control computer is 70% of the initial value T_o of the thrust. (The actual asymptotic value of thrust is about 60% of T_o.) Since this is a reasonably close value in axis one and since the slope is not too important in axis three because of the low rate, we obtain quite satisfactory performance.

This run also used the filter on noisy data.

Figure 4.16 shows a time-fuel curve for the thrust understatement compensation. If we were to optimize the multiplicative factor, using a somewhat smaller value, we could obtain a curve with a minimum time of approximately 140 seconds. This run was made without the filter.

6) Thrust compensation by fuel conservation.

We have seen throughout that axis three is relatively unaffected by thrust decay. This leads us to attempt compensation by keeping the thrust on-time short.

This was done, letting $\lambda = (1, 3, 0)$ in all three axes.

This was quite successful as the phase plane plots Figures 4.13 and 4.14 show. However, there was a problem along the axis one switching curve. This is the curve c_1 in Figure 2.1. Figure 4.15 shows u_1 chattering on this curve. This deserves comment not only in itself but because we showed no chatter in any previous runs. There are two factors causing the situation. The first is quite simply that the c_1 curve

111

has never been softened as the main switching curve and the time

synchronization switches have.

The reason for this is that the c_1 curve falls away from a

constant rate trajectory and this, in the noise-free case, has always

been sufficient to prevent chatter along this switching curve. The

second reason is the previously mentioned over-estimation of rates in

the thrust decay case. When control is set to zero this overestimation

corrects itself and the vehicle then finds itself below the switching

curve.

The combination of these two effects caused the three extra

actuations which appear in u_1. These could be removed by a simple

softening of the c_1 curve.

Using perfect angle and rate information, as in Figure 4.16, a

time-fuel curve Figure 4.17 was generated using the real thrusters with no

thrust understatement. The lesson to be learned from Figure 3.6, Figure 3.10,

and this plot is that not only does a weighting of about (1, 1, 0) put

the vehicle in a favorable time-fuel tradeoff position but it renders

the control quite insensitive to thrust level changes. This is of course

to be expected since time optimal trajectories are well-known to have many

undesirable properties. For instance, notice that the fuel and time

required for (1, 1, 0) in Figure 4.17 is very little different from

that used by ideal thrusters as shown in Figure 3.6.

This is very important. A great deal of study today in theoretical

and applied control is devoted to the design of control systems which are

insensitive to parameter changes. For instance if a parameter can be expected

to change by 5% and this degrades the optimal performance index by a large

amount it may be preferable to choose another control which is not as good

for nominal parameters but is flat over the expected variations.

This is approximately the situation we obtained by using the (1, 1, 0) weighting. By using a trajectory which remains a shorter time on the (possibly incorrect) switching curve, we render our costs less sensitive to system modeling errors. In addition we can expect such trajectories to be somewhat less sensitive to the combined filter-thruster errors.

Thus, unless the required trajectory time exceeds some minimum time available for the slew, time optimal control should be avoided.

FIG. 4.1 Experiment 2 - Phase plane plot of roll (ϕ).

FIG. 4.2 Experiment 2 - Phase plane plot of pitch (θ).

roll angle (ϕ)

-roll control

-pitch control

Time → (5 sec/interval)

FIG. 4.3 Experiment 2 - Time histories

116
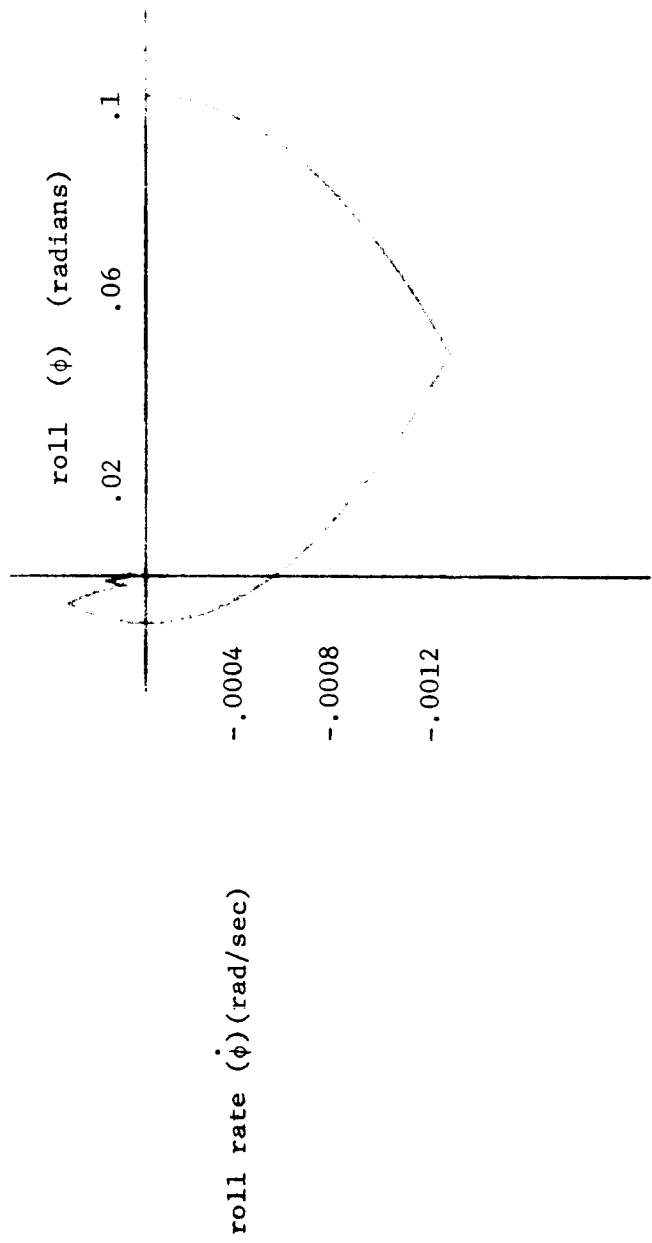
FIG. 4.4 Experiment 3 -- Phase plane plot of roll (ϕ).

117

FIG. 4.5 Experiment 3 - Phase plane plot of pitch (θ).

118

roll angle (ϕ)

-roll control

-pitch control

Time → (5 sec/interval)
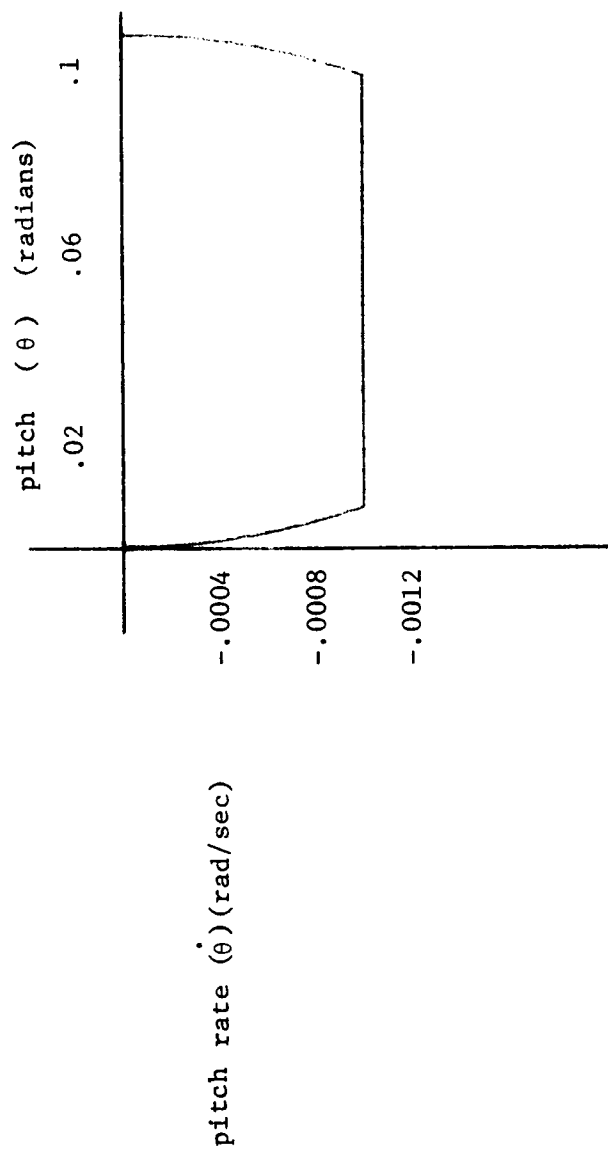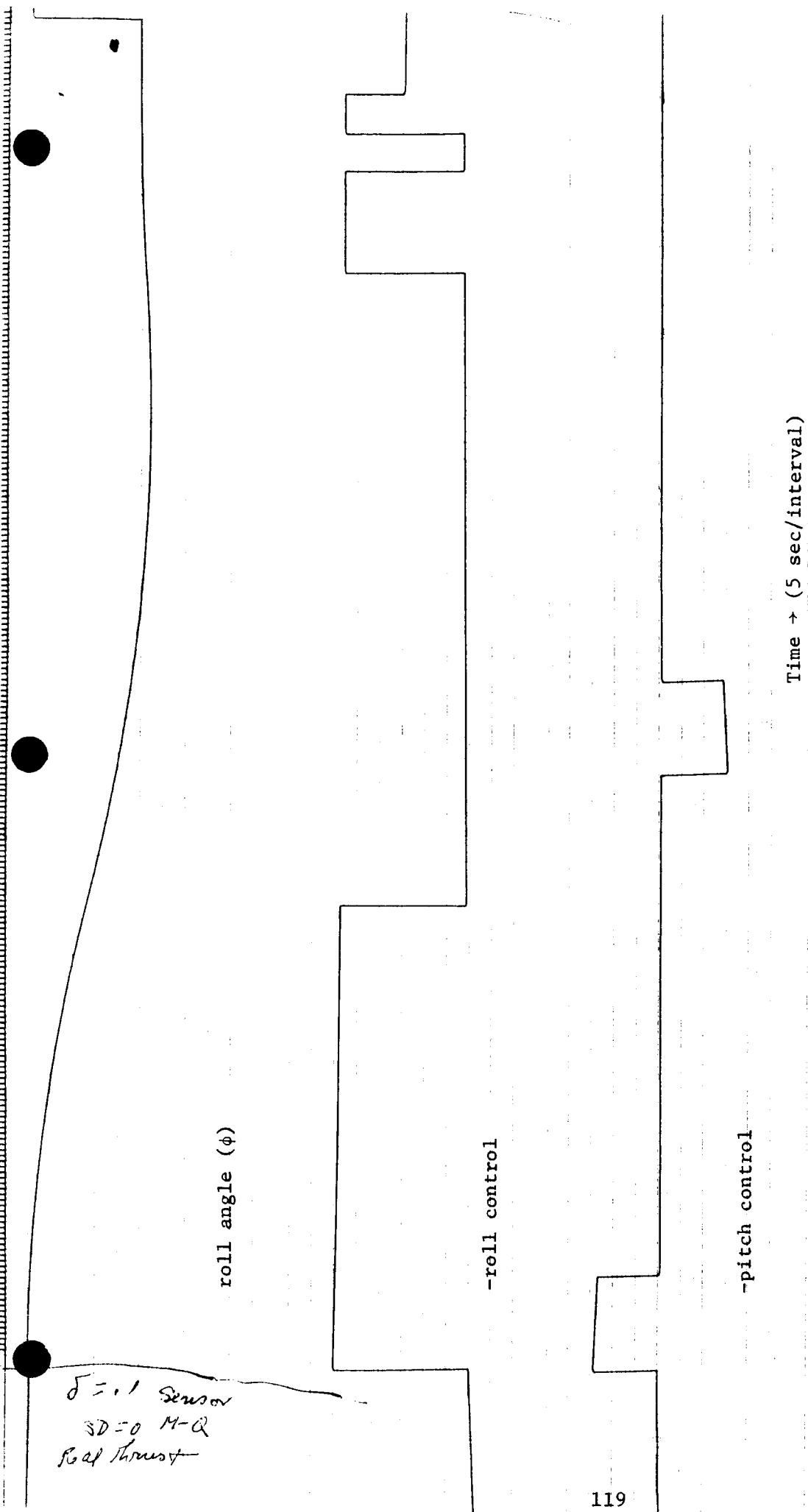
FIG. 4.6 Experiment 3 - Time histories

$\delta = .1$ Sensor
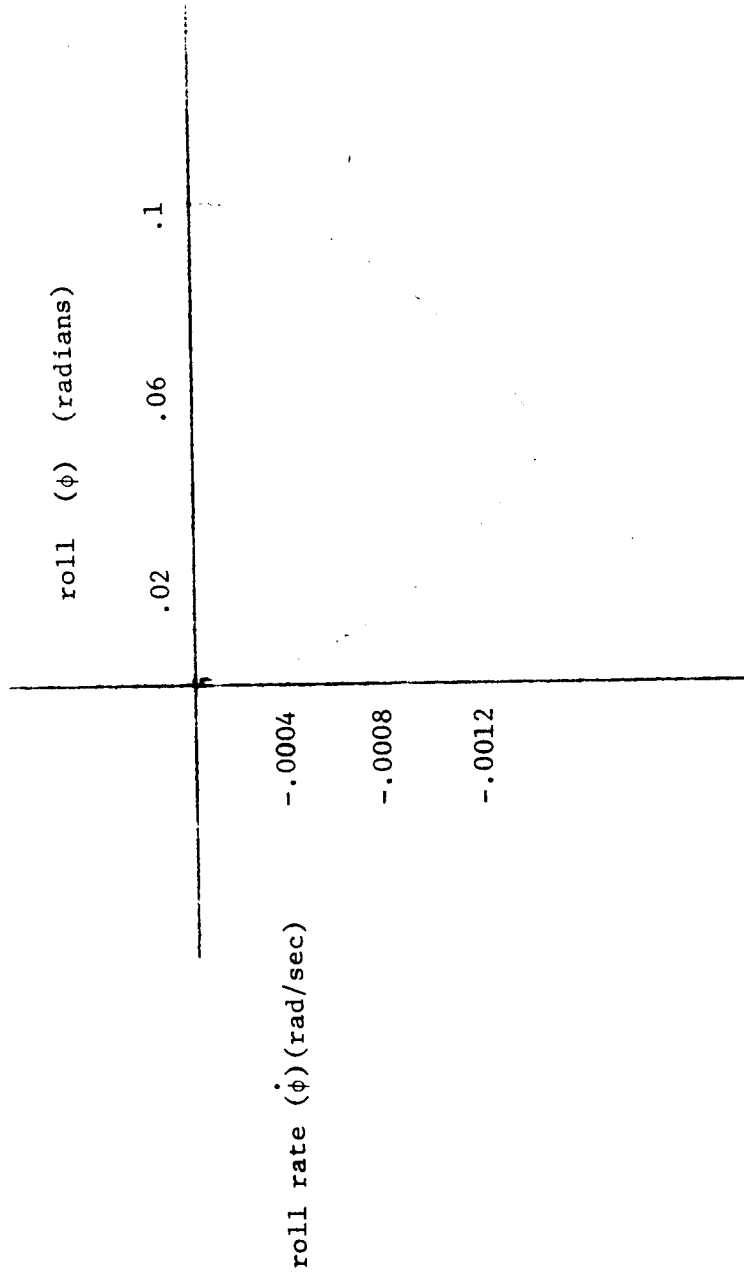$SD = 0$ M-Q
Real thrust

119

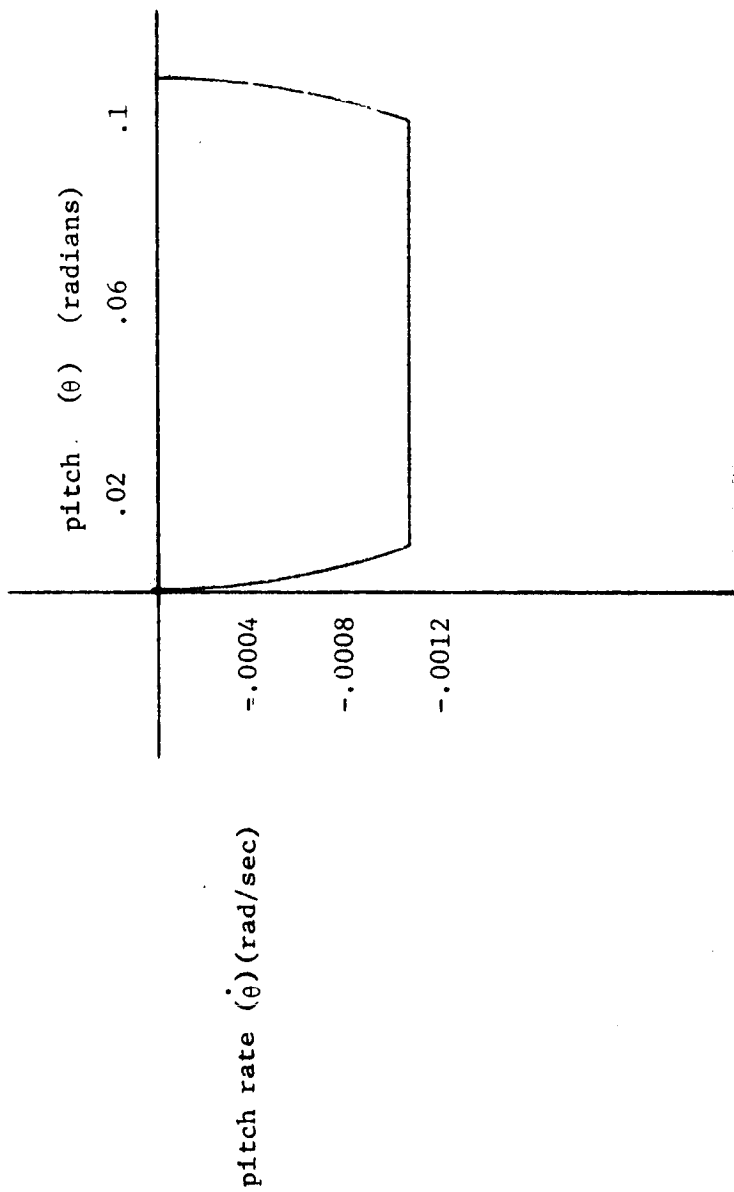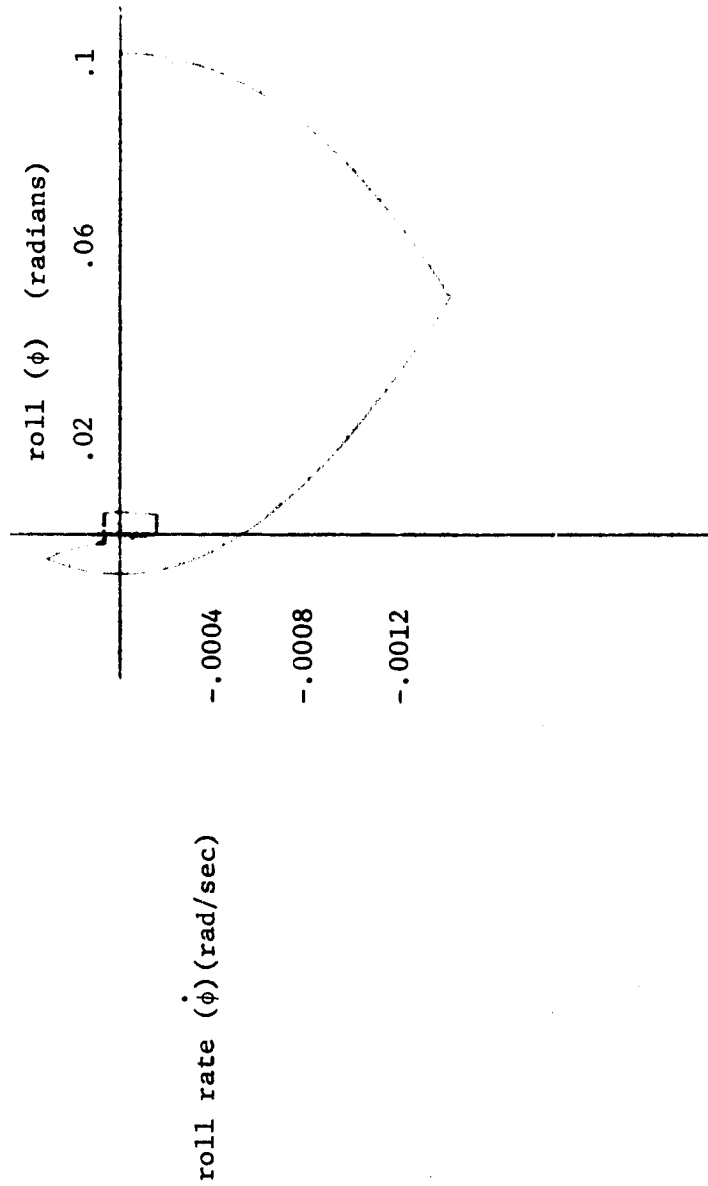FIG. 4.7 Experiment 4 – Phase plane plot of roll (ϕ).

FIG. 4.8 Experiment 4 – Phase plane plot of pitch (θ).

121

roll angle (ϕ)

-roll control

-pitch control

Time → (5 sec/interval)
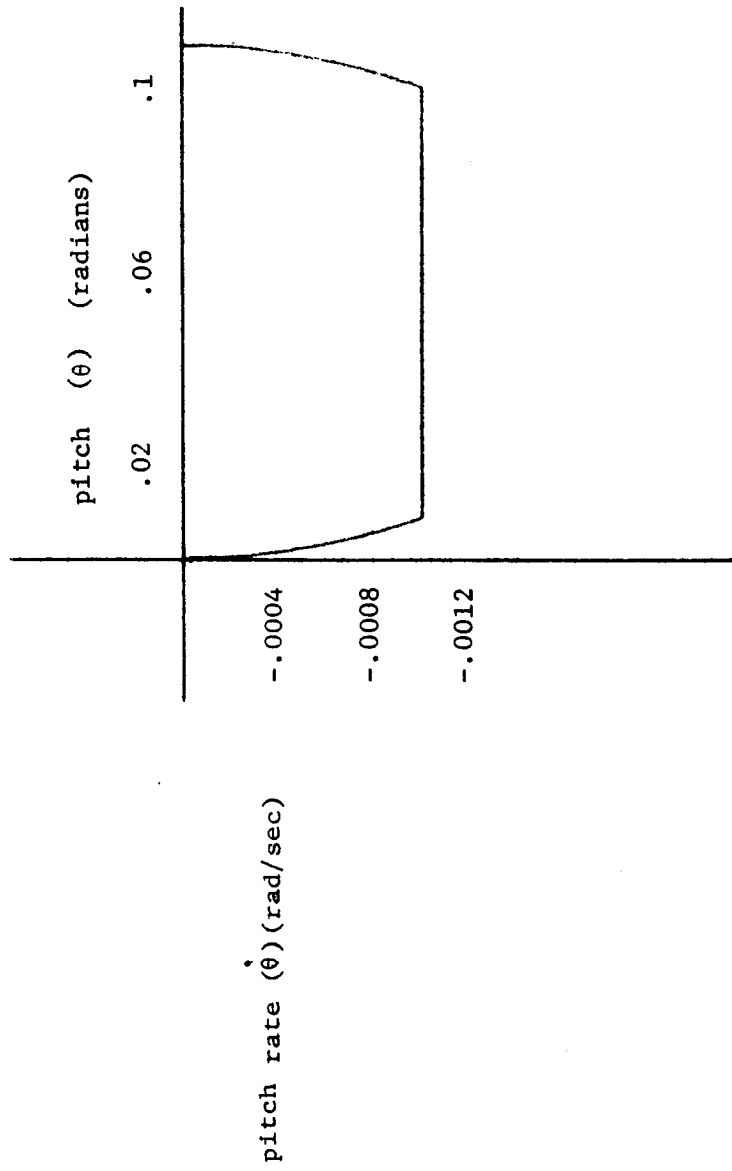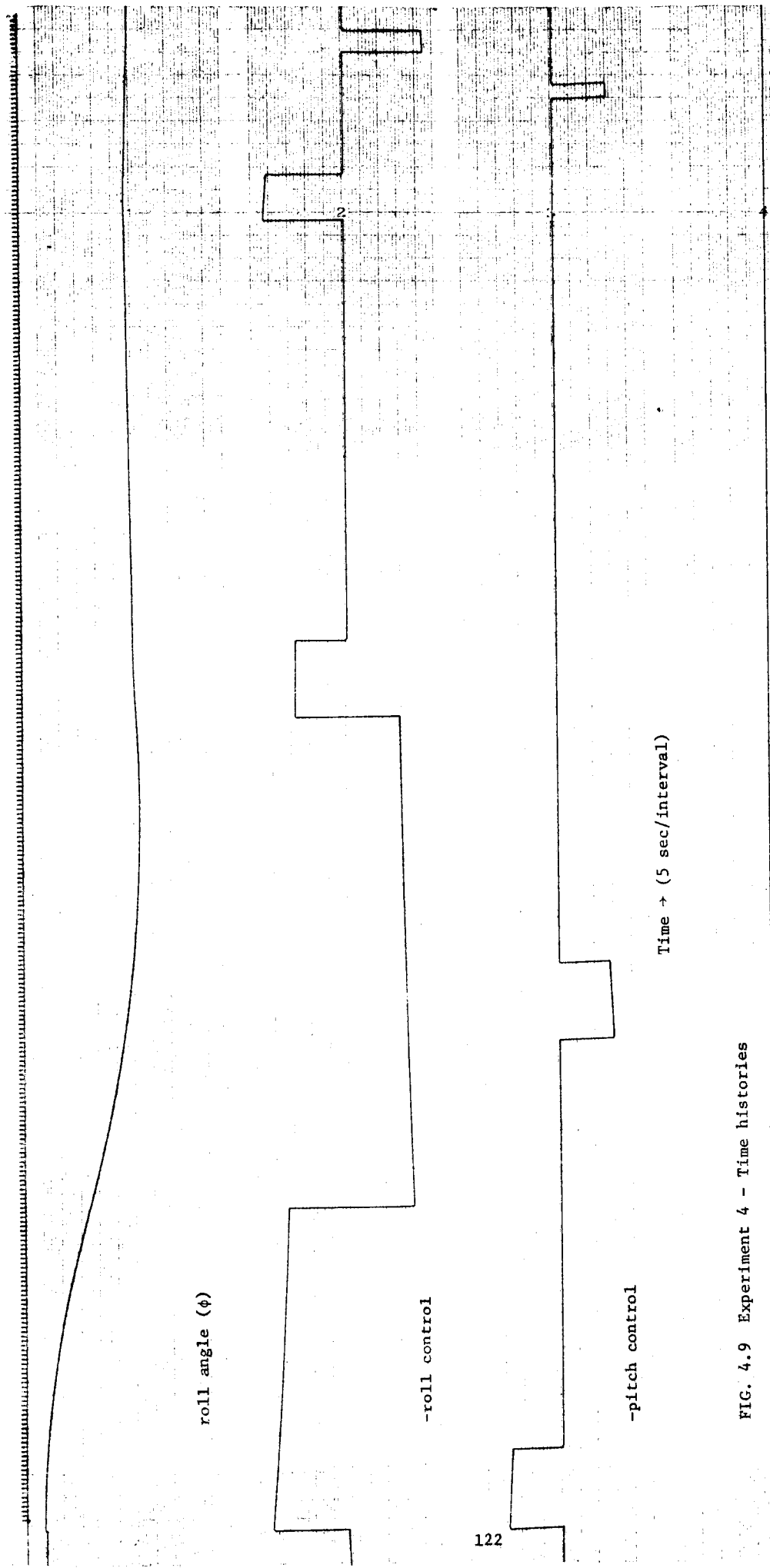
FIG. 4.9 Experiment 4 – Time histories

122
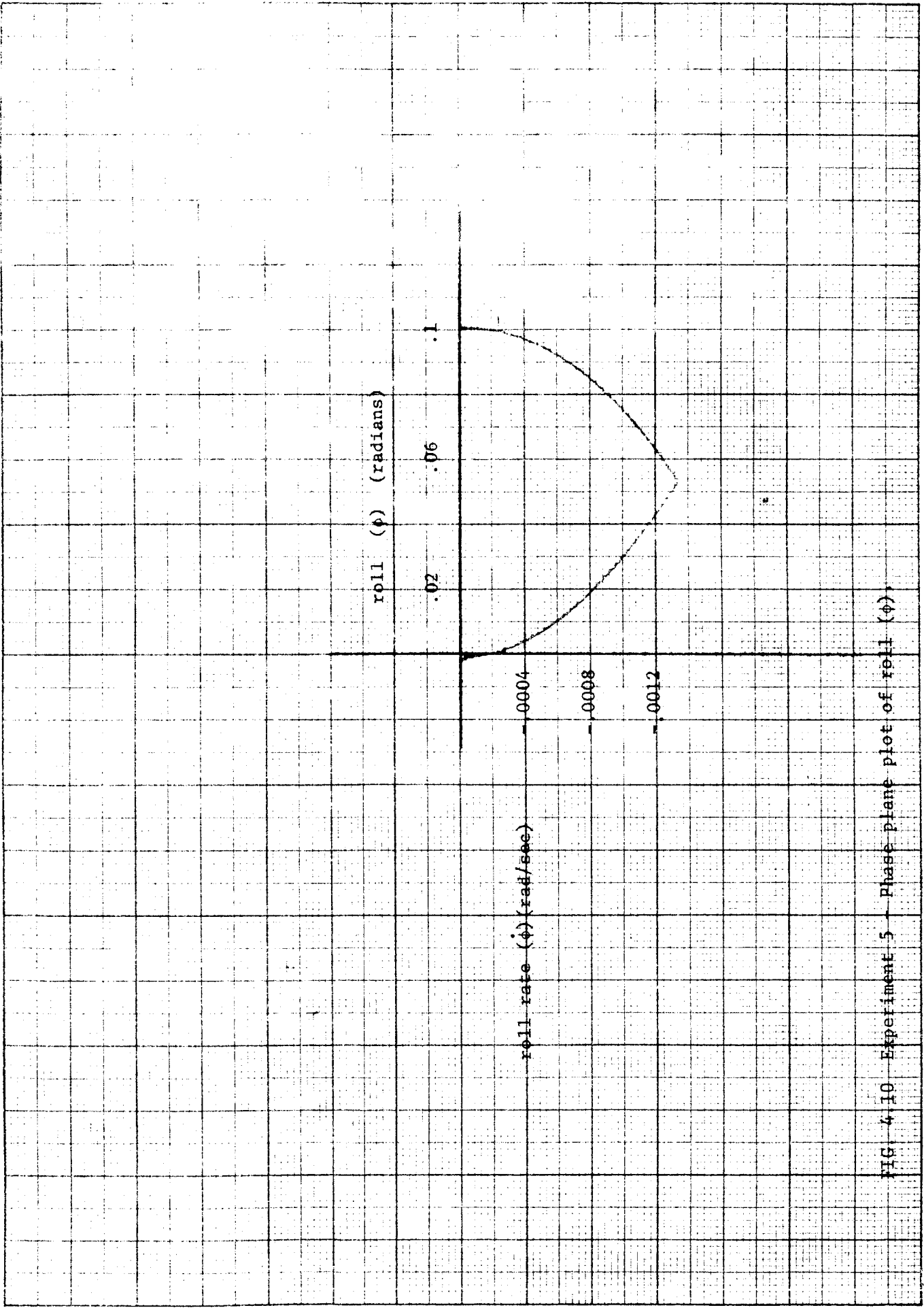
FIG. 4.10 Experiment 5 - Phase plane plot of roll (ϕ).

roll (ϕ) (radians)

.1   .06   .02

roll rate ($\dot{\phi}$) (rad/sec)

.0004   .0008   .0012
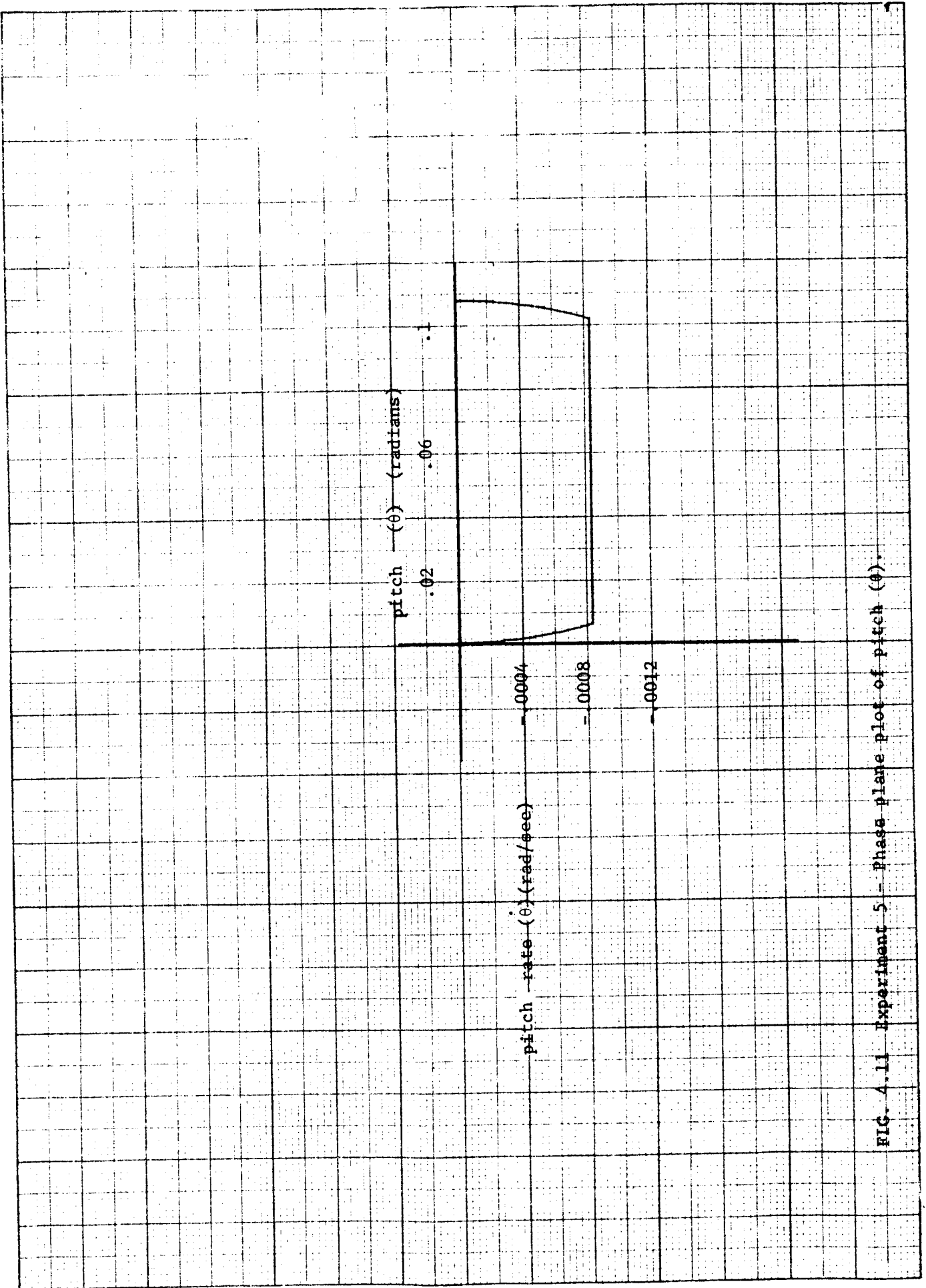
FIG. 4.11.- Experiment 5.- Phase plane plot of pitch (θ).

roll angle (ϕ)

-roll control

-pitch control

Time → (5 sec/interval)

FIG. 4.12   Experiment 5 - Time histories
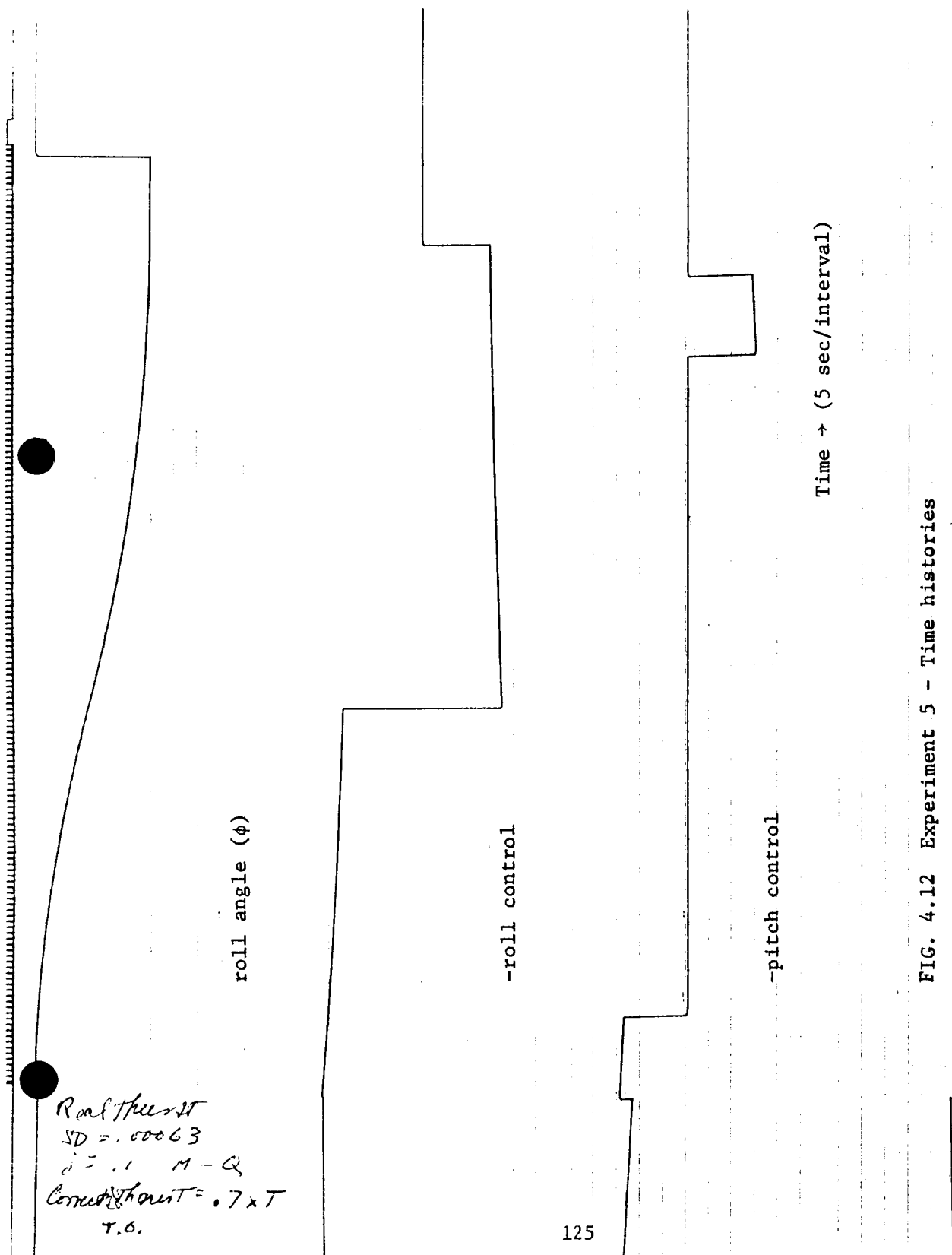
Real thrust
SD = .00063
$\dot{a} = .1$ M - Q
Corrected thrust = .7 x T
T.O.

125
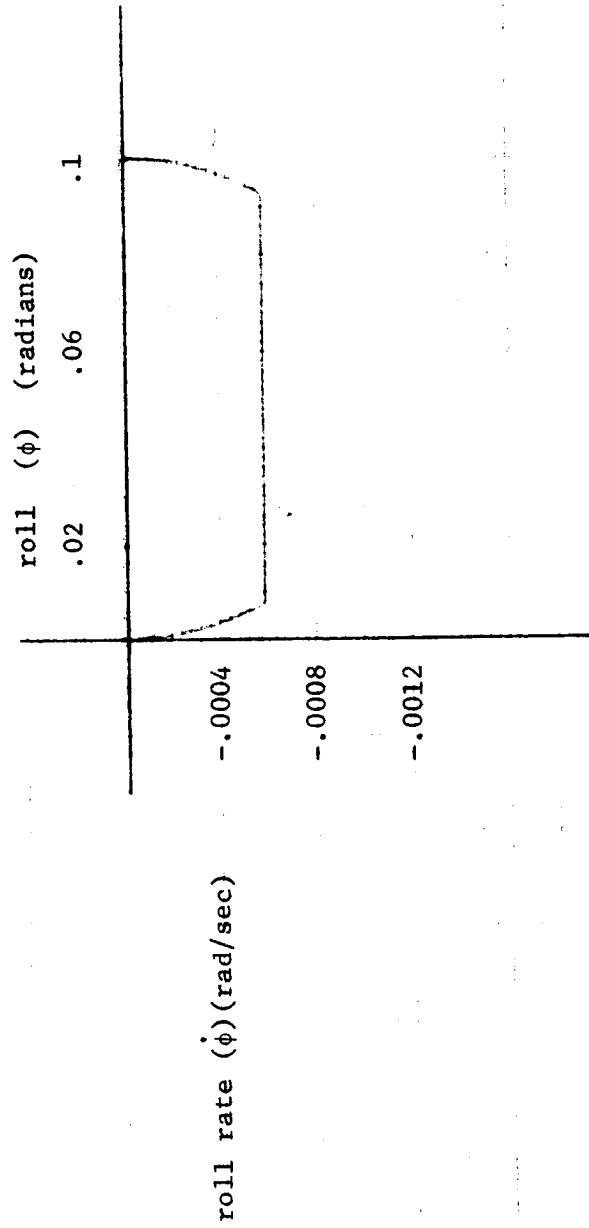
FIG. 4.13 Experiment 6 – Phase plane plot of roll (ϕ).
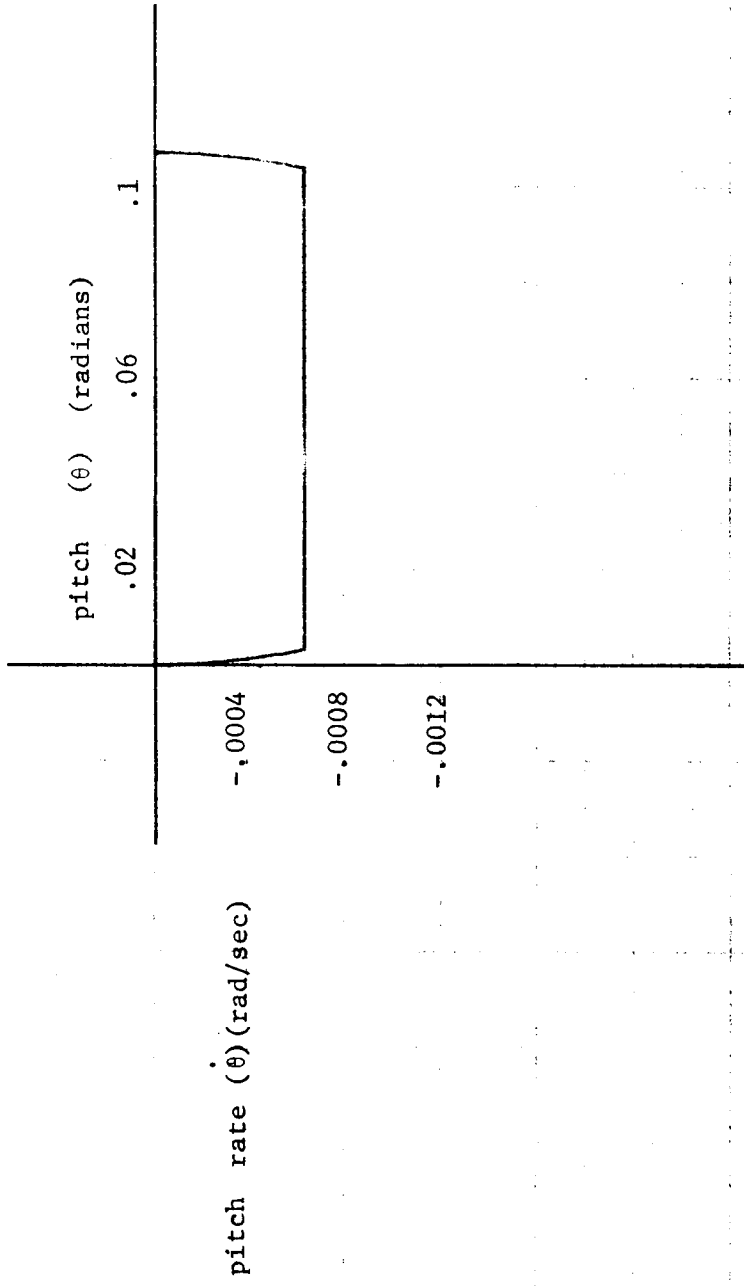
FIG. 4.14 Experiment 6 – Phase plane plot of pitch (θ).

roll angle (φ)
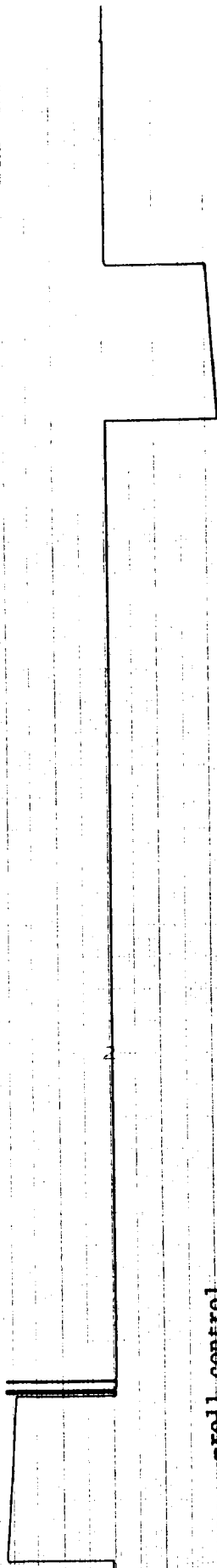
-roll control

-pitch control

Time → (5 sec/interval)
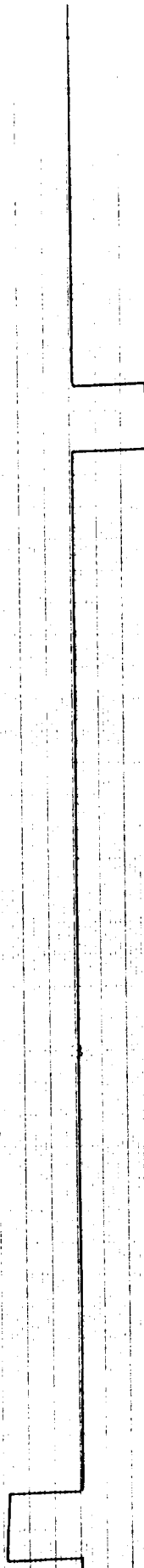
FIG. 4.15 Experiment 6 - Time histories

Real Thruster Effects with Modified Control Time-Fuel Curve (10 % Thrust Factor) (Mohave - QuiTo)

FIGURE 4.16

Slew Time (sec.)

Fuel Expended (lbs/ISP slews)
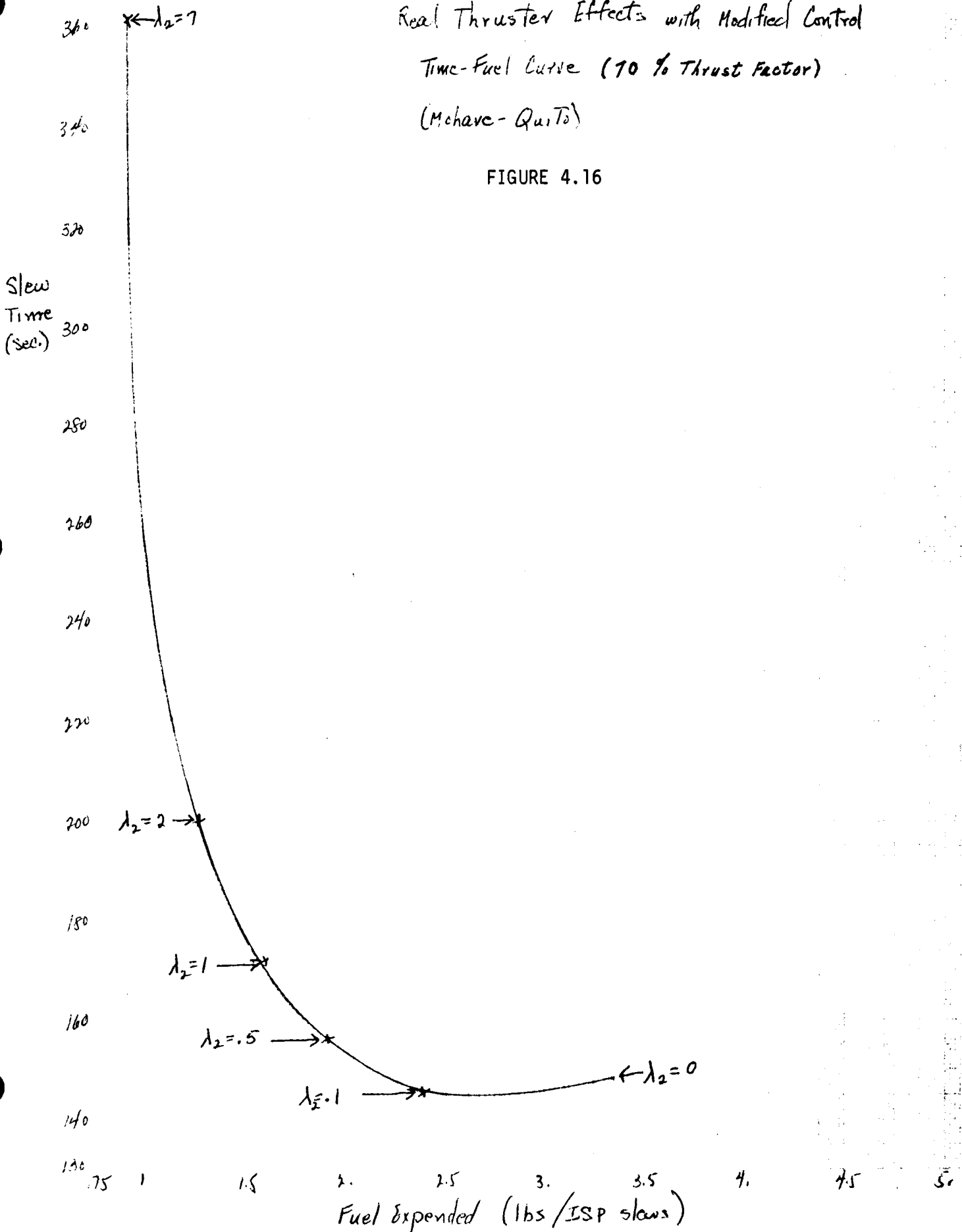
Real Thruster Effects

Time - Fuel Curve

(Mohave to Quito)

FIGURE 4.17

Slew Time (sec.)

$\leftarrow \lambda_2 = 7.$

$\lambda_2 = 0 \rightarrow$

$\lambda_2 = 2, \rightarrow$

$\lambda_{\frac{}{2}} = 1 \rightarrow$

$\lambda_2 = 1. \rightarrow$

$\lambda_2 = .5 \rightarrow$

360
350
340
330
320
310
300
290
280
270
260
250
240
230
220
210
200
190
180
170
160
150
140
130
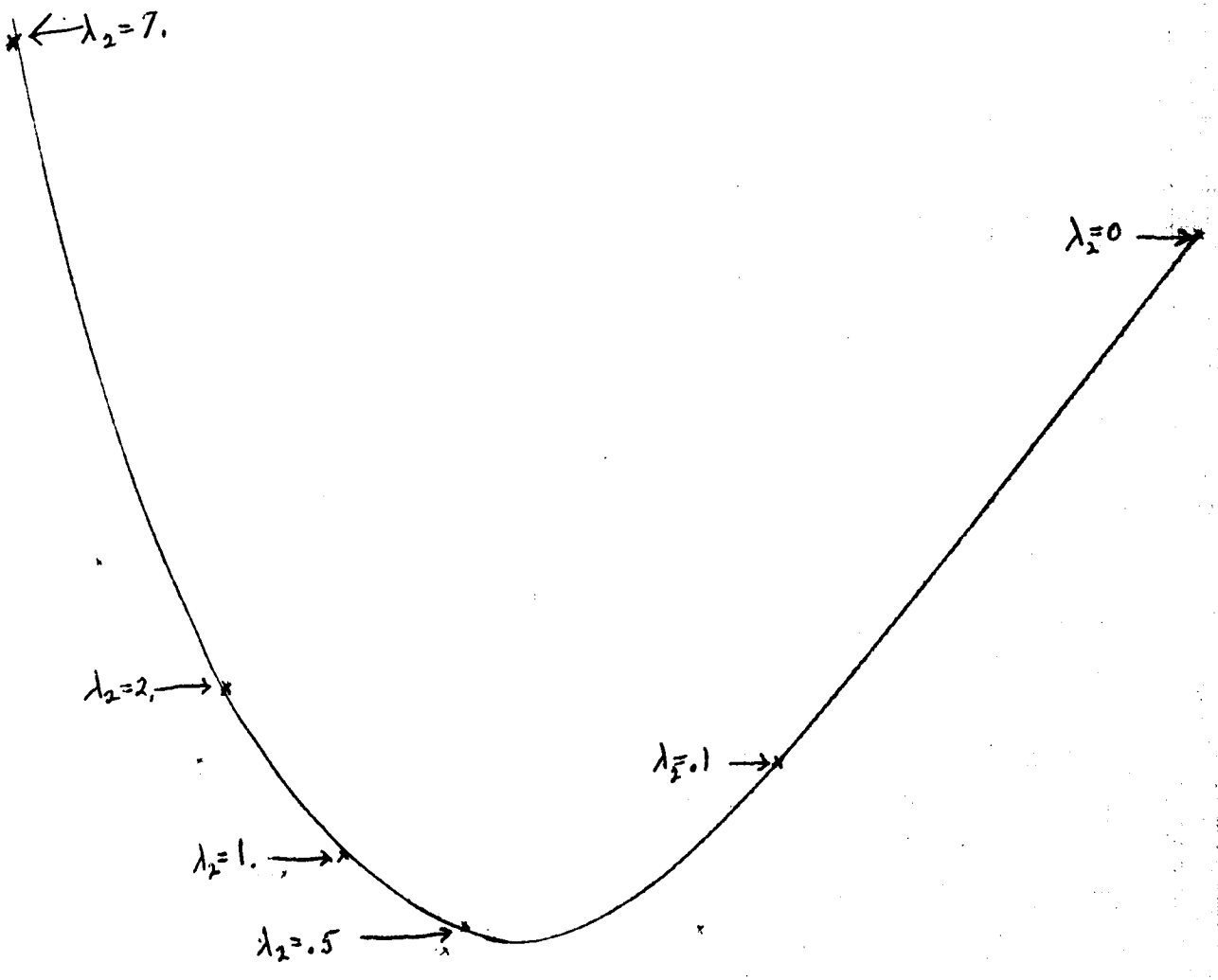
.15   1   1.5   2.   2.5   3.   3.5   4.   4.5   5.   5.25

Fuel Expended (lbs/ISP Slews)

PART V

ELASTIC DYNAMICS AND THE EFFECTS ON SYSTEM PERFORMANCE

5.1 *Control of the Flexing Satellite*

The equations used to simulate the elastic effects are derived in *Appendix F*. In this chapter we give a brief description of: 1) our reasons for choosing lumped parameter simulation; 2) our checking procedures to assure correct translation of the equations to the machine; 3) the results of the simulation.

Our conclusion is important enough to be stated immediately. For the physical parameters which we received from GSFC at the time, the boom is virtually undisturbed by the control and its motion has little effect upon the satellite motion. It appears that these conclusions will hold for reasonably large changes in the boom damping and in the distribution of moments of inertia between loaded boom and satellite, so long as the loaded boom has a natural frequency a thousand times higher than the closed-loop satellite.

The analysis and simulation discussed in previous chapters has considered the satellite to be a rigid body. Such analysis is useful because it is comparatively simple, and because it is usually a very good representation of the actual motion. It has enabled us to gain intuition about the system behavior in successive steps. We have, in particular, demonstrated how a simple model can be made progressively more realistic while our design can be based on a growing knowledge of the actual system. We are in effect following an adaptive design procedure.

We proceed now to initiate an investigation of the effect on our proposed control of the vehicle's elasticity.

Space vehicles by their nature are light and designed close to their structural limits, hence we may expect considerable flexibility in all satellites. Looking to the future, it appears that these problems may be especially serious for large space platforms. In the present case, however, the principal contributors to any lack of rigidity are large booms extending from the satellite and bearing loads at the distal ends.

Because these are the dominant elastic members and because the weight of the boom itself, as opposed to its end loading, is reasonably small, it appeared practical to simulate all the elastic effects by means of a single spring-mass-damper located at some distance from the vehicle center of mass.

The equations of motion for the mass particle appear, with their derivation, in *Appendix F*.

For simplicity we included only one main particle, but to have it most sensitive to control actuation, placed it on axis two, the pointing axis.

A mass of 2.18 slugs was placed 19 feet from the vehicle center of mass. A frequency of 2.3 cps was given and a damping ratio of about 0.3 was assumed. The homogeneous equation describing the movement of the end of the boom relative to the satellite attitude takes the form

$$2.18 \, \ddot{q} + 20 \, \dot{q} + 456 \, q = 0 \quad . \tag{1.1}$$

A time optimal Mojave-Quito run has been made.

By the time two seconds had passed, equilibria were obtained in q_1 and q_3 of -5.4 e-6 and 2.03 e-6 feet, respectively. First we observe that since both $\dot{\omega}_1$ and $\dot{\omega}_3$ are negative, these are the correct signs for a particle located on the positive 2-axis. Next we show that

the values are correct. Restricting our consideration to single axis motion we find that the coupled satellite-particle can be reduced to a single equation for each particle

$$m\ddot{q}_1 + \left(\frac{I_3 + m\ell^2}{I_3}\right)\beta\dot{q}_1 + \left(\frac{I_3 + m\ell^2}{I_3}\right)\alpha q_1 = \frac{m\ell}{I_3} u_3$$

$$m\ddot{q}_3 + \left(\frac{I_1 + m\ell^2}{I_1}\right)\beta\dot{q}_3 + \left(\frac{I_1 + m\ell^2}{I_1}\right)\alpha q_3 = -\frac{m\ell}{I_1} u_1 \ .$$

$$(1.2)$$

Using the values mentioned above for the particle and the standard inertias and torques we can predict much about the behavior and compare it with the computed results.

Let $I_1 = 3580 - m\ell^2 = 2793$

$I_3 = 2000 - m\ell^2 = 1213$

$|u_1| = .08$

$|u_3| = .12 \ .$

Then the equilibria are

$q_1(\infty) = - 5.45e-6$

$q_3(\infty) = 2.03e-6$

which checks with the output.

The damping ratios are $\zeta_1 = .4$, $\zeta_3 = .36$. Natural frequencies are $\omega_1 = 2.95$ cps, $\omega_3 = 2.61$ cps; damped frequencies are $\omega_1 = 2.7$ cps, $\omega_3 = 2.44$ cps. The peaks of q_1 should decay like $e^{-7.5t}$ and those of q_3 like $e^{-5.9t}$.

To check the frequencies we determine the times where the functions cross the equilibrium value. This gives a frequency of 2.7 cps in q_1 and

2.44 cps in c_3.

Determining the damping is rather inaccurate but we have, approximately,

q_1 peaks of -6.8 at .18 and -5.53 at .56

q_3 peaks of 2.65 at .2 and 2.08 at .62.

These indicate, very roughly, that q_1 decays like $e^{-7.45t}$ and q_3 like e^{-6t} which is quite adequate accuracy.

This dynamic analysis is an excellent way to check the overall behavior and gives us both a feel for the system's motion and by predicting the computer output, assures us that the simulation is correct. In addition, however, several spot checks were made on $\ddot{q}_1$ and $\ddot{q}_3$ during their transients. These checked within computational accuracy thus establishing the validity of the mechanization.

As was expected the transient oscillations of the mass particle cause oscillations in the angular acceleration. In fact, we observe oscillations of over 10% in the acceleration at times; however, the frequency of these oscillations is high enough to prevent their affecting the overall motion. In fact the difference between this elastic run and a rigid body run could not be detected, either in fuel expenditure, time required, or phase plane plot. The only time the oscillations could cause a problem is at a switching point, where they might cause chatter and conceivably a resonance. The "softened" switching curves are apparently sufficient to handle this case, however, since we observed no extra switchings and the overall trajectory behavior was as if the boom was rigid. Naturally the dynamics must be handled correctly; that is, the control computer must be aware of the added moment of inertia contributed by the loaded boom.

An additional run was made with $\zeta = 0.05$. The computer output showed again that the overall motion was unaffected by the boom. Furthermore, the influence of the quantity $\frac{I+m\ell^2}{I}$ as a multiplicative factor in the damping term (see 1.2) always insures a higher damping than the homogenous equation (1.1) would lead us to expect.

In short the present simulation leads us to expect very little problems due to elasticity. These results could, of course, be affected by a drastic lowering of the natural frequency of the loaded boom from 2.3 cps to say .1 cps or below.
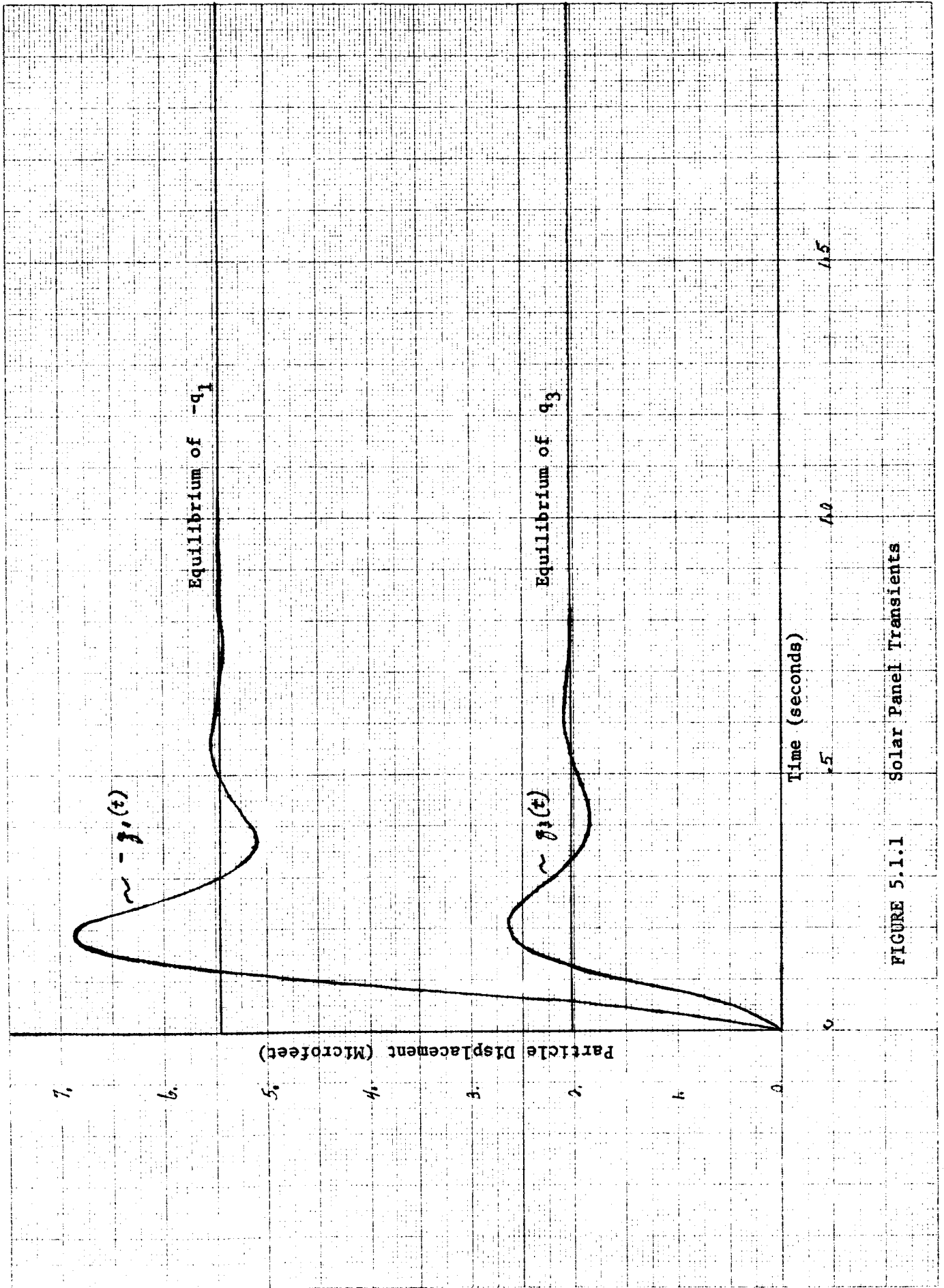
FIGURE 5.1.1   Solar Panel Transients

PART VI

APPENDICES ON DETAILED MATHEMATICAL ANALYSIS

APPENDIX A

GROUND TRACK ANALYSIS

Appendix A

Inverse or Ground Track Program. Given a fixed target latitude and longitude (L_T, ℓ_T) and a varying set of Euler angles θ_{Rb}, Ψ_{Rb}, ϕ_{Rb}, find the corresponding set of initial latitude, longitude and γ, L_I, ℓ_I and γ_I.

In equation (1.3.32), denote the known right hand side by the matrix with elements (c_{ij}), i.e.

$$(A1) \qquad (c_{ij}) \equiv C(\theta_{bR}, \Psi_{bR}, \phi_{bR}) \; C(\theta_{Rs}, 0, \phi_{Rs})$$

or alternatively:

$$(A2) \qquad (c_{ij}) = C(\theta_{bR}, \Psi_{bR}, \phi_{bR}) \; B(L_T, \ell_T, 0)$$

Since the c_{ij} are known, we wish to solve (1.3.32) in the form:

$$(A3) \qquad B(L, \ell, \gamma) = (c_{ij})$$

for the unknown latitude, longitude and γ (subscripts dropped). This is the same as solving the equations (1.2.33) where the a_{ij} elements are replaced by known c_{ij}'s.

We immediately obtain an equation for γ:

$$(A4) \qquad \tan \gamma = \frac{c_{13}}{c_{33}}$$

and two equations for the two unknowns L and ℓ

$$(A5) \qquad \frac{\cos L \sin \ell}{\sin L} = \frac{c_{21}}{c_{23}}$$

$$(A6) \qquad \frac{(k - \cos L \cos \ell)}{\sin L} = \frac{c_{22}}{c_{23}} \quad .$$

Use (A5) to eliminate ℓ in (A6):

$$(A7) \qquad k - \cos L \sqrt{1 - \left(\frac{c_{21}}{c_{23}}\right)^2 \frac{\sin^2 L}{\cos^2 L}} = \left(\frac{c_{22}}{c_{23}}\right) \sin L,$$

an equation reducible to a quadratic in sin L. Replacing cos L and squaring:

$$(A8) \qquad (1 - \sin^2 L) - \left(\frac{c_{21}}{c_{23}}\right)^2 \sin^2 L = \left(\frac{c_{22}}{c_{23}} \sin L - k\right)^2 \; .$$

Collecting terms:

$$(A9) \qquad \sin^2 L(c_{21}^2 + c_{22}^2 + c_{23}^2) - 2kc_{22}\, c_{23} \sin L + (k^2-1)c_{23}^2 = 0$$

Now:

$$(A10) \qquad c_{21}^2 + c_{22}^2 + c_{23}^2 = 1$$

from (1.2.33) and the definition of α_2 (1.2.31).

Solving (A9) yields

$$(A11) \qquad \sin L = c_{23}\left(kc_{22} \pm \sqrt{k^2(c_{22}^2-1) + 1}\right)$$

To determine the proper sign of (A11), we note that the equations (1.2.33) must be satisfied for all values of the variables. Substitute (A11) into (1.2.33f) to obtain:

$$(A12) \qquad \alpha_2 = kc_{22} \pm \sqrt{k^2(c_{22}^2-1) + 1}$$

and let $L = 0 = \ell$. By (1.2.31), we must have

$$(A13) \qquad \alpha_2 = k - 1 \; .$$

By (1.2.33e), we must have:

$$(A14) \qquad c_{22} = \frac{(k-1)}{\alpha_2} = 1 \; .$$

Substitution of (A13) and (A14) into (A12) gives:

$$(A15) \qquad k - 1 = k \pm 1 \; .$$

We, therefore, use the minus sign and write:

$$(A15) \qquad \sin L = c_{23} \left(k c_{22} - \sqrt{k^2(c_{22}^2 - 1) + 1} \; \right) \quad .$$

We may then use (A5) to find $\sin \ell$.

Summarizing:

$$(A16) \qquad \tan \gamma = \frac{c_{13}}{c_{33}}$$

$$(A17) \qquad \sin L = c_{23} \left(k c_{22} - \sqrt{k^2(c_{22}^2 - 1) + 1} \; \right)$$

$$(A18) \qquad \sin \ell = \frac{c_{21}}{c_{23}} \tan L \quad .$$

The known values of c_{ij} may be obtained in several forms. From (A1) and matrix multiplication we may write:

$$(A19) \qquad c_{13} = (\cos \Psi_{bR} \sin \theta_{bR})(\sin \phi_{Rs})$$
$$+ (\sin \Psi_{bR})(\cos \phi_{Rs})$$

$$(A20) \qquad c_{23} = (-\sin \phi_{bR} \sin \Psi_{bR} \sin \theta_{bR} + \cos \phi_{bR} \cos \theta_{bR})(\sin \phi_{Rs})$$
$$+ (\sin \phi_{bR} \cos \Psi_{bR})(\cos \phi_{Rs})$$

$$(A21) \qquad c_{33} = (-\cos \phi_{bR} \sin \Psi_{bR} \sin \theta_{bR} - \sin \phi_{bR} \cos \theta_{bR})(\sin \phi_{Rs})$$
$$+ (\cos \phi_{bR} \cos \Psi_{bR})(\cos \phi_{Rs})$$

$$(A22) \qquad c_{21} = (-\sin \phi_{bR} \sin \Psi_{bR} \cos \theta_{bR} - \cos \phi_{bR} \cos \theta_{bR})(\cos \theta_{Rs})$$
$$+ (-\sin \phi_{bR} \sin \Psi_{bR} \sin \theta_{bR} + \cos \phi_{br} \cos \theta_{bR})(-\cos \phi_{Rs} \sin \theta_{Rs})$$
$$+ (\sin \phi_{bR} \cos \Psi_{bR})(\sin \phi_{Rs} \sin \theta_{Rs})$$

142

(A23) $\quad c_{22} = (-\sin \phi_{bR} \sin \Psi_{bR} \cos \theta_{bR} - \cos \phi_{bR} \sin \theta_{bR})(\sin \theta_{Rs})$

$\quad\quad + (-\sin \phi_{bR} \sin \Psi_{bR} \sin \theta_{bR} + \cos \phi_{bR} \cos \theta_{bR})(\cos \phi_{Rs} \cos \theta_{Rs})$

$\quad\quad + (\sin \phi_{bR} \cos \Psi_{bR})(-\sin \phi_{Rs} \cos \theta_{Rs}) \quad .$

An alternative to equations (A19) to (A23) is to use matrix multiplication in equation (A2)(see equations (1.3.5) and (1.2.29) for the matrices on the right hand side of (A2)).

APPENDIX B

SOLAR PRESSURE TORQUE ANALYSIS

1. *Radiation pressure acting on a flat surface.*

In this section we shall investigate some physical properties of the pressure of the solar radiation on flat surfaces with different inclinations with respect to the incoming solar rays. The solar radiation is composed of photons of various frequencies, emitted by the solar surface in radial directions. The great distance between the sun and the orbiting satellite allow us to consider the solar rays acting on a surface as travelling on parallel paths. If the photons, composing such rays, hit an ideal "geometrical flat surface" then they would be reflected according to the laws of geometrical optic. In real situations, however, part of the photons will be absorbed while others will be reflected in various directions. Each photon carries a momentum whose magnitude is given from the expression

$$|\mathbf{p}| = \frac{h\nu}{c}$$

where h is Planck's energy constant, ν the frequency of the photon and c the speed of light. The principle of conservation of momentum implies the momentum of a photon absorbed by the flat surface is transmitted to the surface. If instead a photon is reflected , it changes its direction so that by the same principle, it transmits to the surface a momentum p_t such that

$$p_b + p_r + p_t = 0$$

where p_b is the vector which characterizes the momentum of the incoming photon. p_r is the vector which characterizes the momentum of the

reflected photons. Thus the effect of the flux of photons on a surface is a transfer of momentum which produces a pressure on the surface.

We shall now proceed with a more detailed analysis of the phenomenon. Let us define the solar pressure constant S as the average momentum associated with a radiation beam through a unit surface normal to the beam in unit time. If complete absorptivity is assumed, S can also be defined as the average force acting on a unit area normal to the radiation beam. S has the dimensions of a pressure.

Let us consider a flat surface α and the unit normal vector n through a point 0. Let b denote the unit vector that gives the direction of the incoming beam of photons and θ the angle between b and n.
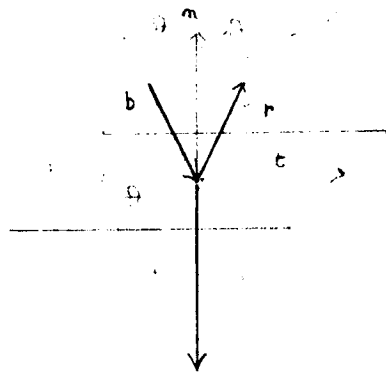
Assume that the surface we are considering is an "ideal flat surface". Then an incoming photon will be reflected in a direction r in the plane defined by the b and n vectors, and such that the angle between r and n will be equal to the angle between b and n. Let us

146

call μ the modulus of the momentum of an incoming photon and τ that of the transmitted momentum. From the law of conservation of momentum μb (momentum of the system photon-surface before the impact) $= \mu r + \tau(-n)$ (momentum of the system after the impact) i.e.:

$$1.1 \qquad -n\tau = \mu b + \mu(-r),$$

that is, the surface will acquire a momentum

$$1.2 \qquad -n\tau = -n \, 2\mu\cos\theta.$$

if complete absorptivity of the surface is assumed, a photon will yield to the surface a momentum equal to μb, whose components will be

$$1.3 \qquad \mu b = \mu \cos\theta \, (-n) + \mu \sin\theta \, t$$

if t is the unitary vector that defines the intersection between the plane defined by b and n, and α. In the average, the total momentum incoming on α in a unit time will be, if A is the area of α,

$$1.4 \qquad S \cdot A|\cos\theta|$$

If complete reflectivity is assumed, α will be subject to a force given by

$$1.5 \qquad F_r = (-n) \, 2SA|\cos\theta| \, \cos\theta \quad .$$

If complete absorptivity is assumed, the force acting on α will be

$$1.6 \qquad F_a = S[A|\cos\theta| \, \cos\theta \, (-n) + A|\cos\theta| \sin\theta \, t].$$

As is evident $|F_r| \leq 2|F_a|$.

Let us now assume that, on a statistical basis, of n photons incoming on a given surface, $n\nu$ be reflected and $(1-\nu)n$ be absorbed (ν is called "reflectivity constant" of a surface); then the total force applied on the surface α will be:

1.7
$$F_t = S[\nu \, F_r + (1-\nu)F_a]$$

$$F_t = S[(-n) \, A|\cos\theta|\cos\theta \, (2\nu + 1-\nu) + t \, A|(\cos\theta| \, \sin\theta(1-\nu)].$$

$$= S[(-n) \, A|\cos\theta| \, \cos\theta \, (1 + \nu) + t \, A|\cos\theta| \, \sin\theta \, (1-\nu)].$$

2. *The satellite model.*

Let us assume that, as far as the radiation is concerned, the satellite we are interested in could be described as a parabolic dish Π whose base radius is 15' and whose height is 3-1/4'. This satellite is assumed to rotate around the earth at a distance in which there will be no appreciable variation in the solar pressure constant, whose value will be assumed to be $9.4 \cdot 10^{-8}$ lbs. per foot squared. It is assumed further that the center of mass is the center of the base circle.
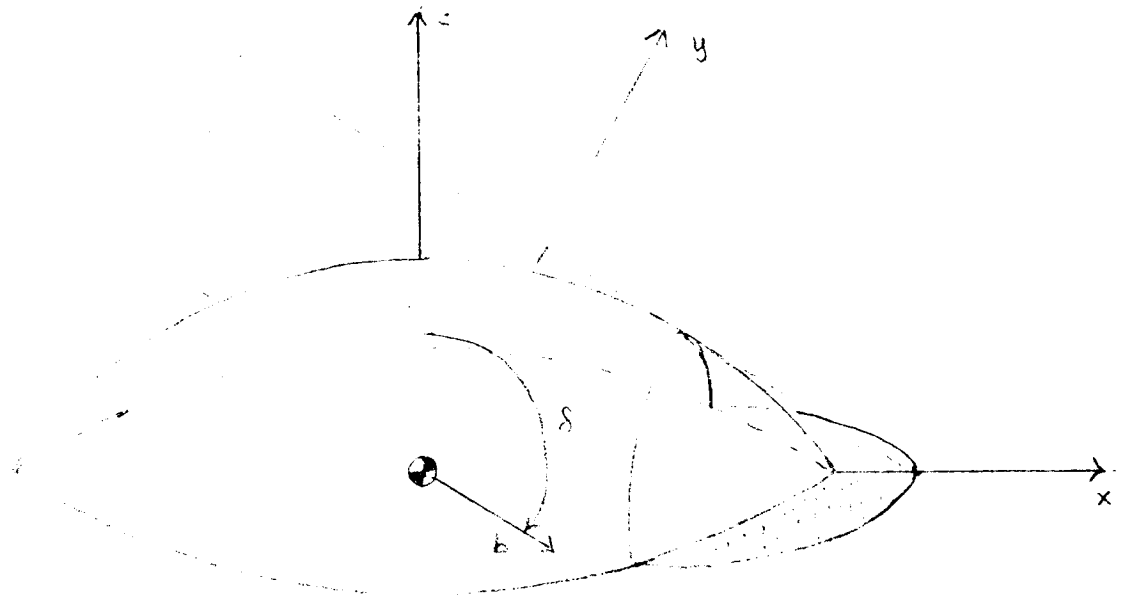
Figure 2.1

Let us define a coordinate system whose origin is the center of mass, whose k axis points along the $-p_2$ axis of the satellite (here it is assumed that the p_2 axis is the symmetry axis of the satellite), whose i axis lies in the plane determined by the p_2 and b directions and such that

$$|b\hat{\ }i| \leq \frac{\pi}{2} , \quad i.e.,$$

2.1 $\qquad \cos b\hat{\ }i \geq 0$

The j axis is then defined so as to complete a usual right handed system.

In this system let us write the equations of the truncated paraboloid as

2.2 $\qquad z = -\gamma(x^2 + y^2) + \ell, \quad z \geq 0;$

and call δ the angle between the k axis and the direction of the beam in counterclockwise direction, looking from the positive j axis. Therefore for 2.1

2.3 $\qquad 0 \leq \delta \leq \pi$

Generally, the condition under which a point P lying on a given surface is lighted by a radiation beam incoming with a direction b is as follows: if $P + \tau b, -\infty < \tau \leq 0$ is the parametric equation of the half-line through P $(\tau = 0)$, for negative τ, this half-line has to have no intersection with the given surface other than $\tau = 0$.

Then, if n is the vector that gives the normal to the surface, if

$$\frac{\pi}{2} \leq b \hat{\ } n \leq \frac{3}{2} \pi$$

the surface at P is lighted "from outside" (in the direction of n);
if

$$-\frac{\pi}{2} \leq b \hat{\ } n \leq \frac{\pi}{2}$$

the surface at P is lighted "from inside" (in the direction of $-n$).

Taking advantage of the formulas 1.4, it is possible to handle, using the coefficient ν, both the cases of reflectivity and absorptivity at once. We shall, on the other hand, consider them separately, both for pointing out the differences between them and for taking full advantage of the symmetries of the proposed body, that makes possible, in the latter case, to derive in a very easy way the applied torque.

3. *Complete absorptivity case.*

Consider the satellite as a rigid body subject to forces all in the same direction, the direction of the incoming beam b. It is well known that it is then possible to translate those forces along their direction and consider them all applied, for instance, on the same plane.

Consider a point P on Π; disregarding infinitesimals of higher order we shall identify an elementary area over Π with the corresponding area on the plane tangent to Π at P.

Let α be a plane, and A_α an area over α; let A_α be subject to a radiation beam with some radiation constant S; from section 1 we know that A_α will be subject to a force in the direction of b, of modulus SA_n, where A_n is the projection of A_α over the plane normal to b. Consider over the plane $z = 0$ the "shadow" of A_α, or A_n, i.e., their projection along the direction b; the area of this projection is A_z, and over this area will act a force of modulus SA_n; δ is the angle between the k axis and b; we have

$$A_n = A_z \cdot |\cos\delta|$$

which means that over an area A_z of $z = 0$, "shadow" of some area A_α, we can consider applied a force of modulus

$$|dF| = SA_z \, |\cos\delta| \ .$$

Let us point out that this force <u>doesn't depend at all on</u> A_α. This means that, in the complete absorptivity case, for computation of the torques, over every elementary area $dx\,dy$ of $z = 0$, in the region projection on

$z = 0$ of the beams that interact with a given surface, there is applied a force

$$S\ dx\ dy\,|\cos\delta|$$

that doesn't depend on the shape of the surfaces: two surfaces of arbitrary shape, having the same "shadow" are completely equivalent.

Consider then the given satellite and suppose, as in figure 2.1, that $\frac{\pi}{2} \leq \delta \leq \pi$. Let us look at the geometrical figure that the shadow of the beam will draw on the $z = 0$ plane. This figure will be composed of: a) the circle base of the paraboloid dish Π, b) the dotted region Δ in figure 2.1, projection of the beam intercepted by Π outside the a) region; an analytical expression of its boundary will be derived further.

Let us fix two coordinates x, y, and search for the elementary torque exerted on 0 by an infinitesimal surface between x and $x + dx$, y and $y + dy$; as we said, it is possible to consider this elementary surface in the plane $z = 0$. The torque applied on 0 by a force of components $F_x F_y F_z$ acting on the point (x, y, z) is

$$\mathsf{T} = \mathsf{i}\,(yF_z - zF_y) + \mathsf{j}\,(zF_x - xF_z) + \mathsf{k}\,(xF_y - yF_x)$$

where $\mathsf{i,j,k}$ are the directions of the x, y, and z axis. Recalling that in our case $z = 0$, let us consider the

torques applied on 0 by four points P_1, P_2, P_3, P_4 of

coordinates respectively (x,y); (-x,y); (x;-y); (-x,-y). The

force applied in each of these points is the same $F(P_1)$ =

$F(P_2)$ = $F(P_3)$ = $F(P_4)$.

It is:

$$T_{P_1+P_2+P_3+P_4} = i(yF_z - yF_z + yF_z - yF_z) + j(-xF_z - xF_z + xF_z + xF_z)$$

$$+ k(xF_y - xF_y + xF_y - xF_y - yF_x - yF_x + yF_x + yF_x)$$

$$= 0i + 0j + 0k$$

So the contribution to the total torque from the points on the circle

base is zero. It remains to compute the torque from the dotted region

in figure 1.

The exterior boundary of this region is the projection on

the z = 0 plane of the radiation beams tangent to the paraboloid dish.

Let us call b the direction of the incoming beam; for a point

x,y,z over Π be lighted "from outside" it is necessary that

$$\frac{\pi}{2} \leq b \hat{\ } n \leq \frac{3}{2} \pi$$

that is $\cos b \hat{\ } n \leq 0$.

So we have

$$\frac{2\gamma x \sin \delta + \cos \delta}{\sqrt{1 + (\frac{\partial z}{\partial x})^2 + (\frac{\partial z}{\partial y})^2}} \leq 0$$

i.e.
$$x \leq \frac{-1}{2\gamma \tan \delta} \; ;$$

and the points on the boundary of the lighted region lie on the plane $x = \frac{-1}{2\gamma t}$, where we put $t = \tan \delta$. Let us fix y_0 in this plane; the corresponding z_0 over Π will be given by

$$z_0 = -\gamma \left(\frac{1}{4\gamma^2 t^2} + y_0^2\right) + \ell$$

The equations of the straight line in the plane $y = y_0$ through the point $\left(\frac{-1}{2\gamma t} , z_0\right)$ with angular coefficient $\tan\left(\frac{\pi}{2} - \delta\right) = \frac{1}{t}$ will be then

$$z + \gamma\left(\frac{1}{4\gamma^2 t^2} + y_0^2\right) - \ell = \frac{1}{t} \left(x + \frac{1}{2\gamma t}\right); \quad y = y_0$$

The intersection with the plane $z = 0$, as function of y, is given by

$$\gamma\left(\frac{1}{4\gamma^2 t^2} + y^2\right) - \ell = \frac{1}{t}\left(x + \frac{1}{2\gamma t}\right) \quad ,$$

i.e. the parabola

$$x = -t\left(-\gamma y^2 + \ell + \frac{1}{4\gamma t^2}\right) \; .$$

It is evident that in the case

$$0 \leq \delta \leq \frac{\pi}{2}$$

on the $z = 0$ plane there will be no more shadow, but the preceding equations will give the projection over $z = 0$ of the beams actually interacting with Π.

For having the torque T on 0 we have to compute the integral (recalling $z = 0$)

$$\int\int_{\Delta} [i \; ydF_z \; - \; j \; xdF_z \; + \; k(xdFy-ydFx)]$$

Now $dF_y = 0$, and let us consider a point (x,y) in Δ and the corresponding point $(x,-y)$; for symmetry the contribution of these two points to $i \; ydF_z$ and $-k \; ydF_x$ is zero whereas their contributions to xF_z sum up; so it remains to compute

$$2 \int\int -j \; xdF_z \qquad ,$$

where the region of integration is that part of Δ that lies in the $y > 0$ half-plane.

From Section 1 we know that

$$dF_z = -S \; dxdy \; |\cos(\delta-\pi)| \cos(\delta-\pi) = S \; dxdy |\cos \delta| \cos \delta =$$

$$= S \; dxdy \; \cos^2\delta \; \text{sign} \; (\cos\delta)$$

So

$$T = -j \; 2S \; \cos^2\delta \; \text{sign} \; (\cos \; \delta) \int_0^{y_f} dy \int_{x_0}^{x_1} xdx$$

where

$$\left. \begin{aligned} x_0 &= \sqrt{\frac{\ell}{\gamma} - y^2} \\ x_1 &= t(-\gamma y^2 + \ell + \frac{1}{4\gamma t^2}) \end{aligned} \right\} \qquad \frac{\pi}{2} \leq \delta \leq \pi$$

$$x_0 = -t(-\gamma y^2 + \ell + \frac{1}{4\gamma t^2}) \quad \Big\}$$

$$x_1 = -\sqrt{\frac{\ell}{\gamma} - y^2} \qquad \qquad \Big\} \quad 0 \leq \delta \leq \frac{\pi}{2}$$

Finally T can be written

$$\mathsf{T} = 2\, j\, S\, \cos^2\delta \int_0^{y_f} dy \int_{x_0 = \sqrt{\frac{\ell}{\gamma} - y^2}}^{x_1 = t(-\gamma y^2 + \ell + \frac{1}{4\gamma t^2})} x\, dx$$

and y_f is given by

$$\frac{1}{4\gamma^2 t^2} + y_f^2 = \frac{\ell}{\gamma} \quad , \quad y_f = \sqrt{\frac{\ell}{\gamma} - \frac{1}{4\gamma^2 t^2}}$$

y_f is real if

$$\tan\delta \geqslant \frac{1}{2\sqrt{\ell\gamma}} \qquad \tan\delta \leqslant -\frac{1}{2\sqrt{\ell\gamma}}$$

if these conditions are not fulfilled, the integral has to be taken as zero.

Under the preceding conditions, the integration gives

$$\mathsf{T} = 2j\, S\, \cos^2\delta \int_0^{y_f} \frac{1}{2}\left[t^2(-\gamma y^2 + \ell + \frac{1}{4\gamma t^2})^2 - \frac{\ell}{\gamma} + y^2\right] dy =$$

$$= j\, S\, \cos^2\delta\, [t^2 \frac{\gamma^2}{5}\, y_f^5 + \frac{1}{3}(\frac{1}{2} - 2\gamma\ell\, t^2)y_f^3 + (\ell^2 t^2 - \frac{\ell}{2\gamma} + \frac{1}{16\gamma^2 t^2})y_f]$$

and recalling $y_f = \sqrt{\frac{\ell}{\gamma} - \frac{1}{4\gamma^2 t^2}}$

$$\mathsf{T} = j\, S\, \cos^2\delta\, \sqrt{\frac{\ell}{\gamma} - \frac{1}{4\gamma^2 \tan^2\delta}}\left[\tan^2\delta\, \frac{\ell^2 8}{15} - \frac{\ell}{\gamma}\frac{4}{15} + \frac{1}{30\gamma^2}\frac{1}{\tan^2\delta}\right]$$

Let us now consider the actual dimensions of the given satellite.

$$\ell = 3\frac{1}{4} \qquad \qquad \sqrt{\frac{\ell}{\gamma}} = 15$$

157

The relation

$$\lceil \tan \delta \rceil \geq \frac{1}{2\sqrt{\ell_\gamma}}$$ gives

$$|\tan \delta| \geq 2.31,$$
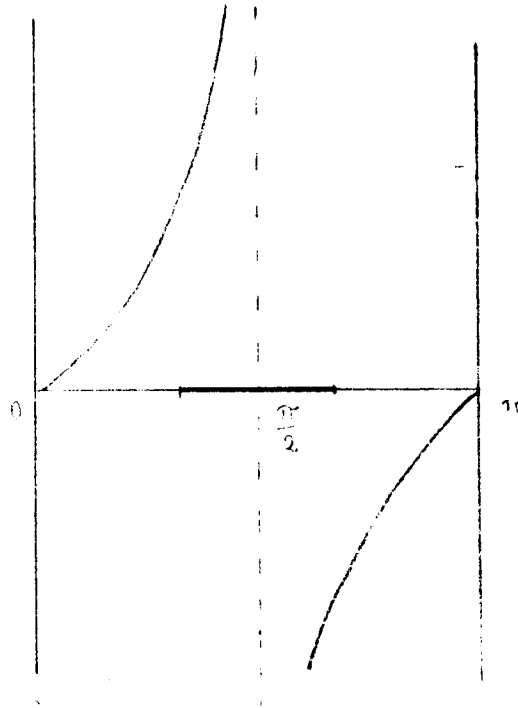
and so

$$T = j\, 9.4 \cdot 10^{-8} \cos^2\delta \sqrt{225 - \frac{10^4}{8.25\ \tan^2\delta}[\tan^2\delta \cdot 5.6 - 60 + \frac{10^3}{6.21\tan^2\delta}]}$$

foot-pounds

$$\lim_{\delta \to +\frac{\pi}{2}} T = j\, 9.4 \cdot 10^{-8} \sqrt{225} \cdot 5.6 = j\, 7.9\ 10^{-6} \quad \text{foot-pounds}$$

4. *The complete reflectivity case. Shadows on the satellite.*

In the absorptivity case, it was not at all necessary to consider exactly which portions of the satellite were actually illuminated but only necessary to consider the global intersection with the beam. This is not the case where reflectivity is concerned. In fact, not only the magnitude of the force but also its direction depend on the characteristics of surface over which the force is applied.

Consider first the case in which the beam comes in from above, i.e. with an angle δ such that

$$\frac{1}{2}\pi \leq \delta \leq \pi$$

Since the surface interacting with the beam is convex, the conditions we gave in the preceding section can be summarized in the following statement.

A point on Π is illuminated from the direction of n by the radiation with direction b iff

4.1
$$\frac{\pi}{2} \leq \widehat{b\,n} \leq \frac{3}{2}\pi$$

i.e.

4.2
$$\cos \widehat{b\,n} \leq 0 \qquad .$$

It is

$$b = i\,\sin\delta + j\,0 - k\,\cos\delta$$

159

$$n = \frac{2\gamma x \mathbf{i} + 2\gamma y \mathbf{j} + \mathbf{k}}{\sqrt{1 + (\frac{\partial z}{\partial x})^2 + (\frac{\partial z}{\partial y})^2}}$$

so that $\cos \widehat{b\ n} = b \cdot n = \dfrac{2\gamma x \ \sin \ \delta - \cos \ \delta}{\sqrt{1 + (\frac{\partial z}{\partial x})^2 + (\frac{\partial z}{\partial y})^2}}$

and recalling $\sin \delta \geqslant 0$ we obtain the conditions

$$-\sqrt{\frac{\ell}{\gamma}} \leqslant x \leqslant \frac{-1}{2\gamma \tan \delta} \quad , \quad \frac{\pi}{2} \leqslant \delta \leqslant \pi$$

if $\left|\dfrac{1}{\tan \delta}\right| > 2\sqrt{\ell\gamma}$, the whole surface will be lighted; in the other case, the boundary of the lighted region will lie on the plane $x = \dfrac{-1}{2\gamma \tan \delta}$. As $\delta \to \dfrac{\pi}{2}$, $x \to 0$, so in this position exactly half of the satellite will be lighted.

Consider now the case $0 \leqslant \delta \leqslant \dfrac{\pi}{2}$. The surfaces interacting with the beam will be both convex and concave, so it will be necessary to verify both the conditions pointed out in the preceding section. In general, if δ is sufficiently close to $\dfrac{1}{2}\pi$, it will be possible to distinguish three different regions on the satellite:
1) A region lighted from outside. 2) A region lighted from inside .
3) A region not lighted from any side, (shadow of the region 1).
Consider figure 4.1

Figure 4.1

160
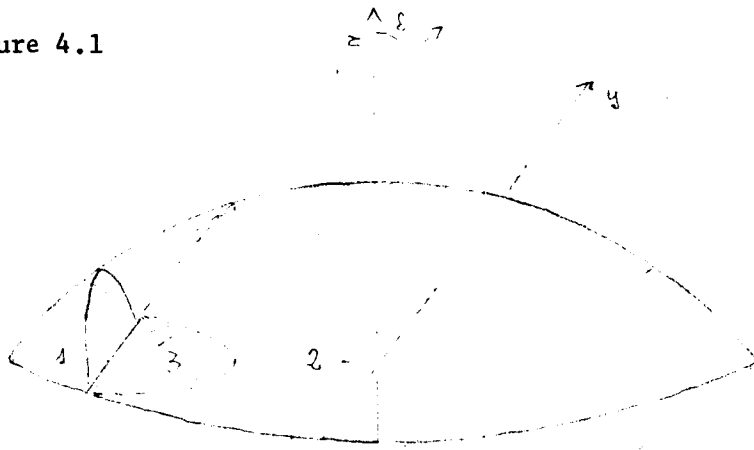
For the first region the usual condition will hold:

$$-\sqrt{\frac{\ell}{\gamma}} \leq x \leq \frac{-1}{2\,\gamma\tan\delta} \qquad 0 \leq \delta \leq \frac{\pi}{2}$$

The second region is the one in which the rays interact from inside without having any previous interaction with the surface. Analytically this condition can be expressed as follows:

Let us fix a plane $y = y_0$, and chose an arbitrary x_0; the corresponding z_0 on π will be given by

$$z_0 = -\gamma(x_0^2 + y_0^2) + \ell$$

The straight line in the given plane through this point with angular coefficient $\tan(\frac{\pi}{2} - \delta) = \frac{1}{\tan\delta} = \frac{1}{t}$ will be

$$z + \gamma(x_0^2 + y_0^2) - \ell = \frac{1}{t}(x - x_0)$$

and will interact with the paraboloid

$$z = -\gamma(x^2 + y^2) + \ell$$

at x_1, x_2 solutions of the system

$$\begin{cases} z = -\gamma(x^2 + y^2) + \ell \\ \\ z + \gamma(x_0^2 + y_0^2) - \ell = \frac{1}{t}(x - x_0) \\ \\ y = y_0 \end{cases}$$

161

This will give:

$$x_1 = x_0$$

$$x_2 = \frac{-1}{t\gamma} - x_0$$

Let us assume that $z_0 > 0$, and impose the condition

$z_2 = -\gamma[(\frac{-1}{t\gamma} - x_0)^2 + y_0^2] + \ell < 0$. This condition will assure that

no other previous interaction occurs with our *truncated* paraboloid.

We can rewrite this condition in the form

$$(x_0 + \frac{1}{t\gamma})^2 + y_0^2 > \frac{\ell}{\gamma}$$

i.e. the exterior of the circle with center at $(\frac{-1}{t\gamma}, 0)$ and

radius $+\sqrt{\frac{\ell}{\gamma}}$. If $2\sqrt{\frac{\ell}{\gamma}} > |\frac{1}{t}|$, the whole base of the satellite

will satisfy this condition; otherwise the intersection of the two

circles will occur at the solution of

$$x^2 + y^2 = \frac{\ell}{\gamma}$$

$$(x + \frac{1}{t\gamma})^2 + y^2 = \frac{\ell}{\gamma}$$

i.e. $\qquad x = \frac{-1}{2\gamma t}$

These points of intersection lie just on the plane that bounds the

corresponding region lighted from outside, so the orthogonal projection

over $z = 0$ of the satellite for a given δ will be as in figure 4.2.
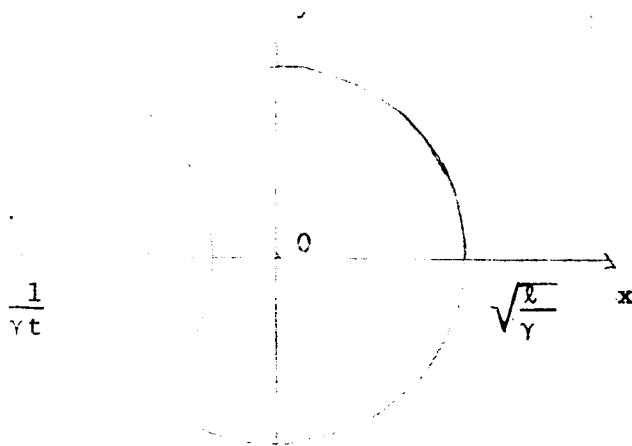
Figure 4.2

The following scheme will clarify the different phenomena occurring
as a function of δ:

$$\delta = \pi - \tan^{-1}\frac{1}{2\sqrt{\ell\gamma}}$$

$$\frac{\pi}{2}$$

$$\delta = \tan^{-1}\frac{1}{2\sqrt{\ell\gamma}}$$

partially from
outside

partially from
inside
partially from
outside

lighted from
outside

lighted from
inside

π

0

Figure 4.2

163
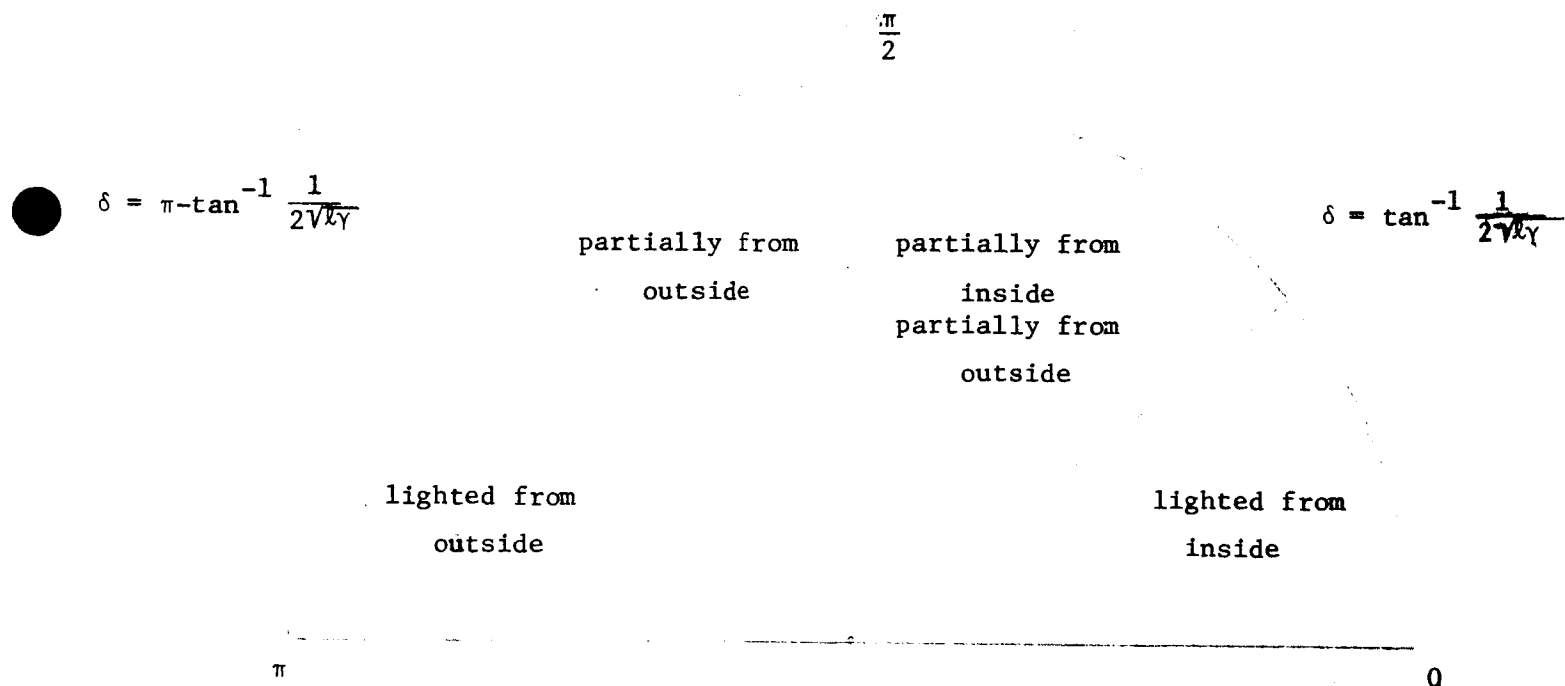
5. *The total reflectivity case - Expressions for the torque*

Let us fix (x,y) on the $z = 0$ plane. As we pointed out in a previous section the force acting on an elementary area dA is

5.1 $\qquad dF = 2S \, dA \cos \theta \; \text{sign} \, (\cos \theta) n = dF \; \text{sign} \, (\cos \theta) n$

where S is the solar radiation constant, n the normal to the surface, θ the angle between the direction of the beam, b , and n.

Let us fix a point $(x,y,0)$ and consider over Π; $z = z(x,y)$ the area whose projection over the $z = 0$ plane is between x and $x + dx$, y and $y + dy$. If ζ is the angle between n and the k axis,

5.2 $\qquad dA = dxdy \, \dfrac{1}{|\cos \zeta|} = dxdy \, \sqrt{1 + (\dfrac{\partial z}{\partial x})^2 + (\dfrac{\partial z}{\partial y})^2}$

Further we have:

$$n = \frac{-\dfrac{\partial z}{\partial x} i - \dfrac{\partial z}{\partial y} j + k}{\sqrt{1 + (\dfrac{\partial z}{\partial x})^2 + (\dfrac{\partial z}{\partial y})^2}}$$

$$b = \sin \delta \, i + \cos \delta \, k$$

so that $\qquad \cos \theta = b \cdot n = \dfrac{-\dfrac{\partial z}{\partial x} \sin \delta + \cos \delta}{\sqrt{1 + (\dfrac{\partial z}{\partial x})^2 + (\dfrac{\partial z}{\partial y})^2}}$

and the 5.1 can be rewritten

$$dF = n\ 2S\ dxdy\ \sqrt{1 + (\tfrac{\partial z}{\partial x})^2 + (\tfrac{\partial z}{\partial y})^2}\ \frac{(-\tfrac{\partial z}{\partial x}\sin\delta + \cos\delta)^2}{1 + (\tfrac{\partial z}{\partial x})^2 + (\tfrac{\partial z}{\partial y})^2}\ \text{sign}\ (\cos\theta)$$

The components of dF over the i,j,k directions are:

$$dF_x = dF\ \frac{-\tfrac{\partial z}{\partial x}}{\sqrt{1 + (\tfrac{\partial z}{\partial x})^2 + (\tfrac{\partial z}{\partial y})^2}}\ \text{sign}\ (\cos\theta)$$

$$dF_y = dF\ \frac{-\tfrac{\partial z}{\partial y}}{\sqrt{1 + (\tfrac{\partial z}{\partial x})^2 + (\tfrac{\partial z}{\partial y})^2}}\ \text{sign}\ (\cos\theta)$$

$$dF_z = dF\ \frac{1}{\sqrt{1 + (\tfrac{\partial z}{\partial x})^2 + (\tfrac{\partial z}{\partial y})^2}}\ \text{sign}\ (\cos\theta)$$

If $z = -\gamma(x^2 + y^2) + \ell$,

$$\frac{\partial z}{\partial x} = -2\gamma x \qquad\qquad \frac{\partial z}{\partial y} = -2\gamma y$$

Consider now the elementary torque over $(0,0,0)$. It is

$$d\overline{T} = i(ydF_z - zdF_y) + j(zdF_x - xdF_z) + k(xdF_y - ydF_x)$$

It is possible to simplify this expression taking advantage of the symmetries of the satellite. Let us consider together two points P_1, P_2 of coordinates (x,y,z) and $(x,-y,z)$, and sum up the two corresponding elementary torques. Since dF_z and dF_x are even in y and dF_y odd in y, $\theta(p_1) = \theta(p_2)$ the resulting torque will be

165

$$i(0-0) + 2j(z dF_x - x dF_z) + k(0-0)$$

i.e.

$$2dT = 2j\ \text{sign}(\cos\theta)(z\ dF\ \frac{-\frac{\partial z}{\partial x}}{\sqrt{1 + (\frac{\partial z}{\partial x})^2 + (\frac{\partial z}{\partial y})^2}} - x dF\ \frac{1}{\sqrt{1 + (\frac{\partial z}{\partial x})^2 + (\frac{\partial z}{\partial y})^2}}\ ) =$$

$$= 2j\ \frac{dF}{\sqrt{1 + (\frac{\partial z}{\partial x})^2 + (\frac{\partial z}{\partial y})^2}}(-z\ \frac{\partial z}{\partial x} - x)\ \text{sign}(\cos\theta) =$$

$$= 4j\,\text{sign}(\cos\theta)\ S\ dxdy\ \frac{(-\frac{\partial z}{\partial x}\sin\delta + \cos\delta)^2}{1 + (\frac{\partial z}{\partial x})^2 + (\frac{\partial z}{\partial y})^2}\ [(-\gamma(x^2+y^2)+ \ell)(\ 2\gamma x)-x]$$

where we did substitute the expression for z. This is the expression
for the elementary torque from two points, (x,y,z) and (x,-y,z).
This expression has to be integrated over the areas described in the
preceding section, or, more precisely, over the y > 0 part of these
areas.

We are interested in three kinds of areas:

1) A semicircle.

2) A semisector.

3) Half of the region between two circumferences.

See Figure 4.2

166

We shall compute the surface integrals as double integrals.

Let us fix a value x, and perform the integration

$$2dT_y = -\text{sign}(\cos\theta)4j\ S dx \int_{y_0}^{y_1} dy \frac{(2\gamma\ x\ \sin\delta + \cos\ \delta)^2}{1+ 4\gamma^2\ x^2 + 4\gamma^2 y^2} \{2\gamma^2 x^3 - x(2\gamma\ell - 1)+2\gamma^2 xy^2\}$$

where the limits are:

for 1),2)

$$\begin{cases} y_0 = 0 \\ \\ y_1 = \sqrt{\dfrac{\ell}{\gamma} - x^2} \end{cases}$$

for 3)

$$\begin{cases} y_0 = \sqrt{\dfrac{\ell}{\gamma} - (x + \dfrac{1}{\gamma\ \tan\ \delta})^2} \\ \\ y_1 = \sqrt{\dfrac{\ell}{\gamma} - x^2} \end{cases}$$

we have

$$2dT_y = -\text{sign}\ (\cos\theta)\ j4\ S dx(2\gamma\ x\ \sin\delta + \cos\ \delta)^2 \left\{ \frac{2\gamma^2 x^3 - x(2\gamma\ell - 1)}{4\ \gamma^2} \right.$$

$$[\ \sqrt{\frac{4\gamma^2}{1 + 4\gamma^2 x^2}} \quad \tan^{-1} \frac{y}{\sqrt{\frac{1 + 4\gamma^2 x^2}{4\gamma^2}}}]$$

$$\left. + \frac{x}{2}\ [y\ -\sqrt{\frac{1 + 4\gamma^2 x^2}{4\gamma^2}}\ \tan^{-1}\frac{y}{\sqrt{\frac{1 + 4\gamma^2 x^2}{4\gamma^2}}}]\right\}\ \begin{matrix} y_1 \\ \\ y_0 \end{matrix}$$

So looking at the expressions for y_0, one should in general evaluate integrals of two kinds:

$$f(x_0,x_1,\delta) = + \int_{x_0}^{x_1} (2\gamma x \sin \delta + \cos \delta)^2 \quad \cdot$$

$$\cdot \left\{ \frac{2\gamma^2 x^3 - x(2\gamma\ell - 1)}{4\gamma^2} \left[\sqrt{\frac{4\gamma^2}{1 + 4\gamma^2 x^3}} \quad \tan^{-1}\frac{\sqrt{\frac{\ell}{\gamma} - x^2}}{\sqrt{\frac{1}{4\gamma^2} + x^2}} \right] \right.$$

$$\left. + \frac{x}{2} \left[\sqrt{\frac{\ell}{\gamma} - x^2} - \sqrt{\frac{1}{4\gamma^2} + x^2} \quad \tan^{-1}\frac{\sqrt{\frac{\ell}{\gamma} - x^2}}{\sqrt{\frac{1}{4\gamma^2} + x^2}} \right] \right\} dx$$

$$g(x_0,x_1,\delta) = + \int_{x_0}^{x_1} (2\gamma x \sin \delta + \cos \delta)^2 \cdot$$

$$\cdot \frac{2\gamma^2 x^3 - x(2\gamma\ell - 1)}{4\gamma^2} \left[\sqrt{\frac{4\gamma^2}{1 + 4\gamma^2 x^2}} \left(\tan^{-1}\frac{\sqrt{\frac{\ell}{\gamma} - x^2}}{\sqrt{\frac{1}{4\gamma^2} + x^2}} - \tan^{-1}\frac{\sqrt{\frac{\ell}{\gamma} - (x + \frac{1}{\gamma\tan\delta})^2}}{\sqrt{\frac{1}{4\gamma^2} + x^2}} \right) \right.$$

$$+ \frac{x}{2} \left[\left(\sqrt{\frac{\ell}{\gamma} - x^2} - \sqrt{\frac{\ell}{\gamma} - (x + \frac{1}{\gamma\tan\delta})^2} \right) - \sqrt{\frac{1 + 4\gamma^2 x^2}{4\gamma^2}} \quad \cdot \right.$$

$$\left. \left. \cdot \left(\tan^{-1}\frac{\sqrt{\frac{\ell}{\gamma} - x^2}}{\sqrt{\frac{1}{4\gamma^2} + x^2}} - \tan^{-1}\frac{\sqrt{\frac{\ell}{\gamma} - (x + \frac{1}{\gamma\tan\delta})^2}}{\sqrt{\frac{1}{4\gamma^2} + x^2}} \right) \right] \right] dx$$

where in the last expression $\frac{\ell}{\gamma} - (x + \frac{1}{\gamma\tan\delta})^2$ has to be taken as zero for $\frac{\ell}{\gamma} - (x + \frac{1}{\gamma\tan\delta})^2 \leq 0$. Consider first the case $\frac{\pi}{2} \leq \delta \leq \pi$. From (4.2), we have sign $(\cos \theta) = -1$. Since only the function $f(x_0,x_1,\delta)$ occurs in this case, we have:

$$T = +j \quad 4S \, f(x_o,x_1,\delta)$$

where:

	x_0	x_1

$$\tan^{-1}(-2\sqrt{\ell\gamma})^{-1} \leq \delta \leq \pi \qquad\qquad -\sqrt{\frac{\ell}{\gamma}} \qquad\qquad +\sqrt{\frac{\ell}{\gamma}}$$

$$\frac{\pi}{2} \leq \delta \leq \tan^{-1}(-2\sqrt{2\gamma})^{-1} \qquad\qquad -\sqrt{\frac{\ell}{\gamma}} \qquad\qquad \frac{-1}{2\gamma \tan \delta}$$

Now consider the case $0 \leq \delta \leq \frac{\pi}{2}$ and suppose first that

$$\delta \leq \tan^{-1}(2\sqrt{\ell\gamma})^{-1}$$

The satellite is lighted from below, and sign $(\cos \theta) = +1$. Thus:

$$T_{\delta \leq \tan^{-1}(2\sqrt{\ell\gamma})^{-1}} = -j \, 4S \, f(x_0, x_1, \delta)$$

where

$$x_0 = -\sqrt{\frac{\ell}{\gamma}} \qquad\qquad x_1 = +\sqrt{\frac{\ell}{\gamma}} \qquad .$$

For $\delta > \tan^{-1}(2\sqrt{\ell\gamma})^{-1}$ the integrals are taken over two distinct regions: one, whose contributions to T are given by the function $f(x,\delta)$, is lighted from above, so sign $(\cos \theta) = -1$, and the other, lighted from below, whose contributions are described by the function $g(x,\delta)$, presents sign $(\cos \theta) = +1$. We get then

$$T_{\delta > \tan^{-1}(2\sqrt{\ell\gamma})^{-1}} = +j \, 4S \, f(x_0, x_1, \delta) - j \, 4S \, g(x_0^1, x_1^1, \delta)$$

where

$$\tan^{-1}(2\sqrt{\ell\gamma})^{-1} \leqq \delta \leqq \frac{\pi}{2}$$

x_0	x_1	$\mathbf{x}_0^1$	x_1^1
$-\sqrt{\dfrac{\ell}{\gamma}}$	$\dfrac{-1}{2\gamma\tan\delta}$	$\dfrac{-1}{2\gamma\tan\delta}$	$\sqrt{\dfrac{\ell}{\gamma}}$

6. *Expression of the torque in the body system*

Let us introduce a new set of coordinates, the c_i system, in the following way:

The plane c_1, c_2 contains the earth orbit, c_1 points toward the first point of Aries, c_3 is normal to the c_1, c_2 plane in such a way so to minimize the angle between the c_2 direction and the polar star; c_3 completes a usual right-handed system.

We also define an e_i system as follows: e_1 coincides with c_1; e_3 is pointing north along the axis of rotation of the earth; e_2 completes a right-handed orthonormal system.

The relation between the c_i system and the e_i system is given by the transformation

$$6.1 \qquad \begin{bmatrix} e_1 \\ e_2 \\ e_3 \end{bmatrix} = \begin{pmatrix} 1 & 0 & 0 \\ 0 & \cos\alpha & \sin\alpha \\ 0 & -\sin\alpha & \cos\alpha \end{pmatrix} \begin{bmatrix} c_1 \\ c_2 \\ c_3 \end{bmatrix}$$

or

$$6.2 \qquad \begin{bmatrix} e_1 \\ e_2 \\ e_3 \end{bmatrix} = C(0,\ 0,\ \alpha) \begin{bmatrix} c_1 \\ c_2 \\ c_3 \end{bmatrix}$$

where α is the angle obtained by rotating c_3 into e_3 (α is actually a negative angle equal approximately to $-23°$).

We shall assume for simplicity that the position of the earth is such that the c_2 vector points from the center of the sun to the center of the earth. With this assumption c_2 is also the direction of the incoming beam b. The relation between the c_i system and the p_i system in terms of α, $(\theta(t)_{se})$, (θ_{Rs}, ϕ_{Rs}), $(\theta(t)_{bR}, \Psi(t)_{bR}, \phi(t)_{bR})$, $(\theta_{bp}, \Psi_{bp}, \phi_{bp})$ (See the sections on Coordinate Systems, and Transformations, and Euler angles) is:

$$6.3 \quad \begin{bmatrix} p_1 \\ p_2 \\ p_3 \end{bmatrix} = C^T(\theta_{bp}, \Psi_{bp}, \phi_{bp}) \; C(\theta(t)_{bR}, \Psi(t)_{bR}, \phi(t)_{bR}) \; C(\theta_{Rs}, 0, \phi_{Rs})$$

$$C(\theta(t)_{se}, 0, 0) \; C(0, 0, \alpha) \qquad \begin{bmatrix} c_1 \\ c_2 \\ c_3 \end{bmatrix}$$

Lets call $G = (g_{ij})$ the matrix of the resulting transformation, so that

$$6.4 \quad \cos \widehat{c_2 p_1} = g_{12}; \quad \cos \widehat{c_2 p_2} = g_{22}; \quad \cos \widehat{c_2 p_3} = g_{32} \quad .$$

In the computation of the torques the set (x,y,z) of coordinates has been introduced. Let us write the transformation between this set and the p-set in terms of an angle β that describes a rotation around the p_2 axis. With reference to fig. 6.2 it is

172

$$6.5 \quad \begin{bmatrix} P_1 \\ P_2 \\ P_3 \end{bmatrix} = \begin{bmatrix} \cos\beta & -\sin\beta & 0 \\ 0 & 0 & -1 \\ \sin\beta & \cos\beta & 0 \end{bmatrix} \begin{bmatrix} x \\ y \\ z \end{bmatrix}$$

or

$$6.6 \quad \begin{bmatrix} P_1 \\ P_2 \\ P_3 \end{bmatrix} = C(0, \beta, \tfrac{\pi}{2})^T \begin{bmatrix} x \\ y \\ z \end{bmatrix}$$
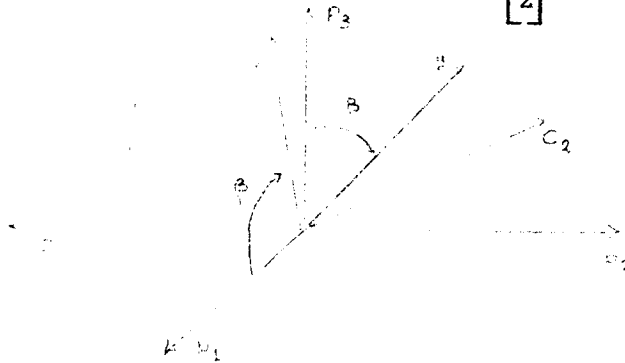
In accordance with the assumptions of section 2, we shall determine the angle β so to fulfill the following conditions:

a) The y-axis is normal to c_2 (direction of the incoming beam). that is $j \cdot c_2 = 0$ or the a_{22} element of $C(0, \beta, \tfrac{\pi}{2}) \cdot G$ is zero.

b) The component of c_2 on the x-axis is greater than or equal to zero. That is $i \cdot c_2 \geqslant 0$ or the a_{12} element of $C(0, \beta, \tfrac{\pi}{2}) \cdot G$ is greater than or equal to zero.

In terms of the elements of $C(0, \beta, \tfrac{\pi}{2}) \cdot G$, these conditions can be written:

$$6.7 \quad -g_{12} \sin\beta + g_{32} \cos\beta = 0$$

$$6.8 \quad g_{12} \cos\beta + g_{32} \sin\beta \geqslant 0$$

6.7 gives

(6.9) $$\tan \beta = \frac{g_{32}}{g_{12}}$$

Eliminating g_{12} in 6.8 using 6.7 (or 6.9),
we obtain

$$\sin \beta \geq 0, \quad \text{if} \quad g_{32} \geq 0$$

$$\sin \beta \leq 0, \quad \text{if} \quad g_{32} \leq 0$$

and the following cases are possible

$$g_{32} \geq 0, \ g_{12} \geq 0; \quad \tan \beta = \frac{g_{32}}{g_{12}}; \quad 0 \leq \beta \leq \frac{\pi}{2}$$

$$g_{32} \geq 0, \ g_{12} \leq 0; \quad \tan \beta = \frac{g_{32}}{g_{12}}; \quad \frac{\pi}{2} \leq \beta \leq \pi$$

$$g_{32} \leq 0, \ g_{12} \leq 0; \quad \tan \beta = \frac{g_{32}}{g_{12}}; \quad \pi \leq \beta \leq \frac{3}{2}\pi$$

$$g_{32} \leq 0, \ g_{12} \geq 0; \quad \tan \beta = \frac{g_{32}}{g_{12}}; \quad \frac{3}{2}\pi \leq \beta \leq 2\pi \quad .$$

The preceding relations completely determine β.

Let us write the computed torque as $T = T_j$ in the p_i system

$$T_{p_1} = -\sin \beta \ \mathbf{T}(\delta)$$

$$T_{p_2} = 0$$

$$T_{p_3} = \cos \beta \ T(\delta)$$

where T is a function of $\cos \delta$, $\sin \delta$ and $\tan \delta$; from the assumption 2.3, we have

$$\sin \delta = + \sqrt{1 - \cos^2 \delta} \qquad \tan \delta = \frac{+ \sqrt{1 - \cos^2 \delta}}{\cos \delta}$$

and finally $\cos \delta = z \cdot c_2 = -g_{22}$, where g_{22} is a function of the angles appearing in equation (6.3).

7. Computations.

Compute the matrix $\{g_{ij}\}$

$$G = C^T(\theta_{bp}, \Psi_{bp}, \phi_{bp})\ C(\theta(t)_{bR}, \Psi(t)_{bR}, \phi(t)_{bR})^*$$

$$C(\theta_{Rs}, 0, \phi_{Rs})\ C(\theta(t)_{se}, 0, 0)\ C(0, 0, \alpha).$$

Compute the angle β from the expression

$$\tan \beta = \frac{g_{32}}{g_{12}}$$

with the following conditions

if

$g_{32} \geq 0;\ g_{12} \geq 0$	$0 \leq \beta \leq \frac{\pi}{2}$
$g_{32} \geq 0;\ g_{12} \leq 0$	$\frac{\pi}{2} \leq \beta \leq \pi$
$g_{32} \leq 0;\ g_{12} \leq 0$	$\pi \leq \beta \leq \frac{3\pi}{2}$
$g_{32} \leq 0;\ g_{12} \geq 0$	$\frac{3}{2}\pi \leq \beta \leq 2\pi$

Set $\cos \delta = -g_{22};$

$$\sin \delta = +\sqrt{1 - g_{22}^2} \qquad \tan \delta = +\frac{\sqrt{1 - g_{22}^2}}{-g_{22}}$$

Set

176

$$T = (1 - \nu) \, T_a + \nu \, T_r$$

$$\nu = 0.75$$

Compute
$$\frac{\ell}{\gamma} - \frac{1}{4 \, \gamma^2 \, \tan^2 \delta}$$

if it is ≤ 0, put $T_a = 0$ if not write

$$T_a = S \, \cos^2 \delta \sqrt{\frac{\ell}{\gamma} - \frac{1}{4\gamma^2 \tan^2 \delta}} \left[\tan^2 \delta \ell^2 \, \frac{8}{15} - \frac{\ell}{\gamma} \, \frac{4}{15} + \frac{1}{30\gamma^2} \, \frac{1}{\tan^2 \delta} \right]$$

where
$$S = 9.4 \times 10^{-8}$$

$$\ell = 3\frac{1}{4} \qquad\qquad \sqrt{\frac{\ell}{\gamma}} = 15$$

Define:

$$f(x_0, x_1, \delta) = \int_{x_0}^{x_1} (2\gamma \, x \sin \delta + \cos \delta)^2 \quad \cdot$$

$$\cdot \left\{ \frac{2\gamma^2 x^3 - x(2\gamma\ell - 1)}{4\gamma^2} \left[\sqrt{\frac{4\gamma^2}{1 + 4\gamma^2 x^2}} \, \tan^{-1} \frac{\sqrt{\frac{\ell}{\gamma} - x^2}}{\sqrt{\frac{1}{4\gamma^2} + x^2}} \right] + \right.$$

$$\left. + \frac{x}{2} \left[\sqrt{\frac{\ell}{\gamma} - x^2} - \sqrt{\frac{1}{4\gamma^2} + x^2} \, \tan^{-1} \frac{\sqrt{\frac{\ell}{\gamma} - x^2}}{\sqrt{\frac{1}{4\gamma^2} + x^2}} \right] \right\} \, dx$$

$$g(x_0^1, x_1^1, \delta) = \int_{x_0^1}^{x_1^1} (2\gamma \, x \sin \delta + \cos \delta)^2 \quad \cdot$$

$$\cdot \left\{ \frac{2\gamma^2 x^3 - x(2\gamma\ell - 1)}{4\gamma^2} \left[\sqrt{\frac{4\gamma^2}{1 + 4\gamma^2 x^2}} \left(\tan^{-1} \frac{\sqrt{\frac{\ell}{\gamma} - x^2}}{\sqrt{\frac{1}{4\gamma^2} + x^2}} - \tan^{-1} \frac{\sqrt{\frac{\ell}{\gamma} - (x + \frac{1}{\gamma \tan \delta})^2}}{\sqrt{\frac{1}{4\gamma^2} + x^2}} \right) \right] \right.$$

177

$$+ \frac{x}{2} \left[\sqrt{\frac{\ell}{\gamma} - x^2} - \sqrt{\frac{\ell}{\gamma} - (x + \frac{1}{\gamma \tan \delta})^2} - \sqrt{\frac{1 + 4\gamma x^2}{4\gamma^2}} \right.$$

$$\left. (\tan^{-1} \frac{\sqrt{\frac{\ell}{\gamma} - x^2}}{\sqrt{\frac{1}{4\gamma^2} + x^2}} - \tan^{-1} \frac{\sqrt{\frac{\ell}{\gamma} - (x + \frac{1}{\gamma \tan \delta})^2}}{\sqrt{\frac{1}{4^2} + x^2}}) \right] \} \quad dx$$

if $g_{22} \geq 0$ compute $\tan^{-1} (-2\sqrt{\ell\gamma})^{-1}$

if $\tan^{-1}(-2\sqrt{\ell\gamma})^{-1} \leq \delta \leq \pi$

put $x_0 = -\sqrt{\frac{\ell}{\gamma}}$; $x_1 = +\sqrt{\frac{\ell}{\gamma}}$

and

$$T_r = +4 \ S \ f(x_0, x_1, \delta)$$

if $\frac{\pi}{2} \leq \delta \leq \tan^{-1} (-2\sqrt{\ell\gamma})^{-1}$

put $x_0 = -\sqrt{\frac{\ell}{\gamma}}$; $x_1 = - \frac{1}{2 \ \gamma \tan \delta}$

and $T_r = +4 \ S \ f(x_0, x_1, \delta)$

if $g_{22} \leq 0$ compute $\tan^{-1}(2\sqrt{\ell\gamma})^{-1}$

if $0 \leq \delta \leq \tan^{-1}(2\sqrt{\ell\gamma})^{-1}$

put $x_0 = -\sqrt{\frac{\ell}{\gamma}}$; $x_1 = +\sqrt{\frac{\ell}{\gamma}}$

and $T_r = -4 \ S \ f(x_0, x_1, \delta)$

if $\tan^{-1} (2\sqrt{\ell\gamma})^{-1} \leq \delta \leq \frac{\pi}{2}$

put $x_0 = -\sqrt{\frac{\ell}{\gamma}}$; $x_1 = \frac{-1}{2 \ \gamma \tan \delta}$; $x_0^1 = \frac{-1}{2 \ \gamma \tan \delta}$; $x_1^1 = +\sqrt{\frac{\ell}{\gamma}}$

and

$$T_r = + 4S \, f(x_0, x_1, \delta) - 4 \, S \, g(x_o^1, \, x_1^1, \delta)$$

Having so computed T for every δ, write

$$T_{P_1} = - \sin \, \beta \, T$$

$$T_{P_2} = 0$$

$$T_{P_3} = \cos \, \beta \, T$$

where T_{P_i} are the components of the torques along the P_i axis.

APPENDIX C

GRAVITY GRADIENT TORQUE ANALYSIS

Consider a satellite, whose geometrical and physical properties are summarized in the given inertia moments and products, with respect to the body system.

Let us describe the position of the satellite by the vector r that points from the center of the earth to the mass center of the satellite, and by the three Euler angles, θ, Ψ, ϕ, between the s_i system and the b_i system.* The interaction between the earth (here considered spherical) and the satellite can be described by a potential U that is a function of the given coordinates r, θ, Ψ, ϕ.

As long as the approximation of the so-called McCullagh formula is within prescribed accuracy, the "rotational" potential of the satellite in the earth field, that is, that part of the potential that depends on the rotational angles, can be written

$$\text{1)} \qquad U = \frac{3}{2} \; \frac{\mu}{r^3} \; I_0 \quad .$$

where I_0, the inertia moment of the satellite around the s_2 axis, is given by the relationship

$$\text{2)} \qquad I_0 = I_{11} \, a_1^2 + I_{22} \, a_2^2 + I_{33} \, a_3^2 + 2 \, I_{12} a_1 a_2 + 2 \, I_{13} \, a_1 a_3 + 2 \, I_{23} a_2 a_3 .$$

Here I_{ii} and I_{ij} are the inertia moments and products and $a_i = s_2 \cdot b_i$; in terms of θ, Ψ, ϕ these can be written

$$\text{3)} \qquad a_1 = \sin \theta \; \cos \Psi$$

$$a_2 = - \sin \theta \sin \phi \sin \Psi + \cos \theta \cos \phi$$

$$a_3 = - \sin \theta \cos \phi \sin \Psi - \cos \theta \sin \phi \quad .$$

---

*In the notation of the Euler angle section, these angles would be designated as $\theta_{bs}, \Psi_{bs}, \phi_{bs}$. In this section, for convenience we drop the subscripts.

With reference to Figure 3.1 of the section on Euler angles, let us consider the three infinitesimal rotations $d\theta$, $d\Psi$, $d\phi$: the expression

4)
$$-dU = -[\frac{\partial U}{\partial \phi} \, d\phi + \frac{\partial U}{\partial \Psi} \, d\Psi + \frac{\partial U}{\partial \theta} \, d\theta]$$

has the dimensions of work and can be interpreted as

(5)
$$\mathsf{T} \cdot d\phi$$

Where T is a vector, representing the total torque acting on the satellite and $d\phi$ is also a vector, the infinitesimal angular displacement.

Both the 4) and 5) are scalars, invariant under change of coordinates, but the 5) is expressed as the scalar product of two vectors, and this scalar product as to be specified in some set of coordinates.

Here there are two natural set of coordinates: the axis of the infinitesimal rotation of the Euler angles, i.e., the set s_3, b_1, s_2' of Figure 3.1 in the section on Euler angles, and the b-axis.

We want to expand the scalar product of 5) so as to have an expression of the following kind:

$$\mathsf{T} \cdot d\phi = \Sigma_i \quad T_i d\phi_i$$

This latter expression is true only if the set of axis along which the expansion is performed are orthogonal. Now the set of rotational axis is not an orthogonal set: this implies that the expansion as to be performed along the b-set, and the 5) can be rewritten as

6)
$$\mathsf{T} \cdot d\phi = \Sigma_i \, T_{b_i} \, d\phi_{b_i}$$

Consider now the 4): $d\theta$, $d\Psi$, $d\phi$ are the components of the vector $d\phi$

along the rotational set of axes: let us transform them into the b-system by means of the matrix $D^{-1}(\Psi, \phi)$ of the section on angular velocities[*]:

7)
$$\begin{bmatrix} d\phi \\ d\Psi \\ d\theta \end{bmatrix} = D^{-1}(\Psi, \theta) \begin{bmatrix} d\phi_{b_1} \\ d\phi_{b_2} \\ d\phi_{b_3} \end{bmatrix}$$

and the 4) can be formally rewritten

8)
$$-dU = - \left[\frac{\partial U}{\partial \phi}, \; \frac{\partial U}{\partial \Psi}, \; \frac{\partial U}{\partial \theta} \right] D^{-1}(\Psi, \theta) \begin{bmatrix} d\phi_{b_1} \\ d\phi_{b_2} \\ d\phi_{b_3} \end{bmatrix}$$

Recalling the 6) and the fact that the infinitesimal angular displacements are arbitrary the following identification can be done:

9)
$$[T_{b_1}, \; T_{b_2}, \; T_{b_3}] = - \left[\frac{\partial U}{\partial \phi}, \; \frac{\partial U}{\partial \Psi}, \; \frac{\partial U}{\partial \theta} \right] D^{-1}(\Psi, \theta)$$

and transposing

10)
$$\begin{bmatrix} T_{b_1} \\ T_{b_2} \\ T_{b_3} \end{bmatrix} = - D^{-1}(\Psi, \theta) \begin{bmatrix} \frac{\partial U}{\partial \phi} \\ \frac{\partial U}{\partial \Psi} \\ \frac{\partial U}{\partial \theta} \end{bmatrix}$$

So we have

11)
$$\begin{cases} T_{b_1} = - \frac{\partial U}{\partial \phi} \\[2mm] T_{b_2} = \tan \Psi \sin \phi \frac{\partial U}{\partial \phi} + \cos \phi \frac{\partial U}{\partial \Psi} - \frac{\sin \phi}{\cos \Psi} \frac{\partial U}{\partial \theta} \\[2mm] T_{b_3} = \tan \Psi \cos \phi \frac{\partial U}{\partial \phi} - \sin \phi \frac{\partial U}{\partial \Psi} - \frac{\cos \phi}{\cos \Psi} \frac{\partial U}{\partial \theta} \end{cases}$$

---

[*]Multiply equation (4.11) by dt and invert $D(\Psi, \phi)$.

It is possible to verify that from the 11) it follows

$$T_{b_1} = \frac{3\mu}{r^3} \{(I_{21}a_1 + I_{22}a_2 + I_{23}a_3) \ (-a_3) \ +$$

$$+ \ (I_{31}a_1 + I_{32}a_2 + I_{33}a_3) \ a_2\}$$

$$T_{b_2} = \frac{3\mu}{r^3} \{(I_{11}a_1 + I_{12}a_2 + I_{13}a_3) \ a_3 \ +$$

$$+ \ (I_{31}a_1 + I_{32}a_2 + I_{33}a_3) \ (-a_1)\}$$

$$T_{b_3} = \frac{3\mu}{r^3} \ (I_{11}a_1 + I_{12}a_2 + I_{13}a_3) \ (-a_2) \ +$$

$$+ \ (I_{21}a_1 + I_{22}a_2 + I_{23}) \ a_1\}$$

The assumed values for the principal inertia moments (in the p_i system) are:

I_1 along the p_1 axis = 2686 slug $\cdot$ ft^2 .

I_2 along the p_2 axis = 1846 slug $\cdot$ ft^2 .

I_3 along the p_3 axis = 1617 slug $\cdot$ ft^2 .

It is possible from these to obtain the values for the I_{ij} components of the inertial matrix in the b_i system recalling the transformation law for tensors of rank two:

$$t'_{\mu\nu} = h_{\mu\alpha} h_{\mu\beta} t_{\alpha\beta} \quad .$$

where

$$h_{\rho\sigma} = i'_\rho \cdot i_\sigma$$

So we have:

$$I_{11} = h_{11}^2 \, I_1 + h_{12}^2 \, I_2 + h_{13}^2 \, I_3$$

$$I_{22} = h_{21}^2 \, I_1 + h_{22}^2 \, I_2 + h_{23}^2 \, I_3$$

$$I_{33} = h_{31}^2 \, I_1 + h_{32}^2 \, I_2 + h_{33}^2 \, I_3$$

$$I_{12} = I_{21} = h_{11}h_{21} \, I_1 + h_{12}h_{22} \, I_2 + h_{13}h_{23} \, I_3$$

$$I_{13} = I_{31} = h_{11}h_{31} \, I_1 + h_{12}h_{32} \, I_2 + h_{13}h_{33} \, I_3$$

$$I_{23} = I_{32} = h_{21}h_{31} \, I_1 + h_{22}h_{32} \, I_2 + h_{23}h_{33} \, I_3$$

in which h_{ij} are the elements of the matrix

$$C(\theta_{bp}, \, \Psi_{bp}, \, \phi_{bp})^T$$

that describes the transformation from the p_i system to the b_i system (see page 47 for the elements of the matrix C).

APPENDIX D

SIMULATION OF ELASTIC BOOMS ON THE SATELLITE

SIMULATION OF ELASTIC BOOMS ON THE SATELLITE

I. <u>Introduction</u>: We wish to investigate the effect upon satellite motion
of elastic booms projecting from the satellite proper. That is, without
compensating for the boom's motion, indeed without any knowledge of it, the
present control law will be used on a satellite with an elastic boom, just
as it is now being used on a satellite with a rigid boom. The degradation of
control can then be observed in terms of changes in fuel and time requirements,
and increased number of control actuations.

The solution of the actual physical problem requires the solution
of the partial differential equation for the elastic beam

$$\frac{\partial^2 q}{\partial t^2} = - \frac{QK^2}{\rho} \frac{\partial^4 q}{\partial s^4}$$

(see Morse, <u>Vibration and Sound</u>, p. 154). $q(t,s)$ is the displacement of the
boom from its equilibrium position (which is itself a function of the satellite
attitude).

The allowed frequencies of the oscillation are

$$\nu_i = \frac{KQ^{1/2}}{2\pi \ell^2 \rho^{1/2}} \lambda_i^2 \quad .$$

Where

K = radius of gyration

Q = Young's modulus

ℓ = length   see Morse, P. 151f

ρ = density

and the first few values of λ_i are given in Morse, p. 158.

$$\lambda_1 = 1.8751, \quad \lambda_2 = 4.6941, \quad \lambda_3 = 7.8548 \quad .$$

Even better we have

$$\nu_2 = 6.267\nu_1$$

$$\nu_3 = 17.548\nu_1$$

$$\nu_4 = 34.387\nu_1 \quad .$$

As an introduction to the effect it appeared advisable to GSFC and MSG to examine the effect upon the motion of a single particle situated off the antenna but linked to it by a spring-damper device. The purpose of this memorandum is the derivation of the equations of motion for the system composed of our present satellite together with such a particle.

The equations which will be given were derived first by a lagrangian technique and second by the vectorial methods which appear here. Since the final results agree, we have great confidence that the equations are in fact, correct.

II. <u>Definitions and Assumptions</u>: ϕ, θ, Ψ, ω_1, ω_2, ω_3 have unchanged definitions. I_1, I_2, I_3 are the principal moments of inertia of the satellite about its center of mass.

Computation of the center of mass and of the moments does not include

the mass particle.

The lagrangian is

$$L = -\frac{1}{2}\alpha(q_1^2+q_3^2) + \frac{1}{2}\,\omega'I\omega + \frac{m}{2}(\dot{u}^2+\dot{v}^2+\dot{w}^2)$$

where α is the spring constant; q_1 and q_3 are the projections of the particle on the body 1 and 3 axes (we assumed the particle to be on the body 2 axis, ℓ units from the c.m.); and $\dot{u}$, $\dot{v}$, and $\dot{w}$ are components, in the target reference system, of the particle's inertial velocity.

Notice that the particle is constrained to move orthogonally to the body 2 axis.

A damping coefficient β will also be assumed.

Given an axis system rotating with velocity $\underline{\omega}$ with respect to an inertial system, it is possible to write the equation of the motion in the following way:

$$ma_o = F - 2m(\underline{\omega}xv_o) - m\underline{\omega}\ x\ (\omega x\underline{r}) - m\dot{\omega}\ x\ r \qquad 1)$$

where

$\underline{a}_o$ is the observed acceleration

$\underline{v}_o$ is the observed velocity

r is the position

F is the force applied.

It is important to point out that in some texts (for example, Goldstein, p. 135) the last term is missing, because the angular velocity is assumed constant.

The force F applied on the body B by the spring and the damping is:

$$F = -\alpha q_1\underline{i} - \alpha q_3\underline{k} - \beta\dot{q}_1\underline{i} - \beta\dot{q}_3\underline{k} \qquad 2)$$

where as usual i, j, k are the unit vectors that give the directions of the

q_1, q_2, q_3 axes.

Writing down the equation 1) along the $\underline{i}$ and $\underline{k}$ axes we have:

$$m\ddot{q}_1 = -\alpha q_1 - \beta \dot{q}_1 - 2m\omega_2\dot{q}_3 - m\omega_1(\omega_1 q_1 + \omega_2 \ell + \omega_3 q_3)$$
$$+ mq_1(\omega_1^2 + \omega_2^2 + \omega_3^2) - m(\dot{\omega}_2 q_3 - \dot{\omega}_3 \ell)$$

$$m\ddot{q}_3 = -\alpha q_3 - \beta \dot{q}_3 + 2m\omega_2\dot{q}_1 - m\omega_3(\omega_1 q_1 + \omega_2 \ell + \omega_3 q_3)$$
$$+ mq_3(\omega_1^2 + \omega_2^2 + \omega_3^2) - m(\dot{\omega}_1 q_2 - \dot{\omega}_2 q_1)$$

These are the equations that describe the movement of B with respect to the antenna.

The equation for the antenna, a rigid body constrained to rotate around a fixed point, will be the Euler equations: if we assume that the system {i, j, k} is the set of principal axes for the antenna, these are:

$$I_1\dot{\omega}_1 + (I_3 - I_2)\omega_2\omega_3 = n_1$$

$$I_2\dot{\omega}_2 + (I_1 - I_3)\omega_1\omega_3 = n_2$$

$$I_3 + (I_2 - I_1)\omega_2\omega_1 = n_3$$

where I_i is the principal moment of inertia and n_i the torque applied along the corresponding axis. These torques will be both those applied directly over the antenna and those arising from the interaction between the antenna and the body B.

Our next step will be deriving these last.

The forces that the antenna applies over B are:

a) the force applied through the spring

b) the frictional force arising from the damping

c) the constraining force.

We did not write the equation of the motion for B in the $\underline{j}$ direction, because

190

the constraints do not allow any motion in that direction. On the other hand the terms in 1) arising from the movement of the reference frame do not have zero components along the j axis. We therefore can use the j component of equation 1) to solve for the force of constraint.

Now if a), b), c) are the forces that are applied on B by the antenna, B will apply forces on the antenna with the same magnitude and opposite directions. More precisely:

a') Through the spring is applied over the antenna, at the point $(0,\ell,0)$, the force

$$F_a = \alpha q_1 \underline{i} + \alpha q_3 \underline{k}$$

b') From the friction is applied over the antenna, at the point (q_1,ℓ,q_3) the force

$$F_b = \beta \dot{q}_1 \underline{i} + \beta \dot{q}_3 \underline{k}$$

c') From the relative motion is applied over the antenna at (q_1,ℓ,q_3) the force (arising from the expansion of the right hand member of 1))

$$F_c = [-2m(\omega_3 \dot{q}_1 - \omega_1 \dot{q}_3) - m\omega_2(\omega_1 q_1 + \omega_2 \ell + \omega_3 q_3)$$
$$+ m\ell(\omega_1^2 + \omega_2^2 + \omega_3^2) - m(\dot{\omega}_3 q_1 - \dot{\omega}_1 q_3)]j$$

Finally, recalling that the torque $\underline{T}$ over $(0,0,0)$ is given by:

$$\underline{T} = \underline{i}(q_2 F_3 - q_3 F_2) + \underline{j}(q_3 F_1 - q_1 F_3) + \underline{k}(q_1 F_2 - q_2 F_3)$$

where F_i is the force in the q_i direction, we have

$$T_1 = \ell(\alpha q_3 + \beta \dot{q}_3) - q_3[2m(\omega_3 \dot{q}_1 - \omega \dot{q}_3) - m\omega_2(\omega_1 q_1 + \omega_2 \ell + \omega_3 q_3) + m\ell(\omega_1^2 + \omega_2^2 + \omega_3^2)$$

$$- m(\dot{\omega}_3 q_1 - \dot{\omega}_1 q_3)]$$

$$T_2 = \beta q_3 \dot{q}_1 - \beta q_1 \dot{q}_3$$

$$T_3 = -\ell(\alpha q_1 + \beta \dot{q}_1) + q_1[-2m(\omega_3 \dot{q}_1 - \omega_1 \dot{q}_3) - m\omega_2(\omega_1 q_1 + \omega_2 \ell + \omega_3 q_3) + m\ell(\omega_1^2 + \omega_2^2 + \omega_3^2)$$

$$- m(\dot{\omega}_3 q_1 - \dot{\omega}_1 q_3)]$$

APPENDIX E

CONTROL SYNTHESIS ANALYSIS

6E.1 *Optimal Synthesis of Scalar Component System*

1.1 *Introduction*

In Part 2 the synthesis of optimal attitude control was reduced to considering three component scalar systems of the form

$$
\begin{cases}
\dot{x}_2 = u + b \\[2ex]
\dot{x}_1 = x_2 \\[2ex]
|u| \leq 1 \\[2ex]
J = \displaystyle\int_{t_o}^{t_1} (\lambda_1 + \lambda_2 x_2^2 + \lambda_3 |u|) dt
\end{cases}
$$

where b is constant with magnitude less than 1 and optimality specifies the minimization of J. Our control objective is to drive the systems to $x_2 = x_1 = 0$. For the synthesis developed in we shall specify in addition that $-1 < b < 0$. For $b = 0$ the proper synthesis is given by passing to the limit as b approaches 0. For $0 < b < 1$ the proper synthesis is easily seen to be the synthesis for $-b$ reflected about the x_2 - coordinate axis.

Following the Pontryagin Maximal Principle we consider the
system

$$
\begin{aligned}
\dot{x}_O &= \lambda_1 + \lambda_2\, x_2^{\,2} + \lambda_3\, |u| \ , \\
\dot{x}_1 &= x_2 \ , \\
\dot{x}_2 &= u + b \ .
\end{aligned}
\right\} \tag{1.1}
$$

We may write the Hamiltonian

$$
H(x_1,\ x_2,\ z_0,\ z_1,\ z_2,\ u) = z_O[\lambda_1 + \lambda_2\, x_2^{\,2} + \lambda_3 |u|]
\tag{1.2}
$$

$$
+ z_1\, x_2 + z_2\, (u + b).
$$

Therefore, the co-state equations are

$$
\begin{aligned}
\dot{z}_O &= - \frac{\partial H}{\partial x_O} = 0 \ , \\
\dot{z}_1 &= - \frac{\partial H}{\partial x_1} = 0 \ , \\
\dot{z}_2 &= - \frac{\partial H}{\partial x_2} = - 2z_O\, \lambda_2\, x_2 - z_1 \ .
\end{aligned}
\right\} \tag{1.3}
$$

It will be necessary to actually solve the equations of motion
(1.1) on intervals of constant control $u(t)$. Let $u(t) \equiv u_O$ on an
interval $[\sigma_1,\ \sigma_2]$. Then for $\sigma_1 \leqslant t \leqslant \sigma_2$, we have from (1.1),

$$x_2(t) = (b + u_o) \ (t - \sigma_1) + x_2(\sigma_1) \ ,$$

$$x_1(t) = \frac{1}{2} \ (b + u_o) \ (t - \sigma_1)^2 + x_2(\sigma_1) \ (t - \sigma_1) + x_1(\sigma_1) \ , \qquad (1.4)$$

hence,

$$x_1(t) = \frac{x_2^{\ 2}(t)}{2(b + u_o)} + k \ , \qquad (1.5)$$

where k is the constant $x_1(\sigma_1) - \dfrac{x_2^{\ 2}(\sigma_1)}{2(b + u_o)}$.

Let $u(t)$ be an optimal control with a corresponding optimal trajectory $(x_1(t), \ x_2(t))$ on $[t_o, \ t_1]$. Then from Pontryagin's Maximum Principle, we have

$$(z_o(t), \ z_1(t), \ z_2(t)) \neq (0, \ 0, \ 0) \quad \text{on} \quad [t_o, \ t_1], \qquad (1.6)$$

$$z_o(t_o) \leqslant 0, \qquad (1.7)$$

and

$$\left. \begin{aligned} &H(x_1(t), \ x_2(t), \ z_o(t), \ z_1(t), \ z_2(t), \ u(t)) \\ &\quad = M(x_1(t), \ x_2(t), \ z_o(t), \ z_1(t), \ z_2(t)) = 0 \end{aligned} \right\} \qquad (1.8)$$

almost everywhere on $[t_o, \ t_1]$, where M is defined by

$$\begin{aligned} M(x_1, \ x_2, \ z_o, \ z_1, \ z_2) = \ &sup\{H(x_1, \ x_2, \ z_o, \ z_1, \ z_2, \ u) \\ &: \ |u| \leqslant 1\} \ . \end{aligned} \qquad (1.9)$$

Since changing the control on a set of measure zero does not change the trajectories nor the cost, we shall usually assume that we have redefined the optimal control so that (1.8) holds for every t in $[t_o, \ t_1]$.

1.2 *Control Law*

We consider separately the cases $z_0(t_0) = 0$ and $z_0(t_0) < 0$.
First, suppose that $z_0(t_0) = 0$. Then H reduces to

$$H = z_1 x_2 + z_2(u + b).$$

Thus $M = z_1 x_2 + |z_2| + z_2 b$; that is, the optimal control $u(t)$ must satisfy

$$u(t) = sgn \; z_2(t) \tag{2.1}$$

for every t in $[t_0, t_1]$. From (1.3), we have

$$\dot{z}_2 = -z_1 \tag{2.2}$$

so that $z_2(t)$ is linear. If $z_2(t) \equiv 0$, then $z_1(t) \equiv 0$ by (2.2) and $z_0(t) \equiv 0$ by assumption. This contradicts (1.6). Thus $z_2(t) \not\equiv 0$, so that from (2.1), $u(t)$ is bang-bang with at most one switch. Let this switch occur at $t = \tau$. Then $z_2(\tau) = 0$, hence $H(\tau) = z_1(\tau) x_2(\tau) = 0$. From (2.1), if $z_1(\tau) = 0$, then $z_2(t) \equiv z_1(t) \equiv 0$ contradicting (1.6). Thus $x_2(\tau) = 0$. For $t > \tau$, either $x_2(t) = (t - \tau)$ or $x_2(t) = -(t-\tau)$. In either case, it can never happen again that $x_2(t) = 0$. Thus $x_2(\tau) = x_1(\tau) = 0$; that is, the trajectory must already have reached the target at $t = \tau$. Thus the point $(x_1(t_0), x_2(t_0))$ must lie in one of the two "optimal parabolas"

$$x_1 = \frac{x_2^{\,2}}{2(b+1)} \; , \quad x_1 \geq 0,$$

$$x_1 = \frac{x_2^{\,2}}{2(b-1)} \; , \quad x_1 \leq 0. \tag{2.3}$$

If $(x_1(t_o), x_2(t_o))$ does not lie on one of the curves (2.3),
then it must be that $z_2(t_o) < 0$. We may assume without loss of generality
that $z_o(t_o) = -1$. We then have

$$H = - [\lambda_1 + \lambda_2 x_2 + \lambda_3 |u|] + z_1 x_2 + z_2 (u + b), \qquad (2.4)$$

and H is maximized with respect to u by choosing

$$u = \begin{cases} + 1 & \text{if} \quad z_2 > \lambda_3, \\ 0 & \text{if} \quad |z_2| < \lambda_3, \\ - 1 & \text{if} \quad z_2 < - \lambda_3. \end{cases} \qquad (2.4)$$

If $z_2 = \lambda_3$, we can conclude only that u is between 0 and 1, while if
$z_2 = - \lambda_3$, we can only conclude that u is between -1 and 0. We must
then determine the sets on which $z_2(t)$ equals λ_3 or $-\lambda_3$, and we must
determine $u(t)$ on these sets. By (1.3), $\dot{z}_2 = 2\lambda_2 x_2 - z_1$, hence

$$\ddot{z}_2 = 2\lambda_2 (u + b) \ .$$

Thus $z_2(t) > \lambda_3$ implies $u(t) = 1$ which implies $\ddot{z}_2(t) > 0$ so that $z_2(t)$
is concave up. Also, $z_2(t) < - \lambda_3$ implies $u(t) = - 1$ which implies
$\ddot{z}_2(t) < 0$ so that $z_2(t)$ is concave down. Similarly, $|z_2(t)| < \lambda_3$ implies
$u(t) = 0$ which implies $\ddot{z}_2(t) < 0$ so that $z_2(t)$ is concave down. If
$z_2(t) \equiv \lambda_3$ on an interval I, $\ddot{z}_2(t) \equiv 0 = 2\lambda_2(u(t) + b)$ which implies
$u(t) \equiv - b > 0$ on I. If $z_2(t) \equiv - \lambda_3$ on an interval I,
$\ddot{z}_2(t) \equiv 0 = 2\lambda_2(u(t) + b)$ which implies $u(t) \equiv - b > 0$ on I, contradicting
the fact that u is between -1 and 0 for $z_2 = - \lambda_3$. Thus $z_2(t)$ cannot
identically equal $-\lambda_3$ on a interval. Furthermore, $\dot{z}_2(t)$ is continuous.

From this analysis we conclude that the set $\{t : z_2(t) = \lambda_3\}$ consists of either one point or a closed interval, while the set $\{t : z_2(t) = -\lambda_3\}$ consists of either one point or two points. Thus an optimal control must obey the control law

$$u(t) = \begin{cases} +1 & \text{if } z_2(t) > \lambda_3 , \\ -b & \text{if } z_2(t) = \lambda_3 , \\ 0 & \text{if } |z_2(t)| < \lambda_3 , \\ -1 & \text{if } z_2(t) < -\lambda_3 , \end{cases} \qquad (2.6)$$

and $z_2(t)$ cannot equal $-\lambda_3$ except on a set of measure zero. Moreover, since $z_2(t)$ is continuous, $u(t)$ cannot assume the values 1 and -1 consecutively, nor the values $-b$ and -1 consecutively. The optimal trajectory segments corresponding to each of the values of $u(t)$ in (2.6) are given below in figure 2.1, using (1.5).
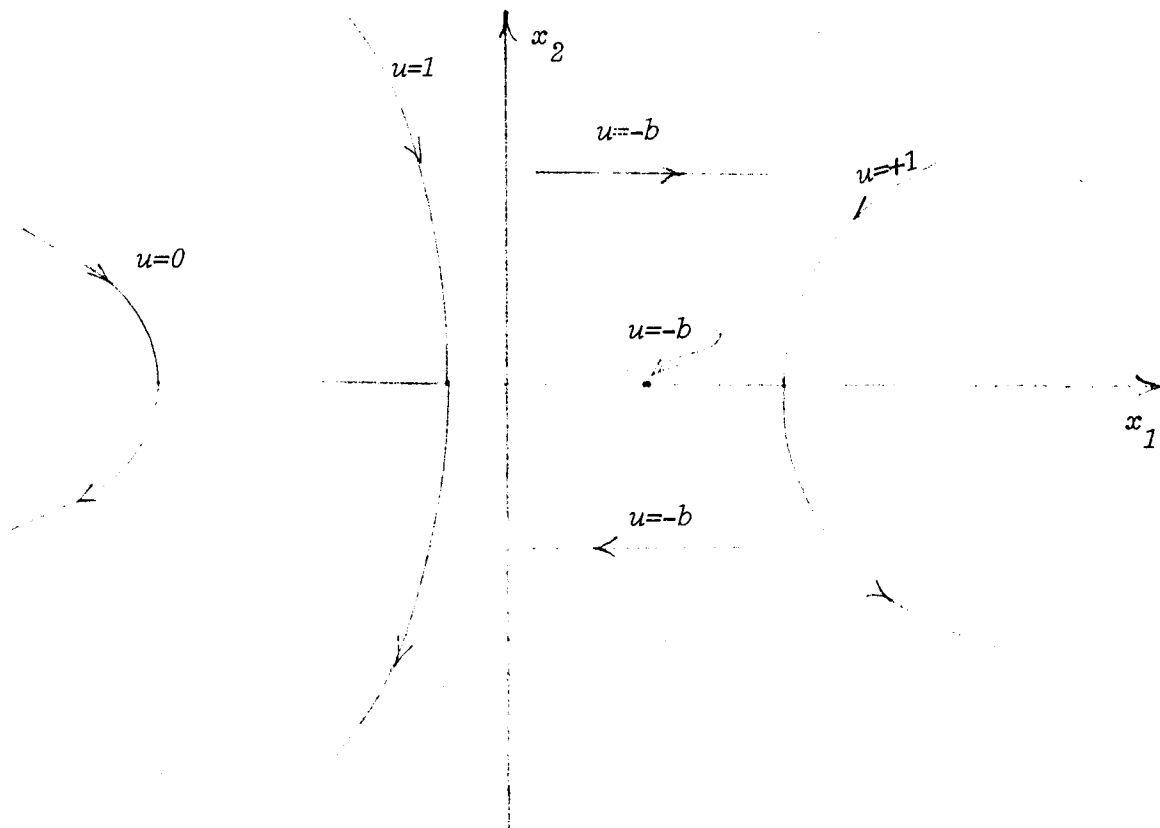

Figure 2.1

Furthermore, only continuous segments of the seven graphs given in Figure 2.2 are possible for $z_2(t)$.
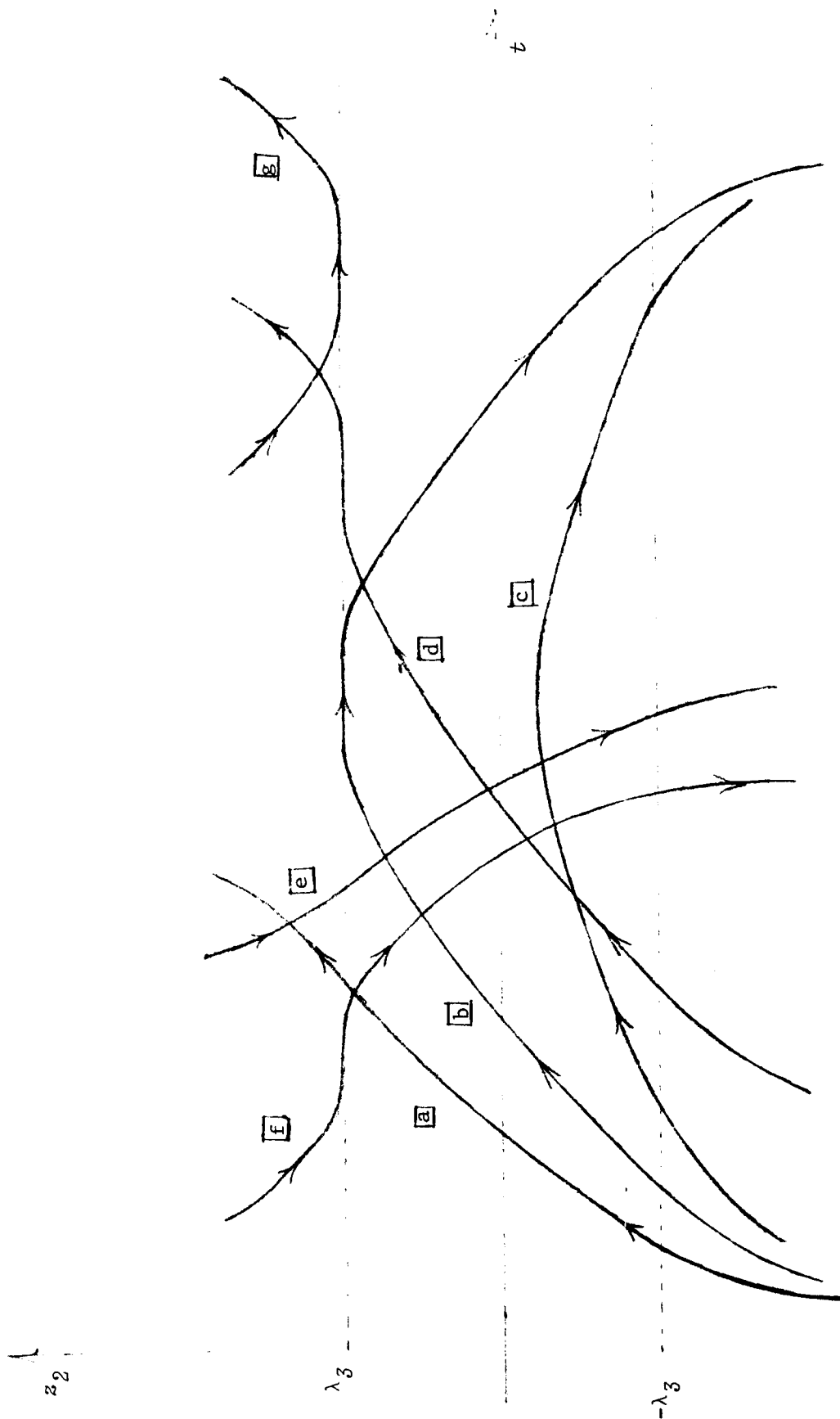
The corresponding strategies are

[a] :   -1, 0, + 1

[b] :   -1, 0, -b, 0, -1

[c] :   -1, 0, -1

[d] :   -1, 0, -b, +1

[e] :   +1, 0, -1

[f] :   +1, -b, 0, -1

[g] :   +1, -b, +1

Of course, "substrategies" may occur, such as $-b$, 0, -1 which is a sub-strategy of [b] .

1.3 *Switching Point Analysis*

We now determine the trajectory segments terminating at the origin. Clearly, a trajectory segment corresponding to $u = -b$ cannot terminate at the origin. If a trajectory segment corresponding to $u = + 1$ ends at the origin, it must lie completely in the 4th quadrant. A trajectory segment corresponding to either $u = 0$ and $u = -1$ and ending at the origin must lie completely in the 2nd quadrant. Consider the case where termination occurs at a final time t_1 with $u = 0$. Then at $t = t_1$, we have

$$H = - \lambda_1 + z_2(t_1) \, b = 0. \tag{3.1}$$

From (2.6), $\left|z_2(t_1)\right| \leq \lambda_3$. Hence using (3.1) we have

$$\frac{\lambda_1}{b} = z_2(t_1) \geq -\lambda_3 \, ,$$

hence,

$$b \leq -\frac{\lambda_1}{\lambda_3} \qquad . \tag{3.2}$$

Now suppose termination occurs at a final time t_1 with $u = -1$
and suppose that the initial value $(x_1(t_o), x_2(t_o))$ does not lie on an
optimal parabola of the form (2.3). Then $z_o(t_o) = -1$, and $z_2(t)$ is
decreasing from the value $-\lambda_3$ as $t \to t_1$. Hence at $t = t_1$, we have

$$H = -\lambda_1 - \lambda_3 + z_2(t_1)(b-1) = 0,$$

therefore,

$$z_2(t_1) = \frac{\lambda_1 + \lambda_3}{b - 1} \qquad . \tag{3.3}$$

From (2.6), $z_2(t_1) < -\lambda_3$, hence

$$\frac{\lambda_1 + \lambda_3}{b-1} < -\lambda_3 \, ,$$

which implies

$$-\frac{\lambda_1}{\lambda_3} < b \tag{3.4}$$

From (3.2) and (3.4) we conclude that if $-1 < b \leq -\frac{\lambda_1}{\lambda_3}$, termination
occurs from the 2nd quadrant only with $u = 0$, unless the entire trajectory
is a subset of the optimal parabola segment $x_1 = \frac{x_2^2}{2(b-1)}$, $x_1 \leq 0$. Also,
if $-\frac{\lambda_1}{\lambda_3} < b < 0$, then termination occurs from the 2nd quadrant only with

$u = -1$. These possibilities are shown in figure 3.1.

$$-\frac{\lambda_1}{\lambda_3} < b < 0$$

$$-1 < b \le -\frac{\lambda_1}{\lambda_3}$$
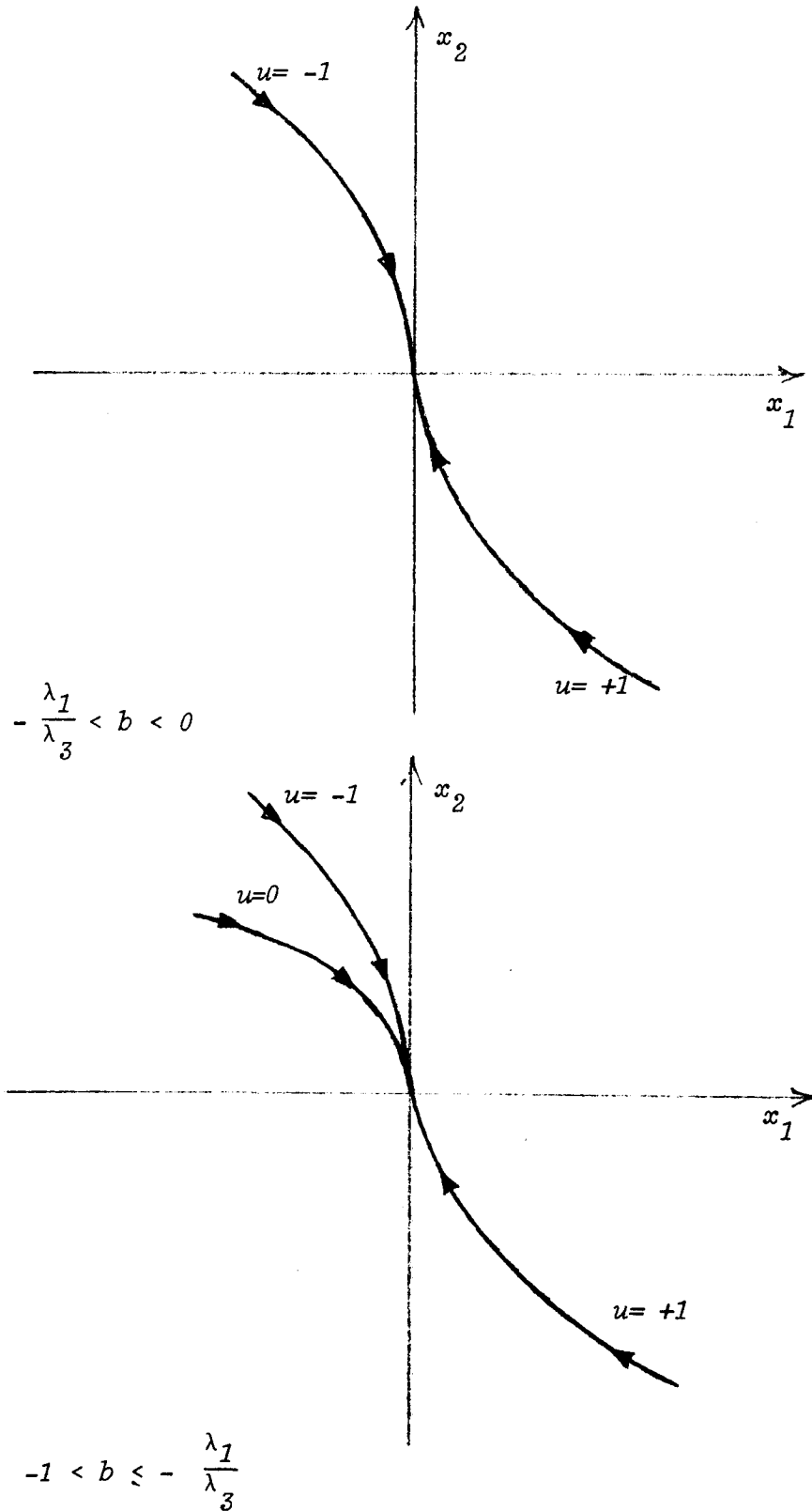
Figure 3.1

1.4 *Relationships at Switching Points*

We next derive relations between x_1 and x_2 at various switching points. The results are presented in table 4.1. For convenience later, let $s = \sqrt{\dfrac{\lambda_1 - \lambda_3\, b}{\lambda_2}}$ and $r = \sqrt{\dfrac{-2\lambda_3\, b}{\lambda_2}}$, and for

$-\dfrac{\lambda_1}{\lambda_3} \leq b < 0$ let $q = \sqrt{\dfrac{\lambda_1 + \lambda_3\, b}{\lambda_2}}$.

Let τ be a point at which u switches to or from $-b$. Then at $t = \tau$

$$H = -\,[\lambda_1 + \lambda_2\, x_2^{\,2}(\tau) + \lambda_3|b|] + z_1(t_o)\, x_2(\tau) = 0 \qquad (4.1)$$

and

$$\dot{z}_2(\tau) = 2\lambda_2\, x_2(\tau) - z_1(t_o) = 0 \ .$$

Thus $z_1(t_o) = 2\lambda_2\, x_2(\tau)$, and using this in (4.1) we have

$$x_2^{\,2}(\tau) = \frac{\lambda_1 - \lambda_3 b}{\lambda_2} \ .$$

A switch from $-b$ to $+1$ occurs in $\boxed{d}$ and $\boxed{g}$ after which u remains $+1$. At this point then,

$$x_2(\tau) = -\sqrt{\frac{\lambda_1 - \lambda_3\, b}{\lambda_2}} = -\,s \ .$$

u switches from	At the switching point, x_1 and x_2 satisfy
$-b$ to -1	no such switch can occur.
-1 to $-b$	no such switch can occur.
$-b$ to $+1$	$x_2 = -s$
$-b$ to 0	$x_2 = s.$
0 to $-b$	$x_2 = s$ or $x_2 = -s.$
$+1$ to $-b$	$x_2 = s$ or $x_2 = -s.$
0 to -1	$-\dfrac{\lambda_1}{\lambda_3} < b < 0$ and $0 < x_2 < q$.
-1 to 0	$\begin{cases} \text{if} \quad -1 < b < -\dfrac{\lambda_1}{\lambda_3} \quad, \quad \text{then } x_2 > 0. \\[2mm] \text{if} \quad b = -\dfrac{\lambda_1}{\lambda_3}, \quad \text{then } x_2 = 0 \text{ or } x_2 > 0. \\[2mm] \text{if} \quad -\dfrac{\lambda_1}{\lambda_3} < b < 0, \text{ then } x_2 > q \text{ or } \\[2mm] \qquad\qquad -q < x_2 < 0. \end{cases}$
0 to $+1$	$-s \lesssim x_2 < 0.$
$+1$ to 0	$0 < x_2 \lesssim s$.

$$s = \sqrt{\frac{\lambda_1 - \lambda_3\, b}{\lambda_2}} \quad, \quad q = \sqrt{\frac{\lambda_1 + \lambda_3\, b}{\lambda_2}}$$

Table 4.1

A switch from $-b$ to 0 occurs in $\boxed{b}$ and $\boxed{f}$ after which u cannot be $+1$. Thus the origin is entered from the 2nd quadriant, hence

$$x_2(\tau) = s.$$

Each of the switches 0 to $-b$ and $+1$ to $-b$ may occur for $x_2(\tau) = s$ or $x_2(\tau) = -s$, see figure 2.2.

Now suppose u switches from 0 to -1 at τ. Then

$$H = -[\lambda_1 + \lambda_2 x_2^2(\tau)] + z_1(t_o) x_2(\tau) - \lambda_3 b = 0, \qquad (4.2)$$

$$\dot{z}_2(\tau) = 2\lambda_2 x_2(\tau) = z_1(t_o) < 0, \qquad (4.3)$$

and $u(t) \equiv -1$ for all $t \geqslant \tau$, see figure 2.2. Thus we must have $-\dfrac{\lambda_1}{\lambda_3} < b < 0$ and $x_2(\tau) > 0$, see figure 3.1. Thus from (4.2) and (4.3),

$$z_1(t_o) = \frac{\lambda_1 + \lambda_2 x_2^2(\tau) + \lambda_3 b}{x_2(\tau)} > 2\lambda_2 x_2(\tau)$$

so that

$$\lambda_1 + \lambda_3 b > \lambda_2 x_2^2(\tau) .$$

Since $x_2^2(\tau) > 0$,

$$0 < x_2(\tau) < \sqrt{\frac{\lambda_1 + \lambda_3 b}{\lambda_2}} = q .$$

Let u switch from -1 to 0 at τ. Then

$$H = - [\lambda_1 + \lambda_2 \, x_2^2(\tau)] + z_1(t_o) \, x_2(\tau) - \lambda_3 \, b = 0 \qquad (4.4)$$

and

$$\dot{z}_2(\tau) = 2\lambda_2 \, x_2(\tau) - z_1(t_o) > 0 \; . \qquad (4.5)$$

There are now several cases. If $b = -\lambda_{1/\lambda_3}$, then (4.4) implies

$$0 = - \lambda_1 - \lambda_2 \, x_2^2(\tau) + z_1(t_o) \, x_2(\tau) + \lambda_1$$

$$= z_1(t_o) \, x_2(\tau) - \lambda_2 \, x_2^2(\tau)$$

so that either $x_2(\tau) = 0$ or $x_2(\tau) = z_1(t_o)/\lambda_2$. Using (4.5),

$$x_2(\tau) = z_1(t_o)/\lambda_2 < 2\lambda_2 \, x_2(\tau)/\lambda_2 = 2x_2(\tau)$$

which implies $x_2(\tau) > 0$. Thus if $b = -\lambda_{1/\lambda_3}$, we can conclude only that either $x_2(\tau) = 0$ or $x_2(\tau) > 0$. If $-1 < b < - \dfrac{\lambda_1}{\lambda_3}$, then from (4.4) we have

$$z_1(\tau_o) \, x_2(\tau) = \lambda_1 + \lambda_2 \, x_2^2(\tau) + \lambda_3 \, b < \lambda_2 \, x_2^2(\tau) \; . \qquad (4.6)$$

If $x_2(\tau) \leq 0$, (4.5) implies

$$z_1(t_o) \, x_2(\tau) \geq 2\lambda_2 \, x_2^2(\tau) \; ,$$

contradicting (4.6). Thus $x_2(\tau) > 0$, for the case $-1 < b < - \dfrac{\lambda_1}{\lambda_3}$.

Finally, if $- \dfrac{\lambda_1}{\lambda_3} < b < 0$, then

$$z_1(t_o) \, x_2(\tau) = \lambda_1 + \lambda_2 \, x_2^2(\tau) + \lambda_3 \, b \; .$$

If $x_2(\tau) = 0$, we have $b = -\dfrac{\lambda_1}{\lambda_3}$, a contradiction. If $x_2(\tau) \neq 0$, we have, using (4.5)

$$z_1(t_o) = \frac{\lambda_1 + \lambda_2 \, x_2^2(\tau) + \lambda_3 \, b}{x_2(\tau)} \; < 2\lambda_2 \, x_2(\tau) \; . \qquad (4.7)$$

If $x_2(\tau) > 0$, (4.7) yields

$$\lambda_2 \, x_2^2(\tau) > \lambda_1 + \lambda_3 \, b \; ,$$

hence

$$x_2(\tau) > q \; .$$

If $x_2(\tau) < 0$, (4.7) yields

$$\lambda_2 \, x_2^2(\tau) < \lambda_1 + \lambda_3 \, b \; ,$$

hence

$$x_2(\tau) > - q.$$

Let u switch from 0 to $+1$ at τ. Then $u(t) \equiv + 1$ for $t \geqslant \tau$, hence $x_2(\tau) < 0$. Also,

$$H = - \left[\lambda_1 + \lambda_2 \, x_2^2(\tau) \right] + z_1(t_o) \, x_2(\tau) + \lambda_2 \, b = 0 \qquad \textbf{and}$$

$$\dot{z}_2(\tau) = 2\lambda_3 \, x_2(\tau) - z_1(t_o) \geqslant 0 \; ,$$

hence

$$z_1(t_o) = \frac{\lambda_1 + \lambda_2 \, x_2^2(\tau) - \lambda_2 \, b}{x_2(\tau)} \leq 2\lambda_2 \, x_2(\tau)$$

which implies

$$- s \leq x_2(\tau) < 0 \ .$$

Let u switch from $+1$ to 0 at τ. In figure 2.2, this happens only in $\boxed{e}$, hence $x_2(\tau) > 0$. The argument of the preceding paragraph yields

$$0 < x_2(\tau) \leq s \ .$$

1.5 *Construction of Optimal Trajectories*

Table 4.1 contains most of the data we need to construct the optimal trajectories in phase space. However, we do require some further analysis by which we determine a bound on trajectory segments corresponding to $u = 0$.

Consider the trajectory corresponding to strategy $\boxed{e}$ of figure 2.2. Let $u(t) = 0$ during $\boxed{e}$ on an interval $[\sigma_1, \sigma_2]$. Then for t in $[\sigma_1, \sigma_2]$, we have $\ddot{z}_2(t) = 2\lambda_2 \, b$, hence $\dot{z}_2(t) = 2\lambda_2 \, b(t - \sigma_1) + \dot{z}_2(\sigma_1)$ and $-2\lambda_3 = z_2(\sigma_2) - z_2(\sigma_1) = \lambda_2 \, b(\sigma_2 - \sigma_1)^2 + \dot{z}_2(\sigma_1) \, (\sigma_2 - \sigma_1)$. Since $\dot{z}_2(\sigma_1) \leq 0$, $-2\lambda_3 \leq \lambda_2 \, b(\sigma_2 - \sigma_1)^2$, hence

$$|x_2(\sigma_2) - x_2(\sigma_1)| = |b(\sigma_2 - \sigma_1)| = -b(\sigma_2 - \sigma_1)$$

$$\leq -b \sqrt{-\frac{2\lambda_3}{\lambda_2 b}}$$

$$= \sqrt{\frac{-2\lambda_3 b}{\lambda_2}} = r .$$

(5.1)

A similar analysis also applies to $\boxed{a}$. For $\boxed{b}$, $\boxed{d}$, and $\boxed{f}$, we have $\dot{z}_2(\sigma_1) = 0$ (or $\dot{z}_2(\sigma_2) = 0$) , hence for these trajectory segments

$$|x_2(\sigma_2) = x_2(\sigma_1)| = r .$$

(5.2)

The one case of $\boxed{b}$ where z_2 takes on the value λ_3 at precisely one point, we have

$$|x_2(\sigma_2) - x_2(\sigma_1)| = 2r .$$

For $\boxed{c}$ we have

$$|x_2(\sigma_2) - x_2(\sigma_1)| \leq 2r .$$

We construct the optimal trajectories by proceeding backwards in time from the final time. The results are given in figures 5.1, 5.2, and 5.3. First, let $-\frac{\lambda_1}{\lambda_3} < b < 0$. Then only segments corresponding to

$u = 1$ or $u = -1$ can end at the origin. Proceeding along the segment

$$x_1 = \frac{x_2^2}{2(b-1)}$$ into the 2nd quadrant, we have two possibilities. Either

the entire optimal trajectory is part of that half-parabola, or this

final segment meets a trajectory segment corresponding to $u = 0$

$0 < x_2 < q$, see table 4.1. Suppose the latter occurs. Then $z_2(t)$

has one of the forms $\boxed{b}$, $\boxed{c}$, $\boxed{e}$, or $\boxed{f}$. Now using

table 4.1 and the first part of section 5, we see that each of these

strategies must actually occur, otherwise vast regions of the 2nd quadrant

will not be reached by optimal trajectories. For example, if $\boxed{f}$

does not occur, the trajectories do not reach the region

$$x_2 < s , \qquad x_1 << 0 .$$

If either $\boxed{f}$ or $\boxed{b}$ occurs, then since $u = -b$ only on

$x_2 = s$ in the 2nd quadrant, and using (5.2), the $u = 0$ segment meets

the final $u = -1$ segment precisely at $x_2 = s - r$. Proceeding further

along this optimal trajectory, either the $u = -b$ segment completes the

full trajectory, or it doesn't. If it does not, then the $u = -b$ meets a

$u = 1$ segment (strategy $\boxed{f}$) completing the trajectory, or it meets

a $u = 0$ segment (strategy $\boxed{b}$). If the latter occurs and does not

complete the trajectory, then by (5.2) the $u = 0$ segment meets a $u = -1$

segment precisely at $x_2 = s + r$, completing the trajectory.

If the $u = 0$ segment meets the final segment for $0 < x_2 < s - r$,

then this corresponds to strategy $\boxed{e}$ because trajectories cannot cross

each other, and the $u = 0$ segment meets a $u = 1$ segment for $0 < x_2 < s$,

211

completing that trajectory. The switching curve C_1 where the $u = 0$ segment meets the initial $u = 1$ segment is computed in section 6.

If the $u = 0$ segment meets the final segment for $s - r < x_2 < q$ (note that $s - r < q$ whenever $-\frac{\lambda_1}{\lambda_3} < b < 0$ and $s - r = q$ when $-\frac{\lambda_1}{\lambda_3} = b$), then this corresponds to strategy $\boxed{c}$ because trajectories cannot cross. This $u = 0$ segment then meets a $u = -1$ segment for $q < x_2 < s + r$, completing that trajectory. The switching curve C_3 where the $u = 0$ segment meets the initial $u = -1$ segment is computed in section 8. This completes the construction for the optimal trajectories whose final segments correspond to $u = -1$. The region so covered is

$$\{(x_1, x_2): x_1 \leq \frac{x_2^2}{2(b-1)} \} \quad U \quad \{(x_1, x_2): x_1 < \frac{x_2^2}{2(b+1)}$$

(5.3)

$$\text{and } x_2 \leq 0\} .$$

Still assuming that $-\frac{\lambda_1}{\lambda_3} < b < 0$, we proceed along the segment $x_1 = \frac{x_2^2}{2(b+1)}$ into the 4th quadrant. Then either the entire optimal trajectory is part of that half-parabola, or this final $u = 1$ segment meets a $u = 0$ trajectory segment, or the $u = 1$ segment meets a $u = -b$ segment. In the first case, this completes the optimal trajectory. The second case corresponds to strategy $\boxed{a}$ and this switch occurs for $-s < x_2 < 0$. Hence this $u = 0$ segment must meet a $u = -1$ segment for $-q < x_2 < 0$ (we shall see later that this switch actually occurs for $-s + r < x_2 < 0$), completing that trajectory. The switching curve C_2 where the $u = 0$ segment meets the initial $u = -1$ segment is computed in section 7.

212

The third case corresponds to one of the strategies $\boxed{d}$ or $\boxed{g}$. As before, each of these must occur, otherwise part of the $x_1 - x_2$ plane will not be reached. In $\boxed{g}$ the $u = -b$ segments meets a $u = 1$ segment, completing the trajectory. In $\boxed{d}$ the $u = -b$ segment meets a $u = 0$ segment which in turn meets a $u = -1$ segment at $x_2 = -s + r$, completing the trajectory. This completes the construction for the optimal trajectories whose final segments correspond to $u = 1$. The region so covered is the complement of the region in (5.3). This finishes the case $-\dfrac{\lambda_1}{\lambda_3} < b < 0$, see figure 5.1.

The two remaining cases $b = -\dfrac{\lambda_1}{\lambda_3}$ and $-1 < b < -\dfrac{\lambda_1}{\lambda_3}$ are treated similarly, except each is slightly easier than the case handled above. The results are shown in figures 5.2 and 5.3.

213

1.6 *Switching Curve* C_1

We start with a procedure which will allow us to derive both C_1 and C_3. Let the interval $[t_o, t_1]$ be divided into three parts so that $u = h$ on $[t_o, \tau_1]$, $u = 0$ on $[\tau_1, \tau_2]$, and $u = -h$ on $[\tau_2, t_1]$. If $h = 1$, we assume that $(x_1(\tau_1), x_2(\tau_1))$ belongs to C_1 while if $h = -1$, we assume that $(x_1(\tau_1), x_2(\tau_1))$ belongs to C_2. Solving the equations (1.1) on these intervals leads to the following:

$$x_2(t) = b(t - \tau_1) + x_2(\tau_1) , \quad \text{and}$$

$$x_1(t) = \frac{1}{2} b (t - \tau_1)^2 + x_2(\tau_1)(t - \tau_1) + x_1(\tau_1)$$

for $\tau_1 \le t \le \tau_2$. Thus

$$x_2(t) = (b-h)(t-\tau_2) + b(\tau_2-\tau_1) + x_2(\tau_1), \quad \text{and}$$

$$x_1(t) = \frac{1}{2} (b - h)(t - \tau_2)^2 + [b(\tau_2 - \tau_1) + x_2(\tau_1)] (t - \tau_2)$$

$$+ \frac{1}{2} b(\tau_2 - \tau_1)^2 + x_2(\tau_1)(\tau_2 - \tau_1) + x_1(\tau_1)$$

for $\tau_2 \le t \le t_1$. At $t = t_1$, the above becomes

$$\left. \begin{aligned}
0 = x_2(t_1) &= (b - h)(t_1 - \tau_2) + b(\tau_2 - \tau_1) + x_2(\tau_1) , \\
0 = x_1(t_1) &= \frac{1}{2} (b - h)(t_1 - \tau_2)^2 + \left[b(\tau_2 - \tau_1) + x_2(\tau_1) \right] (t_1 - \tau_2) \\
&\quad + \frac{1}{2} b(\tau_2 - \tau_1)^2 + x_2(\tau_1)(\tau_2 - \tau_1) + x_1(\tau_1).
\end{aligned} \right\} \quad (6.1)$$

Solving the two equations in (6.1) simultaneously; that is, eliminating $(t_1 - \tau_2)$, we have

$$0 = - bh(\tau_2 - \tau_1)^2 - 2h\, x_2(\tau_1)(\tau_2 - \tau_1) + 2(b-h)\, x_1(\tau_1) - x_2^{\ 2}(\tau_1). \quad (6.2)$$

What we need is a relation between $x_1(\tau_1)$ and $x_2(\tau_1)$ with $(\tau_2 - \tau_1)$ eliminated.

For $\tau_1 \leqslant t \leqslant \tau_2$, we have

$$\ddot{z}_2(t) = 2\lambda_2\, b \;,$$

hence

$$\dot{z}_2(t) = 2\lambda_2\, b(t - \tau_1) + \dot{z}_2(\tau_1)$$

and

$$z_2(t) = \lambda_2\, b(t - \tau_1)^2 + \dot{z}_2(t_1)(t - \tau_1) + z_2(\tau_1).$$

But $z_2(\tau_1) = h\lambda_3$ and $z_2(\tau_2) = - h\lambda_3$, hence

$$- h\lambda_3 = \lambda_2 b(\tau_2 - \tau_1)^2 + \dot{z}_2(\tau_1)(\tau_2 - \tau_1) + h\lambda_3$$

which implies

$$\dot{z}_2(\tau_1) = \frac{-2h\lambda_3 - \lambda_2 b(\tau_2 - \tau_1)^2}{\tau_2 - \tau_1}$$

We also have from (1.3)

$$\dot{z}_2(\tau_1) = 2\lambda_2 \, x_2(\tau_1) - z_1(t_o) \ ,$$

hence

$$z_1(t_o) = 2\lambda_2 \, x_2(\tau_1) + \frac{2h\lambda_3 + \lambda_2 \, b(\tau_2 - \tau_1)^2}{\tau_2 - \tau_1} \ . \qquad (6.3)$$

Using (6.3) in the Hamiltonian at $t = \tau_1$, we have

$$\left. \begin{array}{l} H = - \, [\lambda_1 + \lambda_2 \, x_2^{\,2}(\tau_1)] + z_1(t_o) \, x_2(\tau_1) + z_2(\tau_1)b \\[3mm] \quad = - \, \lambda_1 + \lambda_2 \, x_2^{\,2}(\tau_1) + \left[\dfrac{2h\lambda_3 + \lambda_2 \, b(\tau_2 - \tau_1)^2}{\tau_2 - \tau_1} \right] x_2(\tau_1) \\[8mm] \qquad + \, h\lambda_3 \, b = 0 \ , \end{array} \right\} \qquad (6.4)$$

so that we may eliminate $(\tau_2 - \tau_1)$ between (6.2) and (6.4).

Let $\alpha = \tau_2 - \tau_1$, $x = x_1(\tau_1)$, $y = x_2(\tau_1)$, and $\beta = - \, \lambda_1 + \lambda_2 y^2 + h\lambda_3 \, b$. Then we rewrite (6.2) and (6.4) as

$$bh \, \alpha^2 + 2hy \, \alpha - 2(b-h)x + y^2 = 0 \qquad (6.5)$$

$$\lambda_2 \, by \, \alpha^2 + \beta \, \alpha + 2h\lambda_3 = 0 \ . \qquad (6.6)$$

We now eliminate α. Multiplying (6.5) by $- \dfrac{\lambda_2 y}{h}$ and adding the result to (6.6) gives

$$[-2\lambda_2 y^2 + \beta]\alpha + \frac{2\lambda_2 y(b-h)x}{h} - \frac{\lambda_2 y^3}{h} + 2h\lambda_3 y = 0. \qquad (6.7)$$

Substituting (6.7) into (6.5), we obtain

$$(bh\delta^2 + 2\gamma\delta + \gamma^2)y^2 = 2\gamma^2(b-h)x , \qquad (6.8)$$

where

$$\gamma = -\lambda_1 - \lambda_2 y^2 + h\lambda_3 b$$

and

$$\delta = -2\lambda_3 + \lambda_2 y^2 - 2\lambda_2(b-h)x .$$

Put $h = 1$. Then the switching curve C_1 is part of the curve

$$(b\delta^2 + 2\gamma\delta + \gamma^2)y^2 = 2\gamma^2(b-1)x , \qquad (6.9)$$

where

$$\gamma = -\lambda_1 - \lambda_2 y^2 + \lambda_3 b < 0$$

and

$$\delta = -2\lambda_3 + \lambda_2 y^2 - 2\lambda_2(b-1)x.$$

If we now let $b = -\dfrac{\lambda_1}{\lambda_2}$ and $y^2 = 2bx$ in (6.9), there results an identity, which means that for $b = -\dfrac{\lambda_1}{\lambda_2}$, the switching curve C_1 contains the $u = 0$ final segment of an optimal trajectory, see figure 5.2. The full switching curve C_1 is given by (6.9) together with the boundary conditions

$$0 \leqslant y \leqslant s, \quad \text{and}$$

$$\frac{bs^2 - 2rs + r^2}{2b(b-1)} \leqslant x \leqslant 0.$$

1.7 *Switching Curve* C_2

If we put $h = -1$ in (6.8), we have

$$(-b\delta^2 + 2\gamma\delta + \gamma^2)y^2 = 2\gamma^2(b + 1)x, \qquad (7.1)$$

where

$$\gamma = -\lambda_1 - \lambda_2 y^2 - \lambda_3 b$$

and

$$\delta = -2\lambda_3 + \lambda_2 y^2 - 2\lambda_2(b + 1)x.$$

This time, γ may be zero. In fact, if $b = -\dfrac{\lambda_1}{\lambda_3}$, then

$$\gamma = -\lambda_2 y^2$$

so that $y = 0$ is a solution of (7.1); in fact, it is the only solution that fits the boundary conditions of the switching curve C_2 which are

$$0 \leqslant y \leqslant -s + r,$$

$$0 \leqslant x \leqslant \frac{b(r - s)^2 - 2rs + r^2}{2b(b+1)}$$

if $1 < b \leqslant -\dfrac{\lambda_1}{\lambda_2}$ (i.e., $0 \leqslant -s + r$); and

$$-s + r \leqslant y \leqslant 0,$$

$$0 \leqslant x \leqslant \frac{b(r-s)^2 - 2rs + r^2}{2b(b+1)}$$

if $-\dfrac{\lambda_1}{\lambda_2} \leqslant b < 0.$

1.8 *Switching Curve* C_3

Let the interval $[t_o, t_1]$ be divided into three parts so that $u = -1$ on $[t_o, \tau_1]$, $u = 0$ on $[\tau_1, \tau_2]$, and $u = -1$ on $[\tau_2, t_1]$. We assume $(x_1(\tau_1), x_2(\tau_1))$ belongs to C_3. Just as we derived (6.1), we have

$$
\left.
\begin{aligned}
0 &= (b-1)(t_1-\tau_2) + b(\tau_2-\tau_1) + x_2(\tau_1), \\[6pt]
0 &= \frac{1}{2}(b-1)(t_1-\tau_2)^2 + [b(\tau_2-\tau_1) + x_2(\tau_1)]\,(t_1-\tau_2) \\[6pt]
&\quad + \frac{1}{2}b(\tau_2-\tau_1)^2 + x_2(\tau_1)(\tau_2-\tau_1) + x_1(\tau_1)\ .
\end{aligned}
\right\}
\tag{8.1}
$$

Eliminating $(t_1-\tau_2)$, we obtain

$$
0 = -b(\tau_2-\tau_1)^2 - 2x_2(\tau_1)(\tau_2-\tau_1) + 2(b-1)x_1(\tau_1) - x_2^{\,2}(\tau_1). \tag{8.2}
$$

For $\tau_1 \leqslant t \leqslant \tau_2$, we have

$$
\ddot{z}_2(t) = 2\lambda_2\, b\ ,
$$

hence

$$
\dot{z}_2(t) = 2\lambda_2\, b(t - \tau_1) + \dot{z}_2(\tau_1)
$$

and

$$
z_2(t) = \lambda_2\, b(t - \tau_1)^2 + \dot{z}_2(\tau_1)(t - \tau_1) + z_2(\tau_1)\ .
$$

But $z_2(\tau_1) = z_2(\tau_2) = -\lambda_3$, hence

$$0 = \lambda_2\, b(\tau_2 - \tau_1) + \dot{z}_2(\tau_1)$$

which implies

$$\dot{z}_2(\tau_1) = -\lambda_2\, b(\tau_2 - \tau_1).$$

We also have from (1.3)

$$\dot{z}_2(\tau_1) = 2\lambda_2\, x_2(\tau_1) - z_1(t_o)\ ,$$

hence

$$z_1(t_o) = 2\lambda_2\, x_2(\tau_1) + \lambda_2\, b(\tau_2 - \tau_1). \tag{8.3}$$

Using (8.3) in the Hamiltonian at $t = \tau_1$, we have

$$H = -\,[\lambda_1 + \lambda_2\, x_2^{\,2}(\tau_1)] + z_1(t_o)\, x_2(\tau_1) + z_2(\tau_1)b$$

$$= -\,\lambda_1 + \lambda_2\, x_2^{\,2}(\tau_1) + \lambda_2\, b\, x_2(\tau_1)(\tau_2 - \tau_1) - \lambda_3\, b = 0. \tag{8.4}$$

Using (8.4) in (8.2) to eliminate $(\tau_2 - \tau_1)$ and letting $x = x_1(\tau_1)$ and $y = x_2(\tau_1)$, we have

$$x = \frac{y^2}{2b}\left[1 + \frac{q^4}{(b-1)y}\right]. \tag{8.5}$$

Thus if $b = -\dfrac{\lambda_1}{\lambda_3}$, $q = 0$, and (8.5) reduces to

$$x = \frac{y^2}{2b}$$

which is the same $u = 0$ final segment that (6.9) reduces to, see figure 5.2. The boundary conditions on (8.5) are

$$q \leqslant y \leqslant r + s,$$

$$\frac{b(s+r)^2 - 4\,rs}{2b(b-1)} \leqslant x \leqslant \frac{q^2}{2(b-1)} \quad .$$

1.9 *Variations of Equations*

Now we have treated

$$\dot{x}_1 = x_2 \; ,$$

$$\dot{x}_2 = u - |b| \; , \quad 0 < |b| < 1 \; . \tag{9.1}$$

Suppose we are confronted with

$$\dot{y}_1 = - y_2 \; ,$$

$$\dot{y}_2 = u - |b| \; . \tag{9.2}$$

Let $x_1 = - y_1$. Then

$$\dot{x}_1 = - \dot{y}_1 = y_2 \; ,$$

$$\dot{y}_2 = u - |b| \; . \tag{9.3}$$

Thus we compute u from figures 5.1 – 5.3.

Suppose we are confronted with

$$\dot{y}_1 = y_2 \; ,$$

$$\dot{y}_2 = u + |b| \; . \tag{9.4}$$

Let $x_1 = - y_1, \quad x_2 = - y_2, \quad v = - u.$ Then

$$\dot{x}_1 = - \dot{y}_1 = - y_2 = x_2 \; ,$$

$$\dot{x}_2 = - \dot{y}_2 = - u - |b| = v - |b| \; . \tag{9.5}$$

We compute v from figure 5.1 – 5.3. Then we put $u = -v$.

Finally, suppose we are confronted with

$$\left. \begin{array}{l} \dot{y}_1 = - y_2 \ , \\ \dot{y}_2 = u + |b| \ . \end{array} \right\} \qquad (9.6)$$

Let $x_2 = - y_2$, $v = - u$. Then

$$\left. \begin{array}{l} \dot{y}_1 = - y_2 = x_2 \ , \\ \dot{x}_2 = - \dot{y}_2 = - u - |b| = v - |b| \ . \end{array} \right\} \qquad (9.7)$$

We compute v from figures 5.1 – 5.3. Then we put $u = -v$.

6E.2 *Time of Arrival on Target and Performance Parameter Calculations*

2.1 *Introduction*

In this section of Appendix E we calculate the parameters which are necessary in time synchronization of three second order syntheses such as described in the previous sections. This section together with Section 6E.1 form the heart of our control logic calculations.

2.2 *Preliminary Calculations*

Consider the switching curve C_1 defined as follows:

$$(b\delta + 2\gamma + \gamma^2)y^2 = 2\gamma^2(b - 1)x \tag{2.1}$$

where

$$\gamma = -\lambda_1 - \lambda_2 y^2 + \lambda_3 b < 0 \tag{2.2}$$

$$\delta = -2\lambda_3 + \lambda_2 y^2 - 2\lambda_2(b - 1)x \tag{2.3}$$

$$0 \leq y \leq s$$

$$\frac{bs^2 - 2rs + r^2}{2b(b - 1)} \leq x \leq 0 \quad . \tag{2.4}$$

We shall need the intersections of this curve with the family of parabolas

$$x_1 = \frac{1}{2(b+1)} x_2^2 + k_1 \quad . \tag{2.5}$$

Because direct substitution leads to a third order equation, we shall approximate the C_1 curve with a simpler one.

Precisely, for $b = 0$ the C_1 reduces to

$$x_1 = -\left(\frac{1}{2} + \frac{2\lambda_3}{\lambda_1 - \lambda_2 x_2^2}\right) x_2^2 \quad .$$

Taking advantage of the fact that b is small, we shall approximate the C_1 by the curve C_1'

$$x_1 = - \left(\frac{1}{2} + \frac{2\lambda_3}{\lambda_1 - \lambda_2 \tau x_2^2} \right) \tau x_2^2 \qquad (2.6)$$

where τ will be chosen in such a way that C_1' passes through

$$\frac{bs^2 - 2rs + r^2}{2b(b-1)} , s \qquad , \qquad (2.7)$$

and the conditions (4) are satisfied.

Solving (6) with respect to τ, we have

$$\tau = \frac{x_2^2(\lambda_1 + 4\lambda_3) - 2\lambda_2 x_1 x_2^2 \pm \sqrt{[x_2^2(\lambda_1 + 4\lambda_3) - 2\lambda_2 x_1 x_2^2]^2 + 8\lambda_1\lambda_2 x_1 x_2^4}}{2\lambda_2 x_2^4}$$

$$(2.8)$$

The condition

$$\lim \tau = 1$$
$$x_1 \rightarrow -\infty$$
$$x_2 \rightarrow \sqrt{\frac{\lambda_1}{\lambda_2}}$$

implies that in (2.8) the $+$ sign has to be chosen. Direct substitution in (2.8) of the values of (2.7) gives the τ required.

Let us find now the intersection of (2.5) with the family (2.6); we have

$$x_2^4 \left[\frac{1 + \tau(b+1)(-\lambda_2\tau)}{2(b+1)} \right] + x_2^2 \left[\frac{(1+(b+1)\lambda_1}{2(b+1)} + \tau(2\lambda_3 - \lambda_2 k_1) \right] + k_1\lambda_1 = 0$$

$$(2.9)$$

i.e.,

$$x_2^4 \alpha + x_2^2 \beta + \gamma = 0$$

and

$$x_2^2 = \frac{-\beta \pm \sqrt{\beta^2 - 4\alpha\gamma}}{2\alpha} \ . \tag{2.10}$$

It is

$$\gamma < 0, \quad \beta > 0, \quad \alpha < 0,$$

i.e.,

$$\beta^2 - 4\alpha\gamma \leq \beta^2 \tag{2.11}$$

The two solutions are positive; from the study of the behavior of (2.6) it is clear that the minor has to be chosen, i.e.,

$$x_2^2 = \frac{-\beta - \sqrt{\beta^2 - 4\alpha\gamma}}{2\alpha} \ . \tag{2.12}$$

The intersection we are interested in lies in the positive x_2 half plane, so

$$x_2 = +\sqrt{\frac{-\beta - \sqrt{\beta^2 - 4\alpha\gamma}}{2\alpha}} \tag{2.13}$$

where β and γ are functions of k_1.

The corresponding x_1 is:

$$x_1 = \frac{1}{2(b+1)} \frac{-\beta - \sqrt{\beta^2 - 4\alpha\gamma}}{2\alpha} + k_1 \ . \tag{2.14}$$

227

Switching Curve C_2.

For the same reasons as before, we shall approximate C_2 by C_2':

$$x_1 = \left(\frac{1}{2} + \frac{2\lambda_3}{\lambda_1 - \lambda_2 \, \tau \, x_2^2} \right) \tau \, x_2^2 \qquad (2.15)$$

with the conditions

$$\left. \begin{array}{l} -s + r \leq y \leq 0 \\[2ex] 0 \leq x \leq \dfrac{b(r-s)^2 - 2rs + r^2}{2b(b+1)} \end{array} \right\} \qquad (2.16)$$

τ as a function of (x_1, x_2) is given by:

$$\tau = \frac{x_2^2(\lambda_1 + 4\lambda_3) + 2\lambda_2 \, x_1 \, x_2^2 \pm \sqrt{[x_2^2(x_1 + 4\lambda_3) + 2\lambda_2 \, x_1 \, x_2^2]^2 - 8\lambda_1\lambda_2 \, x_1 \, x_2^4}}{2\lambda_2 \, x_2^4} \qquad (2.17)$$

From the condition

$$\lim_{\substack{x_1 \to +\infty \\ x_2 \to -\sqrt{\frac{\lambda_1}{\lambda_2}}}} \tau = 1,$$

we choose the minus sign.

Direct substitution of the values

$$x_1 = r - s \qquad (2.18)$$

$$x_2 = \frac{b(r-s)^2 - 2rs + r^2}{2b(b+1)} \qquad (2.19)$$

gives the τ required.

The intersection of (14) with the family of parabolas

$$x_1 = \frac{1}{2(b-1)} \; x_2^2 + k_{-1} \; , \qquad k_{-1} > 0 \qquad (2.20)$$

occurs at x_2 solution of

$$x_2^4 \; [\lambda_2\tau-(b-1)\lambda_2\tau^2] + x_2^2[(b-1)(\tau\lambda_1+4\lambda_3\tau+2\lambda_2 k_{-1}\tau)-\lambda_1]-2(b-1)k_{-1}\lambda_1=0$$

i.e.,

$$x_2^4 \; \alpha + x_2^2 \; \beta + \gamma = 0 \; ,$$

$$x_2^2 = \frac{-\beta \pm \sqrt{\beta^2 - 4\alpha\gamma}}{2\alpha}$$

where $\alpha > 0, \quad \beta < 0, \quad \gamma > 0$.

The two solutions are positive. We choose the one with the minus sign.
Therefore,

$$x_2 = \sqrt{\frac{-\beta - \sqrt{\beta^2 - 4\alpha\gamma}}{2\alpha}} \qquad (2.21)$$

where β and γ are functions of k_{-1} .

The corresponding x_1 is:

$$x_1 = \frac{1}{2(b-1)} \; \frac{-\beta - \sqrt{\beta^2 - 4\alpha\gamma}}{2\alpha} + k_{-1} \qquad (2.22)$$

Switching curve C_3

C_3 is:

$$x_1 = \frac{x_2^2}{2b} \left[1 + \frac{q^4}{(b-1)x_2} \right] . \tag{2.23}$$

Its intersections with the family of parabolas

$$x_1 = \frac{1}{2(b-1)} x_2^2 + k_{-1} \tag{2.24}$$

occur at x_2 solution of

$$x_2^2 - q^4 x_2 + 2b(b-1)k_{-1} = 0$$

i.e.,

$$x_2 = \frac{1}{2} \left(q^4 \pm \sqrt{q^4 - 8(b-1)bk_{-1}} \right). \tag{2.25}$$

We are interested in $k_{-1} \leq 0$, $x_2 > 0$, so we choose the plus sign.

$$x_2 = \frac{1}{2} \left(q^4 + \sqrt{q^4 - 8(b-1)bk_{-1}} \right). \tag{2.26}$$

The corresponding x_1 is

$$x_1 = \frac{1}{4(b-1)} \left(q^4 + \sqrt{q^4 - 8(b-1)bk_{-1}} \right)^2 + k_{-1} . \tag{2.27}$$

Finally, these two results will be needed:

In the positive x_2 half plane, the intersections of the family of parabols

$$x_1 = \frac{1}{2b} x_2^2 + k_o$$

with

230

$$x_1 = \frac{1}{2(b-1)} \, x_2^2$$

occur at

$$x_2 = {}^- \sqrt{2b(b-1)k_o} \; .$$

(2.28)

In the negative x_2 half plane, the intersections of the family of parabolas

$$x_1 = \frac{1}{2b} \, x_2^2 + k_o$$

with

$$x_1 = \frac{1}{2(b+1)} \, x_2^2$$

occur at

$$x_2 = -\sqrt{-2b(b+1)k_o} \quad .$$

(2.29)

2.3 *Notations and Conventions*

Given any point (x_1, x_2), we shall call

$$k_o(x_1, x_2) = x_1 - \frac{x_2^2}{2b} \qquad (3.1)$$

$$k_1(x_1, x_2) = x_1 - \frac{x_2^2}{2(b+1)} \qquad (3.2)$$

$$k_{-1}(x_1, x_2) = x_1 - \frac{x_2^2}{2(b-1)} \qquad (3.3)$$

k_o, k_1, k_{-1} are the intersections with the $x_2 = 0$ axis of the parabolas

$$x_1 = \frac{x_2^2}{2b} + k_o$$

$$x_1 = \frac{x_2^2}{2(b+1)} + k_1$$

$$x_1 = \frac{x_2^2}{2(b-1)} + k_{-1}$$

that pass through (x_1, x_2).

We shall use the letters P, Q, R for the points

$$P: \quad x_1 = \frac{b(s+r)^2 - 4rs}{2b(b-1)} \quad , \quad x_2 = (s+r) \qquad (3.4)$$

$$Q: \quad x_1 = \frac{bs^2 - 2sr + r^2}{2b(b-1)} \quad , \quad x_2 = s \qquad (3.5)$$

$$R: \quad x_1 = \frac{b(r-s)^2 - 2rs + r^2}{2b(b+1)} \quad , \quad x_2 = (r - s) \qquad (3.6)$$

232

so that, for instance $k_o(Q)$ will mean the operation (3.1) performed over the point (3.5).

The initial point will be $x_1(0)$, $x_2(0)$; the corresponding operations (3.1), (3.2), (3.3) will be indicated with the letter 0, such that, for instance

$$k_1(x_1(0), x_2(0)) = k_1(0).$$

The operations (3.1), (3.2), (3.3) performed over x_1, x_2 solutions of (2.14), (2.13) will be indicated by the letter C_1; the same over x_1, x_2 solutions of (2.22), (2.21), by the letter C_2, and over x_1, x_2 solutions of (2.27), (2.26) by the letter C_3. For example,

$$k_{-1}(C_2) = k_{-1}(x_1, x_2); \quad x_1 \text{ given by (2.27)}; \quad x_2 \text{ by (2.26)}.$$

2.4 *Time of arrival calculations*

Let us divide the phase plane into four regions, A, B, C, D in the following way:

The region A is composed of

i) those points x_1, x_2 in the second quadrant such that

$$x_2 \leqslant s \tag{4.1}$$

and

$$x_1 \leqslant -\left(\frac{1}{2} + \frac{2\lambda_3}{\lambda_1 - \lambda_2 \, \tau \, x_2^2}\right)\tau \, x_2^2 \tag{4.2}$$

where τ is given by (2.8);

ii) the third quadrant

iii) those points x_1, x_2 in the fourth quadrant such that either

$$x_2 \leqslant -s \tag{4.3}$$

or

$$x_1 \leqslant \frac{x_1^2}{2(b+1)} \qquad . \tag{4.4}$$

The region B is composed of those points x_1, x_2 that lie in the second quadrant that do not belong to A, and such that

$$x_2 \leqslant s + r \tag{4.5}$$

and

$$x_1 \leqslant \frac{x_2^2}{2b}\left[1 + \frac{q^4}{(b-1)x_2}\right]. \tag{4.6}$$

The region C is composed of those points x_1, x_2 in the fourth quadrant that do not belong to A and such that either

$$x_2 \leq - s + r \tag{4.7}$$

or

$$x_1 \leq \left(\frac{1}{2} + \frac{2\lambda_3}{\lambda_1 - \lambda_1 \tau x_2^2} \right) x_2^2 \tag{4.8}$$

where τ is given by (2.17).

The region D is composed of all the other points.

The given system is

$$\dot{x}_1 = x_2$$

$$\dot{x}_2 = u + b$$

where b is assumed constant and u piecewise constant. For every time interval in which u is constant,

if $u \neq - b$

$$t_1 - t_o = \frac{x_2(t_1) - x_2(t_o)}{u + b}$$

if $u = - b$

$$t_1 - t_o = \frac{x_1(t_1) - x_1(t_1)}{x_2} \quad .$$

Take any initial point $x_1(0)$, $x_2(0)$, and call T the time required for getting to the origin:

a) If this point lies in the region A, compute $k_1(0)$ and $k_1(Q)$; then:

i) if $k_1(0) \geq 0$,

$$T = \frac{-k_1(0)}{-s} + \frac{-x_2(0)}{b+1}$$

ii) if $k_1(Q) \leq k_1(0) \leq 0$,

Compute x_2 from $(2.13)^*$; then from (2.13), (2.14) compute $k_0(C_1)$. Then, recalling (2.28),

$$T = \frac{x_2 - x_2(0)}{b+1} + \frac{\sqrt{2b(b-1)k_0(C_1)} - x_2}{b} + \frac{-\sqrt{2b(b-1)k_0(C_1)}}{b-1}$$

iii) if $k_1(0) < k_1(Q)$,

$$T = \frac{k_1(Q) - k_1(0)}{s} + \frac{-r}{b} + \frac{r-s}{b-1} \; .$$

b) If the initial point lies in the region B, compute $k_0(0)$; then:

i) if $k_0(0) \leq k_0(Q)$,

$$T = \frac{s - x_2(0)}{b} + \frac{k_0(Q) - k_0(0)}{s} + \frac{-r}{b} + \frac{r-s}{b-1}$$

*reading k_0 as $k_0(0)$;

236

ii) if $k_o(0) \geqslant k_o(Q)$,   recalling (2.28),

$$T = \frac{\sqrt{2b(b-1)k_o(0)} - x_2(0)}{b} + \frac{-\sqrt{2b(b-1)k_o(0)}}{b-1}$$

c) If the initial point lies in the region C, compute $k_o(0)$; then:

i)   if $k_o(0) > k_o(R)$,

$$T = \frac{-s - x_2(0)}{b} + \frac{k_o(R) - k_o(0)}{-s} + \frac{s}{b+1}$$

ii) if $0 \leqslant k_o(0) \leqslant k_o(R)$,   recalling (2.29)

$$T = -\frac{-\sqrt{-2b(b+1)k_o(0)} - x_2(0)}{b} + \frac{\sqrt{-2b(b+1)k_o(0)}}{b+1}$$

d) If the initial point lies in the region D, compute $k_{-1}(0)$; then

i)   if $k_{-1}(0) < k_{-1}(P)$,

$$T = \frac{s+r - x_2(0)}{b-1} + \frac{-r}{b} + \frac{k_{-1}(P) - k_{-1}(0)}{s} + \frac{-r}{b} + \frac{r-s}{b-1}$$

ii) if $k_{-1}(P) \leqslant k_{-1}(0) < 0$,

compute x_2 from (2.26), reading k_{-1} as $k_{-1}(0)$;

then compute $k_{-1}(C_3)$ from (2.26), (2.27):

237

$$T = \frac{x_2 - x_2(0)}{b-1} + \frac{\sqrt{2b(b-1)k_o(C_3)} - x_2}{b} + \frac{-\sqrt{2b(b-1)k_o(C_3)}}{b-1}$$

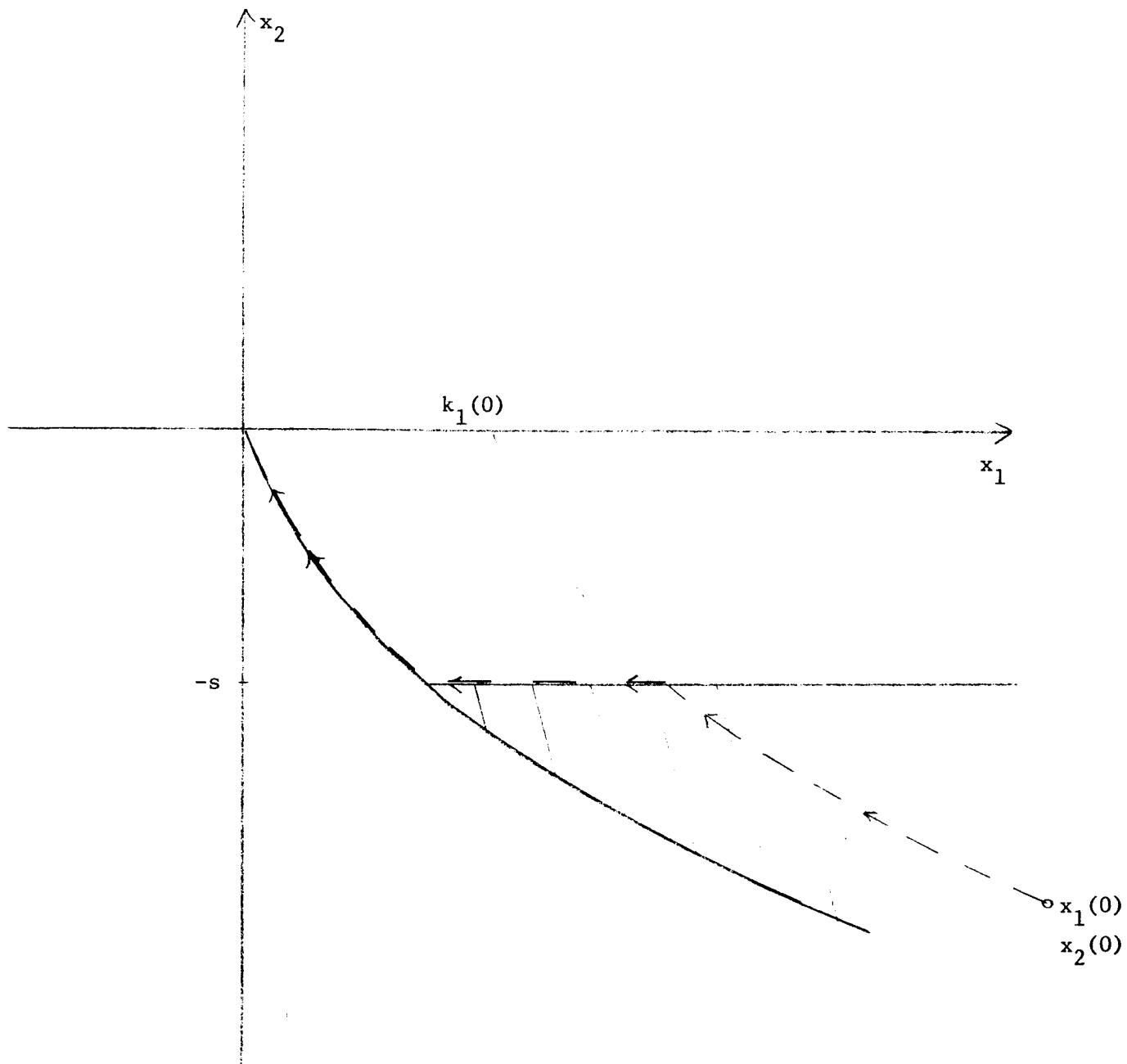iii) if $0 \leqslant k_{-1}(0) < k_{-1}(R)$,

compute x_2 from (2.21) in which k_{-1} has to be
read as $k_{-1}(0)$; then from (2.21), (2.22), compute
$k_o(C_2)$:

$$T = \frac{x_2 - x_2(0)}{b-1} + \frac{-\sqrt{-2b(b+1)k_o(C_2)} - x_2}{b} + \frac{\sqrt{-2b(b+1)k_o(C_2)}}{b+1}$$
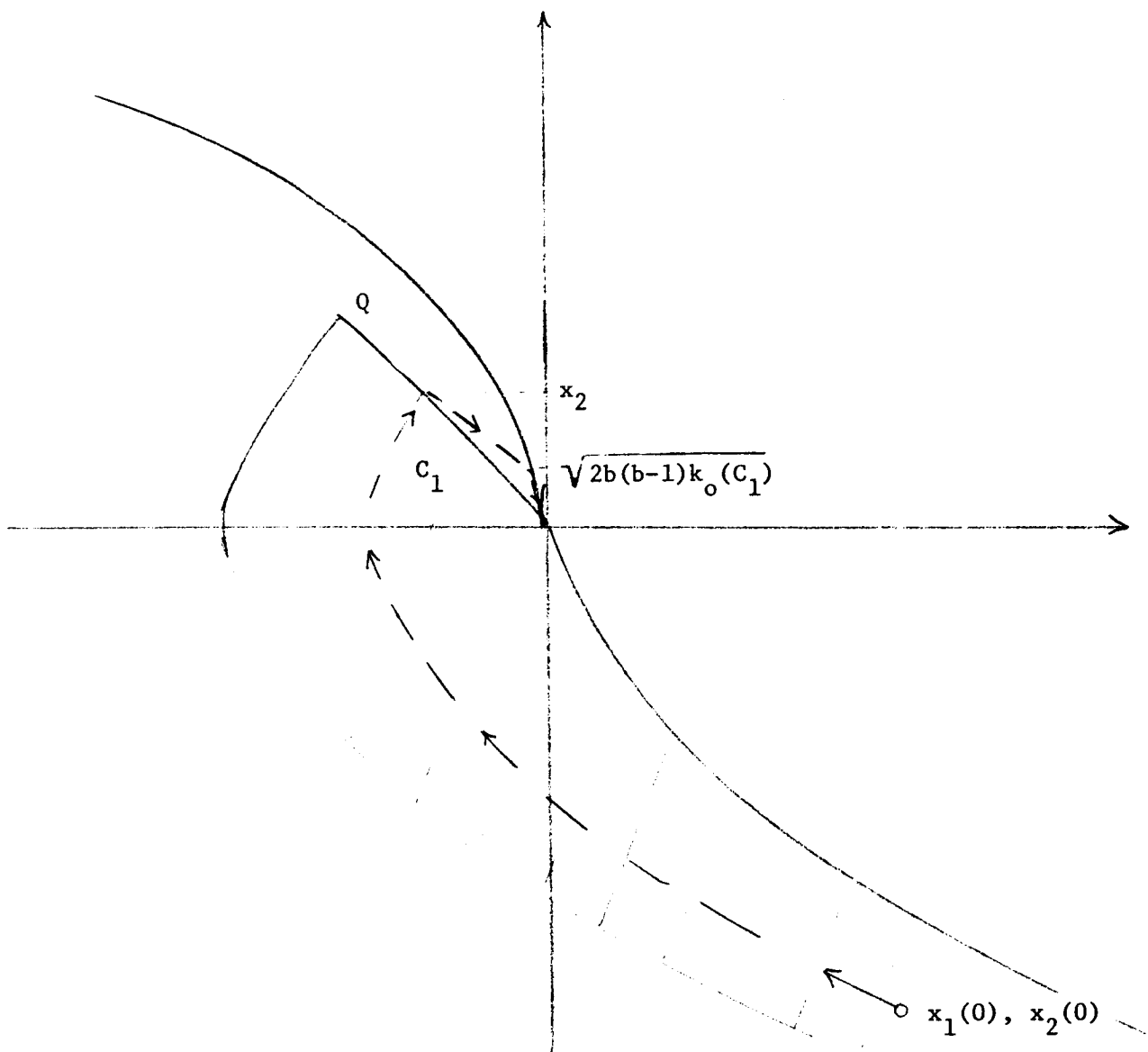
iv) if $k_{-1}(R) \leqslant k_{-1}(0)$,

$$T = \frac{-s+r - x_2(0)}{b-1} + \frac{-s-r}{b} + \frac{k_{-1}(R) - k_{-1}(0)}{-s} + \frac{s}{b+1}$$
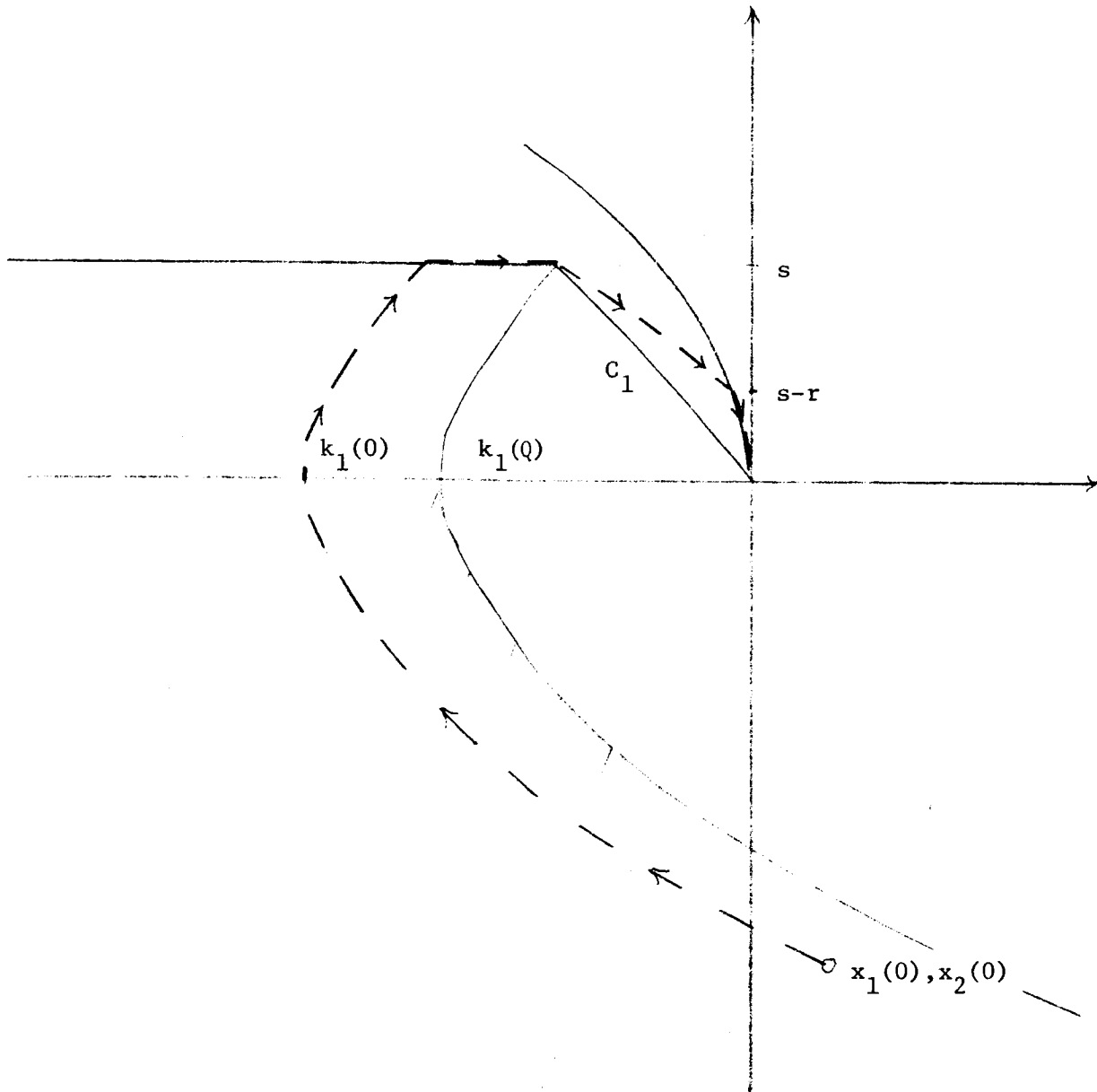
238

Region a, i)

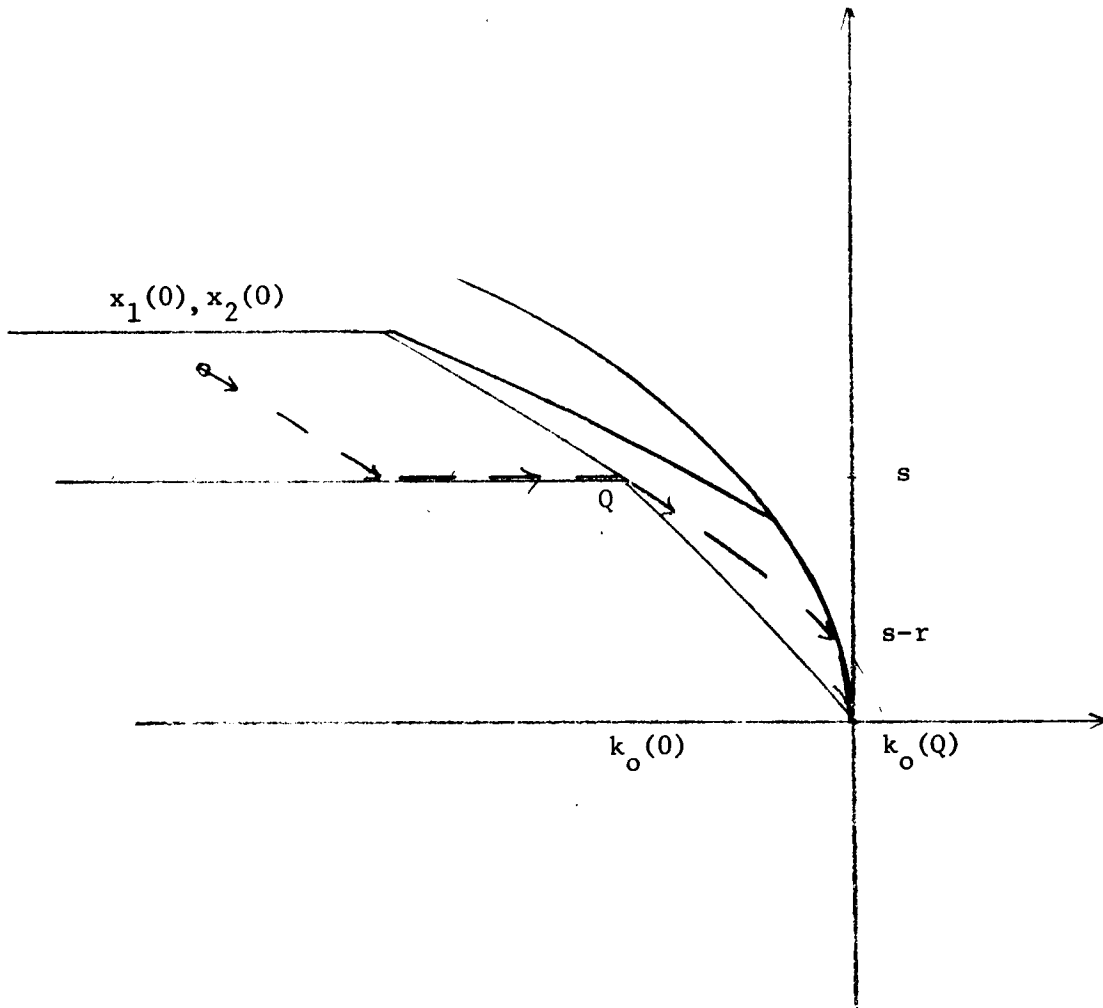$$T = \frac{-s - x_2(0)}{b+1} + \frac{-k_1(0)}{-s} + \frac{s}{b+1}$$

239

Region a, ii)

$$T = \frac{x_2 - x_2(0)}{b+1} + \frac{\sqrt{2b(b-1)k_o(C_1)} - x_2}{b} + \frac{-\sqrt{2b(b-1)k_o(C_1)}}{b-1}$$
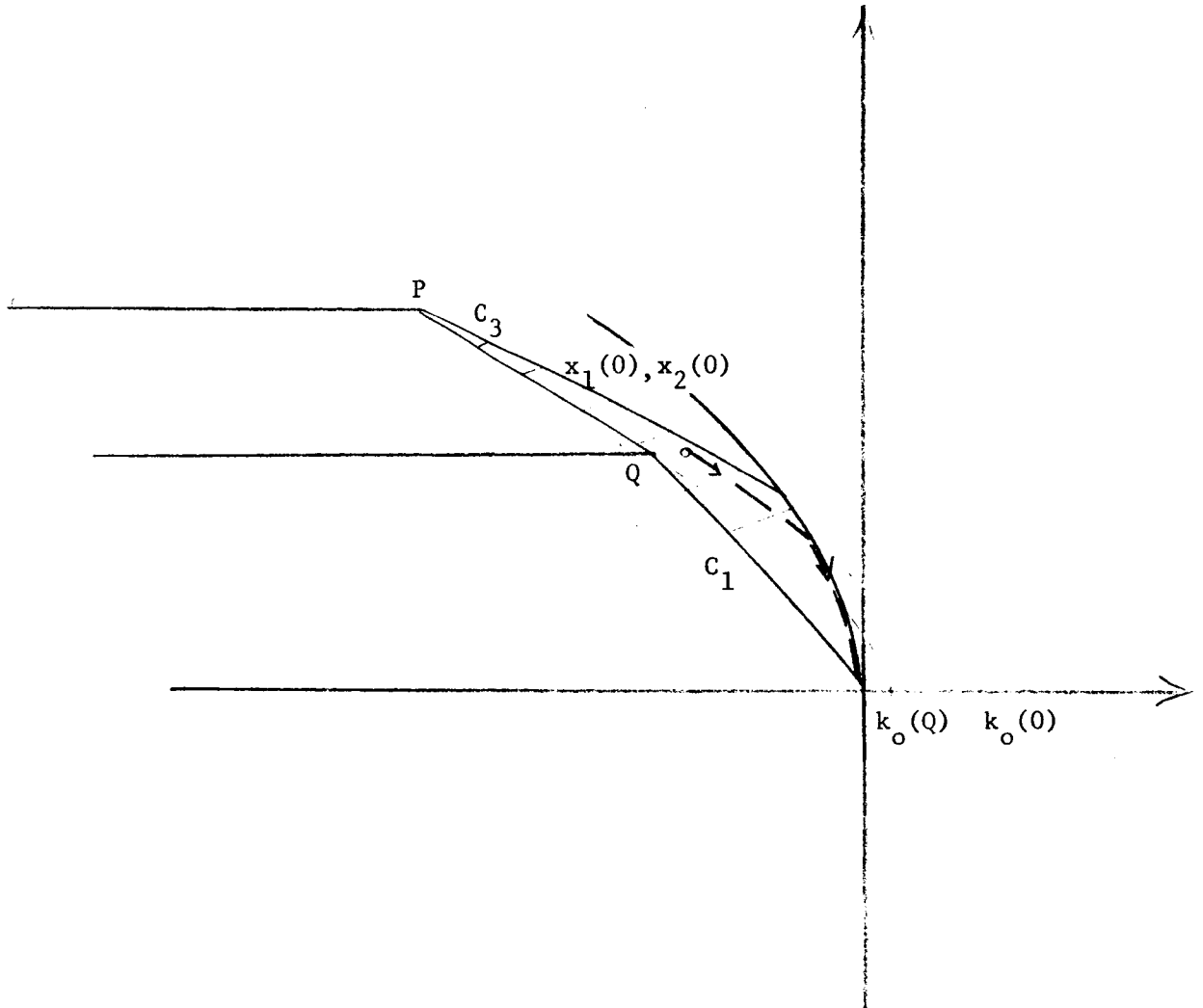
$$T = \frac{s - x_2(0)}{b+1} + \frac{k_1(Q) - k_1(0)}{s} + \frac{-r}{b} + \frac{r-s}{b-1}$$

Region b, i)

$$T = \frac{s - x_2(0)}{b} + \frac{k_o(Q) - k_o(0)}{s} + \frac{-r}{b} + \frac{r-s}{b-1}$$
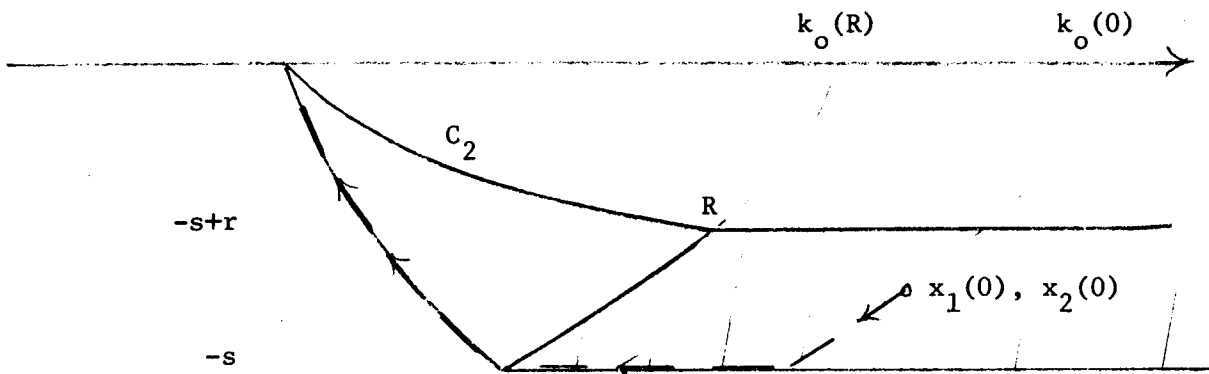
Region b, ii)

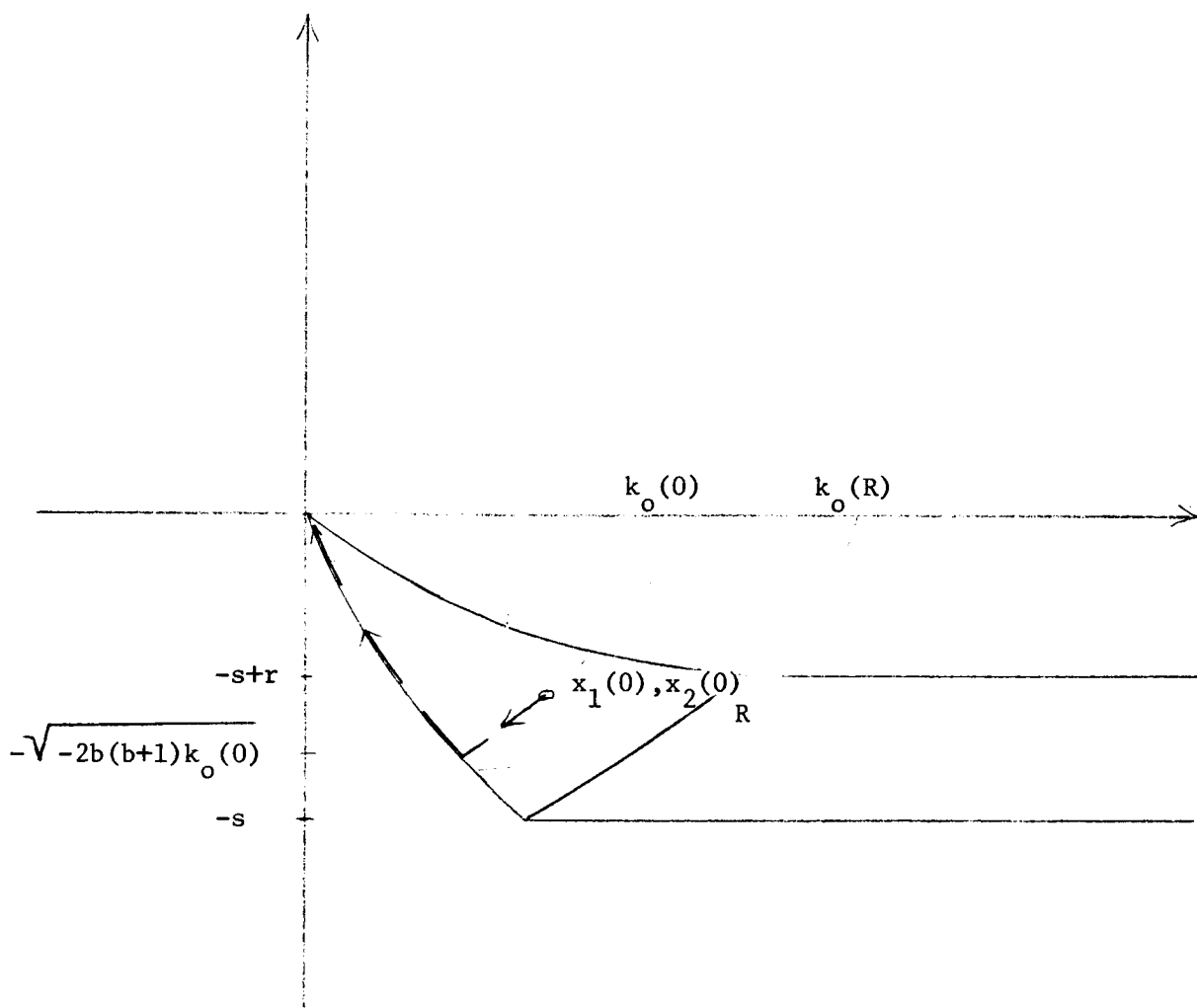$$T = \frac{\sqrt{2b(b-1)k_o(0)} - x_2(0)}{b} + \frac{-\sqrt{2b(b-1)k_o(0)}}{b-1}$$
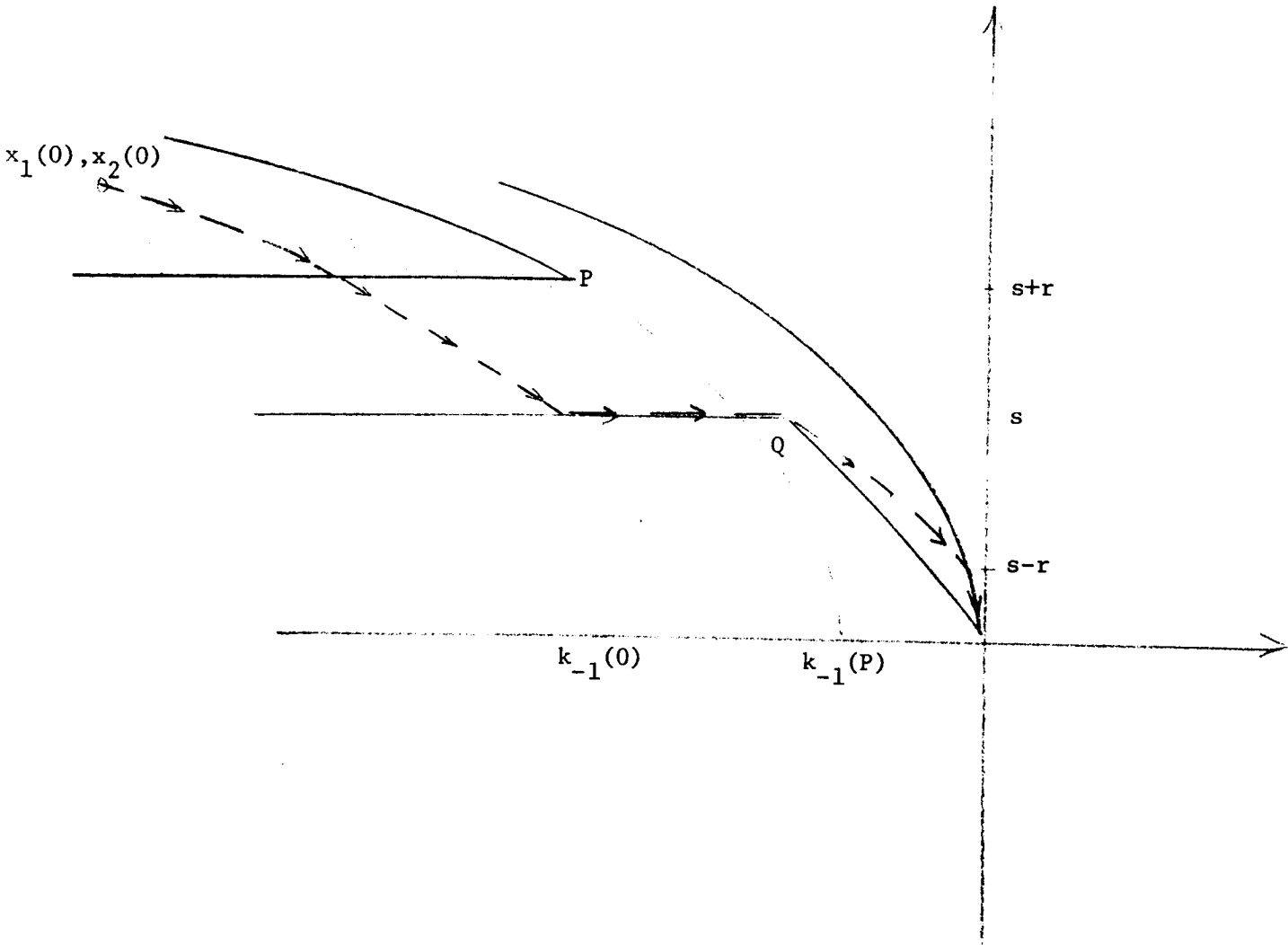
Region c, i)

$$T = \frac{-s - x_2(0)}{b} + \frac{k_o(R) - k_o(0)}{-s} + \frac{s}{b+1}$$

Region c, ii)

$$T = \frac{-\sqrt{-2b(b+1)k_o(0)} - x_2(0)}{b} + \frac{\sqrt{-2b(b+1)k_o(0)}}{b+1}$$

Region d, i)

$$T = \frac{s+r - x_2(0)}{b-s} + \frac{-r}{b} + \frac{k_{-1}(P) - k_{-1}(0)}{s} + \frac{-r}{b} + \frac{r-s}{b-1}$$

246

Region d, ii)

$$T = \frac{x_2 - x_2(0)}{b-1} + \frac{\sqrt{2b(b-1)k_o(C_3)} - x_2}{b} + \frac{-\sqrt{2b(b-1)k_o(C_3)}}{b-1}$$

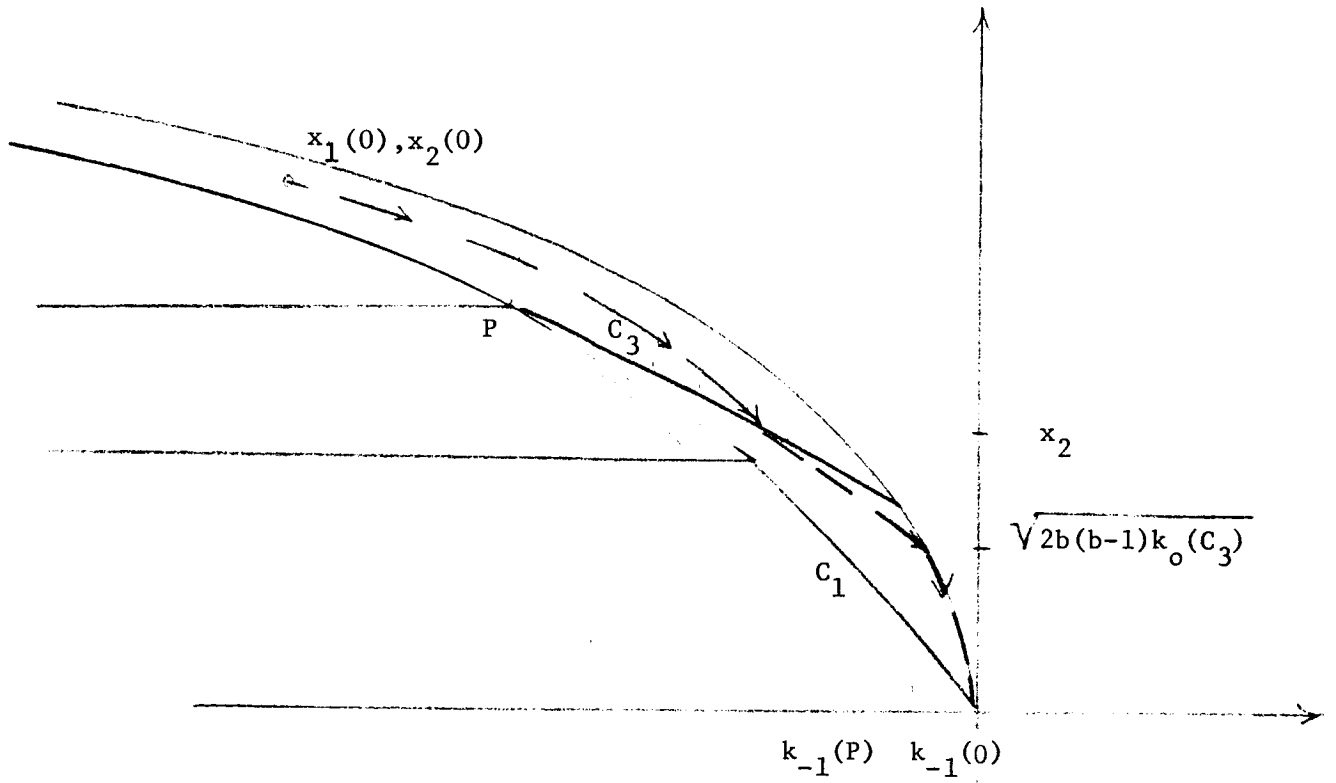Region d, iii)
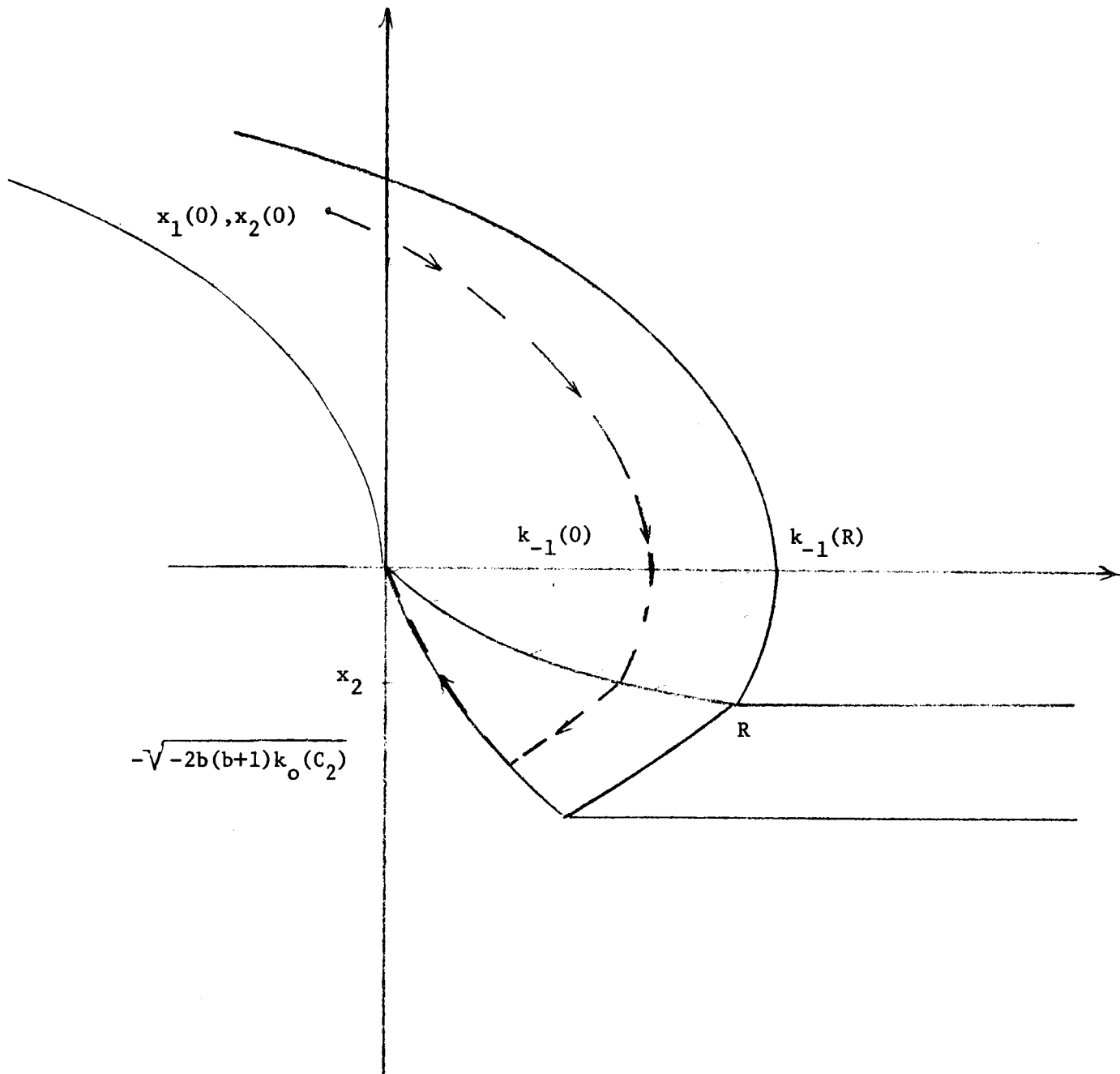
$$T = \frac{x_2 - x_2(0)}{b-1} + \frac{-\sqrt{-2b(b+1)k_o(C_2)} - x_2}{b} + \frac{\sqrt{-2b(b+1)k_o(C_2)}}{b+1}$$
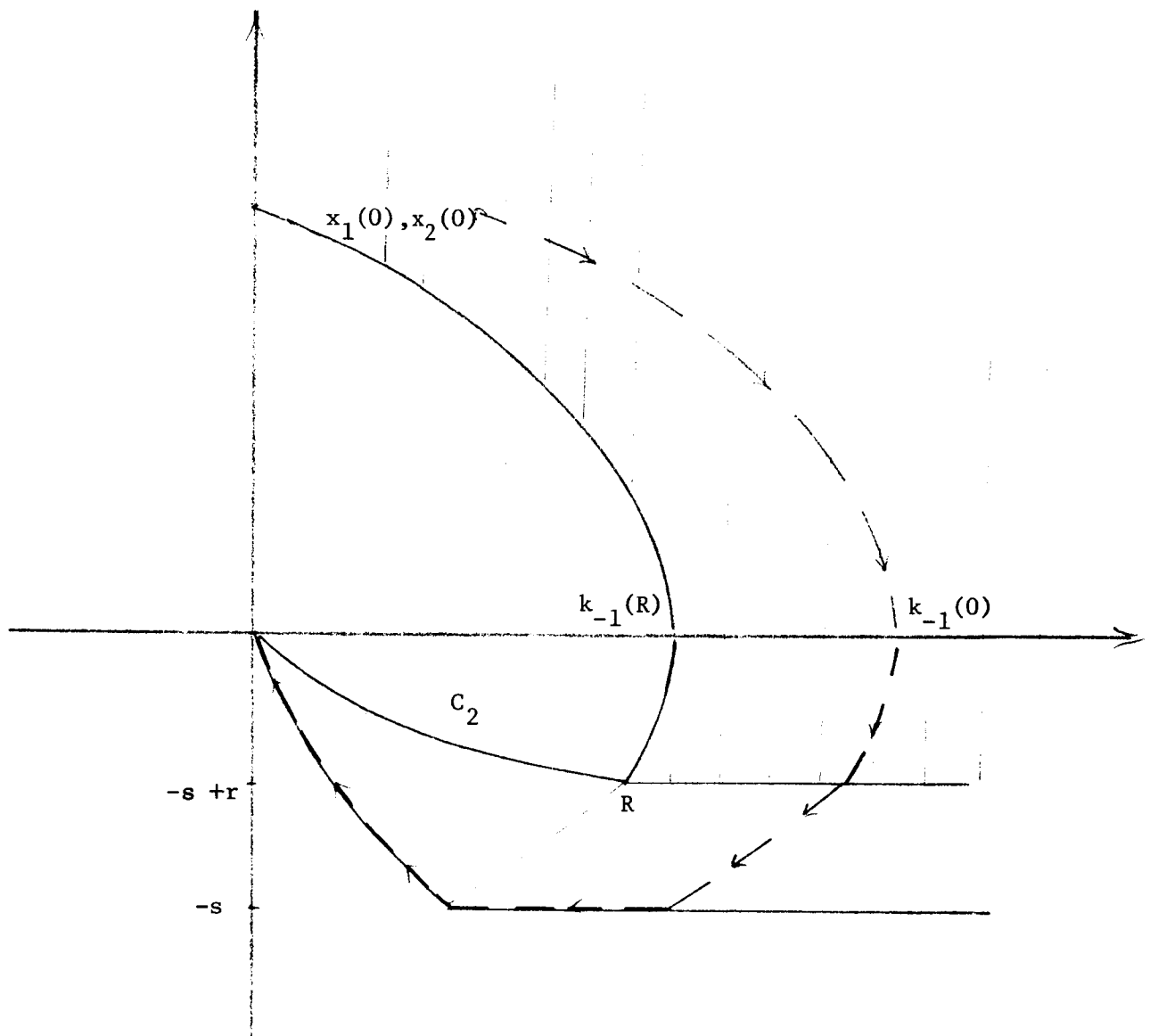
Region d, iv)

$$T = \frac{-s + r - x_2(0)}{b-1} + \frac{-s + r}{b} + \frac{k_{-1}(R) - k_{-1}(0)}{-s} + \frac{s}{b+1}$$

2.5 *Parametric Calculation for Specified Time of Arrival*

The following problem is given: from any initial position with initial velocity zero, reach the origin in fixed time T along optimal paths or, in other words, given $x_1(0)$, $x_2(0) = 0$, T, find $\lambda_1, \lambda_2, \lambda_3$ such that the motion through $(x_1(0), 0)$ at $t = 0$, solution of the optimality problem, reaches the origin at T. Taking into account the fact that b is extremely small, we shall consider it as zero, i.e., we shall treat the system

$$\dot{x}_1 = x_2$$

$$\dot{x}_2 = u$$

(5.1)

Besides, because of the symmetry of the system, we shall limit ourselves to the case $x_1(0) < 0$. The equation of the switching curve is

$$x_1 = - \left(\frac{1}{2} + \frac{2\lambda_3}{\lambda_1 - \lambda_2 x_2^2} \right) x_2^2$$

(5.2)

and the paths are composed of

1) An arc of the parabola through $(x_1(0), 0)$

$$x_1 = \frac{x_2^2}{2} + x_1(0)$$

(5.3)

2) A segment

$$x_2 = \text{const}$$

(5.4)

3) An arc of the parabola through the origin

$$x_1 = - \frac{x_1^2}{2}$$

(5.5)

Suppose the switching from any of these paths to the following occurs at $x_2 = x_2^*$. From the preceding sections we know that the time required for getting the origin along a sequence of paths is:

$$T = x_2^* + \frac{1}{x_2^*} \left[\frac{-(x_2^*)^2}{2} - \frac{(x_2^*)^2}{2} - x_1(0) \right] + x_2^*$$

$$= x_2^* - \frac{x_1(0)}{x_2^*} \tag{5.6}$$

We shall solve this equation with respect to x_2^*:

$$(x_2^*)^2 - T(x_2^*) - x_1(0) = 0$$

i.e.

$$x_2^* = \frac{1}{2} \left(T \mp \sqrt{T^2 + 4x_1(0)} \right)$$

Both the solutions are positive: it is easy to realize from the behavior of the curve

$$T = x_2^* - \frac{x_1(0)}{x_2^*}$$

that the - sign has to be chosen, so

$$x_2^* = \frac{1}{2} \left(T - \sqrt{T^2 + 4x_1(0)} \right) \qquad . \tag{5.7}$$

The first switching occurs at a point x_1^*, x_2^* that lies both on the parabola (5.3) and on the switching curve (5.2).

The switching curve (5.2) depends on the parameters $\lambda_1, \lambda_2, \lambda_3$. We shall assume

one of them, λ_2, as fixed and, taking into account the constraint

$$\lambda_1 + \lambda_2 + \lambda_3 = 1, \qquad\qquad \text{i.e.,}$$

$$\lambda_3 = 1 - \lambda_2 - \lambda_1 \qquad , \qquad\qquad (5.8)$$

we shall solve the problem with respect to λ_1.

From the (5.3) we have

$$x_1^* = \frac{(x_2^*)^2}{2} + x_1(0) \qquad ; \qquad\qquad (5.9)$$

Let us rewrite the (5.2) with the substitution (5.8) as λ_1 function of λ_2, x_1, x_2:

$$(\lambda_1 - \lambda_2 x_2^2)x_1 = -\frac{1}{2}(\lambda_1 - \lambda_2 x_2^2)x_2^2 - 2(1 - \lambda_2 - \lambda_1)x_2^2$$

i.e.

$$\lambda_1 = \frac{x_2^2[x_2^2 \frac{\lambda_2}{2} + \lambda_2 x_1 - 2(1 - \lambda_2)]}{x_1 - \frac{3}{2} x_2^2} \qquad\qquad (5.10)$$

The substitution in (5.10) of the values given by (5.7) and (5.9) gives the λ_1 required.

6E.3 _Despinning mode for large_ ω

Let us consider the general vector equation of motion

$$I\dot{\omega} + \omega \times I\omega = v + f \qquad (3.1)$$

where I is the moment of inertia matrix for the principle axes system, ω the angular velocity vector, v the control torque vector, and f the disturbance torque vector. Let K be a diagonal matrix whose diagonal elements are the hard constraints on the magnitudes of the components of v and let k be the smallest diagonal element of K. The control synthesis is formulated with J as defined in Part 2 takes the form

$$v = -k \frac{I\omega}{||I\omega||} \qquad (3.2)$$

for large $||I\omega||$. We shall show that from an arbitrary initial state that $||\omega||$, subject to control of the form (3.2), tends to zero in finite time. This despinning assures stability for our system and justifies the approximations made in Part 2 regarding the term $\omega \times I\omega$.

Let $z = ||I\omega||$ and note that

$$\dot{z} = \frac{1}{z} (I\omega \cdot I\dot{\omega}) \quad . \qquad (3.3)$$

By (3.1) we have

$$I\omega \cdot I\dot{\omega} + I\omega \cdot \omega \times I\omega = I\omega \cdot (v + f) \quad .$$

Since

$$I\omega \cdot \omega \times I\omega = 0$$

it follows using (3.2) that

$$I\omega \cdot I\dot{\omega} \leq -k \ z + I\omega \cdot f$$

and

$$\dot{z} \leq -k + \frac{1}{||I\omega||} (I\omega \cdot f) \quad .$$

By the Schwartz inequality it follows that

$$\dot{z} \leq -k + ||f||$$

Our assumed design constraints requires that $||f|| < k$ so z is negative and bounded away from zero. It follows that z must decrease monotonically to 0 and arrive there in finite time.

6E.4 _Proof of Proposition 1_

Let b be a constant vector whose components are bounded below _1_ in magnitude. Consider the system of equations

$$\dot{y} = v + b \tag{4.1}$$

and

$$A^*(\xi)\dot{\xi} = y \tag{4.2}$$

together with the constraints $|v_i| \leqslant 1$, for $i = 1,2,3$ and the performance criterion J as defined in Part 2.

Let us consider the functional equation

$$x(t) = -\int_{t_o}^{t_1} A^*(z(\tau))z(\tau)d\tau \tag{4.3}$$

where X and Z are differentiable vector functions defined on the interval $[t_o, t_1]$ which vanish at t_1. It can be proved that for each function X(t) there exists one and only one function Z(t) satisfying (4.3). _Hence there exists a one-to-one correspondence between the functions_ x(t) _and_ z(t) _related through equation (4.3)._

Now consider the system

$$\dot{y} = v + b \tag{4.4}$$
$$\dot{x} = y \tag{4.5}$$

together with J and the constraints on V as previously specified. Let $\xi, y, v = p(\xi, y)$ be functions defined on an interval $[t_o, t_1]$ which satisfy the system of equations (4.1) and (4.2) and are such that $\xi(t_1) = 0$ and $y(t_1) = 0$. Let x and ξ be related by the equation

$$x(t) = \int_t^{t_1} A^*(\xi(\tau))\dot{\xi}(\xi)d\tau \quad . \tag{4.6}$$

Proposition I: $\xi, y, v = p(\ , y; b)$ *is an optimal synthesis for the system of equations* (4.1) *and* (4.2) *relative to* J *if and only if* $x, y, v = q(x, y; b)$ *is an optimal synthesis for the system of equations* (4.4) *and* (4.5) *relative to* J *and*

$$p(\xi, y; b) = q\left(\int_t^{t_1} A^*(\xi(\tau))\dot{\xi}(\tau)d\tau, y; b\right) \quad . \tag{4.7}$$

Proof. Since J is invariant under the change of variables (4.6) to prove this proposition we have only to show that (4.6) establishes a one-to-one correspondence between differentiable functions x and ξ defined on the interval $[t_o, t_1]$ and vanishing at t_1. To establish such a correspondence we shall make use of the contraction principle for complete metric spaces. (A derivation of this principle is contained in the notes on control theory composing part of the final report for contract NASA-9172).

It is tacitly assumed in Proposition I that the coordinates of ξ are bounded away from $\frac{\pi}{2}$. This assures that $A^*(\xi)$ is nonsingular. Equation (4.6) and the fact that $\xi(t_1) = 0$ imply that

$$\xi(t) = -\int_t^{t_1} A^{*-1}(\xi(\tau))\dot{x}(\tau)d\tau \quad . \tag{4.8}$$

If M is an arbitrary three by three matrix we define $||M||$ by the formula

$$||M|| = \max\{||Mr|| : ||r|| \le 1\}$$

Let G be the set of all 3-dimensional vectors whose components are bounded away from $\frac{\pi}{2}$ by some fixed constant. Let $\mathcal{D}(t_o, t_1)$ be the class of all 3-dimensional vector functions $z: [t_o, t_1] \to G$ which are differentiable

on $[t_o, t_1]$ and vanish at t_1. We define a norm on (t_o, t_1) by the formula

$$|z| = \max\{e^{-\eta(t_1 - t)} ||z(t)|| : t \text{ in } [t_o, t_1]\} \quad ,$$

where z is an arbitrary function in (t_o, t_1). For a fixed function x in (t_o, t_1) let us define the mapping $F: (t_o, t_1) \rightarrow (t_o, t_1)$ by the formula

$$F(z)(t) = - \int_t^{t_1} A^{-1}(z(\tau))x(\tau)d\tau.$$

For an arbitrary pair of functions z_1 and z_2 we have

$$F(z_1)(t) - F(z_2)(t) = - \int_t^{t_1}(A^{-1}(z_1(\tau)) - A^{-1}(z_2(\tau)))x(\tau)d\tau.$$

Now we can easily verify that there exists a constant N such that for arbitrary r_1 and r_2 in G

$$||A^{-1}(r_1) - A^{-1}(r_2)|| \leq N||r_1 - r_2||.$$

Hence

$$||F(z_1)(t) - F(z_2)(t)|| \leq N\int_t^{t_1}||\dot{x}(\tau)|| \, ||z_1(\tau) - z_2(\tau)|| \, \tau,$$

$$||F(z_1)(t) - F(z_2)(t)|| \leq N\int_t^{t_1}||\dot{x}(\tau)||e^{\lambda(t_1 - \tau)}e^{-\lambda(t_1 - \tau)}||z_1(\tau)-z_2(\tau)||d\tau,$$

and

$$||F(z_1)(t) - F(z_2)(t)|| \leq N\int_t^{t_1}||\dot{x}(\tau)||e^{\lambda(t_1 - \tau)}d\tau\, |z_1 - z_2|.$$

Letting $m = \max\{||\dot{x}(t)|| : t \text{ in } [t_o, t_1]\}$, we have that

$$e^{-\lambda(t_1 - t)}||F(z_1)(t) - F(z_2)(t)|| \leq (N\, m\, e^{\lambda t}\int_t^{t_1}e^{-\lambda\tau}d\tau)\, |z_1 - z_2|$$

and

$$e^{-\lambda(t_1 - t)}||F(z_1)(t) - F(z_2)(t)|| \leq (\tfrac{1}{\lambda} N\, m(1 - e^{-\lambda(t_1 - t)}))\, |z_1 - z_2|.$$

Thus

$$\left|F(z_1) - F(z_2)\right| \leq \tfrac{1}{\lambda} N\, m(1 - e^{-\lambda(t_1 - t_o)})\, z_1 - z_2 .$$

Now we are free to choose , so we choose it such that

$$\alpha = \tfrac{1}{\lambda} N\, m(1 - e^{-\lambda(t_1 - t_o)}) < 1 .$$

Therefore F is a contraction and by the contraction principle there exist one and only one function z such that $F(z) = z$. That is, there exists one and only one function z such that for fixed $x(t)$

$$z(t) = -\int_t^{t_1}A^{-1}(z(\tau))\dot{x}(\tau)d\tau .$$

This is equivalent, of course, to the existence of one and only one

function z such that

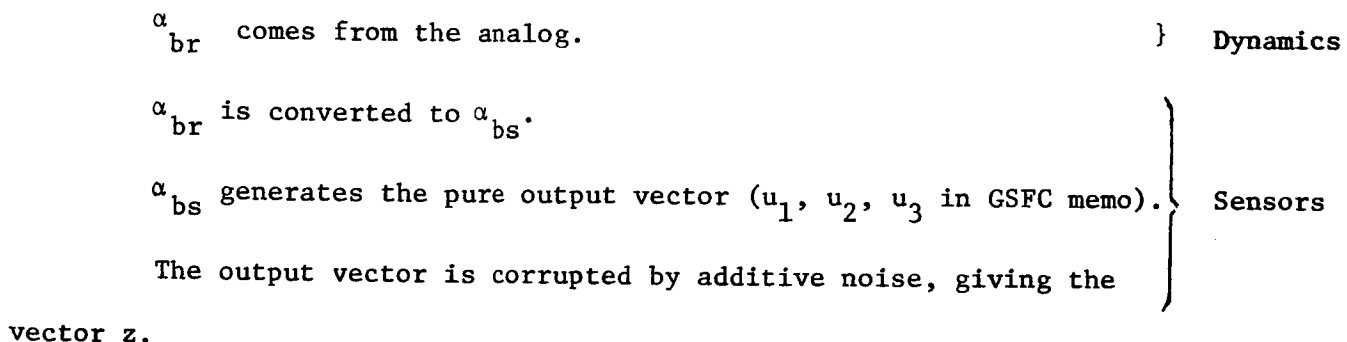$$x(t) = - I \int_t^{t_1} A(z(\tau))\dot{z}(\tau)d\tau \quad .$$

This establishes the desired one-to-one correspondence and the proof of

Proposition I is complete.

APPENDIX F

INCORPORATION OF THE SENSOR INTO

THE SATELLITE CONTROL LOOP

APPLICATION OF THE KALMAN FILTER TO RATE SENSOR

I. The control being used is computed from the satellite location (α_{br} and ω) in the phase plane. Until now this location has been obtained directly from the dynamics. We now wish to use the sensor output to obtain the required information. This will entail quite a bit of programming since 1) the rates are not directly available, and therefore a filter must be used, 2) the angles α_{br} are not directly available but must be obtained from three independent, nonlinear functions of α_{bs}.

II. In broad outline the flow of information is: (See Figures 1 and 2.)

    α_{br} comes from the analog.   } **Dynamics**

    α_{br} is converted to α_{bs}.

    α_{bs} generates the pure output vector (u_1, u_2, u_3 in GSFC memo). **Sensors**

    The output vector is corrupted by additive noise, giving the vector z.

<div align="center">Real world</div>

<div align="center">Estimate world</div>

The angles α'_{bs} are computed as if the z_i were u_i.

The angles α'_{br} are computed as if the α'_{bs} were α_{bs}.

The estimated $\hat{\alpha}_n$, $\hat{\omega}_n$ of $\hat{\theta}_{bs}$ and $\hat{\omega}$ are computed from the old

estimate by

$$\begin{bmatrix} \hat{\alpha}_n \\ \hat{\omega}_n \end{bmatrix} = \begin{bmatrix} 1 & \sigma \\ 0 & 1 \end{bmatrix} \begin{bmatrix} \hat{\alpha}_o \\ \hat{\omega}_o \end{bmatrix} + \begin{bmatrix} \frac{\sigma^2}{2} \\ \sigma \end{bmatrix} u_o + K \begin{bmatrix} \alpha'_{br} - (\hat{\alpha}_o + \sigma \hat{\omega}_o + \frac{\sigma^2}{2} u_o) \end{bmatrix} \quad (2.1)$$

where K is a constant matrix computed externally.

III. Specifications.

1) Initialization

The commands x and y must be computed from

$$x = + \frac{\sin \theta_{rs}}{\sqrt{\sin^2 \theta_{rs} + \cos^2 \theta_{rs} \cos^2 \psi_{rs}}} \qquad 3.1)$$

$$y = \sin \phi_{rs} \sqrt{1 - x^2} \qquad 3.2)$$

where, in accord with our previous notation, θ_{rs} and ϕ_{rs} are the angles

through which the s system must be rotated (θ_{rs} first) to align finally

with the R system.

Thus

$$\tan \theta_{rs} = - \frac{\cos \gamma \sin \beta}{K - \cos \gamma \cos \beta}$$

$$\tan \phi_{rs} = \frac{\sin \gamma \sec \theta_{rs}}{K - \cos \gamma \cos \beta - \cos \gamma \sin \beta \tan \theta_{rs}}$$

where γ = target latitude, positive north,

β = target longitude, positive east of Greenwich,

and K is the ratio of satellite orbit radius to earth radius.

These formulae are based on the GSFC letter, Isley to Jones

May 5, 1967, giving sensor transformations; equations 1.3.28a and 1.3.28b;

and the fact that in MSG notation A (of the GSFC memo) is

$$
A = \begin{bmatrix}
c\theta c\Psi & -s\Psi & s\theta c\Psi \\
c\theta c\phi s\Psi - s\theta s\phi & c\phi c\Psi & s\phi c\theta + s\Psi s\theta c\phi \\
-s\theta c\phi - s\phi s\Psi c\theta & -s\phi c\Psi & c\theta c\phi - s\theta c\phi s\Psi
\end{bmatrix}
$$

where all angles are subscripted (bs). (The subappendix of Appendix G may prove a helpful reference.)

    2) <u>Transformation to Euler angles.</u>

    We assume that Polaris is due north, a simplification which we believe justified in this study on the grounds that:

    1) The satellite hardware will probably remove the effect, and

    2) Attacking the problem without this assumption will probably involve us in numerical (as opposed to analytic) solution of the sensor output to α_{bs} transformation. This will almost certainly involve us in more computer time and space than we have. In any case the effect should be small and we can easily put the effect in the sensors and run a simulation.

If Polaris is due north, then, letting

$$
z = \sqrt{1 - x^2 - y^2} \;,
$$

$$
u_1 = -x \sin \Psi_{bs} + y \cos\phi_{bs} \cos \Psi_{bs} - z \sin \phi_{bs} \cos \Psi_{bs}
$$

$$
u_2 = x \cos \theta_{bs} \cos \Psi_{bs} + y(\cos \theta_{bs} \cos \phi_{bs} \sin \Psi_{bs} - \sin \theta_{bs} \sin \phi_{bs})
$$

$$
- z(\sin \theta_{bs} \cos \phi_{bs} + \sin \phi_{bs} \sin \Psi_{bs} \cos \theta_{bs})
$$

$$
u_3 = \sin \Psi_{bs} \;.
$$

This can be solved as $\Psi_{bs} = \sin^{-1} u_3$

$$\phi_{bs} = \sin^{-1} \frac{1}{b(1-x^2)} [2\sqrt{b^2(1-x^2) - (u_1+xu_3)^2} - 2(u_1+xu_3)].$$

where $b = \sqrt{1 - u_3^2}$, and

$$\theta_{bs} = \sin^{-1} \frac{u_2}{\sqrt{A^2+B^2}} - \tan^{-1} \frac{A}{B}$$

where $A = bx + yu_3 \cos \phi_{bs} - 2u_3 \sin \phi_{bs}$

$B = -y \sin \phi_{bs} - 2 \cos \phi_{bs}$.

In Figure 2 this transformation inversion is written as

$$\begin{bmatrix} \phi \\ \Psi \\ \theta \end{bmatrix}'_{bs} = \alpha'_{bs} = u^{-1}(z) = u^{-1} \begin{pmatrix} u_1 + n_1 \\ u_2 + n_2 \\ u_3 + n_3 \end{pmatrix},$$

the parameters (x,y) having been set by the target command coming from the ground.

From α_{bs} it is a simple task to compute α_{br} since α_{rs} is implicit in the ground command. These are (Englar $\rightarrow$ Isley, May 22, 1967)

$$\Psi_{br} = \sin^{-1}(\sin \phi_{rs} \cos \Psi_{bs} \sin(\theta_{rs} - \theta_{bs}) + \cos \phi_{rs} \sin \Psi_{bs})$$

$$\theta_{br} = \sin^{-1}[\frac{\sin \phi_{rs} \sin \Psi_{bs} + \cos \phi_{rs} \cos \Psi_{bs} \sin (\theta_{bs}-\theta_{rs})}{\cos \Psi_{br}}]$$

$$\phi_{br} = \sin^{-1}[(\cos \phi_{rs} \sin \phi_{bs} \cos \Psi_{bs} - \sin \phi_{rs} \cos \phi_{bs} \cos (\theta_{rs}-\theta_{bs})$$

$$- \sin \phi_{rs} \sin \phi_{bs} \sin \Psi_{bs} \sin (\theta_{rs}-\theta_{bs}))/\cos \Psi_{br}]$$

These formulae are applied to the parameters α_{rs} and the calculated quantities α'_{bs} to compute α'_{br} and these are filtered by the Kalman filter

appearing in (2.1).

3) <u>Filter specification (choice of K).</u>

The remaining task is to select K. From a purely theoretical standpoint, this is done for a linear system by obtaining an approximate idea of the statistics of the observation noise and the dynamical or input noise, these in turn determine K. Generally input noise is an expression of your failure in the filter to model the complete system exactly -- this is the situation here where we allow input noise to compensate for ignoring the coupling terms. Usually however this technique cannot be applied directly. It will be necessary to test various gains and try to determine a satisfactory one. That is one sufficiently stable under the observation noise at low signal levels (primary consideration) yet sensitive enough to compensate for the lack of accurate modeling.

The expected bias on the output signal is 0.008° (Isley - Englar, oral, June 12, 1967) and the expected peak noise is 0.05° and independent of signal amplitude (ibid). We will simulate the noise by gaussian noise of standard deviation (0.05·0.707/57.3 = 0.00063) and mean (0.008/57.3 = 0.00014).

No attempt will be made to solve for the bias in the instruments. It could be done but since the deadband is a factor of ten larger, it doesn't seem worthwhile.

IV. Computation of K.

An important reference for the notation here is (Englar - Isley, June 16, 1967).

The R matrix (covariance matrix of the observation noise) is $39.7 \cdot 10^{-8} = (6.3 \cdot 10^{-4})^2$.

The K matrix ultimately must be tested to see what kind of trajectory it gives, but we should be able to eliminate a large amount of trial and error

by some preliminary analysis.

Let us rewrite the filter equation as

$$\hat{x}(k+1) = A \hat{x}(k) + K[y(k) - H\hat{x}(k)] \quad ,$$

$$\hat{x}(k+1) = (A-KH)\hat{x}(k) + Ky(k) \quad .$$

A fundamental requirement, in every way analogous to the same re-
quirement in the control problem, is that the closed loop system be stable.
That is, the matrix (A-KH) must have its eigenvalues inside the unit disk.
In our case

$$A = \begin{bmatrix} 1 & \delta \\ 0 & 1 \end{bmatrix} \quad H = [1 \quad 0] \quad K = \begin{bmatrix} k_1 \\ k_2 \end{bmatrix}$$

and the value of δ at present is $\delta = 0.1$. In what follows we take $\delta = 0.1$.
Remember that if the sampling interval changes, K must change.

Figure 3 shows the unit square in the $k_1 - k_2$ plane with regions of
interest to us delineated. Naturally the small wedge-shaped region yielding
an unstable system must be avoided.

Moreover our particular dislike for control "chatter" which is
caused by crossing of switching lines, leads us to believe that we should avoid
the oscillatory systems to the left of the critical damping line, even if they
should be otherwise optimal.

Furthermore, because of the very high signal to noise ratio at low
signal levels, the k_i should almost certainly be less than 0.2. Looking at
Figure 1, we see that such restrictions have already greatly limited our
choice.

Now let us attempt to estimate the input noise levels and apply
optimal filtering to obtain another estimate of K.

The perturbing action in the $\dot{\alpha}$ equation is caused by terms like $\alpha\omega$. We must make sure that our filter works best in the vicinity of the origin so we compute this at $\alpha = 0.1° = 0.002$ rad. When $\alpha = .002$ rad, we expect ω to be about $5\cdot10^{-5}$ rad/sec. Therefore the noise on $\dot{\alpha}$ will be about $1\cdot10^{-7}$. The maximum value for $\alpha\omega$ is about $0.2\cdot0.002 = 4\cdot10^{-4}$.

The perturbing action in $\dot{\omega}$ is caused by solar and gravitational torques which are constant throughout a slew, by the term $\omega \times I\omega$, and by control torque uncertainties such as the jet misalignments.

The solar and gravitational torques are apparently less than $1.5\cdot10^{-4}$ and their input bounded by

$$\frac{1.5\cdot10^{-4}}{2000} = .8\cdot10^{-7} \quad .$$

The jet misalignments are less than $2°$. Therefore the orthogonal torques are bounded by $\frac{2\cdot0.12}{57.3}$ and their input bounded by

$$\frac{0.24}{57.3\cdot2000} = 2\cdot10^{-6} \quad .$$

The Euler torques $\omega \times I\omega$ are bounded by $0.75\omega_i\omega_j$ which will **never** exceed $0.75\cdot4\cdot10^{-6} = 3\cdot10^{-6}$ and in the region close to the origin will be much smaller.

We might say then that the Q matrix is larger than

$$\begin{bmatrix} 10^{-14} & 0 \\ 0 & 4\cdot10^{-12} \end{bmatrix}$$

but less than

$$\begin{bmatrix} 1.5\cdot10^{-7} & 0 \\ 0 & 13\cdot10^{-12} \end{bmatrix}$$

while R is constant at $4\cdot10^{-7}$.

Various values of Q were used, the results are presented in Table 1. The numbers p_{ij} are the elements of the covariance matrix and $\sqrt{p_{11}}$, $\sqrt{p_{22}}$ are respectively the theoretical standard deviations of the estimation errors in angle and rate.

The noise simulation is not theoretically valid since we have used the errors in the differential equations directly rather than using the equivalent errors in the discrete system. However, this tends to over-estimate the noise by about a factor of 10 and since we have obtained apparently satisfactory gains, we will ignore the question.

The discrete versus differential question will arise again in testing K.

IV. <u>Testing of K.</u> Somewhere in this spectrum of K values lies the one we should use. One of the tasks that is always faced in such problems is that of determining a proper gain while using the most realistic assumptions possible. In our case this means while using the simulation. Before doing that however, we wish to demonstrate that at least one of these K's appears to give tolerable results under circumstances similar to those which we have hypothesized.

Allowing some engineering judgement to operate, one of these gains looks particularly good, that is [0.13, 0.0054]. Primarily this is because it has a small k_1 and a reasonably large k_2.

We also mention that k_2 is about the right magnitude. A magnitude for k_1 of 0.1 seems quite reasonable and the rates are approximately a hundredth of the angles.

Let us take this gain and make two runs with it, both having observation noise of s.d. $6.3 \cdot 10^{-4}$, and constant perturbations in $\dot{\omega}$ of 10^{-5},

which is large by a factor of five.

The first run will have $\alpha(0) = 0.005\text{rad} = 0.286°$ and $\omega(0) = -0.0005\text{rad/sec}$. These are fairly typical values in the vicinity of the origin. While in this region we might expect perturbations on $\dot{\alpha}$ of $2.5\cdot10^{-6}$ so we will enter a constant term of 10^{-5}. We put $\hat{\alpha}(0) = \alpha(0)$ and $\hat{\omega}(0) = \omega(0)$.

We are able to investigate the behavior of this filter in the absence of control because the control is known (up to misalignments which have been accounted for otherwise) and can be entered exactly in the filter.

We expect to be in a region such as this for a maximum of 20 seconds.

Figures 4 and 5 show the results of this run. $\hat{\omega}$ is steadily deteriorating because the constant rate does not appear in the modeling and because the observation errors are insufficient to correct the estimate. $\hat{x}$ is oscillating about the true value with errors of about 0.00016 radians which is one fourth of the observation noise.

The second run has $\alpha(0) = \hat{\alpha}(0) = 0.05$ rad and $\omega(0) = \hat{\omega}(0) = -0.0015\text{rad/sec}$. We will use a bias in $\dot{\alpha}$ of $4\cdot10^{-4}$.

In this high signal run $\hat{x}$ is very close to x, but $\hat{\omega}$ appears to be somewhat affected by the noise. Except for the observation noise, all these perturbations are much too high and perhaps our major conclusion should be that adequate testing of the filter can be done only on the full simulator.

q_{11}	q_{22}	k_1	k_2	p_{11}	p_{12}	p_{22}	$k_2 < 2.5k_1^2$
1E-14	4E-12	0.025	0.0031	1.0E-8	1.3E-9	3.2E-10	No
5E-12	1E-11	0.032	0.0049	1.3E-8	2.0E-9	6.5E-10	No
1E-10	1.3E-11	0.037	0.0056	1.5E-8	2.3E-9	8.6E-10	No
2.5E-9	1.3E-11	0.083	0.0055	3.6E-8	2.4E-9	2.0E-9	Yes
7.5E-9	1.3E-11	0.13	0.0054	6.1E-8	2.5E-9	3.3E-9	Yes
2.5E-8	1.3E-11	0.22	0.0048	1.1E-7	2.5E-9	5.5E-9	Yes
1.5E-7	1.3E-11	0.45	0.0036	3.3E-7	2.7E-9	1.2E-8	Yes
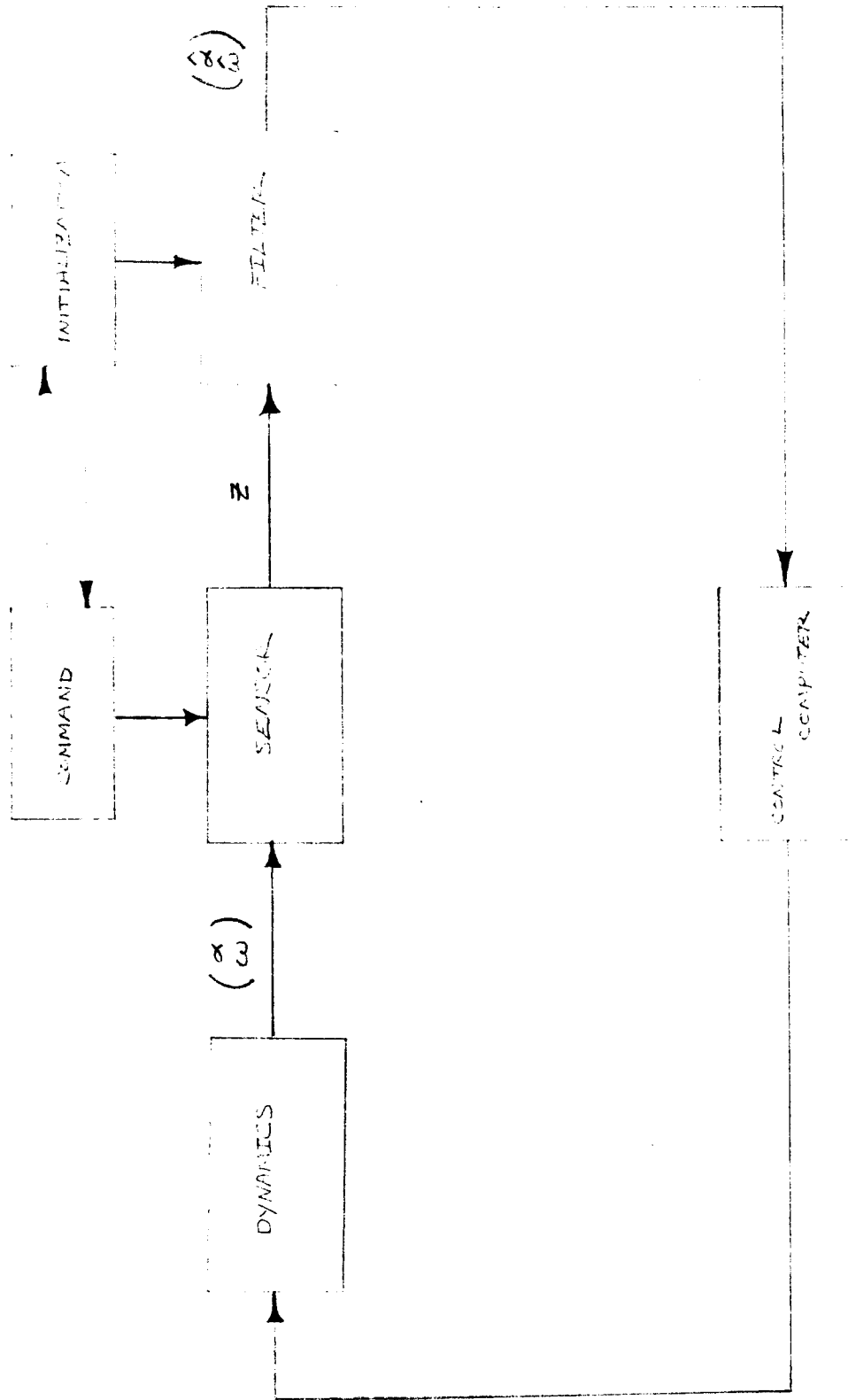
Table 1

BLOCK DIAGRAM OF FULL DYNAMIC LOOP

FIG. 1.

$u + \eta = z$

$\alpha'_{bs} = LL^{-1}(z)$

α'_{bs}

$\alpha'_{br} = \alpha_{br}(\alpha'_{bs}, \alpha_{rs})$

α_{rs}

COMMAND

$$\begin{pmatrix} \hat{\alpha}_{i+1} \\ \hat{\omega}_{i+1} \end{pmatrix} = \begin{pmatrix} 1 & \sigma \\ 0 & 1 \end{pmatrix} \begin{pmatrix} \hat{\alpha}_i \\ \hat{\omega}_i \end{pmatrix} + \begin{pmatrix} \sigma^2/2 \\ \sigma \end{pmatrix} u_i + K\left[\alpha'_{br} - \left(\hat{\alpha}_i + \sigma\hat{\omega}_i + \tfrac{\sigma^2}{2} u_i \right) \right]$$

$\begin{pmatrix} \hat{\alpha} \\ \hat{\omega} \end{pmatrix}$
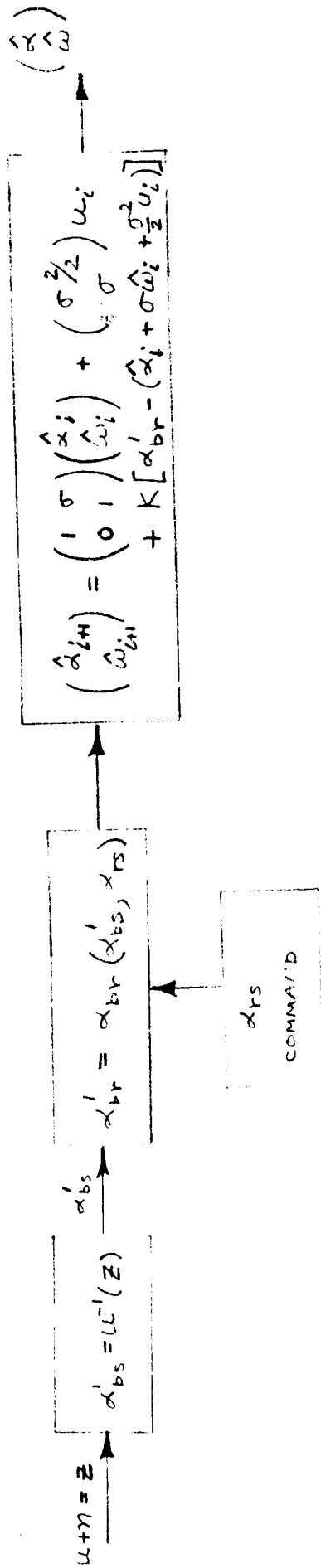
FIG. 2.   DETAILED DESCRIPTION OF FILTER

UNSTABLE REGION

CRITICAL DAMPING

h_z

1.0

0.5

0   0.5   1.0 h_x

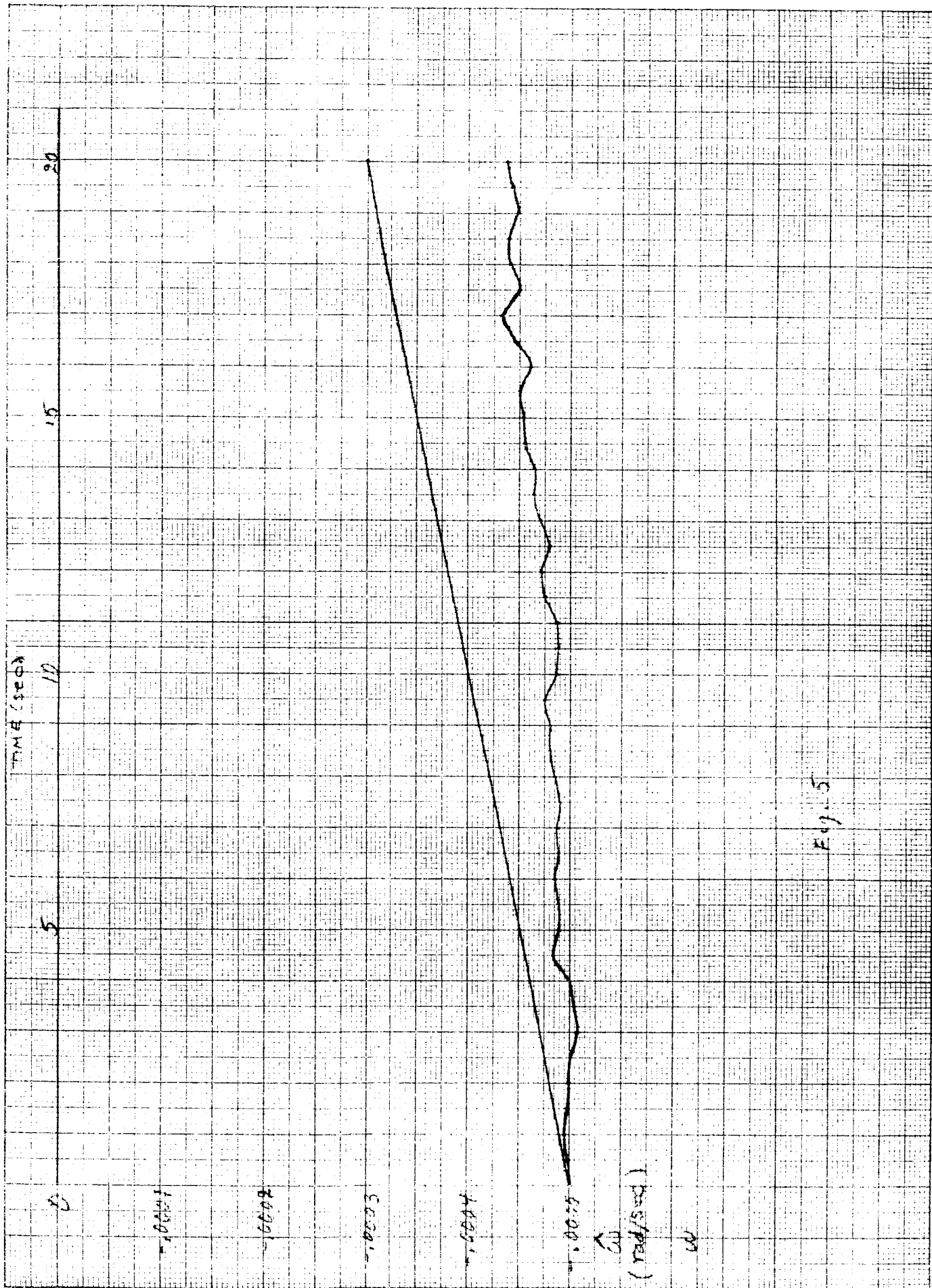$\delta = 0.1$

Fig. 3

Fig. 9.4

274

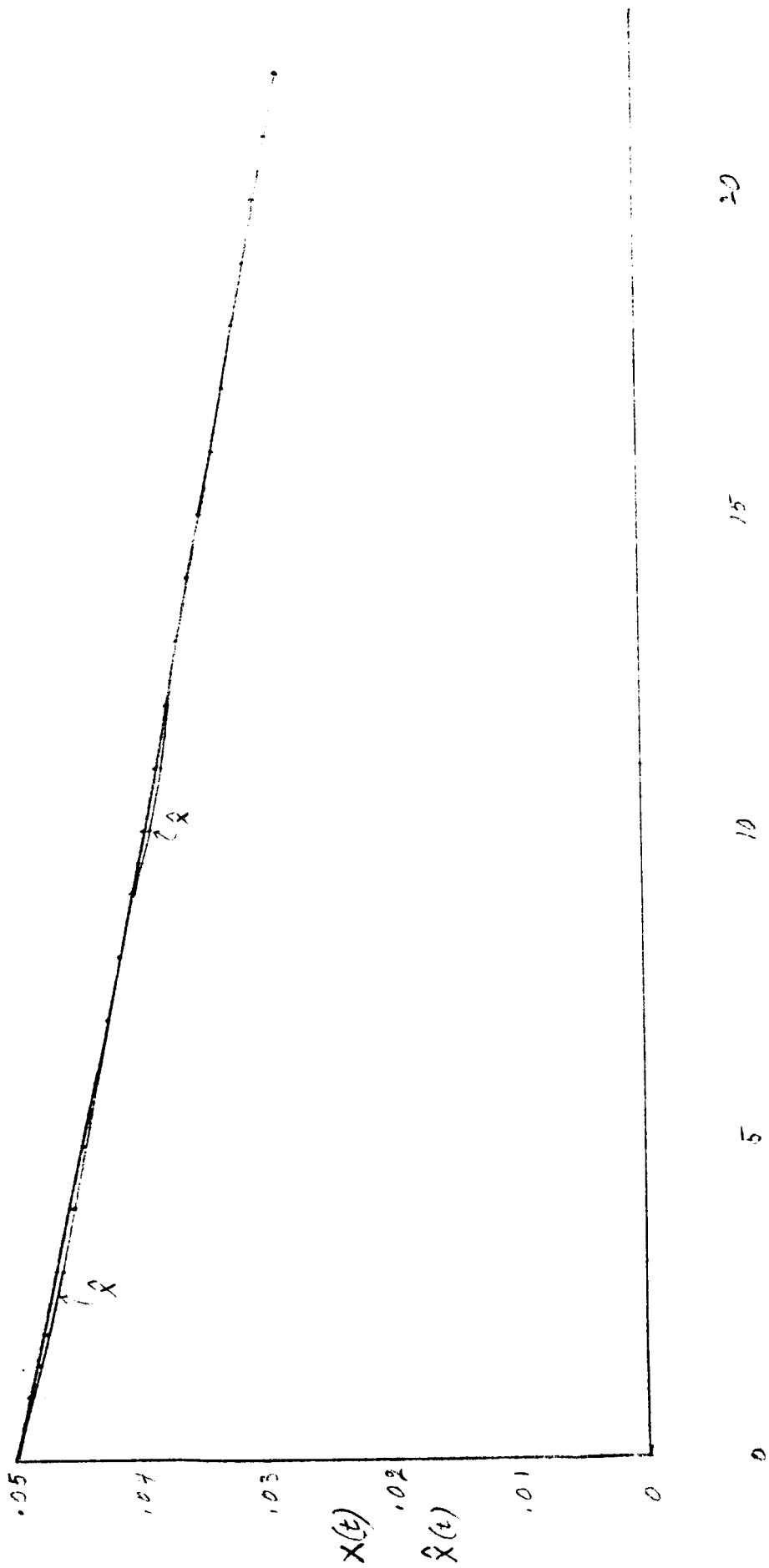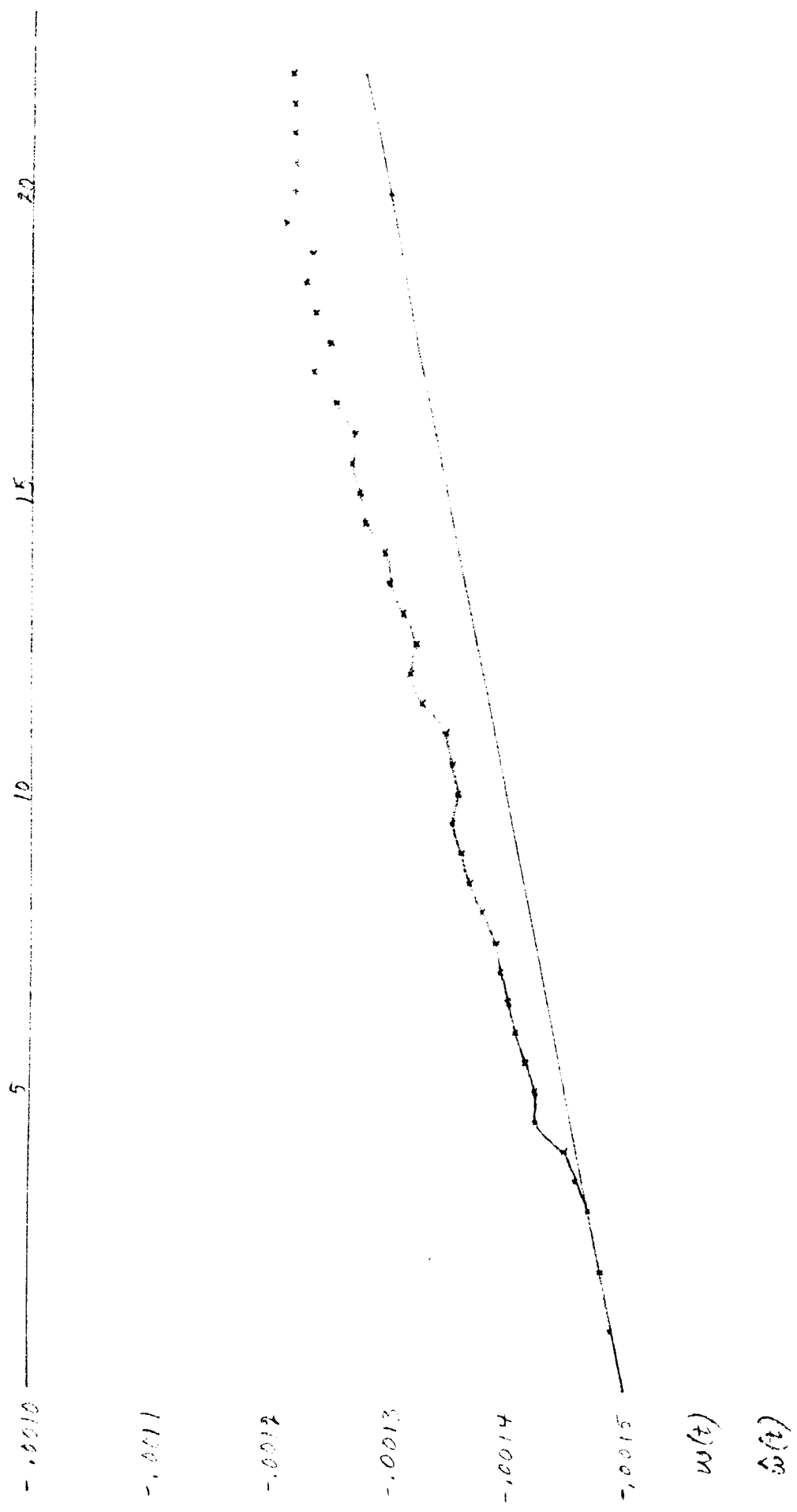Fig. 5

Fig. 6

276
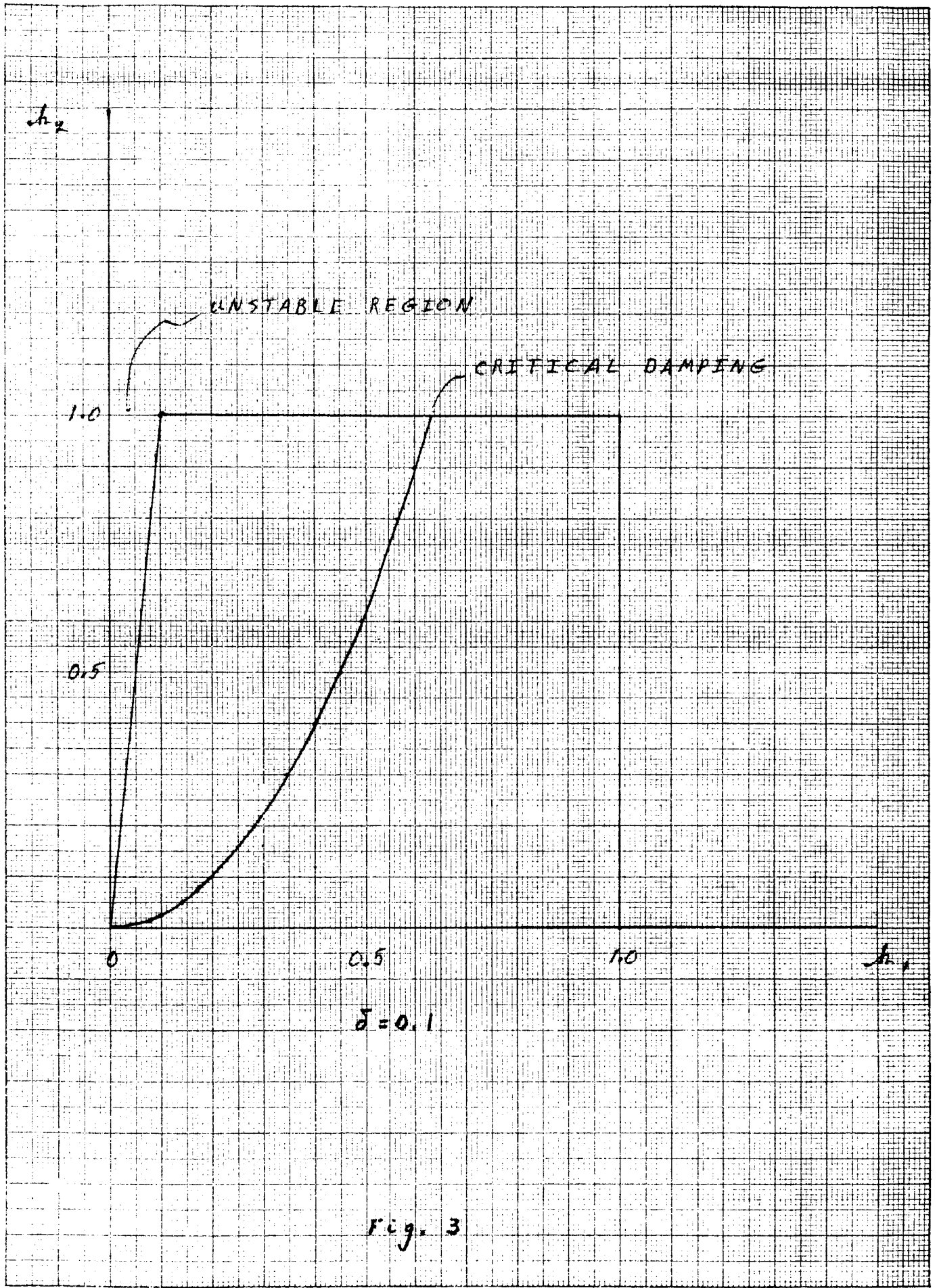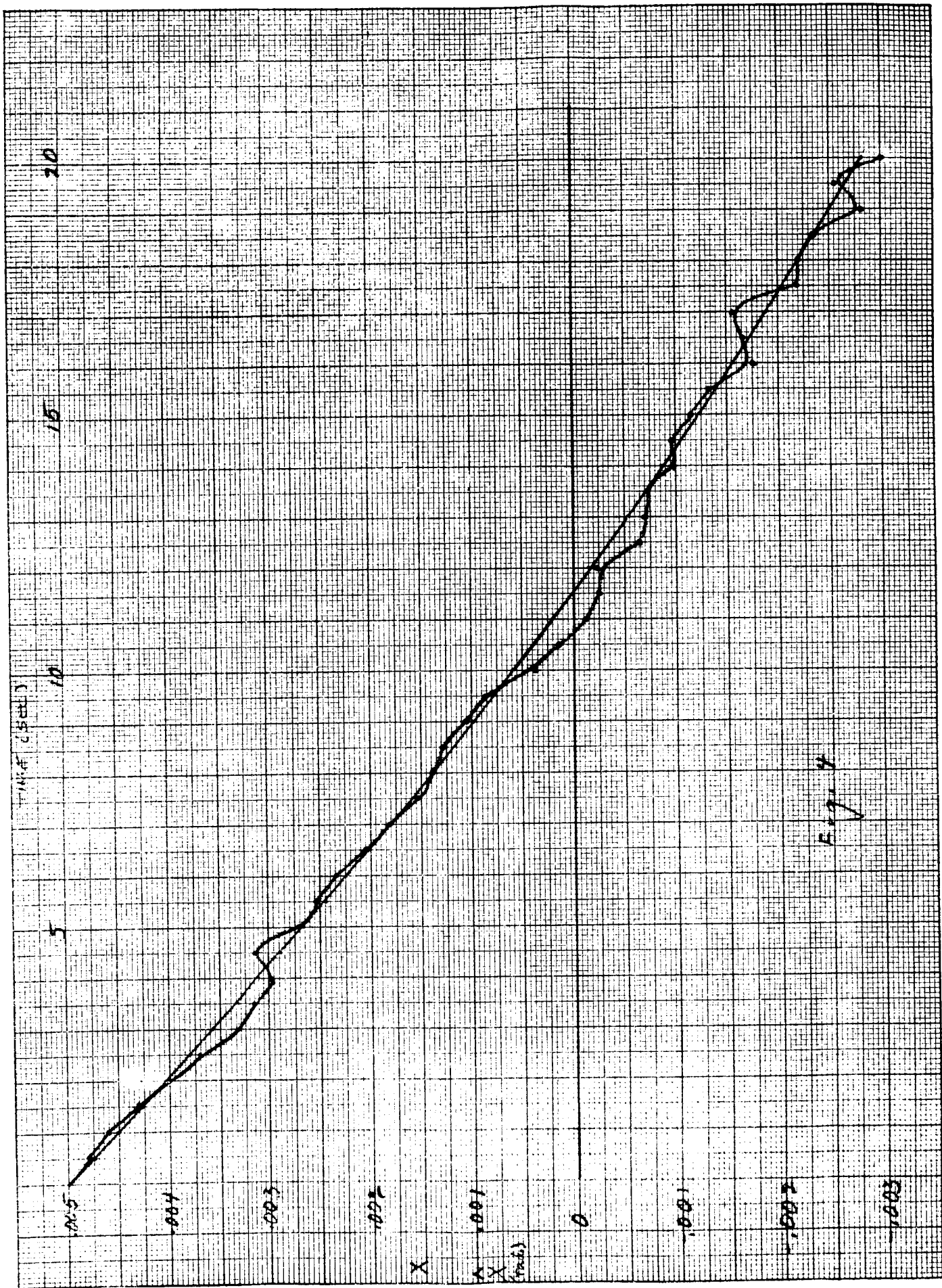
Fig. 7

277

IDENTIFICATION OF SENSOR OUTPUTS WITH EULER ANGLES

I. <u>Introduction</u>. We now wish to show that the (u_i) sensor outputs are, to first order, proportional to the (br) Euler angles.

II. <u>Sensor Math Model</u>. We first re-state the sensor math model as follows:

(a) A certain vector is fed into the body axis system (via the command inputs x and y).

(b) The spacecraft is slewed until the vector in (a) (constant in the body system) is pointing along the local vertical.

(c) During the slewing maneuver, the sensor detects the direction of Polaris relative to the body system and detects the vector in (a) relative to the orbit coordinate system (the s-system in MSG notation).

Let $\vec{v}_2$ be the unit vector given in (a), and let $\vec{v}_1$ be a unit vector pointing in the direction of Polaris. Then in our notation, we may express (c) in the form:

278

$$\vec{v}_2 = \begin{pmatrix} u_2 \\ u_0 \\ -u_1 \end{pmatrix}_s \qquad , \qquad \vec{v}_1 = \begin{pmatrix} u_3 \\ u'_3 \\ u'_0 \end{pmatrix}_b$$

where u_1, u_2, u_3 and u'_3 are the sensor outputs described in the GSFC letter, and $u_0^2 \equiv 1 - u_2^2 - u_1^2$, $(u'_0)^2 \equiv 1 - (u_3)^2 - (u'_3)^2$ (to make $\vec{v}_2$ and $\vec{v}_1$ unit vectors), and the s and b subscripts denote that the respective vector components are taken in the s-system (orbit coordinate system) and in the b-system (body coordinate system).

According to (a), the vector $\vec{v}_2$ is given in the b-system in terms of the command inputs. Thus we may write:

$$\vec{v}_2 = \begin{pmatrix} x \\ z \\ -y \end{pmatrix}_b$$

where x and y are the command inputs given in the GSFC letter and $z^2 \equiv 1 - x^2 - y^2$.

From astronomical information, we may also write $\vec{v}_1$ in the s-system as follows:

$$\vec{v}_1 = \begin{bmatrix} -\sin(0.8°)\ \cos\ q \\ +\sin(0.8°)\ \sin\ q \\ \cos(0.8°) \end{bmatrix}_s$$

where q is the satellite orbit angle. (The angle q is taken to be zero when Polaris is in the $\vec{s}_3\vec{s}_1$ plane and $\vec{s}_1$ makes an angle greater than 180° with $\vec{v}_1$.)

By a transformation of coordinates, we may relate the components in the b and s systems. In particular, for any vector $\vec{\omega}$:

$$(\vec{\omega})_b = C(\theta_{bs},\ \Psi_{bs},\ \phi_{bs})\ (\vec{\omega})_s$$

where $\theta_{bs}, -\Psi_{bs}$ and ϕ_{bs} are the Euler angles in rotating the s-system into the b-system, and the matrix C is:

$$C(\theta,\ \Psi,\ \phi) = \begin{pmatrix} C\Psi C\theta & C\Psi S\theta & S\Psi \\ -S\phi S\Psi C\theta & -S\phi S\Psi S\theta & S\phi C\Psi \\ -C\phi S\theta & +C\phi C\theta & \\ -C\phi S\Psi C\theta & -C\phi S\Psi S\theta & C\phi C\Psi \\ +S\phi S\theta & -S\phi C\theta & \end{pmatrix}$$

Thus for the $\vec{v}_2$ vector, we can write:

$$\begin{pmatrix} u_2 \\ u_0 \\ -u_1 \end{pmatrix}_s = C^T(\theta_{bs},\ \Psi_{bs},\ \phi_{bs}) \begin{pmatrix} x \\ z \\ -y \end{pmatrix}_b$$

where C^T is the transpose of C and $C^T = C^{-1}$ since C is an orthogonal matrix.

Writing out the preceding equation in component form, we have:

$$u_1 = - x \sin\Psi_{bs} - z \sin\phi_{bs} \cos\Psi_{bs} + y \cos\phi_{bs} \cos\Psi_{bs}$$

$$u_2 = x \cos\Psi_{bs} \cos\theta_{bs} - z(\sin\phi_{bs} \sin\Psi_{bs} \cos\theta_{bs} + \cos\phi_{bs} \sin\theta_{bs})$$
$$- y(-\cos\phi_{bs} \sin\Psi_{bs} \cos\theta_{bs} + \sin\phi_{bs} \sin\theta_{bs})$$

Similarly, for the $\vec{v}_1$ vector:

$$\begin{pmatrix} u_3 \\ u_3' \\ u_0' \end{pmatrix}_b = C(\theta_{bs}, \Psi_{bs}, \phi_{bs}) \begin{pmatrix} -S(0.8°) \ Cq \\ +S(0.8°) \ Sq \\ C(0.8°) \end{pmatrix}_s$$

and:

$$u_3 = (-\sin(0.8°) \cos q)(\cos\Psi_{bs} \cos\theta_{bs}) + (\sin(0.8°) \sin q)\cdot$$
$$(\cos\Psi_{bs} \sin\theta_{bs}) + (\cos(0.8°))(\sin\Psi_{bs}) \quad ,$$

$$u_3' = (-\sin 0.8° \cos q)(-\sin\phi_{bs} \sin\Psi_{bs} \cos\theta_{bs} - \cos\phi_{bs} \sin\theta_{bs})$$
$$+ (\sin 0.8° \sin q) (-\sin\phi_{bs} \sin\Psi_{bs} \sin\theta_{bs} + \cos\phi_{bs} \cos\theta_{bs})$$
$$+ (\cos 0.8°)(\sin\phi_{bs} \cos\Psi_{bs}) \quad .$$

The sensor outputs have all been expressed in terms of Euler angles. The command inputs x and y may also be so expressed. That is, we wish to find an expression for $(\vec{v}_2)_b$ in terms of Euler angles. According to (b), at

the end of the slewing maneuver, $\vec{v}_2$ is along the local vertical, i. e.,
at this time $\vec{v}_2 = \vec{s}_2$. In MSG notation, the body coordinate system coincides
with the r-system (or reference system) at the end of the slewing maneuver.
That is the components of $\vec{v}_2$ in the b-system and in the r-system are the
same or $(\vec{v}_2)_b = (\vec{v}_2)_r$. Combining with the preceding equation, we have
$(\vec{v}_2)_b = (\vec{v}_2)_r = (\vec{s}_2)_r$.

By coordinate transformation between the s-system and the r-system,
we may write:

$$(\vec{s}_2)_r = C(\theta_{rs}, \; 0, \; \phi_{rs}) \; (\vec{s}_2)_s$$

since $\Psi_{rs} = 0$. Then from $(\vec{v}_2)_b = (\vec{s}_2)_r$ and the definition of $(\vec{v}_2)_b$, we have:

$$\begin{pmatrix} x \\ z \\ -y \end{pmatrix}_b = C(\theta_{rs}, \; 0, \; \phi_{rs}) \begin{pmatrix} 0 \\ 1 \\ 0 \end{pmatrix}_s .$$

In component form, this gives:

$$x = \sin\theta_{rs}$$

$$y = \sin\phi_{rs} \cos\theta_{rs} .$$

The relations between the bs, rs and br Euler angles have been
determined previously (see Englar → Isley, June 12, 1967 or Englar → Isley,
May 22, 1967) and are:

$$\sin\Psi_{br} = \sin\phi_{rs}\ \cos\Psi_{bs}\ \sin(\theta_{rs} - \theta_{bs}) + \cos\phi_{rs}\ \sin\Psi_{bs}$$

$$\sin\theta_{br} = \frac{\sin\phi_{rs}\ \sin\Psi_{bs} + \cos\phi_{rs}\ \cos\Psi_{bs}\ \sin(\theta_{bs} - \theta_{rs})}{\cos\Psi_{br}}$$

$$\sin\phi_{br} = \frac{\begin{pmatrix} \cos\phi_{rs}\ \sin\phi_{bs}\ \cos\Psi_{bs} \\ - \sin\phi_{rs}\ \cos\phi_{bs}\ \cos(\theta_{rs} - \theta_{bs}) \\ - \sin\phi_{rs}\ \sin\phi_{bs}\ \sin\Psi_{bs}\ \sin(\theta_{rs} - \theta_{bs}) \end{pmatrix}}{\cos\Psi_{br}}$$

III. <u>Linearized Equations.</u> So far, we have made no approximations, and the preceding equations are exact. We now make the following two assumptions:

(1) Polaris is due north.

(2) All of the Euler angles are small.

One effect of assumption (1) is to remove the orbit angle q from all calculations. Assumption (1) also simplifies the inversion of the u_i equations (to express the Euler angles as functions of the u_i). Assumption (1) can be examined later (both analytically and numerically) to see what errors it may introduce. As far as the preceding equations are concerned, the 0.8° angle appearing in the u_3 and u_3' equations becomes a zero angle. Thus:

$$u_3 = \sin\Psi_{bs}$$

$$u_3' = \sin\phi_{bs}\ \cos\Psi_{bs}\quad .$$

Assumption (2) is the linearizing approximation we are interested in. Using (2) we obtain the following equations (retaining first order terms only):

$$u_3 = \Psi_{bs}$$

$$u_3' = \phi_{bs}$$

$$x = \theta_{rs}$$

$$y = \phi_{rs}$$

$$z = 1.0$$

$$u_1 = -\phi_{bs} + \phi_{rs}$$

$$u_2 = \theta_{rs} - \theta_{bs}$$

$$\Psi_{br} = \Psi_{bs}$$

$$\theta_{br} = \theta_{bs} - \theta_{rs}$$

$$\phi_{br} = \phi_{bs} - \phi_{rs} \quad .$$

If we combine certain equations above, we may write u_1, u_2 and u_3 as functions of the br Euler angles. Thus:

$$u_1 = -\phi_{br}$$

$$u_2 = -\theta_{br}$$

$$u_3 = \Psi_{br}$$

These are the linearized equations for u_i showing that, in fact, u_1, u_2 and u_3 are proportional to the br Euler angles.

APPENDIX G

MINIMIZATION OF POLARIS SENSOR DEVIATION

MINIMIZATION OF POLARIS SENSOR DEVIATION

The purpose of this appendix is to justify the assumption made throughout the report that the definition herein used of the R system is such as to minimize the angle between a polar axis (in particular $\hat{z}_s$, the 3-axis of the system) and the target 3-axis. That is, for all orthogonal systems whose 2-axis points at the target (possible target coordinate systems), our definition of the R system renders the angle between $\hat{z}_r$ and the polar axis a minimum.

We will give two proofs of this here. The first geometric and conceptual - the second computational.

A.   Given a target point define a plane P containing the satellite, the target point, and $\hat{z}_s$. Rotate about $\hat{z}_s = \hat{z}_b$ until the pointing vector $\hat{y}_b$ lies in this plane. Notice that $\hat{z}_s = \hat{z}_b$ still and therefore the polaris sensor has no deviation.

Naturally $\hat{x}_b$ is normal to this plane and the rotation ρ about $\hat{x}_b$ which brings $\hat{y}_b$ to bear on the target leaves

$\hat{z}_b$ in P , hence

$$\hat{z}_b \cdot \hat{z}_s = \cos \rho. \tag{A-1}$$

The ($\hat{x}_b$, $\hat{y}_b$, $\hat{z}_b$) system as it now appears is that defined by MSG to be the target system - R. The claim is that any other system pointing at the target will have ($\hat{z}_b \cdot \hat{z}_s$) smaller and hence a larger deviation.

Any other system pointing at the target is obtained by rotating this system about the pointing vector $\hat{y}_r$. Because $\hat{y}_r$ lies in the plane P, any rotation about $\hat{y}_r$ will move $\hat{z}_b$ out of P in a plane perpendicular to P. This alone is sufficient to tell us that the angle between $\hat{z}_b$ and $\hat{z}_s$ will increase.

However the proof is given by reference to some spherical trig formulae. Let us take a unit sphere Q centered on the satellite. Let P_s

be the intersection of $\hat{z}_s$ and Q, P_r the intersection of $\hat{z}_r$ and Q, and P_b the intersection of $\hat{z}_b$ and Q after rotation through y about $\hat{y}_r$.
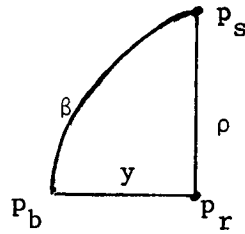
The angle β is the polaris sensor deviation and from the law of cosines

$$\cos \beta = \cos y \cos \rho . \tag{A-2}$$

Therefore β is minimum when y is zero.

B. The following analysis develops explicitly the formulae for the body unit vectors in terms of the S unit vectors. The results will show that

$$\cos \beta = \cos \rho \cos y$$

as in (A-2).

From the appendix we find that after the R system pointing at the target is defined by rotating through π and ρ, we have

$$B^T(\pi,\rho) \begin{bmatrix} \hat{x}_s \\ \hat{y}_s \\ \hat{z}_s \end{bmatrix} = \begin{bmatrix} \hat{x}_r \\ \hat{y}_r \\ \hat{z}_r \end{bmatrix}$$

where

$$B(\pi,\rho) = \begin{bmatrix} c\pi & -s\pi\ c\rho & s\pi\ s\rho \\ s\pi & c\pi\ c\rho & -c\pi\ s\rho \\ 0 & s\rho & c\rho \end{bmatrix}$$

Therefore

$$\hat{z}_r = \sin \pi \sin \rho\ \hat{x}_s - \cos \pi \sin \rho\ \hat{y}_s + \cos \rho\ \hat{z}_s .$$

This agrees with (A-1).

Now if we rotate about $\hat{y}_r$ through an angle y, we have

$$B^T(y)\ B^T(\pi,\rho) \begin{bmatrix} \hat{x}_s \\ \hat{y}_s \\ \hat{z}_s \end{bmatrix} = \begin{bmatrix} \hat{x}_b \\ \hat{y}_b \\ \hat{z}_b \end{bmatrix}$$

where

$$B(y) = \begin{bmatrix} cy & 0 & -sy \\ 0 & 1 & 0 \\ sy & 0 & cy \end{bmatrix}$$

and therefore

$$\hat{z}_b \cdot \hat{z}_s = \cos\rho \cos y \ .$$

This agrees with (A-2) and again proves the claim.

Appendix

The two pages following derive the expressions for vector components and for unit vectors after rotation through Euler angles in accordance with the MSG convention.

Let R, $\mathcal{B}$ be the names of two right-handed orthogonal coordinate systems having the same origin. Let π, y, ρ be the names of the Euler angles which take R to $\hat{\mathcal{B}}$ by the following procedure:

Rotate thru an angle π about

$\hat{r}_3$ to create the axis system R^1. Rotate thru an angle -y about

$\hat{r}_2^1$ to create the axis system R^2. Rotate thru an angle ρ about

$\hat{r}_1^2$ to create R^3.

Then system R^3 is system $\mathcal{B}$.

Define the matrix

$$
B = \begin{bmatrix}
c\pi\ cy & -c\pi\ s\rho\ sy - s\pi\ c\rho & -c\pi\ c\rho\ sy + s\pi\ s\rho \\
s\pi\ cy & -s\pi\ s\rho\ sy + c\pi\ c\rho & -s\pi\ c\rho\ sy - c\pi\ s\rho \\
sy & s\rho\ cy & c\rho\ cy
\end{bmatrix}
$$

Let v be a vector in three-space and v_r, v_b its vector of components in the R, $\mathcal{B}$ systems respectively.
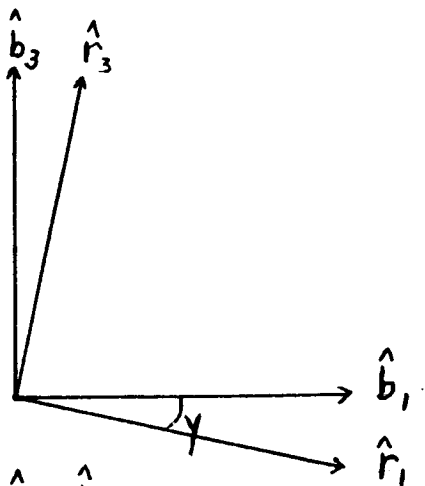
Then
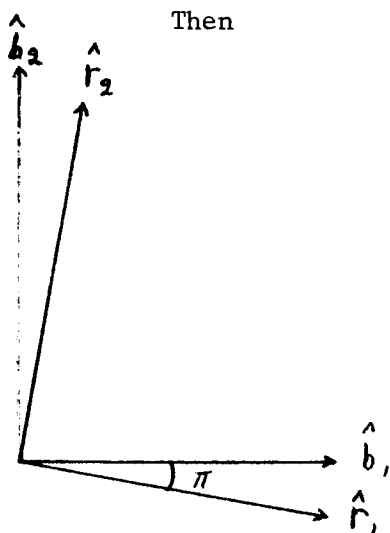
$$v_r = B\ v_b \quad ; \quad v_b = B^T\ v_r .$$

Checks: Let y = ρ = 0

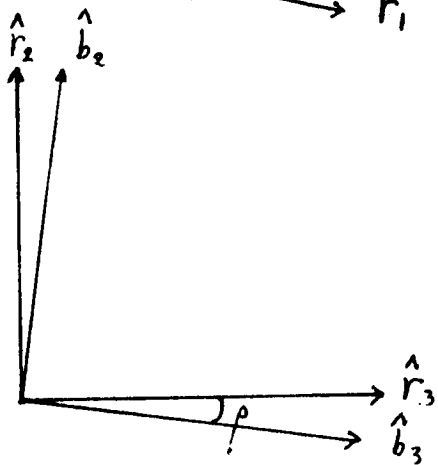$$v_b = [1\ 0\ 0] \quad [0\ 1\ 0] \quad [0\ 0\ 1]$$

$$v_r = \begin{bmatrix} \cos\pi \\ \sin\pi \\ 0 \end{bmatrix} \quad \begin{bmatrix} -\sin\pi \\ \cos\pi \\ 0 \end{bmatrix} \quad \begin{bmatrix} 0 \\ 0 \\ 1 \end{bmatrix}$$

Let $\pi = \rho = 0$

$$v_b = [1\ 0\ 0] \qquad [0\ 1\ 0] \qquad [0\ 0\ 1]$$

$$v_r = \begin{bmatrix} \cos y \\ 0 \\ \sin y \end{bmatrix} \qquad \begin{bmatrix} 0 \\ 1 \\ 0 \end{bmatrix} \qquad \begin{bmatrix} -\sin y \\ 0 \\ \cos y \end{bmatrix}$$

Let $\pi = y = 0$

$$v_b = [1\ 0\ 0] \qquad [0\ 1\ 0] \qquad [0\ 0\ 1]$$

$$v_r = \begin{bmatrix} 1 \\ 0 \\ 0 \end{bmatrix} \qquad \begin{bmatrix} 0 \\ \cos\rho \\ \sin\rho \end{bmatrix} \qquad \begin{bmatrix} 0 \\ -\sin\rho \\ \cos\rho \end{bmatrix}$$

Furthermore, we can write the unit vectors as

$$\begin{bmatrix} \hat{r}_1 \\ \hat{r}_2 \\ \hat{r}_3 \end{bmatrix} = B \begin{bmatrix} \hat{b}_1 \\ \hat{b}_2 \\ \hat{b}_3 \end{bmatrix}$$

APPENDIX H

EXPERIMENT PLAN FOR IDEAL MODEL

I. The significant criteria for evaluating the performance of the control system for a given slewing maneuver are:

1) The total fuel consumption.

2) The time required.

3) The rates achieved.

4) The number of control actuations.

The first three can be manipulated by varying the performance index. The fourth cannot be treated generally and has been minimized by experimental tuning of the control. These criteria will be called the control system output or costs.

The range of values of these costs is determined by what we shall call the input parameters which split into three groups

A. Vehicle-fixed

B. Performance weights

C. Initial conditions.

Vehicle-fixed parameters are the moments of inertia, available control torques, and the values of perturbation torques.

Fixed for each space mission but somewhat less hardware fixed are the weights appearing in the performance index.

Finally, a specific initial condition and target location pair generate the values of the criteria given by any slewing maneuver.

The purpose of this initial set of experiments is to investigate the changes in the criteria produced by changes in the input parameters described above.

The major portion of testing groups A) and B) can be done by fixing terminal points α and initial point β on the Earth and performing a fixed slewing maneuver. Suggested pairs might be Canberra-Mojave, Mojave-Rosman, or Rosman-Ascension. Canberra-Mojave provide a good latitude-longitude split. A study of this type would give a good idea of the cost of such a slew as input varied.

II. Perturbation torque study.

The first object of this sequence would be to point out that the perturbation torques-gravitational and solar torques -- have little effect upon costs. This would be done by running a long-time (not time optimal) trajectory from station α to station β and back with zero torques, the true torques, and fixed torques ten times larger than the maximum naturally available.

The expected results would show little change in fuel, rates, or time. The number of actuations might increase in the large torque case because our softened switching curves would be overpowered.

Phase plane plots of the three runs would be made with tables of fuel, time, and stations used. This sequence could dispose of the torque question.

III. Fuel vs. time tradeoff with effect of hardware changes.

Using $\lambda_1 = 1$, $\lambda_3 = 0$, λ_2 can be varied to produce a graph of time vs. fuel.

Thus far all problems have been computed with the nominal values of hardware constants. Now the control moment of inertia ratio should be changed, to provide information about performance changes caused by

specification changes. We suggest that the ratio be changed by ± 10% in all axes at once and then the pitch and roll axes have their ratios changed by 10% so as to separate them. This will give four curves on the graph.

IV. <u>Extremum studies</u>.

Determine the max-min time for a hemispheric slew and its associated fuel cost.

For this particular slew determine the time-fuel relationship.

V. <u>Catastrophic control</u>.

An additional study could investigate costs and the phase plane trajectories for perturbation torques having a significant percentage of the control torque, say 50%. This might illustrate the case of a jet which cannot be shut off.

VI. <u>Ground track illustration</u>.

For several station pairs, perhaps the three named above, we would like to graph the ground track of the pointing vector for time optimal control. This control is chosen since it will probably give the least smooth trajectory.

In addition the ground tracks would be made for a longtime trajectory. We anticipate very little difference. These ground tracks would be paired with the phase-plane plots.

This work does require additional programming and checkout estimated at two weeks and additional analysis of two days.

VII. Time and fuel contours.

Assume the target is at face-center. Draw two contours of constant time and two of constant fuel for min time control and a longtime control.

This is only tentative since such contours, though they need be constructed only for one quadrant require iteration and will thus consume a great deal of time.

APPENDIX I

EXPERIMENT PLAN FOR REAL EFFECTS

The real satellite differs from the ideal primarily in having control torques which decrease with on-time and in having available for state information only noisy angles as opposed to the precise angles and rates available in the ideal model.

We need then to investigate the effect of these changes upon the overall control system. Since the control system includes a filter designed to handle the noisy, angle-only data problem we should expect to find more problems arising from the modeling error given by the thrust decay than from the real sensor simulation.

The following experiments test combinations of these effects on the standard Mojave-Quito time optimal slew and also exhibit one non-time-optimal run.

1. For comparison with the ideal model, a run using the filter on exact sensor data with ideal thrusters. That is, only angles available, but no noise added.

2. Ideal thruster, realistic sensor. Angles only available and gaussian noise added of standard deviation $\sigma = 0.00063$. This run isolates the errors introduced by the filter.

3. Real thrusters, using the filter on noiseless, angle-only data. This will isolate the thruster effects except for a small contribution from the inherent filter lag.

4. Both sensor and thruster real effects. This gives us the worst case situation and leads into the next set of runs which involve compensation.

5. A non-time-optimal run will serve to illustrate control law response in another situation and also probably compensate for thrust decay.

6. Other possible control error compensation runs.

APPENDIX J

TORQUE MISALIGNMENT CALCULATIONS

Torque Misalignment Calculations

1. <u>Introduction</u>: Although the control torque vectors are nominally aligned with the vehicle principal axes, small misalignments of the thrusters may give control torque vectors which have projections on all three principal axes. It is expected, however that ground testing of the satellite will reveal the actual orientation of these torques. That is the detection of the misalignment can be done with much greater precision than the hardware can actually be aligned. In short we have misalignments existing but they are known to us. In such a case we would expect to improve our control by some compensation for these misalignments.

The purpose of this appendix is to describe: 1) how these misalignments enter the vehicle dynamics, 2) how the misalignments are parameterized -- that is how the misalignments are entered in the simulation, and 3) how they are compensated in the control law.

2. <u>Equations of Motion</u>: In both the analog and digital dynamics simulations the following torque equations are used

$$I_1\dot\omega_1 = (I_2 - I_3)\omega_2\omega_3 + T_1 + b_{11}u_1 + b_{12}u_2 + b_{13}u_3$$

$$I_2\dot\omega_2 = (I_3 - I_1)\omega_1\omega_3 + T_2 + b_{21}u_1 + b_{22}u_2 + b_{23}u_3$$

$$I_3\dot\omega_3 = (I_1 - I_2)\omega_1\omega_2 + T_3 + b_{31}u_1 + b_{32}u_2 + b_{33}u_3$$

Here $\{I_i\}$ are the principal axis moments of inertia, $\{\omega_i\}$ are the principal axis angular rates and $\{T_i\}$ are the principal axis torques arising from the solar and gravitational forces. The remaining terms on the right hand side arise from the misalignment torques.

The terms b_{ij} are the influence coefficients of the jth control torque on the ith principal axis rate. Usually we expect b_{ii} to be close to unity and the off diagonal elements to be small. Since all of the jth torque operates on the vehicle,

$$b^2_{1j} + b^2_{2j} + b^2_{3j} = 1.$$

That is, the length of each column vector is one. The matrix $B = [b_{ij}]$ is not orthogonal however, since the torques need not be mutually orthogonal.

The direction of thrust for a fixed jet is assumed to be constant. Therefore, the influence coefficients $\{b_{ij}\}^3_{i=1}$ are constant for a fixed sign of u_j. However when the sign of u_j changes, the misalignment of the control torque u_j also changes. Therefore the coefficients $\{b_{ij}\}$ must change, and this is provided for in the simulation by having two matricies $B^+ = [b^+_{ij}]$ and $B^- = [b^-_{ij}]$ the columns of which are associated with the respective signs of the control u_j. These are treated independently in the dynamics of course so that b^+_{11}, b^+_{21}, and b^+_{31} may be used for the one-axis torque while b^-_{13}, b^-_{23}, and b^-_{33} are being used for the three-axis torque.

The computation of B^+ and B^- is done in the initialization and setup stage of the control computer. For hybrid operation the

matrices B^+ and B^- are printed so that the appropriate potentiometer settings can be made.

3. _Parameterization of Misalignments_. The following diagram illustrates how the misalignment parameters α and ϵ act to move the torque u_2 from the e_2 axis to its final prosition. This diagram is placed here for easy reference from the subsequent description.
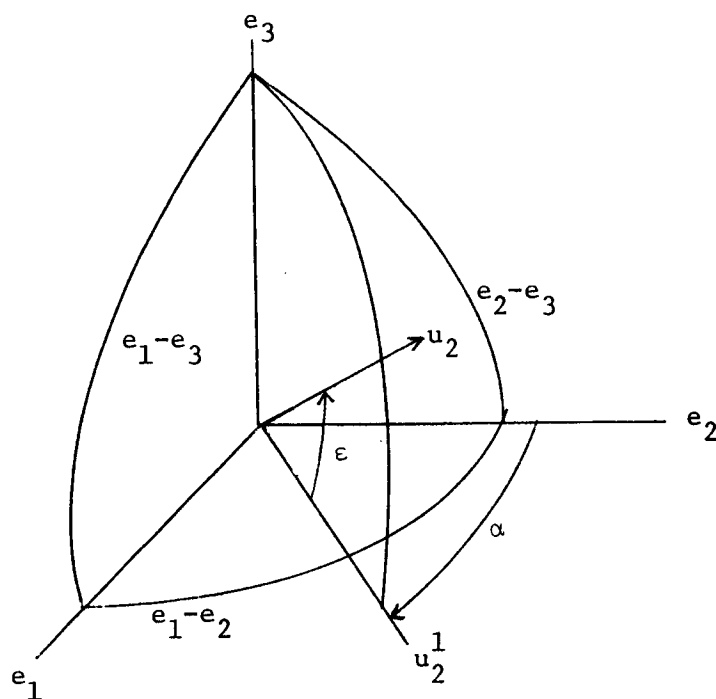
With this parameterization, and defining

$$b_{j-1k} = b_{3k} \quad \text{for} \quad j = 1 \quad \text{and} \quad b_{j+1k} = b_{1k} \quad \text{for} \quad j = 3,$$

we have

$$b_{jj} = \cos \alpha \cos \epsilon, \quad b_{j-1j} = \sin \alpha \cos \epsilon, \quad b_{j+1j} = \sin \epsilon.$$

The torque misalignment is specified by azimuth α and elevation ϵ angles in each direction of the torque. The total misalignment requires twelve parameters, two angles for each axis, in each direction.

Consider positive torque first, and for convenience denote the axes by e_1, e_2, and e_3. Let $e_{i-1} = e_3$ when $i = 1$ and let $e_{i+1} = e_1$ when $i = 3$. Then positive azimuth angle α on u_j causes the torque vector to be rotated α degrees toward e_{j-1} in the $e_j - e_{j-1}$ plane. That is, a positive α for u_j gives a positive projection of u_j on e_{j-1}, that is a positive $b_{j-1, j}$. This new position u_j^1 of the torque is then rotated ϵ degrees toward the e_{j+1} axis in the $e_{j+1} - u_j^1$ plane. The diagram at the beginning of this section shows the rotations for the torque on axis two and may prove helpful.

The remaining task is to define the sense in which angles are defined for negative torques.

The simplest manner of characterizing the definition is to say that angles are defined for negative torques so that $\alpha^+ = \alpha^-$ and $\epsilon^+ = \epsilon^-$ implies that the $u^+ = - u^-$, that is the two torques lie on a straight line. This can be achieved by applying the same procedure as described above to the negative torque after reversing the sense of each axis e_i.

4. <u>Control Computations</u>: No qualitative changes were required in the control computer by the introduction of misalignments. The disturbing force b (see Part I, section 6 and Part II, section 2) includes in axis j the terms $b_{jj-1} u_{j-1} + b_{jj+1} u_{j+1}$. Also the available control torque is replaced by $b_{jj} u_j$.

Control computation then proceeds as before.